Charles University in Prague

Faculty of Mathematics and Physics

DOCTORAL THESIS

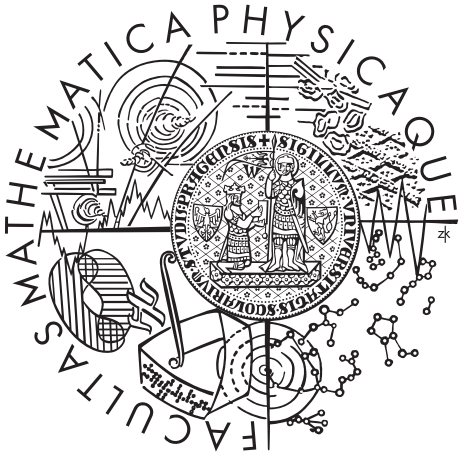

Viktor Holubec

Teoretický popis nerovnovážných procesů transformace energie na úrovni molekulárních struktur

Theoretical description of unequilibrium energy transformation processes on the level of molecular structures

Department of Macromolecular Physics

Supervisor of the doctoral thesis: prof. RNDr. Petr Chvosta, CSc.

Study programme: Physics

Specialization: Theoretical Physics, Astronomy and Astrophysics

Prague 2013

In the first place I would like to thank my supervisor, prof. RNDr. Petr Chvosta CSc., for his guidance and help during our long cooperation and to my colleague, RNDr. Artem Ryabov, for many inspiring discussions. Also I must thank to all other colleagues who cooperate on writing the common publications. Special thanks should go to my co-workers from the Universitaet Osnabrueck for their active interest in my research work. Further I feel obliged to thank my colleagues at the department and at the faculty for providing me friendly and inspiring conditions during my study. Finally I would like to thank my family and my friends. Without their support and tolerance the preparation of the manuscript would either be impossible or I would have no family and friends after its finishing.

I declare that I carried out this doctoral thesis independently, and only with the cited sources, literature and other professional sources.

I understand that my work relates to the rights and obligations under the Act No. 121/2000 Coll., the Copyright Act, as amended, in particular the fact that the Charles University in Prague has the right to conclude a license agreement on the use of this work as a school work pursuant to Section 60 paragraph 1 of the Copyright Act.

In Prague, July 26, 2013 signature of the author

Název práce: Teoretický popis nerovnovážných procesů transformace energie na úrovni molekulárních struktur

Autor: Viktor Holubec

Katedra: Katedra makromolekulární fyziky

Vedoucí disertační práce: prof. RNDr. Petr Chvosta, CSc., Katedra makromolekulární fyziky

Abstrakt:

Práce je věnována termodynamice mezoskopických systémů, které jsou vystaveny časově závislým vnějším silám. Systémů tak malých, že neplatí termodynamická limita a explicitně se vyjevuje pravděpodobnostní charakter druhého termodynamického zákona. Tepelné síly jsou srovnatelné s ostatními silami působícími na systém a musí být tedy explicitně zahrnuty ve výchozí pohybové rovnici. Pro diskrétní systémy je pohybovou rovnicí mistrovská rovnice, pro spojité systémy Fokker-Planckova rovnice. V první části práce studujeme dynamiku a energetiku mezoskopických systémů v průběhu nerovnovážných izotermických procesů. Vzhledem k stochastickému charakteru dynamiky je náhodnou veličinou i práce konaná na systému vnějšími silami. Pro několik modelových systémů odvozujeme přesný analytický tvar hustoty pravděpodobnosti pro práci. Explicitní formule jsou důležité zejména s ohledem na analýzu experimentálních dat při současném využití nedávno odvozených fluktuačních teorémů. V druhé části práce studujeme nerovnovážný cyklický proces zahrnující dvě izotermy s rozdílnými teplotami. V průběhu cyklu může systém konat kladnou práci na okolí. Analyzujeme dva modely takových mezoskopických tepelných motorů a optimalizujeme jejich výkonnostní charakteristiky.

Klíčová slova: stochastická termodynamika, hustota pravděpodobnosti pro práci, stochastické tepelné motory, účinnost při maximálním výkonu, přesná řešení

Title: Theoretical description of unequilibrium energy transformation processes on the level of molecular structures

Author: Viktor Holubec

Department: Department of Macromolecular Physics

Supervisor: prof. RNDr. Petr Chvosta, CSc., Department of Macromolecular Physics

Abstract:

The thesis is devoted to the thermodynamics of externally driven mesoscopic systems. These systems are so small that the thermodynamic limit ceases to hold and the probabilistic character of the second law cannot be ignored. Thermal forces becomes comparable to other forces acting on the system and they have to be incorporated in the underlying dynamical law, i.e., in the master equation for discrete systems, and in the Fokker-Planck equation for continuous ones. In the first part of the thesis we investigate dynamics and energetics of mesoscopic systems during non-equilibrium isothermal processes. Due to the stochastic nature of the dynamics, the work done on the system by the external forces must be treated as a random variable. We derive an exact analytical form of the work probability density for several model systems. In particular, the knowledge of the exact formula improves the analysis of experimental data using the recently discovered fluctuation theorems. In the second part of the thesis we study a non-equilibrium cyclic process which incorporates two isotherms with different temperatures. During the cycle, the system can produce a positive work on the environment. We analyze two specific models of such mesoscopic heat engines and we optimize their performance.

Keywords: stochastic thermodynamics, work probability density, stochastic heat engines, efficiency at maximum power, exact results

Contents

Introduction

More than two centuries ago, a desire to understand energy transformation processes in nature had given birth to the classical thermodynamics [26, 132]. The famous theory which expounded the connection between the concepts of heat and work and introduced general laws governing the system transformations, in particular, those involving the exchange of heat, work and matter with an environment. Cornerstones of this classical theory, the first and the second law of thermodynamics, are so universal that they are successfully exploited in all branches of physics. The first law claims that the total energy of a closed system is conserved. The second law introduces the notion of the total entropy production and says that, during any process, the entropy of the universe can never decrease. The second law, contrary to the first one, has statistical character. It is valid with certain (in most cases very large) probability and is exact only in the thermodynamic limit, the limit of infinite number of particles in the system. Inter alia, the two laws imply fundamental limits on the efficiency of heat engines and refrigerators.

The thermodynamic description of systems in equilibrium was justified by equilibrium statistical mechanics [74, 96]. This theory states that the probability to find a system in contact with a heat bath in its specific microstate is given by the Boltzmann factor. In the language of the statistical mechanics the statistical character of the second law becomes obvious. The most striking example is the famous Boltzmann definition of entropy $\mathcal{S} = k_{\mathrm{B}} \log \Omega$, where k_{B} stands for the Boltzmann constant and Ω denotes the number of microstates corresponding to a given macrostate. The most probable macrostate is compatible with the largest number of microstates Ω. The corresponding entropy is maximal possible and coincides with that defined in the classical thermodynamics. Nevertheless, the system may visit also other macrostates, although the probability of these fluctuations rapidly decreases with the number of particles in the system. For small deviations from equilibrium, linear response theory allows to express transport properties of systems under influence of small external fields through equilibrium correlation functions. On a more phenomenological level, linear irreversible thermodynamics provides a relation between such transport coefficients and entropy production in terms of forces and fluxes. For a long time, no universal exact results beyond this linear response regime were available.

One of the most challenging and exciting fields of science today is a living cell which is, by definition, a non-equilibrium system (equilibrium = dead). Within the cell, one permanently observes many non-equilibrium processes such as activity of molecular motors [156, 157], ion diffusion through membranes [145], DNA replication [111, 180] etc. These systems are mostly so small that the thermal fluctuations inevitably play an important role in their dynamics and, at the same time, they are large enough that the quantum effects can be neglected. Such systems are often referred to as *mesoscopic* systems. An example is a dielectric colloidal particle diffusing in water (heat bath) and driven by an externally controlled potential, which can be for instance realized by a focused laser beam – the so called optical trap [133]. Assume that we modulate the potential and detect the position of the particle. If we repeat the experiment many times with the

same initial state of the particle and with the same driving, we find out that the particle seldom evolves twice along a given trajectory. The reason is simple, we can never guarantee that the bath itself is at the beginning of each realization in the same state. The particle dynamics is characterized by a stochastic process and, from the many repetitions of the experiment, we obtain an ensemble of possible trajectories together with their probabilities. Along each trajectory a different amount of work is done on the particle and, similarly, a different amount of heat is dissipated into the water. These basic thermodynamic variables themselves become stochastic and are described by certain probability densities.

The necessity to describe the thermodynamics of these non-equilibrium processes led to the generalization of classical thermodynamics and equilibrium statistical mechanics. This generalization was developed during the last two decades. Using the new approaches based, both on stochastic dynamics and on thermostatted Hamiltonian dynamics, new general laws applicable to non-equilibrium mesoscopic system were revealed. These exact results, valid in an arbitrary non-equilibrium regime, generically refer to the probability densities of thermodynamic quantities like exchanged heat, applied work or entropy production, which are, for the strongly non-equilibrium processes, typically non-Gaussian. In this sense they represent a generalization of the second law of thermodynamics that is valid only for average values of these thermodynamic quantities. In particular these results allow to quantify the probability that, during a non-equilibrium process, a negative amount of entropy is produced. Occasionally such events have been called (transient) violations of the second law. It turns out that the probability of these events becomes typically exponentially small in the relevant system size. Short review of these results is given below (for more details see for example the review [166]).

First, for a thermostated shear-driven fluid in contact with a heat bath, a remarkable symmetry of the probability distribution for the entropy production in the steady state was discovered numerically and justified heuristically by Evans et al. [64]. This result, known as the steady state fluctuation theorem, was first proven by Gallavotti and Cohen [69] for a large class of systems using concepts from chaotic dynamics. Later the theorem was proven also for driven Langevin dynamics [112] and for driven diffusive dynamics [116]. As a variant of the steady state fluctuation theorem, Evans and Searles [64, 65] also derived a transient fluctuation theorem valid for relaxation towards the steady state.

Second, Jarzynski proved an elegant equality which allows to express the free energy difference between two equilibrium states by a nonlinear average of the random work required to drive the system, during an arbitrary non-equilibrium (finite time) isothermal process, from one state to the other [103, 104]. By comparing probability distributions for the work done during the process used by Jarzynski with that for the work done during the time-reversed one, Crooks found a refinement of the *Jarzynski equality*, the so called *Crooks fluctuation theorem* [42–44]. These two theorems, together with a further refinement of the Jarzynski equality, the *Hummer-Szabo relation* [97], became particularly useful for determining free energy differences and landscapes of biomolecules [19, 36, 40, 129, 148, 151]. Due to their experimental importance these relations are the most prominent ones within this class of exact results (some of which were found even much earlier [16, 17] and then rediscovered) valid for non-equilibrium systems driven by

time-dependent forces. Some of them are also used in this thesis and, hence, we review them in more detail in Sec. 1.3. A theorem which applies to transitions between two non-equilibrium steady states, and, therefore, is analogous to the Jarzynski equality, was derived by Hatano and Sasa [87].

Third, for driven Brownian motion, Sekimoto realized that three central concepts of classical thermodynamics, namely the internal energy, the exchanged heat and the applied work, can be meaningfully defined on the level of individual trajectories of the stochastic process [167, 168]. These stochastic quantities are entering the first law of thermodynamics, which remains valid separately for each individual trajectory of the process. These considerations gave birth to what Sekimoto called *stochastic energetics* in his monograph [169]. Fourth, Maes emphasized that the entropy production in the medium is related to the part of the stochastic action, which determines the weight of the trajectories, that is odd under the time-reversal [120, 121].

Finally, building systematically on the concepts briefly noticed previously [43, 143], a theory unifying the described results emerged. Seifert realized that one should not only make account of the fluctuating entropy produced in the heat bath, but one should also properly assign a stochastic entropy to the system itself [164]. This last step allowed to define the key quantities known from classical thermodynamics along the individual trajectories and, hence, make them accessible to experimental measurements and numerical simulations. Such approach which considers both the first law (energy conservation) and the entropy production along the individual trajectories, was called *stochastic thermodynamics* [165]. A theory with the same name has been originally introduced by the Brussels school in the mid-eighties [131, 186]. It describes non-equilibrium steady states in chemical reaction systems.

Stochastic thermodynamics as considered in this thesis represents a generalization of classical thermodynamics. It applies to various non-equilibrium phenomena in the presence of time varying external fields, where in particular the systems are in contact with a thermal reservoir. Such phenomena are of vital interest in many areas of current research [66, 151, 165, 166]. Examples are ageing and rejuvenation effects in the rheology of soft-matter systems and in the dynamics of spin glasses, the phenomenon of stochastic resonance [34, 70, 106, 107], relaxation and transport processes in biological systems such as molecular motors [4, 7, 9, 23, 83, 139, 145, 170, 181], ion diffusion through membranes, or DNA replication, driven diffusion systems with time-dependent bias such as colloidal particles, and Nano-engines. Most of these systems are embedded in an aqueous solution which serves as a heat reservoir.

Let us mention that the behavior of the systems driven by time-varying forces can be understood intuitively using the famous horse-carrot analogy. The position of the horse (depicted in Fig. 1 by the monkey) represents the immediate state of the system and the carrot (depicted in Fig. 1 by the banana) reflects the external driving. More precisely, the position of the carrot is determined by the thermal equilibrium state corresponding to the current value of the external potential. If the potential remains constant (the banana does not move) the system relaxes towards the equilibrium state corresponding to the immediate value of the potential (the monkey approaches the banana). Since the potential varies with time (the banana moves) the system "lacks behind" the equilibrium

FIG. 1: The horse (the monkey) chasing the carrot (the banana). The position of the banana corresponds to the equilibrium state of the system determined by the instantaneous value of the driving parameters. The position of the monkey depicts the immediate state of the system which is attracted to this equilibrium state. Sadly, in the models presented in this thesis the driving parameters are always modulated, the banana never stops and, hence, the monkey never gets it. In order to calm down the animal rights activists, let us note that both the monkey and the banana in the figure are plastic. Photo Jana Benešová ©.

state (the monkey chases the banana, which constantly escapes). This analogy is precise, except for time scales. If one would not move the banana, any monkey would catch it in a twinkling of an eye. On the contrary the physical relaxation towards equilibrium state is the slower the closer the system is to the equilibrium. To behave like this would be quite unpleasant for any monkey, indeed.

Three types of non-equilibrium situations can be distinguished for the above described systems. First, one can prepare the system in a non-equilibrium initial state and study its relaxation towards equilibrium (the monkey approaches an immobilized banana). Second, general driving can be caused by the action of time-dependent external forces, fields, flows or unbalanced chemical reactions (the monkey chases a constantly moving banana). Third, in the case of time independent driving the system will eventually reach a non-equilibrium steady state (here it is assumed that no equilibrium state exists, the situation can be depicted by the monkey traveling with a constant velocity towards the banana which is infinitely far away). In this thesis we focus only on the second setting.

In all these cases, even under strong non-equilibrium conditions, the temperature of the heat reservoir remains well-defined. This property together with the time-scale separation between the observable, typically slow, degrees of freedom of the system and the unobservable fast ones of the thermal bath (and, in the case of (bio)polymers etc, by fast internal ones of the system) allows for a consistent thermodynamic description. The collection of the relevant slow degrees of freedom yields the possible microstates of the system. The state of the system at a given time is then determined by the probability to find the system at this

time in a given microstate. Since this microstate changes both due to the driving and due to the random thermal fluctuations, the system dynamics is necessarily stochastic. Similarly to the case of a driven colloidal particle, a series of measurements performed on the system under the same conditions (except for the internal coordinates of the bath) would lead to a set of possible trajectories with their relative frequencies. By inspecting the individual trajectories it is therefore possible to measure (both experimentally and in numerical simulations) the probability densities of the thermodynamic variables defined along the individual trajectories.

This ensemble of the trajectories is fully characterized by 1) the initial state of the system, 2) the properties of the thermal noise, and 3) the (possibly time-dependent) external driving. Mathematically, the time-scale separation implies that the underlying stochastic dynamics becomes Markovian one, i.e., the future state of the system depends solely on the present one (the dynamical law has no memory). If the state space of the system is a discrete one the dynamics of the system state can be described by a master equation [78, 187]. For the systems with a continuous state space the dynamics of the system microstate may follow a Langevin equation. In this case the dynamics of the system state (ensemble) is driven by a Fokker-Planck equation [78, 187]. Within such stochastic dynamics, the above-quoted fluctuation theorems can be derived for any system using a rather unsophisticated mathematics. It is sufficient to invoke a "conjugate" dynamics, typically, but not exclusively, time-reversal, to derive these theorems in a few lines [151]. Going beyond the thermodynamic framework, it turns out that many of the fluctuation theorems hold formally true for any kind of Markovian stochastic dynamics [86].

In the present work we always assume that the system dynamics is stochastic and fulfills the above mentioned dynamical laws. Other approaches, which can be also used to describe the time evolution of the systems in question, are the Hamiltonian dynamics [72] and the thermostated dynamics [63, 66]. In fact, many of the fluctuation theorems were originally derived within these deterministic frameworks. Although sometimes these descriptions are considered to be more fundamental than the stochastic one, for the purposes of this thesis, the stochastic approach provides two crucial advantages. First, contrary to the deterministic descriptions, it allows to describe transitions between discrete states like in (bio)chemical reactions with essentially the same conceptual framework used for the systems with a continuous state space. Second, it allows to focus on the relevant (and measurable) degrees of freedom and ignore the water molecules etc. The possibility of this coarse-graining enables the analytical study of the dynamics of relatively complex systems like biomolecules. Using the deterministic approaches this is possible only numerically. Finally, let us note that some of the fluctuation theorems can be formulated also for open quantum systems [27,58,62]. In this thesis we do not consider quantum systems explicitly, however, the obtained results are directly applicable to open quantum systems whenever quantum coherences, i.e., the role of the non-diagonal elements in the density matrix [39], can be neglected. The dynamics of the driven or open quantum system is then equivalent to a classical stochastic one.

In this thesis we focus on exactly solvable models from the field of stochastic thermodynamics, the basic theoretical concepts of which are reviewed in Chap. 1.

First, in CHAPS. 2 and 3, we consider externally driven mesoscopic systems with both discrete (CHAP. 2) and continuous (CHAP. 3) state space which, moreover, are in contact with a thermal reservoir at a constant temperature. We analytically investigate the dynamics and energetics during the emerging isothermal processes. In particular, we calculate the probability density for work, heat and internal energy. Although, from the theoretical point of view, these results are themselves interesting, they can also help to better utilize the experimental data. For instance, as mentioned above, in many experiments the Jarzynski equality is used in order to extract the equilibrium free energy differences from non-equilibrium stretching experiments [151]. The extracted free energy difference strongly depends on the tail of the work distribution for large negative work values, which correspond to highly improbable realizations of the experiment and hence can not be measured accurately enough. Therefore it is important to use the correct fit (the Jarzynski estimator) of the measured work distribution in order to accurately obtain the tail [138]. Although complicated from the mathematical point of view, the models where the work fluctuations can be treated analytically are often too simple from the physical point of view. More realistic models can be studied using computer simulations, which can also help to find suitable Jarzynski estimators. In APP. C we present a new algorithm which can be used for these simulations.

In the second part of the thesis we focus on periodically driven mesoscopic systems which communicate with two heat reservoirs at different temperatures. During the cyclic process the system can perform a positive mean work on the environment. Such stochastic heat engines have been studied during the last decade [14, 23, 31, 59, 166, 167, 170, 181, 195]. First, in SEC. 1.4, we present a more detailed review of the results obtained in the field and also the basic theoretical concepts needed for the analytical treatment of such stochastic heat engines. Next, in CHAP. 4, we present two exactly solvable models. In the first one we consider a two-state system exposed to a simple two two-branch isothermal driving. Within this setting we derive the probability density for the work performed per operational cycle and we discuss its properties. In the second example we consider a system with a continuous state space, the colloidal particle diffusing in an asymmetric log-harmonic potential. For this system we impose the driving which consists of two isotherms and two adiabatic branches. This setting, in particular, allows us to found the exact form of the protocol which yields the maximum output power of the engine and verify the recent general results concerning the corresponding efficiency [59, 61, 159, 195] reviewed in SEC. 1.4. In the both models we have also discussed the possibility to minimize the power fluctuations. Majority of the available studies concerning stochastic heat engines focus on calculating the mean values of the thermodynamic quantities. Our analysis of the corresponding fluctuations provides new insights into the performance of the engines.

To sum up, the main results of the thesis are given in CHAPS. 2-4 and also in APPS. A-C. Some of them were already published (see the List of Original Publications). Specifically, the zipper model (SEC. 2.4) was published in [93], the sliding parabola model in [94], and the two-level motor (SEC. 4.1) is described in [31, 32]. Finally, the new algorithm for Monte Carlo simulation of stochastic jump processes (APP. C) has been published in [92].

1. Stochastic Thermodynamics

Stochastic thermodynamics is an advancing field with many applications to small systems of current interest [20, 28, 82, 104, 176]. Its brief history is summarized in the Introduction. In this CHAP. we review the basic theoretical concepts involved in this domain. Specifically, in SECS. 1.1 and 1.2, we review the dynamical equations for the mesoscopic systems with discrete and with continuous state space, respectively. Further, in these two SECS. , we present equations which describe fluctuations of work, heat and internal energy of the system during isothermal processes. In SEC. 1.3 we give a short review of the celebrated work fluctuation relations [42–44, 103, 104], which represent a generalization of the second law of thermodynamics. Finally, in SEC. 1.4, we review the recent results in the field of stochastic heat engines and present the theory needed to their analytical description.

1.1 Discrete systems

Let us consider a general N-level system in contact with a thermal reservoir at the temperature T. We assume that the system is driven by an external agent. Let $\mathcal{G}_i = \mathcal{U}_i - k_{\mathrm{B}} T \log \Omega_i$ denote free energy landscape (FEL) of the *system alone*, where $\mathcal{U}_i$ (Ω_i) stands for the energies (degeneracies) of the individual levels and k_{B} is the Boltzmann constant. Moreover, let $\tilde{\mathcal{V}}_i[\boldsymbol{Y}(t)] = \mathcal{V}_i(t)$ denote an additional energy due to the interaction with the external agent. The discrete index $i = 1, 2, \ldots, N$ labels the individual microstates (levels) available to the system and $\boldsymbol{Y}(t)$ stands for a vector of *control parameters* driven by the external agent. The FEL of the *compound system*, $\mathcal{F}_i(t)$, and the energies of its individual levels, $\mathcal{E}_i(t)$, read

$$\mathcal{F}_i(t) = \mathcal{G}_i + \tilde{\mathcal{V}}_i[\boldsymbol{Y}(t)] = \mathcal{G}_i + \mathcal{V}_i(t) , \qquad i = 1, 2, \ldots, N , \tag{1.1}$$

$$\mathcal{E}_i(t) = \mathcal{U}_i + \tilde{\mathcal{V}}_i[\boldsymbol{Y}(t)] = \mathcal{U}_i + \mathcal{V}_i(t) , \qquad i = 1, 2, \ldots, N . \tag{1.2}$$

Note that the external driving can not force the system to follow a specific sequence of microstates. It just influences, through the level free energies, just the transition probabilities between the individual microstates.

1.1.1 Dynamics

At an arbitrary fixed time t, the state of the system is specified by the column vector $\boldsymbol{p}(t)$. The components of this vector $[\boldsymbol{p}(t)]_i = p_i(t)$, $i = 1, \ldots, N$, are the occupation probabilities of the individual microstates (levels), i.e., the probabilities to find the system at the time t in the microstate i.

In many experimentally important situations, the time evolution of the system can be described as a Markov process. Such process is governed by the master equation [187]. The transition rates in the equation depend on the temperature of the bath and on the external parameters which influence the FEL of the system. Since the free energies depend on time, the rates must be time dependent as well. Hence the underlying Markov process is time nonhomogeneous one.

One possible probabilistic approach [33, 35] to the analysis of a continuous time Markov process uses its decomposition into a discrete time Markov chain and a system of random points on the time axis. The transitions between the states of the Markov chain occur just at random instants. Usually, the time intervals between individual transitions are taken as independent exponentially distributed random variables. This decomposition can be used for simple and fast simulations of time nonhomogeneous Markov processes. The details are discussed in App. C.

Formally speaking, the time evolution of the system is described by the time-inhomogeneous Markov process $\mathsf{D}(t)$, where $\mathsf{D}(t) = k$ if the system resides in the microstate k at the time t. The master Eq. can be written as

$$\frac{\mathrm{d}}{\mathrm{d}t}\mathbb{R}(t\,|\,t') = -\nu\mathbb{L}(t)\,\mathbb{R}(t|t') \;, \qquad \mathbb{R}(t'\,|\,t') = \mathbb{1} \;, \tag{1.3}$$

where $\mathbb{1}$ is the $(N \times N)$ unity matrix, $\mathbb{L}(t)$ is the $(N \times N)$ matrix of transition rates, and $\mathbb{R}(t\,|\,t')$ is the $(N \times N)$ matrix of transition probabilities. ν^{-1} sets the elementary time scale. In the limit $\nu \to \infty$ ($\nu \to 0$) the relaxation processes are infinitely fast (slow).

If the transition rates would remain constant, the system should relax towards thermal equilibrium specified by the instantaneous values of the level free energies (1.1). In order to guarantee this behavior it is often assumed that the transition rates fulfill the so called (time local) detail balance condition

$$\exp[-\beta\mathcal{F}_j(t)]L_{ij}(t) = L_{ji}(t)\exp[-\beta\mathcal{F}_i(t)] \;, \tag{1.4}$$

where $\beta = 1/(k_{\mathrm{B}}T)$. The matrix of the transition probabilities, $\mathbb{R}(t\,|\,t')$, is a stochastic matrix [130]. Its elements are given by

$$R_{ij}(t\,|\,t') = \mathrm{Prob}\,\{\,\mathsf{D}(t) = i\,|\,\mathsf{D}(t') = j\,\} \;. \tag{1.5}$$

This means that the matrix $\mathbb{R}(t\,|\,t')$ evolves an arbitrary column vector of the initial occupation probabilities, $\boldsymbol{p}(t')$, as

$$\boldsymbol{p}(t) = \mathbb{R}(t\,|\,t')\,\boldsymbol{p}(t') \;. \tag{1.6}$$

Because this formula is valid for any initial vector $\boldsymbol{p}(t')$, it already suggests that the matrix $\mathbb{R}(t\,|\,t')$ fulfills the Chapman-Kolmogorov condition [78, 187]

$$\mathbb{R}(t\,|\,t') = \mathbb{R}(t\,|\,t'')\,\mathbb{R}(t''\,|\,t') \;. \tag{1.7}$$

Here the matrix multiplication on the right hand side amounts for the summation over the intermediate states at the time t''. This formula is valid for any intermediate time t'' and reflects the Markov property of the underlying stochastic process $\mathsf{D}(t)$.

1.1.2 Energetics

The random internal energy of the system at the time t,

$$\mathsf{U}(t) = \mathcal{E}_{\mathsf{D}(t)}(t) \;, \tag{1.8}$$

changes according to the first law of thermodynamics as

$$\dot{\mathsf{U}}(t)\,\mathrm{d}t = \mathsf{W}(t+\mathrm{d}t,t) + \mathsf{Q}(t+\mathrm{d}t,t) = \\ = \left[\mathcal{E}_{\mathsf{D}(t)}(t+\mathrm{d}t) - \mathcal{E}_{\mathsf{D}(t)}(t)\right] + \left[\mathcal{E}_{\mathsf{D}(t+\mathrm{d}t)}(t) - \mathcal{E}_{\mathsf{D}(t)}(t)\right] \ , \quad (1.9)$$

where we use the abbreviation $\dot{f}(t) = \mathrm{d}f(t)/\mathrm{d}t$. The first (the second) term on the right hand side represents the random work (heat) accepted by the system during the infinitesimal time interval $[t, t+dt]$ [165]. Differently speaking, if the system dwells in the level i during the time interval $[t, t+dt]$ then the work done on the system *by the eternal agent*, $\mathsf{W}(t+\mathrm{d}t,t)$, equals $\mathcal{E}_i(t+dt) - \mathcal{E}_i(t)$ and no heat is accepted. On the other hand if the system changes its microstate from j to i during the infinitesimal time interval $[t, t+dt]$ and the level energies $\mathcal{E}_i(t)$, $\mathcal{E}_j(t)$ remain constant, then the heat accepted by the system *from the thermal environment*, $\mathsf{Q}(t+\mathrm{d}t,t)$, is $\mathcal{E}_i(t) - \mathcal{E}_j(t)$ and no work is done. These definitions are further discussed in detail in Subs. 1.2.3, also see Fig. 1.1.

The random work done on the system by the external agent when the control parameter is altered from $\boldsymbol{Y}(t')$ to $\boldsymbol{Y}(t)$ is

$$\mathsf{W}(t,t') = \int_{t'}^{t} \mathrm{d}t'' \sum_{i=1}^{N} \dot{\mathcal{E}}_i(t'')\delta_{i\mathsf{D}(t'')} \ , \quad (1.10)$$

and represents a *functional* of the stochastic process $\mathsf{D}(t)$. Due to the first law of thermodynamics (1.9), the random heat accepted from the reservoir represents another functional of the process $\mathsf{D}(t)$, specifically

$$\mathsf{Q}(t,t') = \mathsf{U}(t) - \mathsf{U}(t') - \mathsf{W}(t,t') \ . \quad (1.11)$$

For an analytical treatment of work and heat fluctuations it is useful to introduce the *augmented process* $\{\mathsf{W}(t,t'),\, \mathsf{D}(t)\}$ [98, 99, 179] which describes both the work and the microstate variable. This augmented process is again a time nonhomogeneous Markov process and its two-time properties are described by the $(N \times N)$ matrix $\mathbb{G}(w,t\,|\,w',t')$ with the matrix elements

$$G_{ij}(w,t\,|\,w',t') = \frac{1}{\epsilon}\,\mathrm{Prob}\left\{ \begin{array}{c|c} \mathsf{W}(t,0) \in (w, w+\epsilon) & \mathsf{W}(t',0) = w' \\ \mathsf{D}(t) = i & \mathsf{D}(t') = j \end{array} \right\} \ , \quad (1.12)$$

where $\epsilon \to 0$. The time evolution of $\mathbb{G}(w,t\,|\,w',t')$ is given by [98, 99, 179]

$$\frac{\partial}{\partial t}\mathbb{G}(w,t\,|\,w',t') = -\left[\frac{\partial}{\partial w}\,\dot{\mathbb{E}}(t) + \nu\mathbb{L}(t)\right]\,\mathbb{G}(w,t\,|\,w',t') \quad (1.13)$$

with the initial condition $\mathbb{G}(w,t'\,|\,w',t') = \delta(w-w')\,\mathbb{1}$. Here $\dot{\mathbb{E}}(t)$ is the diagonal matrix $\dot{\mathbb{E}}(t) = \mathrm{diag}\{\dot{\mathcal{E}}_1(t), \ldots, \dot{\mathcal{E}}_N(t)\}$. Note that $\mathbb{R}(t\,|\,t') = \int_{-\infty}^{\infty} \mathrm{d}w\, \mathbb{G}(w,t\,|\,0,t')$ and that $\mathbb{G}(w,t\,|\,w',t') = \mathbb{G}(w-w',t\,|\,0,t')$. Eq. (1.13) represents a hyperbolic system of N^2 coupled partial differential equations with time-dependent coefficients. It can be derived in several ways. For example, as explained in reference [100], one considers at the time t the family of all realizations, which display at that time the work in the infinitesimal interval $(w, w+dw)$ and, simultaneously, which occupy a given microstate. During the infinitesimal time interval $(t, t+dt)$, the number of such paths can change due to two reasons. First, while residing in the

given microstate, some paths enter (leave) the set, because the energy levels move and an additional work has been done. Secondly, some paths can enter (leave) the described family, because they jump out of (into) the specified level. These two contributions correspond to the two terms on the right hand side of Eq. (1.13). Another derivation [179] is based on an explicit probabilistic construction of all possible paths and their respective probabilities.

The Chapman-Kolmogorov condition for the augmented process assumes the form

$$\mathbb{G}(w,t\,|\,w',t') = \int_{-\infty}^{\infty} dw''\,\mathbb{G}(w,t\,|\,w'',t'')\,\mathbb{G}(w'',t''\,|\,w',t')\ . \tag{1.14}$$

Here the matrix multiplication on the right hand side amounts for the summation over the intermediate states at the time t'', and the integration runs over all possible intermediate values of the work variable w''. The equation is valid for any intermediate time $t'' \in [t',t]$.

Eqs. (1.3) and (1.13) are exactly solvable only in several cases. Investigations have been conducted for simple spin systems driven by a time-dependent external field [30,31,35,52,90,179]. As a result, analytical solutions are known for several two-level systems [31,35,122,179]. A generalization of these results and also some other exactly solvable models are presented in Chap. 2. Further, in App. A, we discuss the limit of infinitely fast (slow) relaxation ($\nu \to 0,\ \infty$). In these limiting cases Eqs. (1.3) and (1.13) can be solved for any model.

The matrix $\mathbb{G}(w,t\,|\,w',t')$ provides a complete description of the energetics of the process $\mathsf{D}(t)$. The joint probability density for the internal energy $\mathsf{U}(t)$ and the work $\mathsf{W}(t,t')$ performed on the system during the time interval $[t',t]$, given the internal energy initially was u', (regardless of the final state of the system at the time t) is given by

$$\xi(u,w,t;u') = \sum_{i,\,j=1}^{N} \delta\left[u-\mathcal{E}_i(t)\right]\delta\left[u'-\mathcal{E}_j(t')\right]\ G_{ij}(w,t\,|\,0,t')\,p_j(t')\ . \tag{1.15}$$

Here $\delta(x)$ stands for the Dirac δ-function and $p_j(t')$ denotes the initial occupation probabilities. The function $\xi(u,w,t;u')$ already yields the probability density for the work,

$$\rho(w,t) = \int_{-\infty}^{\infty}\mathrm{d}u\ \int_{-\infty}^{\infty}\mathrm{d}u'\ \xi(u,w,t;u')\ . \tag{1.16}$$

An analogous integration over the variables u' and w gives the probability density for the internal energy $\mathsf{U}(t)$,

$$\varsigma(u,t) = \int_{-\infty}^{\infty}\mathrm{d}u'\ \int_{-\infty}^{\infty}\mathrm{d}w\ \xi(u,w,t;u')\ . \tag{1.17}$$

Furthermore, using the definition (1.11), the function $\xi(u,w,t;u')$ gives also the probability density for the heat $\mathsf{Q}(t,t')$ transferred from the reservoir during the time interval $[t',t]$ [31]

$$\chi_(q,t) = \int_{-\infty}^{\infty}\mathrm{d}u\ \int_{-\infty}^{\infty}\mathrm{d}u'\ \int_{-\infty}^{\infty}\mathrm{d}w\ \delta\left[q-(u-u'-w)\right]\ \xi(u,w,t;u')\ . \tag{1.18}$$

The functions (1.16)–(1.18) yield all raw moments of internal energy (1.8), work (1.10) and heat (1.11) by single integration

$$\langle [\mathsf{U}(t)]^n \rangle = \int_{-\infty}^{\infty} \mathrm{d}u\, u^n\, \varsigma(u,t) \ , \tag{1.19}$$

$$\langle [\mathsf{W}(t,t')]^n \rangle = \int_{-\infty}^{\infty} \mathrm{d}w\, w^n\, \rho(w,t) \ , \tag{1.20}$$

$$\langle [\mathsf{Q}(t,t')]^n \rangle = \int_{-\infty}^{\infty} \mathrm{d}q\, q^n\, \chi(q,t) \ . \tag{1.21}$$

Let us note that these moments can be also calculated directly from the definitions (1.8), (1.10), and (1.11) only using the solution of the master Eq. (1.3). This approach is convenient for the internal energy where one can use the identity $\int_{-\infty}^{\infty} \mathrm{d}u\, u^n\, \varsigma(u,t) = \sum_{i=1}^{N} [\mathcal{E}_i(t)]^n p_i(t)$. For the work and the heat the situation is more complicated and this approach is useful only for the first few moments. For example, the mean values of the internal energy, work and heat, are

$$U(t) = \langle \mathsf{U}(t) \rangle = \sum_{i=1}^{N} \mathcal{E}_i(t) p_i(t) \ , \tag{1.22}$$

$$W(t,t') = \langle \mathsf{W}(t,t') \rangle = \sum_{i=1}^{N} \int_{t'}^{t} \mathrm{d}t''\, \dot{\mathcal{E}}_i(t'') p_i(t'') \ , \tag{1.23}$$

$$Q(t,t') = \langle \mathsf{Q}(t,t') \rangle = \sum_{i=1}^{N} \int_{t'}^{t} \mathrm{d}t''\, \mathcal{E}_i(t'') \dot{p}_i(t'') \ . \tag{1.24}$$

In order to calculate the second moments of the work and the heat without the probability densities (1.16) and (1.18), one needs the two-time correlation function

$$\left\langle h_{\mathsf{D}(t)}\, f_{\mathsf{D}(t')} \right\rangle_{\mathrm{C}} = \begin{cases} \sum_{i=1}^{N} \sum_{j=1}^{N} h_i\, f_j R_{ij}(t \,|\, t') p_j(t') \ , & t \geq t' \\ \sum_{i=1}^{N} \sum_{j=1}^{N} f_i\, h_j R_{ij}(t' \,|\, t) p_j(t) \ , & t \leq t' \end{cases} \ . \tag{1.25}$$

The second raw moments of the work (1.10) and the heat (1.11) are then given by

$$\left\langle [\mathsf{W}(t,t')]^2 \right\rangle = \int_{t'}^{t} \mathrm{d}t'' \int_{t'}^{t} \mathrm{d}t''' \left\langle \frac{\partial \mathcal{E}_{\mathsf{D}(t'')}(t'')}{\partial t''} \frac{\partial \mathcal{E}_{\mathsf{D}(t''')}(t''')}{\partial t'''} \right\rangle_{\mathrm{C}} \tag{1.26}$$

and

$$\left\langle [\mathsf{Q}(t,t')]^2 \right\rangle = \left\langle [\mathsf{W}(t,t')]^2 \right\rangle + \sum_{i,\,j=1}^{N} \left[\mathcal{E}_i(t) - \mathcal{E}_j(t')\right]^2 R_{ij}(t \,|\, t') p(t') -$$

$$- 2 \sum_{i,\,j,\,k=1}^{N} \left[\mathcal{E}_i(t) - \mathcal{E}_k(t')\right] \int_{t'}^{t} \mathrm{d}t'' \frac{\partial \mathcal{E}_{\mathsf{D}(t'')}(t'')}{\partial t''} R_{ij}(t \,|\, t'') R_{jk}(t'' \,|\, t') p_k(t') \ , \tag{1.27}$$

where $\partial \mathcal{E}_{\mathsf{D}(t)}(t)/\partial t \equiv \mathrm{d}\mathcal{E}_i(t)/\mathrm{d}t|_{i=\mathsf{D}(t)}$. Obviously, in order to obtain the higher moments of the work and the heat, the higher time correlation functions must

be defined and the resulting expressions become too complicated. Finally, let us define the variances of internal energy, heat and work which corresponds to the widths of the individual probability densities

$$[\Delta U(t)]^2 = \left\langle [\mathsf{U}(t)]^2 \right\rangle - [U(t)]^2 \ , \tag{1.28}$$

$$[\Delta W(t,t')]^2 = \left\langle [\mathsf{W}(t,t')]^2 \right\rangle - [W(t,t')]^2 \ , \tag{1.29}$$

$$[\Delta Q(t,t')]^2 = \left\langle [\mathsf{Q}(t,t')]^2 \right\rangle - [Q(t,t')]^2 \ . \tag{1.30}$$

The entropy of the system at the time t is given by the standard formula [165]

$$S_{\mathrm{s}}(t) = -k_{\mathrm{B}} \sum_{i=1}^{N} p_i(t) \log \left[p_i(t) \right] \ . \tag{1.31}$$

Its increment during the time interval $[t', t]$

$$S_{\mathrm{s}}(t,t') = S_{\mathrm{s}}(t) - S_{\mathrm{s}}(t') \ , \tag{1.32}$$

together with the entropy transfered to the reservoirs during the time interval $[t', t]$

$$S_{\mathrm{r}}(t,t') = -\frac{Q(t,t')}{T} \ , \tag{1.33}$$

determines the total entropy produced during the time interval $[t', t]$

$$S_{\mathrm{tot}}(t,t') = S_{\mathrm{s}}(t,t') + S_{\mathrm{r}}(t,t') \geq 0 \ . \tag{1.34}$$

1.2 Continuous systems

Consider an externally driven one dimensional microscopic system in contact with a thermal reservoir at the temperature T. Let $\mathcal{G}(x) = \mathcal{U}(x) - k_{\mathrm{B}} T \log \Omega(x)$ denote the FEL of the system alone, where $\mathcal{U}(x)$ denotes the energy of the xth microstate and $\Omega(x)$ stands for its multiplicity. Moreover, let $\tilde{\mathcal{V}}\left[x, \boldsymbol{Y}(t)\right] = \mathcal{V}(x,t)$ denote an additional energy due to the interaction with the external agent. The continuous index $x \in (-\infty, \infty)$ labels the individual microstates available to the system and $\boldsymbol{Y}(t)$ stands for the vector of the parameters controlled by the external agent. As in the discrete case, the external driving can not force the system to follow a specific sequence of microstates. It just influences, through the FEL, the transition probabilities between the individual microstates. The FEL, $\mathcal{F}(x,t)$, and the energy landscape, $\mathcal{E}(x,t)$, of the compound system read

$$\mathcal{F}(x,t) = \mathcal{G}(x) + \tilde{\mathcal{V}}\left[x, \boldsymbol{Y}(t)\right] = \mathcal{G}(x) + \mathcal{V}(x,t) \ , \tag{1.35}$$

$$\mathcal{E}(x,t) = \mathcal{U}(x) + \tilde{\mathcal{V}}\left[x, \boldsymbol{Y}(t)\right] = \mathcal{U}(x) + \mathcal{V}(x,t) \ . \tag{1.36}$$

Two examples of such setting are depicted in Figs. 3.1 and 3.2 and further discussed in Sec. 3.1.

1.2.1 Dynamics

In the present work we assume that the thermal forces can be described as the sum of the linear friction force and the Langevine white-noise force. We neglect the inertial forces. Then the equation of motion for the particle position (microstate of the system) is the stochastic diferential equation [78, 147, 187]

$$\Gamma \frac{\mathrm{d}}{\mathrm{d}t}\mathsf{X}(t) = -\frac{\partial}{\partial x}\mathcal{F}(x,t)\bigg|_{x=\mathsf{X}(t)} + \mathsf{N}(t) \ , \tag{1.37}$$

with initial condition $\mathsf{X}(t') = x'$. In Eq. (1.37) Γ stands for the particle mass times the viscous friction coefficient, and $\mathsf{N}(t)$ represents the delta-correlated white noise, $\langle \mathsf{N}(t)\mathsf{N}(t')\rangle = 2D\Gamma^2\,\delta(t-t')$. Here $D = k_{\mathrm{B}}T/\Gamma$ denotes the diffusion constant. The Fokker-Planck equation corresponding to the stochastic differential equation (1.37) is [78, 147, 187]

$$\frac{\partial}{\partial t}R(x,t\,|\,x',t') = \left\{ D\,\frac{\partial^2}{\partial x^2} + \frac{1}{\Gamma}\frac{\partial}{\partial x}\left[\frac{\partial}{\partial x}\mathcal{F}(x,t)\right]\right\} R(x,t\,|\,x',t') \ , \tag{1.38}$$

with the initial condition $R(x,t'\,|\,x',t') = \delta(x-x')$. The conditional probabilities $R(x,t\,|\,x',t')\,\mathrm{d}x$ play the same role as the matrix elements (1.5) for the discrete process $\mathsf{D}(t)$. More precisely, the function $R(x,t\,|\,x',t')$ evolves an arbitrary initial probability distribution $p(x,t')$ as

$$p(x,t) = \int_{-\infty}^{\infty} \mathrm{d}x'\, R(x,t\,|\,x',t')\,p(x',t') \ . \tag{1.39}$$

The function $p(x,t)$ specifies the state of the system at the time t. Concretely, the probability to find the system at the time t in a microstate which lies in an infinitesimal neighborhood of the microstate x reads $p(x,t)\,\mathrm{d}x$, or, mathematically, $\mathrm{Prob}\{\mathsf{X}(t) \in (x, x+\mathrm{d}x)\} = p(x,t)\,\mathrm{d}x$.

This setting represents a continuous analogy of the discrete one described in Sec. 1.1. However, it should be noted that the master Eq. formulation is more general than the continuous one, including the Langevin and Fokker-Planck cases as its special limits [78, 187]. The matrix multiplication (summation over the microstates) in the discrete model is now represented by x-integration. For example the Champan-Kolmogorov Eq. (1.7) presently assumes the form

$$R(x,t\,|\,x',t') = \int_{-\infty}^{\infty} \mathrm{d}x'' R(x,t\,|\,x'',t'')R(x'',t''\,|\,x',t') \ . \tag{1.40}$$

1.2.2 Energetics

The random internal energy of the system at the time t,

$$\mathsf{U}(t) = \mathcal{E}[\mathsf{X}(t),t] \ , \tag{1.41}$$

changes according to the first law of thermodynamics (1.11) as

$$\begin{aligned}\dot{\mathsf{U}}(t)\,\mathrm{d}t &= \mathsf{W}(t+\mathrm{d}t,t) + \mathsf{Q}(t+\mathrm{d}t,t) = \\ &= \{\mathcal{E}[\mathsf{X}(t),t+\mathrm{d}t] - \mathcal{E}[\mathsf{X}(t),t]\} + \{\mathcal{E}[\mathsf{X}(t+\mathrm{d}t),t] - \mathcal{E}[\mathsf{X}(t),t]\} \ .\end{aligned} \tag{1.42}$$

The first (the second) term on the right hand side corresponds to the random work (heat) accepted by the system during the infinitesimal time interval $[t, t+dt]$ [165]. Differently speaking, if the system dwells at the position x during the time interval $[t, t+dt]$ then the work done on the system by the eternal agent, $\mathsf{W}(t+\mathrm{d}t, t)$, equals $\mathcal{E}(x, t+dt) - \mathcal{E}(x, t)$ and no heat is accepted. On the other hand if the system changes its position from x' to x during the infinitesimal time interval $[t, t+dt]$ and the energies $\mathcal{E}(x, t)$, $\mathcal{E}(x', t)$ remain constant, then the heat accepted by the system from the thermal environment, $\mathsf{Q}(t+\mathrm{d}t, t)$, is $\mathcal{E}(x, t) - \mathcal{E}(x', t)$ and no work is done.

As a result the random work satisfies the stochastic differential equation [167]

$$\frac{\mathrm{d}}{\mathrm{d}t}\mathsf{W}(t, t') = \frac{\partial}{\partial t}\mathcal{E}[\mathsf{X}(t), t] \equiv \frac{\mathrm{d}}{\mathrm{d}t}\mathcal{E}(x, t)\bigg|_{x=\mathsf{X}(t)} \tag{1.43}$$

with the initial condition $\mathsf{W}(t', t') = 0$. Although this work definition, which we use in the whole thesis, naturally stems from the stochastic thermodynamic definition (1.10), it recently raised a heated discussion in the literature [140, 188, 189, 197] and an alternative work definition was proposed [188]. This question is discussed in detail in Subs. 1.2.3.

The random work done on the system by the external agent when the control parameter is altered from $\boldsymbol{Y}(t')$ to $\boldsymbol{Y}(t)$ reads

$$\mathsf{W}(t, t') = \int_{t'}^{t} \mathrm{d}t'' \int_{-\infty}^{\infty} \mathrm{d}x\, \dot{\mathcal{E}}(x, t'')\delta[x - \mathsf{X}(t'')] \ . \tag{1.44}$$

It represents a functional of the process $\mathsf{X}(t)$. Due to the first law of thermodynamics (1.42) the random heat accepted from the reservoir corresponds to another functional of the process $\mathsf{X}(t)$. This functional is given by (1.11).

The Fokker-Planck equation corresponding to the stochastic differential equations (1.37) and (1.43) reads [147, 187]

$$\frac{\partial}{\partial t}G(x, w, t \,|\, x', w', t') = \left\{ D\,\frac{\partial^2}{\partial x^2} + \frac{1}{\Gamma}\frac{\partial}{\partial x}\left[\frac{\partial}{\partial x}\mathcal{F}(x, t)\right] - \right. \\ \left. - \dot{\mathcal{E}}(x, t)\frac{\partial}{\partial w}\right\} G(x, w, t \,|\, x', w', t') \ , \tag{1.45}$$

with the initial condition $G(x, w, t' \,|\, x', w', t') = \delta(x - x')\delta(w - w')$. The conditional probabilities $G(x, w, t \,|\, x', w', t')\,\mathrm{d}x\,\mathrm{d}w$ play similar role for the continuous process $\mathsf{X}(t)$ as the matrix elements (1.12) for the discrete process $\mathsf{D}(t)$.

Specifically, if we define the function $\xi(u, w, t; u')$ as

$$\xi(u, w, t; u') = \int_{-\infty}^{\infty}\int_{-\infty}^{\infty} \mathrm{d}x\,\mathrm{d}x'\,\delta\left[u - \mathcal{E}(x, t)\right] \times \\ \times\, \delta\left[u' - \mathcal{E}(x', t')\right]\, G(x, w, t \,|\, x', 0, t')\, p(x', t') \ . \tag{1.46}$$

the definitions (1.16)-(1.21) remain valid. In analogy with the discrete model the moments of the random variables in question can be also calculated from the definitions (1.41), (1.44), and (1.11) only using the solution of Eq. (1.38). One just substitutes the continuous variables in the formulas in question for their discrete

equivalents and change the summations to the integrations. The raw moments of the internal energy are now given by $\int_{-\infty}^{\infty} \mathrm{d}u\, u^n \varsigma(u,t) = \int_{-\infty}^{\infty} \mathrm{d}x\, [\mathcal{E}(x,t)]^n p(x,t)$. The mean values of the internal energy, the work and the heat (1.22)-(1.24) now read

$$U(t) = \langle \mathsf{U}(t) \rangle = \int_{-\infty}^{\infty} \mathrm{d}x\, \mathcal{E}(x,t) p(x,t) \;, \tag{1.47}$$

$$W(t,t') = \langle \mathsf{W}(t,t') \rangle = \int_{-\infty}^{\infty} \mathrm{d}x \int_{t'}^{t} \mathrm{d}t''\, \dot{\mathcal{E}}(x,t'') p(x,t'') \;, \tag{1.48}$$

$$Q(t,t') = \langle \mathsf{Q}(t,t') \rangle = \int_{-\infty}^{\infty} \mathrm{d}x \int_{t'}^{t} \mathrm{d}t''\, \mathcal{E}(x,t'') \dot{p}(x,t'') \;. \tag{1.49}$$

Similarly, the second moment of the work (1.26) is given by

$$\left\langle [\mathsf{W}(t,t')]^2 \right\rangle = \int_{t'}^{t} \mathrm{d}t'' \int_{t'}^{t} \mathrm{d}t''' \left\langle \frac{\partial \mathcal{E}[\mathsf{X}(t''),t'']}{\partial t''} \frac{\partial \mathcal{E}[\mathsf{X}(t'''),t''']}{\partial t'''} \right\rangle_{\mathrm{C}} \;, \tag{1.50}$$

with the two-time correlation function defined as

$$\begin{aligned} &\langle h[\mathsf{X}(t)]\, f[\mathsf{X}(t')] \rangle_{\mathrm{C}} = \\ &\quad = \begin{cases} \int_{-\infty}^{\infty} \mathrm{d}x \int_{-\infty}^{\infty} \mathrm{d}x'\, h(x)\, f(x') R(x,t \,|\, x',t') p(x',t') \;, & t \geq t' \\ \int_{-\infty}^{\infty} \mathrm{d}x \int_{-\infty}^{\infty} \mathrm{d}x'\, f(x)\, h(x') R(x,t' \,|\, x',t) p(x',t) \;, & t \leq t' \end{cases} \;. \end{aligned} \tag{1.51}$$

The entropy of the system at the time t is given by the standard formula [165]

$$S_{\mathrm{s}}(t) = -k_{\mathrm{B}} \int_{-\infty}^{\infty} \mathrm{d}x\, p(x,t) \log [p(x,t)] \;. \tag{1.52}$$

Its increase during the time interval $[t',t]$, $S_{\mathrm{s}}(t,t')$, the entropy $S_{\mathrm{r}}(t,t')$ transfered to the reservoirs during the time interval $[t',t]$ and the total entropy produced during the time interval $[t',t]$, $S_{\mathrm{tot}}(t,t')$, are given by Eqs. (1.32)-(1.34).

As in the discrete case, Eqs. (1.38) and (1.45) can be solved analytically only for few simple settings. Examples can be found in the works [11, 125, 152]. In Chap. 3 we present a generic exactly solvable model – the sliding parabola model. Another exactly solvable model is discussed in Sec. 4.2.

1.2.3 On the work definition

Recently, an extensive criticism of the work definition has been raised (1.44) [188, 189]. The objections against the definition presented in [188] are:

- The work (1.44) done during a quasi-static process does not equal the free energy change of the system itself.
- After a gauge transformation $\mathcal{F}(x,t) \to \mathcal{F}(x,t) + g(t)$, $\mathcal{E}(x,t) \to \mathcal{E}(x,t) + g(t)$ one obtains a transformed system which possess the same dynamics as the original one, however, the work (1.44) done on the transformed system and that done on the original differ.

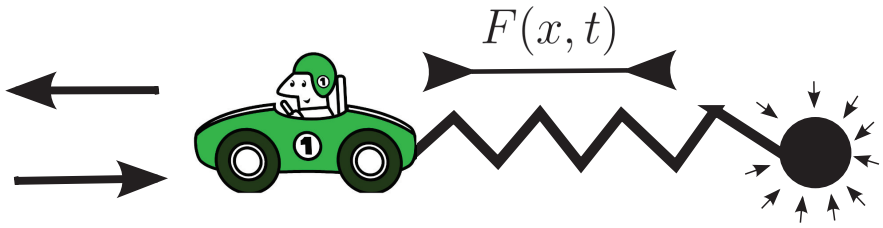

FIG. 1.1: Sketch illustrating the meaning of thermodynamic work (1.44) and that of the mechanical work (1.53).

- The work should be defined in the traditional mechanical way as (force $\times$ displacement). Using this definition, the random work done on the system by the external agent when the control parameter is altered from $\boldsymbol{Y}(t')$ to $\boldsymbol{Y}(t)$ reads [1]

$$\mathsf{W}_{\mathrm{E}}(t,t') = -\int_{t'}^{t} \mathrm{d}t'' \, \frac{\partial}{\partial x}\mathcal{V}\left(x,t''\right)\Big|_{x=\mathsf{X}(t'')} \frac{\mathrm{d}\mathsf{X}(t'')}{\mathrm{d}t''} \;, \tag{1.53}$$

  where $-\partial\mathcal{V}(x,t)/\partial x = F(x,t)$ denotes the force applied on the system by the external agent. The work (1.53) done during a quasi-static process equals the free energy change of the system itself and is gauge invariant.

The papers [27, 140, 197] explain that the controversies caused by the above objections can be easily resolved. To this end we compare the the two work definitions on a specific, simple, example.

The thermodynamic work represents the work done by the external agent on the compound system system-interaction [74, 140, 161]. As an example consider the situation depicted in FIG. (1.1). The microscopic system (the black ball) is driven by an external agent (the car). The interaction between the car and the ball is realized by the spring with zero unloaded length, which contains the interaction energy $\mathcal{V}(x,t)$ and acts on the ball (car) by the force $F(x,t)$ $[-F(x,t)]$. The ball is surrounded by thermal environment and the impacts of its molecules (small arrows) can cause that the ball moves against the force applied. In such case the energy of the impacts [the heat (1.11)] is stored in the spring and the internal energy of the compound system (ball-spring), $\mathcal{E}(x,t)$, increases. If the spring moves the ball, its kinetic energy immediately dissipates into the environment. Part of the energy $\mathcal{E}(x,t)$ is transfered as heat (1.11) into the bath. Another way how to increase (decrease) the energy $\mathcal{E}(x,t)$ is to drive the car [externally manipulate with the interaction potential $\mathcal{V}(x,t)$]. Assume that the impacts of the molecules from the environment cause the ball to stand still. If one drives the car to the left, the spring must be stretched and the work (1.44) is done on the compound system [$\mathcal{E}(x,t)$ increases and the petrol is consumed]. However, if one drives to the right, the spring pulls the car and the compound system does the work (1.44) on the car [$\mathcal{E}(x,t)$ decreases and one can store the energy in an accumulator].

Contrary to the thermodynamic work (1.44), the mechanical work (1.53) describes the work done by the external agent on the system itself [74, 140, 161].

[1] Note that the generalization of this definition for the discrete models is not very natural, because, in such case, one has to substitute a finite difference for the position derivative in the force definition.

Consider again the situation depicted in FIG. (1.1). If the ball moves towards the car, the energy $\mathcal{E}(x,t)$ decreases at the expense of the ball kinetic energy which is quickly (immediately) transfered as heat into the bath. The work (1.53) is done on the ball by the spring, it causes its movement against the friction. Similarly, if the distance between the ball and the car decreases the heat is transfered into the spring and the ball (the thermal environment via the ball) does the work on the spring.

From the last two paragraphs one can deduce that the work definition (1.53) is similar to the definition of heat (1.11). Indeed the mechanical work can be rewritten as

$$\mathsf{W}_{\mathrm{E}}(t,t') = -\mathcal{V}\left[\mathsf{X}(t),t\right] + \mathcal{V}\left[\mathsf{X}(t'),t'\right] + \mathsf{W}(t,t') \tag{1.54}$$

and thus, using EQS. (1.11) and (1.36), we have $\mathsf{W}_{\mathrm{E}}(t,t') = \mathcal{U}\left[\mathsf{X}(t)\right] - \mathcal{U}\left[\mathsf{X}(t')\right] - \mathsf{Q}(t,t')$. For freely diffusing particle $[\mathcal{U}(x)=0]$ the mechanical work thus equals the (minus) heat transfered from the compound system to the thermal environment, $\mathsf{W}_{\mathrm{E}}(t,t') = -\mathsf{Q}(t,t')$. This is not surprising. If one neglects the inertia and sets $\mathcal{U}(x)=0$, the only agent which protects the system from moving freely (without consuming work) is the thermal environment.

In [105] the thermodynamic work (1.44) is referred to as the *inclusive work*. Similarly, the mechanical work (1.53) was called the *exclusive work*. The reason for these terms is the following. During a quasi-static isothermal process the inclusive work is trajectory independent and it equals the change of the Helholtz free energy $F(t)$ of the system described by the full free energy landscape (1.35), i.e.,

$$\left[\mathsf{W}(t,t')\right]_{\mathrm{eq}} = \Delta F(t,t') = F(t) - F(t') = -\frac{1}{\beta}\ln\frac{Z(t)}{Z(t')}\ , \tag{1.55}$$

where $F(t) = -\ln[Z(t)]/\beta$ and the partition function $Z(t)$ reads

$$Z(t) = \int_{-\infty}^{\infty} \mathrm{d}x\, \exp\left[-\beta\mathcal{F}\left(x,t\right)\right]\ . \tag{1.56}$$

The free energy obtained from the inclusive work thus *includes* the terms which stem from the interaction with the external agent. A general proof is presented for example in [140] a proof using EQ. (1.13) for discrete systems is presented in APP. A. The gauge transormation $\mathcal{F}(x,t)+g(t)$ changes the quasi-static work as $[\mathsf{W}(t,t')]_{\mathrm{eq}} \to [\mathsf{W}(t,t')]_{\mathrm{eq}} + g(t) - g(t')$ and the free energy difference as $\Delta F(t,t') \to \Delta F(t,t') + g(t) - g(t')$, indeed. However, the possibility to insert a function $g(t)$ into $\mathcal{F}(x,t)$ is not unphysical – the work can be done on the system without changing its dynamics. For instance the function $g(t)$ may represent an energy input which is the same for all microstates of the system. Consider that the one dimensional microscopic system from FIG. 1.1 is putted into an elevator placed in a gravitational field. If one neglects the inertial effects, the energy flow into the system caused by the elevator movement up and down would be described exactly by the gauge therm $g(t)$.

From EQ. (1.54) one can see that the exclusive work done during a quasi-static isothermal process equals $\left[\mathsf{W}_{\mathrm{E}}(t,t')\right]_{\mathrm{eq}} = -\mathcal{V}\left[\mathsf{X}(t),t\right] + \mathcal{V}\left[\mathsf{X}(t'),t'\right] + \Delta F(t)$. Note that, in contrary to the equilibrium inclusive work, $\left[\mathsf{W}_{\mathrm{E}}(t,t')\right]_{\mathrm{eq}}$ still depends on the random initial and final states of the system, $\mathsf{X}(t)$ and $\mathsf{X}(t')$. Nevertheless, its average value equals to the increase of the free energy $F_0(t,t')$ of the system

alone, i.e.,

$$\left\langle [\mathsf{W}_{\mathrm{E}}(t,t')]_{\mathrm{eq}} \right\rangle = \Delta F(t) - \int_{-\infty}^{\infty} \mathrm{d}x\, \mathcal{V}(x,t) \frac{\exp[-\beta \mathcal{F}(x,t)]}{Z(t)} + \\ + \int_{-\infty}^{\infty} \mathrm{d}x\, \mathcal{V}(x,t') \frac{\exp[-\beta \mathcal{F}(x,t')]}{Z(t')} = F_0(t) - F_0(t') = \Delta F_0(t,t') \ , \quad (1.57)$$

where the free energy of the unperturbed system at the time t reads

$$F_0(t) = \mathcal{G}\big(\langle [\mathsf{X}(t)]_{\mathrm{eq}} \rangle \big) \ . \quad (1.58)$$

Here $\langle [\mathsf{X}(t)]_{\mathrm{eq}} \rangle$ stands for the mean equilibrium state of the system corresponding to the instantaneous FEL $\mathcal{F}(x,t)$. It is given by

$$\langle [\mathsf{X}(t)]_{\mathrm{eq}} \rangle = \int_{-\infty}^{\infty} \mathrm{d}x\, x \frac{\exp[-\beta \mathcal{F}(x,t)]}{Z(t)} \ . \quad (1.59)$$

The free energy obtained from the exclusive work thus *excludes* the terms which stem from the interaction with the external agent and therefore it is also invariant with respect to the gauge transformation $\mathcal{F}(x,t) + g(t)$.

Let us stress that the both equilibrium works can be used for measuring the free energy differences between the states of the system alone, $\Delta F_0(t)$. The average equilibrium exclusive work is exactly $\Delta F_0(t,t')$. The average equilibrium inclusive work yields the free energy difference of the compound system, $\Delta F(t,t')$, which translates to $\Delta F_0(t,t')$ as

$$\Delta F_0(t,t') = -\mathcal{V}\left(\langle [\mathsf{X}(t)]_{\mathrm{eq}} \rangle , t \right) + \mathcal{V}\left(\langle [\mathsf{X}(t')]_{\mathrm{eq}} \rangle , t' \right) + \Delta F(t,t') \ . \quad (1.60)$$

The formula (1.60) can be used once one knows the correct form of the interaction energy $\mathcal{V}(x,t)$. However, in most experimentally relevant situations this function is known indeed. In Sec. 3.1 we illustrate the connection between the exclusive and inclusive work in the form of a specific, physically relevant, model.

1.3 Work fluctuation relations

Investigation of dynamics and thermodynamics of mesoscopic systems under influence of (external) time dependent forces is of great interest over last two decades [24, 150]. As we mentioned in the Introduction, one of the most interesting theoretical result in this field was the discovery of the so called fluctuation theorems [56, 86, 104, 151, 151, 153, 154, 160]. General relations depicting time-irreversibility of various non-equilibrium stochastic processes occurring in microscopic systems exposed to non-equilibrium conditions, such as entropy production [22, 43, 57, 71, 87, 112, 163–165] and work done on the environment [11, 105, 113, 151, 165].

In this Sec. , we focus on the theorems involving the two work definitions (1.44) and (1.53) presented in Sec. 1.2 [2]. The two works represent different random variables and hence they possess different probability densities [105].

[2] In this Sec. , we use the notation introduced in Sec. 1.2 for the continuous models, nevertheless the results remains valid also for the discrete models described in Sec. 1.1, indeed.

Fluctuation theorems for the thermodynamic work (1.44) are studied in detail for last two decades [11, 113, 151, 165]. The most important results in the field are Jarzynski equality [104, 151]

$$\langle \exp\left[-\beta\, \mathsf{W}(t,t')\right]\rangle = \exp\left[\,-\beta \Delta F(t,t')\right] \tag{1.61}$$

and Crooks fluctuation theorem [42–44]

$$\frac{\rho_{\rm F}(w)}{\rho_{\rm R}(-w)} = \exp\left\{-\beta\big[\Delta F(t,t') - w\big]\right\}\ . \tag{1.62}$$

The average on the right-hand side of Eq. (1.61) is taken over the work distribution (1.16) given that the system is initially in equilibrium, i.e., $p(x,t') = \pi(x,t') = \exp\left[-\beta \mathcal{F}(x,t')\right]/Z(t')$. In Eq. (1.62) this work distribution is denoted as $\rho_{\rm F}(w)$. By the subscript F (*forward*) we stress that the externally controlled parameters are driven from $\boldsymbol{Y}(t')$ to $\boldsymbol{Y}(t)$, $t' < t$. $\rho_{\rm R}(w)$ in Eq. (1.62) stands for the work probability distribution for the *time-reversed* process. Here the externally controlled parameters are driven from $\boldsymbol{Y}(t)$ to $\boldsymbol{Y}(t')$ and the system starts from the equilibrium state corresponding to the FEL of the compound system at the time t, $\mathcal{F}(x,t)$. The free energy difference $\Delta F(t,t')$ in Eqs. (1.61) and (1.62) is given by (1.55). The only assumption needed for validity of Eqs. (1.61) and (1.62) is the microscopic reversibility of the underlying dynamics. The discrete models (Sec. 1.1) are reversible if the detailed balance condition (1.4) is fulfilled. The time-reversibility for the continuous models is already incorporated in the Langevin Eq. (1.37). The theorems (1.61) and (1.62) represent an elegant refinement of the second law of thermodynamics. For example, using Jensen's inequality, the well known form of the second law, $\Delta F(t,t') \leq W(t,t')$, follows from Eq. (1.61). Note that Eq. (1.61) is a corollary of Eq. (1.62), but not vice versa.

Equivalent fluctuation theorems for the mechanical work (1.53) were discovered nearly three decades earlier [16, 17, 105, 161]

$$\langle \exp\left[-\beta\, \mathsf{W}_E(t,t')\right]\rangle = 1\ , \tag{1.63}$$

$$\frac{\bar{\rho}_{\rm F}(w)}{\bar{\rho}_{\rm R}(-w)} = \exp(\beta w)\ . \tag{1.64}$$

Here the average in Eq. (1.63) is taken over the probability density for the work (1.53) given that the system starts at the time t' from the state $\bar{\pi}(x) = \exp\left[-\beta \mathcal{G}(x)\right]/Z_0$, $Z_0 = \int_{-\infty}^{\infty} {\rm d}x\, \exp\left[-\beta \mathcal{G}(x)\right]$, the thermal equilibrium state corresponding to the FEL of the unperturbed system, $\mathcal{G}(x)$. This probability density is in Eq. (1.64) denoted by $\bar{\rho}_{\rm F}$. The subscripts F and R have the same meaning as in Eq. (1.62) with the difference that the system starts the reversed process again from the state $\bar{\pi}(x)$.

The theorems for the thermodynamic work (1.44) relate, different from the theorems for the mechanical work (1.53), the work done during a *non-equilibrium* process (easy to measure experimentally) to the increase of the *equilibrium* free energy of the compound system (sometimes hard to measure experimentally), and thus they received much more attention in the literature. The obtained free energy difference $\Delta F(t,t')$ can be interesting in itself or can be used for calculating the increment of the free energy of the unperturbed system, $\Delta F_0(t,t')$, via Eq. (1.60).

Moreover, another generalization of Eq. (1.61) allows the reconstruction of the whole FEL of the unperturbed system, $G(z)$, using the work measurements. This result is called Hummer-Szabo relation and reads [97]

$$Z(t') \exp\left\{\beta\, \tilde{\mathcal{V}}[z, \boldsymbol{Y}(t)]\right\} \, \langle \delta[\mathsf{X}(t) - z] \exp[-\beta\, \mathsf{W}(t,t')]\rangle = \exp[-\beta\, \mathcal{G}(z)] \ . \quad (1.65)$$

The knowledge of $\mathcal{G}(z)$ allows to calculate the equilibrium free energy differences $\Delta F(t,t')$ and $\Delta F_0(t,t')$ from their definitions (1.55) and (1.58). Here we have to stress that there exist also different, and often more accurate, methods which allow to obtain $\mathcal{G}(z)$ etc experimentally. One possibility is to measure the time which the system needs to leave the individual microstates (survival probability), see, for example, [129, 135].

Validity of the equalities (1.61), (1.62) and (1.65) was confirmed in various theoretical models [31, 45, 125], in many experiments [15, 40, 80, 117] and also in numerous numerical simulations [92, 193]. They can be derived for thermostated reversible deterministic systems [171], and also for microscopically reversible stochastic dynamics using both the Langevin equation [43], and the Master equation formulation [151]. In single-molecule experiments [123], all the relations (1.61), (1.62) and (1.65) are used for reconstructing free energy profiles of biomolecules [40,117]. Influence of the experimental errors originating both from the instrument noise and from the uncertainty of measurements on the free energy difference estimate was studied in [25, 124]. It was found that the obtained free-energy difference is correct if the stochastic errors are statistically the same for the conjugate forward and reverse protocols [124], cf. the example in App. C. The discussion about the correct work definition also occurred in the field of fluctuation relations [3, 105]. The result is that the correct work definition, which fulfills the experimentally useful fluctuation theorems (1.61), (1.62) and (1.65), is the definition of the thermodynamic work (1.44).

In order to close this Sec. let us note that the *integral* fluctuation theorems (1.61), (1.63) and (1.65) can be immediately derived from the single relation [165]

$$\left\langle \exp\left[\frac{-\mathsf{S}_{\mathrm{r}}(t,t')}{k_{\mathrm{B}}}\right] \frac{p_{\mathrm{B}}(x)}{p_{\mathrm{F}}(x)} \right\rangle = 1 \ , \quad (1.66)$$

where

$$\mathsf{S}_{\mathrm{r}}(t,t') = -\frac{\mathsf{Q}(t,t')}{T} \quad (1.67)$$

is the (random) entropy transfered from the system into the thermal environment during the time interval $[t', t]$ and the auxiliary function $p_{\mathrm{B}}(x)$ fulfills the normalization condition $\int_{-\infty}^{\infty} \mathrm{d}x\, p_{\mathrm{B}}(x) = 1$. The average in Eq. (1.66) is taken over all trajectories of the stochastic process $\mathsf{X}(t)$ that depart at the time t' with an arbitrary probability $p_{\mathrm{F}}(x)\,\mathrm{d}x$ from the position that lies in the infinitesimal interval $(x, x + \mathrm{d}x)$. The values of the arbitrary functions $p_{\mathrm{B}}(x)$ and $p_{\mathrm{F}}(x)$ that yield the individual relations (1.61), (1.63) and (1.65) are given in Tab. 1.1. Even more general formula, which contains *all* the presented fluctuation relations, was derived by Harris [86].

Eq.	$p_{\mathrm{F}}(x)$	$p_{\mathrm{B}}(x)$
(1.61)	$\dfrac{\exp\left[-\beta\mathcal{F}(x,t')\right]}{\int_{-\infty}^{\infty}\mathrm{d}x\,\exp\left[-\beta\mathcal{F}(x,t')\right]}$	$\dfrac{\exp\left[-\beta\mathcal{F}(x,t)\right]}{\int_{-\infty}^{\infty}\mathrm{d}x\,\exp\left[-\beta\mathcal{F}(x,t)\right]}$
(1.63)	$\dfrac{\exp\left[-\beta\mathcal{G}(x)\right]}{\int_{-\infty}^{\infty}\mathrm{d}x\,\exp\left[-\beta\mathcal{G}(x)\right]}$	$\dfrac{\exp\left[-\beta\mathcal{G}(x)\right]}{\int_{-\infty}^{\infty}\mathrm{d}x\,\exp\left[-\beta\mathcal{G}(x)\right]}$
(1.65)	$\dfrac{\exp\left[-\beta\mathcal{F}(x,t')\right]}{\int_{-\infty}^{\infty}\mathrm{d}x\,\exp\left[-\beta\mathcal{F}(x,t')\right]}$	$\delta\left[\mathsf{X}(t)-z\right]\dfrac{\exp\left\{-\beta\mathcal{F}\left[\mathsf{X}(t),t\right]\right\}}{\exp\left[-\beta\mathcal{F}(z,t)\right]}$

Tab. 1.1: The values of the arbitrary functions $p_{\mathrm{F}}(x)$ and $p_{\mathrm{B}}(x)$ that yield the individual relations (1.61), (1.63) and (1.65) from Eq. (1.66)

1.4 Heat engines

One of the hot topics in the field of stochastic thermodynamics are stochastic heat engines [14, 23, 31, 59, 61, 159, 166, 167, 170, 181, 195]. The variety of models can be roughly classified according to the dynamical laws involved. In the case of the classical stochastic heat engines, the state space can either be discrete [6, 31, 60, 166, 195] or continuous [14, 23, 159, 166, 170, 195]. Examples of the quantum heat engines are studied, e.g., in [1, 4, 89, 146].

In the present work we consider periodically operating classical stochastic heat engines which communicate with two baths at the temperatures T_+ and T_-. Let t_{p} denote the duration of one operational cycle, $W_{\mathrm{out}} \equiv -W(t_{\mathrm{p}},0)$ stands for the (mean) work performed by the engine during one period and

$$Q_{\mathrm{in}} = \int_0^{t_{\mathrm{p}}} \mathrm{d}t\, \frac{\mathrm{d}Q(t,0)}{\mathrm{d}t} \left\{ 1 - \Theta\left[\frac{\mathrm{d}Q(t,0)}{\mathrm{d}t} \right] \right\} , \tag{1.68}$$

where the function $\Theta(\bullet)$ equals to 1 for a positive argument and to 0 otherwise, denotes the heat transfered into the engine from the reservoirs per cycle. The engine efficiency is then defined by the standard formula

$$\eta = \frac{W_{\mathrm{out}}}{Q_{\mathrm{in}}} . \tag{1.69}$$

Similarly, the (mean) power output of the engine reads

$$P_{\mathrm{out}} = \frac{W_{\mathrm{out}}}{t_{\mathrm{p}}} . \tag{1.70}$$

The traditional consideration of efficiency of heat engines operating between the two baths leads to the Carnot's upper bound [3]

$$\eta_{\mathrm{C}} = 1 - \frac{T_-}{T_+} . \tag{1.71}$$

This bound is only achieved under reversible conditions where the state changes require infinite time and hence the power output is zero. Real heat engines generate a finite power output (1.70), i.e., they perform finite work W_{out} during

[3] Without loose of generality we assume that $T_+ > T_-$.

a cycle of a finite duration $t_{\rm p}$. The Carnot's inequality $\eta \leq \eta_{\rm C}$ was recently generalized by Sinitsyn [172] (see also [114]) who derived a fluctuation theorem which relates the statistics of the (random) heat extracted from the hot reservoir during the cycle and that of the (random) work performed by the engine per cycle.

An alternative way to classify the performance of the heat engines is to compare their efficiencies at maximum power. On the macroscopic level, the first works on this subject were performed by Chambadal [29] and Novikov [136]. They studied, in the framework of endoreversible thermodynamics, the efficiency of nuclear power plants and derived the famous formula for the efficiency at maximum power

$$\eta_{\rm CA} = 1 - \sqrt{\frac{T_-}{T_+}} \; . \tag{1.72}$$

This result have been referred to as the Curzon-Ahlborn efficiency since it was, nearly twenty years later, independently rediscovered by Curzon and Ahlborn [47]. After the derivation of $\eta_{\rm CA}$, the discussion whether or not it represents the upper bound for the efficiency at maximum power has been initiated. The result was negative. The efficiency at maximum power is always *model dependent* and no universal upper bound was discovered, yet (see, for example, the reviews [49,195]).

Nevertheless Tu [185] recently realized that large variety of heat engines [47, 60,159,185] (see also the reviews [166,195]) exhibit similar efficiency at maximum power in the case of small difference between the two reservoir temperatures (i.e., $\eta_{\rm C}$ is small). Later it was proven [61] that the Taylor expansion of the efficiency at maximum power

$$\eta_{\rm P} \approx \frac{\eta_{\rm C}}{2} + \frac{\eta_C^2}{8} + o\left(\eta_C^3\right) \tag{1.73}$$

is general for "strong coupling" models (the term $\eta_{\rm C}/2$) that possess a "left-right symmetry" (the term $\eta_{\rm C}^2/8$). In the strong coupling models the energy (heat) flow is proportional to the flow that performs the work (matter flow). The left-right symmetry means that the heat flow through the system changes its sign when the two heat reservoirs are interchanged. If the second assumption is relaxed, only the term $\eta_{\rm C}/2$ of the expansion (1.73) remains generally valid.

The authors of the study [61] also derived a lower and an upper bound for the efficiency at maximum power for a non-equilibrium analogue of the Carnot's cycle [59], the cycle which consists of two non-equilibrium isotherms (say branches I and III) and two non-equilibrium adiabatic branches. More precisely, assume that the durations of the two isothermal branches are t_+ and t_- and that the total entropies produced during those isotherms are S_+ and S_-, respectively. If these variables fulfill the relations $t_{\rm p} \approx (t_+ + t_-)$, $S_+ \approx 1/t_+ \geq 0$ and $S_- \approx 1/t_- \geq 0$, then the efficiency at maximum power is bounded by the inequalities

$$\frac{\eta_{\rm C}}{2} \leq \eta_{\rm P} \leq \frac{\eta_{\rm C}}{2 - \eta_{\rm C}} \; . \tag{1.74}$$

In Chap. 4 we present two examples of stochastic heat engines [14, 31, 166]. An engine based on the two-level system, which is introduced in Subs. 2.1.2, is investigated in Sec. 4.1 (see also [31]). An engine based on a particle diffusing in an external log-harmonic potential is studied in Sec. 4.2. The both models

represent examples of the above mentioned non-equilibrium Carnot's cycle. The second one demonstrates the validity of the relations (1.73) and (1.74). In the next SUBS. we describe the generic periodic driving used in the two models.

1.4.1 Limit cycle

An important part of the driving of a heat engine is represented, except the externally controlled parameters $\boldsymbol{Y}(t)$, by the time dependence of the reservoir temperature $T = T(t)$. Under a periodic driving, $\boldsymbol{Y}(t) = \boldsymbol{Y}(t + t_\mathrm{p})$, $T(t) = T(t + t_\mathrm{p})$, the state of the system eventually, after a transient regime, becomes also periodic. The system attains an uniquely defined *limit cycle*, the operational cycle of the engine. An example of such cycle is depicted in FIG. 4.8. As mentioned above, the generic driving used in the models presented in this thesis is consists of two adiabatic branches and two isotherms. Specifically, we assume the following driving:

- *Branch I (isothermal):* The temperature equals T_+ and the control parameters changes smoothly from $\boldsymbol{Y}(0)$ to $\boldsymbol{Y}(t_+^-)$.

- *Branch II (adiabatic):* The temperature and the control parameters changes rapidly from T_+ to T_- and from $\boldsymbol{Y}(t_+^-)$ to $\boldsymbol{Y}(t_+^+)$, respectively. We assume that the process is so fast that the state of the system remains unchanged (no heat is exchanged with the reservoir). The work done on the system $W(t_+^+, t_+^-)$ equals $U(t_+^+) - U(t_+^-)$ and no entropy is produced.

- *Branch III (isothermal):* The temperature equals T_- and the control parameters changes smoothly from $\boldsymbol{Y}(t_+^+)$ to $\boldsymbol{Y}(t_\mathrm{p}^-)$.

- *Branch IV (adiabatic):* The temperature and the control parameters changes rapidly back from T_- to T_+ and from $\boldsymbol{Y}(t_\mathrm{p}^-)$ to $\boldsymbol{Y}(t_\mathrm{p}) = \boldsymbol{Y}(0)$, respectively. We assume that the process is so fast that the state of the system remains unchanged (no heat is exchanged with the reservoir). The work done on the system $W(t_\mathrm{p}, t_\mathrm{p}^-)$ equals $U(t_\mathrm{p}) - U(t_\mathrm{p}^-)$ and no entropy is produced.

Up to now, both the master EQ. (1.3) and the Fokker-Planck EQ. (1.38) have been considered only for an isothermal process. However, neither in the case of EQ. (1.3) nor in the case of EQ. (1.38) the time dependence of the temperature does not break the Markov property of the underlying stochastic dynamics. Therefore one can use the Chapman-Kolmogorov EQS. (1.7) and (1.40) to compose the solution of EQS. (1.3) and (1.38) for the periodic driving above from their solutions for the isotherms I and III (during the adiabatic branches II and IV the system state does not change). In the next two paragraphs we execute the proposed procedure for the systems with discrete and with continuous state space, respectively.

Discrete systems

Let $\mathbb{R}_+(t\,|\,t') = \mathbb{R}(t\,|\,t')$, $t', t \in (0, t_+^+)$ and $\mathbb{R}_-(t\,|\,t') = \mathbb{R}(t\,|\,t')$, $t', t \in (t_+^+, t_\mathrm{p})$ denote the solution of EQ. (1.3) during the isothermal branches I and III, respectively. Using the Chapman-Kolmogorov EQ. (1.7) the solution of the master

Eq. (1.3) for the above described periodic driving reads[4]

$$\mathbb{R}_{\mathrm{p}}(t\,|\,t') = \begin{cases} \mathbb{R}_{+}(t\,|\,t')\,, & t',t \in \left[0,t_{+}^{+}\right]\,, \\ \mathbb{R}_{-}(t\,|\,t_{+}^{+})\,\mathbb{R}_{+}(t_{+}^{+}\,|\,t')\,, & t' \in \left[0,t_{+}^{+}\right] \;\wedge\; t \in \left[t_{+}^{+},t_{\mathrm{p}}\right]\,, \\ \mathbb{R}_{-}(t\,|\,t')\,, & t',t \in \left[t_{+}^{+},t_{\mathrm{p}}\right]\,. \end{cases} \tag{1.75}$$

The matrix $\mathbb{R}_{\mathrm{p}}(t\,|\,t')$ can be used for calculation of the time correlation function (1.25) during the cycle. Further we focus on the matrix $\mathbb{R}_{\mathrm{p}}(t) \equiv \mathbb{R}_{\mathrm{p}}(t\,|\,0)$, which evolves any initial state of the system as $\boldsymbol{p}(t) = \mathbb{R}_{\mathrm{p}}(t)\,\boldsymbol{p}(0)$. The system states at the ends of the individual periods form a Markov chain and, in order to obtain the periodic state of the system during the limit cycle, $\boldsymbol{p}(t) = \boldsymbol{p}(t+t_{\mathrm{p}})$, we are interested in its fixed point behavior $\lim_{n\to\infty}\left[\mathbb{R}_{\mathrm{p}}(t)\right]^{n}\boldsymbol{p}(0)$. If we take the stationary state as the initial condition, $\boldsymbol{p}(0) = \boldsymbol{p}^{\mathrm{stat}}$, the system revisits this special state after each period of the driving. Therefore, to find the vector $\boldsymbol{p}^{\mathrm{stat}}$, it suffices to solve the eigenvalue problem [130]

$$\boldsymbol{p}^{\mathrm{stat}} = \mathbb{R}_{\mathrm{p}}(t_{\mathrm{p}})\,\boldsymbol{p}^{\mathrm{stat}}\,. \tag{1.76}$$

Similarly, let the matrix $\mathbb{G}_{+}(w,t\,|\,w') = \mathbb{G}(t,w\,|\,w',0)$, $t \in (0,t_{+}^{+})$ and the matrix $\mathbb{G}_{-}(w,t\,|\,w') = \mathbb{G}(t,w\,|\,w',t_{+}^{+})$, $t \in (t_{+}^{+},t_{\mathrm{p}})$ denote the solution of Eq. (1.13) during the isothermal branches I and III, respectively. According to the Chapman-Kolmogorov Eq. (1.14) the solution of Eq. (1.13) for the periodic driving reads

$$\mathbb{G}_{\mathrm{p}}(w,t) = \begin{cases} \mathbb{G}_{+}(w,t\,|\,0)\,, & t \in [0,t_{+}^{+}]\,, \\ \displaystyle\int_{-\infty}^{\infty}\mathrm{d}w'\,\mathbb{G}_{-}(w,t\,|\,w')\,\mathbb{G}_{+}(w',t_{+}^{+}\,|\,0)\,, & t \in [t_{+}^{+},t_{\mathrm{p}}]\,. \end{cases} \tag{1.77}$$

These results completely describe dynamics and energetics of the engine during the limit cycle. Specifically, the system state during the cycle reads

$$\boldsymbol{p}(t) = \mathbb{R}_{\mathrm{p}}(t)\,\boldsymbol{p}^{\mathrm{stat}} \tag{1.78}$$

and the energetics of the engine during the cycle is determined by the function

$$\xi(u,w,t;u') = \sum_{i,j=1}^{N}\delta\left[u-\mathcal{E}_{i}(t)\right]\delta\left[u'-\mathcal{E}_{j}(0)\right]\left[\mathbb{G}_{\mathrm{p}}(w,t)\right]_{ij}\,p_{j}^{\mathrm{stat}} \tag{1.79}$$

which enters Eqs. (1.16)-(1.18).

Continuous systems

The description for the continuous systems is similar. Let $R_{+}(x,t\,|\,x',t') = R(x,t\,|\,x',0)$, $t',t \in (0,t_{+}^{+})$ and $R_{-}(x,t\,|\,x',t') = R(x,t\,|\,x',t_{+}^{+})$, $t',t \in (t_{+}^{+},t_{\mathrm{p}})$ denote the solution of Eq. (1.38) during the isothermal branches I and III, respectively. Using the Chapman-Kolmogorov Eq. (1.40) the solution of the Fokker-Planck Eq. (1.38) for the periodic driving above reads

$$\begin{cases} R_{+}(x,t\,|\,x',t')\,, & t',t \in [0,t_{+}^{+}]\,, \\ \displaystyle\int_{-\infty}^{\infty}\mathrm{d}x''\,R_{-}(x,t\,|\,x'',t_{+}^{+})\,R_{+}(x'',t_{+}^{+}\,|\,x',t')\,, & t' \in [0,t_{+}^{+}] \;\wedge\; t \in [t_{+}^{+},t_{\mathrm{p}}]\,, \\ R_{-}(x,t\,|\,x',t')\,, & t',t \in [t_{+}^{+},t_{\mathrm{p}}]\,. \end{cases} \tag{1.80}$$

[4] It is important to note that the matrix $\mathbb{R}_{\mathrm{p}}(t) \equiv \mathbb{R}_{\mathrm{p}}(t\,|\,0)$ is, contrary to the driving $\boldsymbol{Y}(t)$, always continuous, i.e., $\mathbb{R}_{\mathrm{p}}(t_{+}^{-}) = \mathbb{R}_{\mathrm{p}}(t_{+}^{+})$ and $\mathbb{R}_{\mathrm{p}}(t_{\mathrm{p}}^{-}) = \mathbb{R}_{\mathrm{p}}(t_{\mathrm{p}})$.

The eigenvalue problem (1.76) now translates into the integral Eq.

$$\int_{-\infty}^{\infty} \mathrm{d}x'\, R_{\mathrm{p}}(x, t_{\mathrm{p}} \,|\, x', 0)\, p^{\mathrm{stat}}(x') = p^{\mathrm{stat}}(x) \ . \tag{1.81}$$

The dynamics of the engine is described by the (periodic) state of the system during the limit cycle

$$p(x,t) = \int_{-\infty}^{\infty} \mathrm{d}x'\, R_{\mathrm{p}}(x, t \,|\, x', 0)\, p^{\mathrm{stat}}(x') \ . \tag{1.82}$$

The energetics of the engine is determined by the function $p(x,t)$, which enters Eqs. (1.48)-(1.49) for the mean values of the work, the heat and the internal energy and by the functions $R_{\mathrm{p}}(x, t \,|\, x', t')$ and $p^{\mathrm{stat}}(x)$, which yield the time correlation function (1.51) and hence describe the fluctuations of the work and the heat.

1.4.2 Diagrams of the limit cycle

In this Subs. we discuss the possibility to depict the limit cycle of an engine in a diagram similar to the pressure volume (PV) diagram known from classical thermodynamics. The mean work done per cycle by a discrete system can be rewritten as [cf. Eqs. (1.23) and (1.48)]

$$\begin{aligned} W_{\mathrm{out}} = -W(t_{\mathrm{p}}, 0) = \\ - \int_0^{t_{\mathrm{p}}} \mathrm{d}t \sum_{i=1}^{N} \left[\frac{\mathrm{d}}{\mathrm{d}t} \mathcal{E}_i(t) \right] p_i(t) = - \int_{\boldsymbol{Y}(0)}^{\boldsymbol{Y}(t_{\mathrm{p}})} \mathrm{d}\boldsymbol{Y} \sum_{i=1}^{N} \left[\frac{\mathrm{d}}{\mathrm{d}\boldsymbol{Y}} \tilde{\mathcal{V}}_i(\boldsymbol{Y}) \right] \tilde{p}_i(\boldsymbol{Y}) = \\ = - \sum_{j=1}^{K} \int_{Y_j(0)}^{Y_j(t_{\mathrm{p}})} \mathrm{d}Y_j \sum_{i=1}^{N} \left[\frac{\partial}{\partial Y_j} \tilde{\mathcal{V}}_i(Y_1, \ldots, Y_K) \right] \tilde{p}_i(\boldsymbol{Y}) = \\ = \sum_{i=1}^{K} \int_{Y_i(0)}^{Y_i(t_{\mathrm{p}})} \mathrm{d}Y_i\, f_i(Y_i) \ , \end{aligned} \tag{1.83}$$

where K stands for the number of components of the external driving $\boldsymbol{Y}(t)$ and $\tilde{p}_i[\boldsymbol{Y}(t)] = p_i(t)$. The individual terms on the right-hand side of Eq. (1.83) correspond to the work done by the individual components of the driving. For the continuous models the functions $f_i(Y_i)$ are given by ($p(x,t) = \tilde{p}[x, \boldsymbol{Y}(t)]$)

$$\begin{aligned} f_i(Y_i) = - \int_{\infty}^{\infty} \mathrm{d}x \left[\frac{\partial}{\partial Y_i} \tilde{\mathcal{V}}(x, \boldsymbol{Y}) \right] \tilde{p}(x, \boldsymbol{Y}) = \\ = - \int_{\infty}^{\infty} \mathrm{d}x \left[\frac{\partial}{\partial Y_i} \tilde{\mathcal{V}}(x, Y_1, \ldots, Y_k) \right] \tilde{p}(x, \boldsymbol{Y}) \ . \end{aligned} \tag{1.84}$$

Since $\boldsymbol{Y}(t_{\mathrm{p}}) = \boldsymbol{Y}(0)$, each of the K contributions on the right-hand side of Eq. (1.83) equals the *oriented* area enclosed by the parametric plot of the system response, represented by the average $f_i(Y_i)$, versus the ith component of the driving, $Y_i(t)$. The parameter t runs from 0 to t_{p}. Similar decomposition of work is well known from classical thermodynamics. As an example consider a magnetic gas and let the driving possess two components, the volume $Y_1 = V$ and

the magnetic field (spatially homogeneous magnetic flux density) $Y_2 = B$. The thermodynamic work done by the system per cycle then reads [26]

$$W_{\mathrm{out}} = \int_{V(0)}^{V(t_{\mathrm{p}})} \mathrm{d}V\, p(V) - \int_{B(0)}^{B(t_{\mathrm{p}})} \mathrm{d}B\, I(B)\ , \tag{1.85}$$

where $f_1 = p$ denotes the gas pressure and $-f_2 = I$ stands for the component of the total magnetic moment of the gas parallel to the external magnetic field. The parametric plots corresponding to the individual terms on the right-hand side of Eq. (1.83) thus represent an analogy of the well known PV diagrams. In the field of stochastic thermodynamics such diagrams were used for the first time in the works [31,32,91]. Several examples of the diagrams are presented in Chap. 4 (see Figs. 4.1, 4.4, 4.9 and 4.11).

Important eye-guides in the diagrams can be formed by the so called *equilibrium isotherms*. The curves corresponding to the values of the functions f_i if a given cycle would be carried out quasi-statically. They are given by

$$f_i^{\mathrm{eq}}[Y_i(t)] = \sum_{j=1}^{N} \left\{ \frac{\partial \tilde{\mathcal{V}}_j[Y_1(t), \ldots, Y_K(t)]}{\partial Y_i(t)} \right\} \frac{\exp[\beta(t)\mathcal{F}_j(t)]}{\sum_{j=1}^{N} \exp[\beta(t)\mathcal{F}_j(t)]} \tag{1.86}$$

and

$$f_i^{\mathrm{eq}}[Y_i(t)] = \int_{-\infty}^{\infty} \mathrm{d}x \left[\frac{\partial \tilde{\mathcal{V}}(x, Y_1(t), \ldots, Y_K(t))}{\partial Y_i(t)} \right] \frac{\exp[\beta(t)\mathcal{F}(x,t)]}{\int_{-\infty}^{\infty} \mathrm{d}x' \, \exp[\beta(t)\mathcal{F}(x',t)]} \tag{1.87}$$

for the discrete and for the continuous models, respectively. The equilibrium isotherm corresponding to the first isothermal branch is obtained if one takes in Eqs. (1.86) and (1.87) $t \in (0, t_+^-)$ and $\beta(t) = 1/(k_{\mathrm{B}} T_+)$. Similarly, the equilibrium isotherm corresponding to the second isothermal branch is obtained if one assumes $t \in (t_+^+, t_{\mathrm{p}}^-)$ and $\beta(t) = 1/(k_{\mathrm{B}} T_-)$. In Figs. 4.1, 4.4, 4.9 and 4.11 it can be clearly seen that the non-equilibrium functions f_i are "attracted" to the equilibrium isotherms, which represent the carrot (the banana) in the horse-carrot (banana-monkey) analogy depicted in Fig. 1. The more "reversible" the individual non-equilibrium isotherms are the stronger this attraction is (cf. Fig. 4.9).

2. Discrete State Space Models

2.1 Two-level system

Consider a two-level system ($N = 2$) with the general transition rate matrix

$$\mathbb{L}(t) = \begin{pmatrix} \lambda_{\mathrm{U}}(t) & -\lambda_{\mathrm{D}}(t) \\ -\lambda_{\mathrm{U}}(t) & \lambda_{\mathrm{D}}(t) \end{pmatrix} . \tag{2.1}$$

The transition rate from the level 1 to the level 2 equals $\nu L_{21}(t) = -\nu\lambda_{\mathrm{U}}(t)$. Similarly, the transitions from the level 2 to the level 1 occur with the rate $\nu L_{12}(t) = -\nu\lambda_{\mathrm{D}}(t)$. The model is depicted in Fig. 2.1.

2.1.1 Dynamics

The master Eq. (1.3) with the general transition rate matrix (2.1) can be solved analytically using the variation of parameters [21]. The result is

$$\begin{aligned} \mathbb{R}(t\,|\,t') = \mathbb{1} - \frac{1}{2}\begin{pmatrix} 1 & -1 \\ -1 & 1 \end{pmatrix}\left\{1 - \exp\left[-\int_{t'}^{t} \mathrm{d}t''\gamma_{+}(t'')\right]\right\} + \\ + \frac{1}{2}\begin{pmatrix} -1 & -1 \\ 1 & 1 \end{pmatrix}\int_{t'}^{t} \mathrm{d}t'' \exp\left[-\int_{t''}^{t} \mathrm{d}t'''\gamma_{+}(t''')\right]\,\gamma_{-}(t'') \ , \end{aligned} \tag{2.2}$$

where $\gamma_{\pm}(t) = \nu[\,\lambda_{\mathrm{U}}(t) \pm \lambda_{\mathrm{D}}(t)\,]$. This matrix describes dynamics of the system.

2.1.2 Energetics

The master Eq. (1.3) for $N = 2$ can be solved for arbitrary transition rates. On the contrary, exact solutions of the corresponding Eq. (1.13), which describes energetics during a given process, are known only for few specific settings. In the following we give two exactly solvable models [35, 179] and one model which was, up to now, solved only approximately, nevertheless is quite important from the physical point of view [122]. Without loose of generality we assume for all the three models that the degeneracy of the two levels, Ω_i, equals 1, i.e., the free

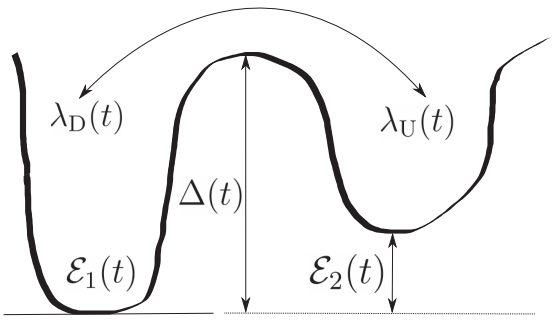

Fig. 2.1: The two-level model.

energies (1.1) and energies (1.2) coincide. We consider the symmetric, linear form of the driving

$$\mathcal{E}_1(t) = \mathcal{F}_1(t) = -\mathcal{E}_2(t) = -\mathcal{F}_2(t) = \frac{U}{2} + \frac{V}{2}(t - t') \ , \tag{2.3}$$

i.e., the gap between the two energy levels changes with the constant velocity $V/2$. The matrix $\dot{\mathbb{E}}(t)$ in Eq. (1.13) then assumes the form

$$\dot{\mathbb{E}}(t) = \frac{V}{2} \, \mathrm{diag}\{1, -1\} \ . \tag{2.4}$$

In all the three settings we assume that the transition rates $\lambda_{\mathrm{L}}(t)$, $\lambda_{\mathrm{R}}(t)$ fulfill the (time local) detailed balance condition (1.4), i.e.,

$$\lambda_{\mathrm{D}}(t) = \exp\left\{-\beta \left[\mathcal{E}_1(t) - \mathcal{E}_2(t)\right]\right\} \lambda_{\mathrm{U}}(t) = \exp\left[2\beta \mathcal{E}_2(t)\right] \lambda_{\mathrm{U}}(t) \ . \tag{2.5}$$

In such case the rate matrix (2.1) reads

$$\mathbb{L}(t) = \lambda_{\mathrm{U}}(t) \begin{pmatrix} 1 & -\exp\left(-\beta U\right) \exp\left[-\beta V (t - t')\right] \\ -1 & \exp\left(-\beta U\right) \exp\left[-\beta V (t - t')\right] \end{pmatrix} \tag{2.6}$$

and the only function which remains to be specified is the rate $\lambda_{\mathrm{U}}(t)$. Assume that the two levels are separated by the free energy barrier (see Fig. 2.1)

$$\Delta(t) = \Delta - V_{\Delta}(t - t') \ , \tag{2.7}$$

which decreases/increases with the constant velocity V_{Δ}. Intuitively, the transition rate $\lambda_{\mathrm{U}}(t)$ should be a decreasing function of the barrier height $\Delta(t)$. In the following we give three examples of possible physical choices of $\lambda_{\mathrm{U}}(t)$.

Metropolis scenario

The simplest possible choice reads $\lambda_{\mathrm{U}}(t) = \exp\left[-2\beta \mathcal{E}_2(t)\right]$, i.e., $\lambda_{\mathrm{D}}(t) = 1$. It is inspired by Monte Carlo simulations, namely by the so-called *Metropolis algorithm* [126]. In the simulations, the Metropolis algorithm is used for its fast relaxation of the system towards the thermal equilibrium. It does not describe well the relaxation processes themselves. However, it turns out that the choice $\lambda_{\mathrm{U}}(t) = \exp\left[-2\beta \mathcal{E}_2(t)\right]$ is mathematically very similar to the more physical choice

$$\lambda_{\mathrm{U}}(t) = \exp\left[-\beta \Delta(t)\right] \ , \qquad V_{\Delta} = V \ . \tag{2.8}$$

We call this choice of the transition scenario the *Metropolis scenario*.

The resulting Eq. (1.13) for this model can be written in the form

$$\frac{\partial}{\partial \tau} \bar{\mathbb{G}}(\eta, \tau) = -\left[\begin{pmatrix} 1 & 0 \\ 0 & -1 \end{pmatrix} \frac{\partial}{\partial \eta} + a \begin{pmatrix} \exp(\tau) & -c \\ -\exp(\tau) & c \end{pmatrix} \right] \bar{\mathbb{G}}(\eta, \tau) \ , \tag{2.9}$$

with the initial condition $\bar{\mathbb{G}}(\eta, 0) = \delta(\eta) \mathbb{1}$. In Eq. (2.9) we used the abbreviations

$$\begin{aligned} \tau &= \tau(t, t') = \beta |V| (t - t') \ , \\ \eta &= \eta(w, w') = 2\beta (w - w') \ , \\ a &= \frac{\nu}{\beta |V|} \exp(-\beta \Delta) \ , \\ c &= \exp\left(-\beta U \frac{|V|}{V}\right) \ . \end{aligned} \tag{2.10}$$

Solution of Eq. (2.9) for $U = \Delta = 0$ was derived in [35] (see also [179]). However, following similar lines as in [35] one can solve Eq. (2.9) also for a general U and Δ. This solution, for $V \geq 0$, reads

$$\begin{aligned}
\bar{G}_{11}(\eta,\tau) &= \delta(\tau-\eta)\exp[a(1-\mathrm{e}^{\tau})] + \frac{a^2 c}{2}\,\Theta(-\tau,\tau;\eta)\,y^{ac}\left(\frac{1}{x}-1\right)\times \\
&\times \exp\left[a\left(1-\frac{1}{x}\right)\right]{}_1\mathrm{F}_1\left(1-ac,2;\phi\right)\ , \qquad (2.11)\\
\bar{G}_{12}(\eta,\tau) &= \frac{ac}{2}\,\Theta(-\tau,\tau;\eta)\,y^{ac}\exp\left[a\left(1-\frac{1}{x}\right)\right]{}_1\mathrm{F}_1\left(1-ac,1;\phi\right)\ , \qquad (2.12)\\
\bar{G}_{21}(\eta,\tau) &= \frac{a}{2}\,\Theta(-\tau,\tau;\eta)\,\frac{y^{ac}}{x}\exp\left[a\left(1-\frac{1}{x}\right)\right]{}_1\mathrm{F}_1\left(-ac,1;\phi\right)\ , \qquad (2.13)\\
\bar{G}_{22}(\eta,\tau) &= \delta(\tau+\eta)\mathrm{e}^{-ac\tau} + \frac{a^2 c}{2}\,\Theta(-\tau,\tau;\eta)\,\frac{y^{ac}}{x}\left(\frac{1}{y}-1\right)\times \\
&\times \exp\left[a\left(1-\frac{1}{x}\right)\right]{}_1\mathrm{F}_1\left(1-ac,2;\phi\right)\ , \qquad (2.14)
\end{aligned}$$

where the auxiliary functions x, y and ϕ are defined by the formulas

$$\begin{aligned}
x &= x(\eta,\tau) = \exp\left(-\frac{\tau+\eta}{2}\right) \qquad (2.15)\\
y &= y(\eta,\tau) = \exp\left(-\frac{\tau-\eta}{2}\right)\ , \qquad (2.16)\\
\phi &= \phi(\eta,\tau) = -a\left(1-\frac{1}{x}\right)\left(1-\frac{1}{y}\right)\ . \qquad (2.17)
\end{aligned}$$

The solution of Eq. (2.9) for $V < 0$ follows from interchanging the indices 1 and 2 in Eqs. (2.11)-(2.14). In these Eqs., the terms proportional to the Dirac δ-function, $\delta(\cdot)$, represent *singular* parts of the diagonal elements of the matrix $\bar{\mathbb{G}}(\eta,\tau)$. Their weights equal to the relative frequencies of the trajectories of the process $\mathsf{D}(t)$ that dwell in a given microstate during the whole time interval $[t',t]$. The *non-singular* parts of the functions (2.11)-(2.14) possess finite supports, i.e., they are proportional to the differences of the unit-step functions $\Theta(a,b;x) = \Theta(x-a) - \Theta(x-b)$. The probability density for the work done on a system with a discrete state space, for finite time processes, always consists of these two parts. The singular part of the work probability density (WPD) can be always obtained analytically (see App. B). The symbol ${}_1\mathrm{F}_1(a,b;z)$ stands for the Kummer function of the variable z with the parameters a and b [2,173]. Finally, the matrix $\mathbb{G}(w,t\,|\,w',t')$ can be calculated from the matrix $\bar{\mathbb{G}}(\eta,\tau)$ as

$$\mathbb{G}(w,t\,|\,w',t') = 2\beta\,\bar{\mathbb{G}}\left[2\beta(w-w'),\beta|V|(t-t')\right]\ . \qquad (2.18)$$

Heat bath scenario

The choice $\lambda_{\mathrm{U}}(t) = 1/(1+\exp\{\beta\Delta(t)]\}^{-1}$, which is often referred to as the *Glauber form* [79], is also inspired by the Monte Carlo simulations, namely by the so-called *heat-bath algorithm* [41]. This algorithm is customarily used to simulate non-equilibrium dynamics of, for example, spin systems [128]. For the spin systems

one often identifies the free energy barrier $\Delta(t)$ with the energy difference $\mathcal{E}_2(t) - \mathcal{E}_1(t) = 2\mathcal{E}_2(t)$. In such case the transition rate $\lambda_{\mathrm{U}}(t)$ reads

$$\lambda_{\mathrm{U}}(t) = \frac{1}{1+\exp[2\beta\mathcal{E}_2(t)]} \ . \tag{2.19}$$

We call this choice of the transition scenario the *Heat bath scenario*.

It is interesting to note that the finite time thermodynamics of this system at a fixed temperature has been studied recently in connection with a single-level fermion model for a quantum dot that interacts with a thermal reservoir (metal lead) through a tunneling junction [60]. Within a description based on a quantum master equation (neglect of quantum coherency and entanglement between the system and the reservoir), the level $\mathcal{E}_2(t)$ in the rates (2.19), being valid in a wide band approximation, then represents the chemical potential of the metal lead. When changing the gap between the level and the chemical potential in a given time interval, the optimal protocol $[\mathcal{E}_1(t) - \mathcal{E}_2(t)]$ for extracting the maximal work was shown to exhibit jumps at the beginning and end of the time interval (see [60] for a further discussion and [159] for related findings). In this thesis, in Sec. 4.1, we present a detailed analysis of a heat engine based on the hereby described two-level system (see also [31, 32, 91]).

The resulting Eq. (1.13) for this model can be written in the form

$$\frac{\partial}{\partial\tau}\bar{\mathbb{G}}(\eta,\tau) = -\left[\begin{pmatrix} 1 & 0 \\ 0 & -1 \end{pmatrix}\frac{\partial}{\partial\eta} + \frac{a}{1+c\mathrm{e}^{-\tau}}\begin{pmatrix} 1 & -c\mathrm{e}^{-\tau} \\ -1 & c\mathrm{e}^{-\tau} \end{pmatrix}\right]\bar{\mathbb{G}}(\eta,\tau) \ , \tag{2.20}$$

with the initial condition $\bar{\mathbb{G}}(\eta,0) = \delta(\eta)\mathbb{1}$. In this Eq. we again used the abbreviations (2.10), but now with $\Delta = 0$. Solution of Eq. (2.20) for $U = 0$ ($c = 1$) was derived in [179]. The solution for a general U was obtained in [91] (see also [31]) and, for $V \geq 0$, reads

$$\begin{aligned}
\bar{G}_{11}(\eta,\tau) &= \left[\frac{(1+c)\exp(-\tau)}{1+c\exp(-\tau)}\right]^a \delta(\tau-\eta) + \Theta(-\tau,\tau;\eta)\,\frac{ac}{2}x^a(1-x)y \times \\
&\times \left[-\frac{1}{(1+cx)^{1+a}(1+cy)^{1-a}}{}_2\mathrm{F}_1(1+a,-a;1;\phi) + \right. \\
&+ \left.\frac{(1+a)(1+c)(1+cxy)}{(1+cx)^{2+a}(1+cy)^{2-a}}{}_2\mathrm{F}_1(2+a,1-a;2;\phi)\right] \ ,
\end{aligned} \tag{2.21}$$

$$\bar{G}_{12}(\eta,\tau) = \frac{1}{2}\Theta(-\tau,\tau;\eta)\,acx^a y\,\frac{{}_2\mathrm{F}_1(a,1-a;1;\phi)}{(1+cx)^a(1+cy)^{1-a}} \ , \tag{2.22}$$

$$\bar{G}_{21}(\eta,\tau) = \frac{1}{2}\Theta(-\tau,\tau;\eta)\,ax^a\,\frac{{}_2\mathrm{F}_1(1+a,-a;1;\phi)}{(1+cx)^{1+a}(1+cy)^{-a}} \ , \tag{2.23}$$

$$\begin{aligned}
\bar{G}_{22}(\eta,\tau) &= \left[\frac{1+c\exp(-\tau)}{1+c}\right]^a \delta(\tau+\eta) + \Theta(-\tau,\tau;\eta)\,\frac{ac}{2}x^a(1-y) \\
&\times \left[+\frac{1}{(1+cx)^{1+a}(1+cy)^{1-a}}{}_2\mathrm{F}_1(a,1-a;1;\phi) - \right. \\
&- \left.\frac{(1-a)(1+c)(1+cxy)}{(1+cx)^{2+a}(1+cy)^{2-a}}{}_2\mathrm{F}_1(1+a,2-a;2;\phi)\right] \ ,
\end{aligned} \tag{2.24}$$

where the auxiliary functions x and y are again given by Eqs. (2.15) and (2.16). The function ϕ now reads

$$\phi = \phi(\eta, \tau) = -c \frac{1-x}{1+cx} \frac{1-y}{1+cy} \ . \tag{2.25}$$

The solution for $V < 0$ follows from interchanging the indices 1 and 2 in Eqs. (2.21)-(2.24). In these Eqs. the terms proportional to the Dirac δ-function, $\delta(\cdot)$, and those proportional to the differences of the unit-step functions, $\Theta(a, b; x)$, have the same meaning as the corresponding terms in Eqs. (2.11)-(2.14). The symbol ${}_2\mathrm{F}_1(a, b, c; z)$ stands for the Gauss hypergeometric function of the variable z with the parameters a, b and c [2, 174]. Finally, the matrix $\mathbb{G}(w, t \,|\, w', t')$ can be calculated from the matrix $\bar{\mathbb{G}}(\eta, \tau)$ using Eq. (2.18).

Diffusive scenario

The function $\lambda_{\mathrm{U}}(t)$ used for diffusive systems assumes the form [84]

$$\lambda_{\mathrm{U}}(t) = \exp[-\beta \Delta(t)] \ , \tag{2.26}$$

where the parameters of the barrier height Δ and V_Δ are general. We call this choice of the transition scenario the *Diffusive scenario*. The resulting Eq. (1.13) for this model can be written in the form

$$\frac{\partial}{\partial \tau} \bar{\mathbb{G}}(\eta, \tau) = - \left[\begin{pmatrix} 1 & 0 \\ 0 & -1 \end{pmatrix} \frac{\partial}{\partial \eta} + a \, \mathrm{e}^{\frac{V_\Delta}{V} \tau} \begin{pmatrix} 1 & -c\mathrm{e}^{-\tau} \\ -1 & c\mathrm{e}^{-\tau} \end{pmatrix} \right] \bar{\mathbb{G}}(\eta, \tau) \ , \tag{2.27}$$

with the initial condition $\bar{\mathbb{G}}(\eta, 0) = \delta(\eta) \mathbb{1}$. Here we used again the abbreviations (2.10). For $V_\Delta = V$ one regains the exactly solvable Eq. (2.9). However, for $V_\Delta \neq V$ new computational difficulties in comparison with Eqs. (2.9) and (2.20) arises and Eq. (2.27) was not solved, yet. An approximate solution using saddle point technique was given in [122], where the authors theoretically studied unfolding of a specifically designed DNA hairpin that, during experiments with optical tweezers, shows two-state cooperative unfolding [129]. Analysis of such systems shows usefulness of the method of computer simulations described in App. C (see also [92]).

2.2 Ehrenfest model

Consider the traditional discrete-time Ehrenfest urn model [50, 108, 162] with the total number of balls in the two urns N_{B} (see the illustration in Fig. 2.2). In each round of the system evolution, a ball is selected with the probability $1/N_{\mathrm{B}}$ and moved to the other urn. The stochastic process of moving the balls between the two urns can be described as a Markov chain. We adopt the continuous-time generalization of the Ehrenfest model introduced in [88], where the time intervals between the individual moves are taken as independent exponentially distributed random variables.

Let us denote the (random) number of balls in the left urn at the time t as $\mathsf{M}(t)$. We will investigate the stochastic process $\mathsf{D}(t) = \mathsf{M}(t) + 1$, which assumes the values $1, 2, \ldots, N_{\mathrm{B}} + 1$. In order to describe dynamics and energetics of this

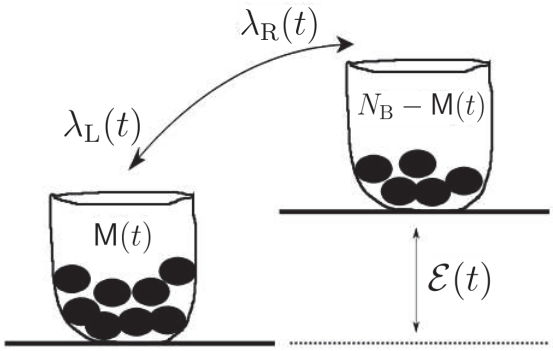

FIG. 2.2: The Ehrenfest model.

process, we can use all the formulas introduced in SEC. 1.1. Assume that the balls in the left (right) urn are moved to the other urn with the transition rate $\nu\lambda_{\mathrm{R}}(t)$ $[\nu\lambda_{\mathrm{L}}(t)]$, where the time dependence of the rates stems from an external manipulation with the two urns. In such case the rate matrix $\mathbb{L}(t)$, which determines via EQ. (1.3) the system dynamics, for the Ehrenfest model reads [88]

$$\begin{pmatrix} \lambda_{\mathrm{L}}(t) & -\dfrac{\lambda_{\mathrm{R}}(t)}{N_{\mathrm{B}}} & 0 & \dots & 0 \\ -\lambda_{\mathrm{L}}(t) & \left[\dfrac{\lambda_{\mathrm{R}}(t)}{N_{\mathrm{B}}} + \dfrac{(N_{\mathrm{B}}-1)\lambda_{\mathrm{L}}(t)}{N_{\mathrm{B}}}\right] & -\dfrac{2\lambda_{\mathrm{R}}(t)}{N_{\mathrm{B}}} & \ddots & \vdots \\ 0 & -\dfrac{(N_{\mathrm{B}}-1)\lambda_{\mathrm{L}}(t)}{N_{\mathrm{B}}} & \ddots & \ddots & 0 \\ \vdots & \ddots & \ddots & \ddots & -\lambda_{\mathrm{R}}(t) \\ 0 & \dots & 0 & -\dfrac{\lambda_{\mathrm{L}}(t)}{N_{\mathrm{B}}} & \lambda_{\mathrm{R}}(t) \end{pmatrix} . \quad (2.28)$$

2.2.1 Dynamics

The Ehrenfest model describes dynamics of N_{B} uncoupled two-level systems (balls) [88]. Hence it should be possible to compose the solution of EQ. (1.3) for a general N_{B} from its solutions for $N_{\mathrm{B}} = 1$. Indeed, for time independent transition rates, such solution was constructed in [88]. For time dependent transition rates one can proceed in a similar way. Specifically, let $\mathbb{T}(t\,|\,t')$ denote the solution of EQ. (1.3) with the rate matrix

$$\mathbb{L}_{\mathrm{T}}(t) = \frac{1}{N_{\mathrm{B}}} \begin{pmatrix} \lambda_{\mathrm{L}}(t) & -\lambda_{\mathrm{R}}(t) \\ -\lambda_{\mathrm{L}}(t) & \lambda_{\mathrm{R}}(t) \end{pmatrix} , \quad (2.29)$$

i.e., the matrix $\mathbb{T}(t\,|\,t')$ is given by EQ. (2.2) with $\gamma_{\pm}(t) = \nu/N_{\mathrm{B}}[\,\lambda_{\mathrm{L}}(t) \pm \lambda_{\mathrm{R}}(t)\,]$. Then the solution of EQ. (1.3) with the rate matrix (2.28) reads

$$R_{m+1n+1}(t\,|\,t') = \sum_{k=0}^{m} \binom{n}{k} \binom{N_{\mathrm{B}}-n}{m-k} [T_{11}(t\,|\,t')]^{N_{\mathrm{B}}-n-m+k} [T_{21}(t\,|\,t')]^{m-k} \times \\ \times [T_{12}(t\,|\,t')]^{n-k} [T_{22}(t\,|\,t')]^{k} , \quad (2.30)$$

where m (n) stands for the number of balls in the left urn at the time t (t'). In (2.30) we assume that $\binom{a}{b}$ equals zero whenever $b > a$.

2.2.2 Energetics

In order to study the energetics of the Ehrenfest model, one has to specify the level energies (1.2). We will assume that whenever the ball is in the left urn, its energy equals $-\mathcal{E}(t)/2$ and, similarly, whenever the ball is in the right urn, its energy reads $\mathcal{E}(t)/2$ (see FIG. 2.2). Such setting yields the level energies

$$\mathcal{E}_i(t) = -(i-1)\frac{\mathcal{E}(t)}{2} + (N_{\mathrm{B}} - i + 1)\frac{\mathcal{E}(t)}{2} = \mathcal{E}(t)\left(\frac{N_{\mathrm{B}}}{2} - i + 1\right) \tag{2.31}$$

and, hence, the matrix $\dot{\mathbb{E}}(t)$ in EQ. (1.13) assumes the form

$$\dot{\mathbb{E}}(t) = \dot{\mathcal{E}}(t)\left[\frac{N_{\mathrm{B}}}{2}\,\mathbb{1} - \mathrm{diag}\{0, 1, \ldots, N_{\mathrm{B}}\}\right] . \tag{2.32}$$

As in the case of the master EQ. (1.3), it should be possible to compose the solution of EQ. (1.13), with the matrices $\mathbb{L}(t)$ and $\dot{\mathbb{E}}(t)$ given by EQS. (2.28) and (2.32), from "one ball solutions". Indeed, let $\mathbb{J}(w, t \,|\, w', t')$ solve EQ. (1.13) with the rate matrix (2.29) and with the matrix $\dot{\mathbb{E}}(t)$ defined as

$$\dot{\mathbb{E}}_{\mathrm{T}}(t) = \frac{\dot{\mathcal{E}}(t)}{2}\,\mathrm{diag}\{1, -1\} . \tag{2.33}$$

Then the matrix $G_{m+1n+1}\,(w, t \,|\, w', t')$ for the Ehrenfest model with N_{B} ball reads

$$G_{m+1n+1}(w, t \,|\, w', t') = \sum_{k=0}^{m} \binom{n}{k}\binom{N_{\mathrm{B}} - n}{m - k}\Bigg(\underbrace{J_{11} * \cdots * J_{11}}_{N_{\mathrm{B}}-n-m+k} * \underbrace{J_{21} * \cdots * J_{21}}_{m-k} * \\ * \underbrace{J_{12} * \cdots * J_{12}}_{n-k} * \underbrace{J_{22} * \cdots * J_{22}}_{k}\Bigg)\left([w], t \,\middle|\, \frac{w'}{N_{\mathrm{B}}}, t'\right) , \tag{2.34}$$

where $(A_1 * A_2 * \cdots * A_n)([w], t \,|\, w', t') = \int_{-\infty}^{\infty} \mathrm{d}w''\, A_1(w - w'' \,|\, w', t')\, B(w'', t \,|\, w', t')$, $B(w, t \,|\, w', t') = (A_2 * \cdots * A_n)([w], t \,|\, w', t')$, denotes the multi-convolution in the work variable w. Validity of this result can be proven by the direct substitution of the Laplace (Fourier) transformed formula (2.34) into the Laplace (Fourier) transformed system (1.13). Two specific examples of the transition rates $\lambda_L(t)$ and $\lambda_R(t)$ and of the driving $\mathcal{E}(t)$ when the matrix $\mathbb{J}(w, t \,|\, w', t')$ can be obtained analytically are discussed in SEC. 2.1.

If the transition rates assume the Glauber form (2.19) (see also [79] and SUBS. 2.1.2) the presented Ehrenfest model describes dynamics and energetics of the system of N_{B} non-interacting spins in a time dependent magnetic field. In such case $\mathsf{M}(t)$ and $\mathsf{D}(t)$ reflect the total magnetization of the system at the time t and $\mathsf{W}(t, t')$ corresponds to the (random) work needed to arrange the individual spins. The work distribution (1.16) for this system for the case of large N_{B} was investigated analytically in the works [100, 149]. It was found that the WPD exhibits exponential tails: $\rho(w, t) \propto \exp[-N_{\mathrm{B}}\,\phi(w, t)]$. On the other hand, for an arbitrary N_{B}, the work distribution was investigated only using Monte Carlo simulations [90]. As far as we know this is for the first time the exact WPD for an arbitrary N_{B}, given by EQS. (2.21)-(2.24) and (2.34), is presented.

2.3 Infinite-level model

Consider a system with infinite number of energy levels and with the infinite three-diagonal transition rate matrix

$$\mathbb{L}(t) = [\lambda_{\mathrm{R}}(t) + \lambda_{\mathrm{L}}(t)]\mathbb{1} - \lambda_{\mathrm{R}}(t)\mathbb{E}_{\mathrm{R}} - \lambda_{\mathrm{L}}(t)\mathbb{E}_{\mathrm{L}} \ , \tag{2.35}$$

where $\mathbb{1}$ stands for the infinite unity matrix and the matrices $\mathbb{E}_{\mathrm{R}}$ and $\mathbb{E}_{\mathrm{L}}$ have the matrix elements

$$[\mathbb{E}_{\mathrm{R}}]_{ij} = \delta_{ij+1} \ , \qquad [\mathbb{E}_{\mathrm{L}}]_{ij} = \delta_{ij-1} \ , \qquad i = \ldots, -1, 0, 1, \ldots \ . \tag{2.36}$$

Here δ_{ij} stands for the Kronecker δ. The transition rate from the level i to the level $i+1$ thus is, for any integer i, given by $\nu\lambda_{\mathrm{R}}(t)$. Similarly, the transitions from the level i to the level $i-1$ occur, for any integer i, with the rate $\nu\lambda_{\mathrm{L}}(t)$.

2.3.1 Dynamics

The dynamics of the system is described by the master Eq. (1.3) with the rate matrix (2.35). Owing to the special form of the matrices $\mathbb{E}_{\mathrm{R}}$ and $\mathbb{E}_{\mathrm{L}}$ this Eq. can be solved analytically regardless the specific form of the functions $\lambda_{\mathrm{R}}(t)$ and $\lambda_{\mathrm{L}}(t)$. Below we derive the solution using the algebraic approach introduced in [194].

Formally, the solution of Eq. (1.3) reads

$$\mathbb{R}(t\,|\,t') = \exp\left[-\nu\int_{t'}^{t} \mathrm{d}t''\,\mathbb{L}(t'')\right] = \\ = \exp\left[-(\Lambda_{\mathrm{R}} + \Lambda_{\mathrm{L}})\mathbb{1} + \Lambda_{\mathrm{R}}\mathbb{E}_{\mathrm{R}} + \Lambda_{\mathrm{L}}\mathbb{E}_{\mathrm{L}}\right] \ , \tag{2.37}$$

where the functions Λ_{R} and Λ_{L} are given by

$$\begin{aligned} \Lambda_{\mathrm{R}} &= \Lambda_{\mathrm{R}}(t,t') = \nu\int_{t'}^{t} \mathrm{d}t''\,\lambda_{\mathrm{R}}(t'') \ , \\ \Lambda_{\mathrm{L}} &= \Lambda_{\mathrm{L}}(t,t') = \nu\int_{t'}^{t} \mathrm{d}t''\,\lambda_{\mathrm{L}}(t'') \ . \end{aligned} \tag{2.38}$$

All the matrices in the exponent in Eq. (2.37) commute, i.e., $\mathbb{E}_{\mathrm{R}}\mathbb{E}_{\mathrm{L}} - \mathbb{E}_{\mathrm{L}}\mathbb{E}_{\mathrm{R}} = 0$ etc, and therefore one can rewrite the formal solution (2.37) as

$$\mathbb{R}(t\,|\,t') = \exp[-(\Lambda_{\mathrm{R}} + \Lambda_{\mathrm{L}})]\exp(\Lambda_{\mathrm{R}}\mathbb{E}_{\mathrm{R}})\exp(\Lambda_{\mathrm{L}}\mathbb{E}_{\mathrm{L}}) \ . \tag{2.39}$$

This formula already represents the exact solution of the master Eq. (1.3). The individual matrix elements of $\mathbb{R}(t\,|\,t')$ read

$$[\mathbb{R}(t\,|\,t')]_{ij} = \exp[-(\Lambda_{\mathrm{R}} + \Lambda_{\mathrm{L}})]\left[\frac{\Lambda_{\mathrm{R}}}{\Lambda_{\mathrm{L}}}\right]^{\frac{i-j}{2}} \mathrm{I}_{i-j}\left(2\sqrt{\Lambda_{\mathrm{R}}\Lambda_{\mathrm{L}}}\right) \ , \tag{2.40}$$

where $\mathrm{I}_{\nu}(x)$ stands for the modified Bessel function of the first kind [2].

2.3.2 Energetics

Let the energies (1.2) of the individual levels of the system read

$$\mathcal{E}_i(t) = -\epsilon\, iF(t) = -\epsilon\, i\,(F_0 + Vt) \ . \tag{2.41}$$

In such case the matrix $\dot{\mathbb{E}}(t)$ in Eq. (1.13), which describes the energetics of the system, assumes the form

$$\dot{\mathbb{E}}(t) = -\epsilon\, V\mathbb{Z} \ , \qquad [\mathbb{Z}]_{ij} = i\delta_{ij} \ . \tag{2.42}$$

Instead of solving Eq. (1.13) directly, we focus on its Laplace transform [1]. This means that we face the set of ordinary differential equations

$$\frac{\mathrm{d}}{\mathrm{d}t}\tilde{\mathbb{G}}(s,t\,|\,t') = -\,[-\epsilon V s\mathbb{Z} + \nu\{[\lambda_{\mathrm{R}}(t) + \lambda_{\mathrm{L}}(t)]\mathbb{1} - \\ -\lambda_{\mathrm{R}}(t)\mathbb{E}_{\mathrm{R}} - \lambda_{\mathrm{L}}(t)\mathbb{E}_{\mathrm{L}}\}]\,\tilde{\mathbb{G}}(s,t\,|\,t') \ , \tag{2.43}$$

with the initial condition $\tilde{\mathbb{G}}(s,t'\,|\,t') = \mathbb{1}$. The Laplace variable s corresponds to the work variable $(w - w')$. The matrices on the right-hand side of Eq. (2.43) do not commute. In order to solve this Eq., we again follow the procedure proposed in [194]. Let us define two auxiliary matrices, $\tilde{\mathbb{H}}(s,t\,|\,t')$ and $\tilde{\mathbb{L}}(t)$, by the formulas

$$\begin{aligned} \tilde{\mathbb{G}}(s,t\,|\,t') &= \exp[x(t-t')\mathbb{Z}]\,\tilde{\mathbb{H}}(s,t\,|\,t') \ , \\ \tilde{\mathbb{L}}(t) &= \exp[-x(t-t')\,\mathbb{Z}]\,\mathbb{L}(t)\,\exp[x(t-t')\,\mathbb{Z}] \ , \end{aligned} \tag{2.44}$$

where

$$x = x(s) = \epsilon V s \ . \tag{2.45}$$

The matrix $\tilde{\mathbb{H}}(s,t\,|\,t')$ obeys the set of ordinary differential equations

$$\frac{\mathrm{d}}{\mathrm{d}t}\tilde{\mathbb{H}}(s,t\,|\,t') = -\nu\left\{[\lambda_{\mathrm{R}}(t) + \lambda_{\mathrm{L}}(t)]\mathbb{1} - \tilde{\lambda}_{\mathrm{R}}(t)\mathbb{E}_{\mathrm{R}} - \tilde{\lambda}_{\mathrm{L}}(t)\mathbb{E}_{\mathrm{L}}\right\}\tilde{\mathbb{H}}(s,t\,|\,t') \ , \tag{2.46}$$

with the initial condition $\tilde{\mathbb{H}}(s,t'\,|\,t') = \mathbb{1}$. Here the auxiliary functions $\tilde{\lambda}_{\mathrm{L}}(t)$ and $\tilde{\lambda}_{\mathrm{R}}(t)$ are given by

$$\begin{aligned} \tilde{\lambda}_{\mathrm{R}}(t) &= \tilde{\lambda}_{\mathrm{R}}(s,t) = \lambda_{\mathrm{R}}(t)\exp(xt) \ , \\ \tilde{\lambda}_{\mathrm{L}}(t) &= \tilde{\lambda}_{\mathrm{L}}(s,t) = \lambda_{\mathrm{L}}(t)\exp(-xt) \ . \end{aligned} \tag{2.47}$$

Eq. (2.46) can be derived using the commutation relations $\mathbb{E}_{\mathrm{R}}\mathbb{Z} - \mathbb{Z}\mathbb{E}_{\mathrm{R}} = -\mathbb{E}_{\mathrm{R}}$ and $\mathbb{E}_{\mathrm{L}}\mathbb{Z} - \mathbb{Z}\mathbb{E}_{\mathrm{L}} = \mathbb{E}_{\mathrm{L}}$. Note that for $u = 0$ this Eq. coincide with Eq. (1.3) for the matrix (2.37). All the matrices on the right hand side of Eq. (2.46) commute and hence, as in the case of the matrix $\mathbb{R}(t\,|\,t')$, we have

$$\mathbb{H}(s,t\,|\,t') = \exp[-(\Lambda_{\mathrm{R}} + \Lambda_{\mathrm{L}})]\exp\left(\tilde{\Lambda}_{\mathrm{R}}\mathbb{E}_{\mathrm{R}}\right)\exp\left(\tilde{\Lambda}_{\mathrm{L}}\mathbb{E}_{\mathrm{L}}\right) \ , \tag{2.48}$$

where the two auxiliary functions $\tilde{\Lambda}_{\mathrm{R}}$ and $\tilde{\Lambda}_{\mathrm{L}}$ are defined as

$$\begin{aligned} \tilde{\Lambda}_{\mathrm{R}} &= \tilde{\Lambda}_{\mathrm{R}}(s,t,t') = \nu\int_{t'}^{t}\mathrm{d}t''\,\tilde{\lambda}_{\mathrm{R}}(s,t'') \ , \\ \tilde{\Lambda}_{\mathrm{L}} &= \tilde{\Lambda}_{\mathrm{L}}(s,t,t') = \nu\int_{t'}^{t}\mathrm{d}t''\,\tilde{\lambda}_{\mathrm{L}}(s,t'') \ . \end{aligned} \tag{2.49}$$

[1] Here we assume that the transformation exists.

Finally, the matrix elements of the matrix $\tilde{\mathbb{G}}(s,t\,|\,t') = \exp[x(t-t')\,\mathbb{Z}]\,\tilde{\mathbb{H}}(s,t\,|\,t')$ are given by

$$[\tilde{\mathbb{G}}(s,t\,|\,t')]_{ij} = \exp[-(\Lambda_{\mathrm{R}}+\Lambda_{\mathrm{L}})]\exp(ixt)\left[\frac{\tilde{\Lambda}_{\mathrm{R}}}{\tilde{\Lambda}_{\mathrm{L}}}\right]^{\frac{i-j}{2}} \mathrm{I}_{i-j}\left(2\sqrt{\tilde{\Lambda}_{\mathrm{R}}\tilde{\Lambda}_{\mathrm{L}}}\right) \ . \quad (2.50)$$

Note that $\tilde{\mathbb{G}}(0,t\,|\,t') = \mathbb{R}(t\,|\,t')$. Once the two transition rates $\lambda_{\mathrm{L}}(t)$ and $\lambda_{\mathrm{R}}(t)$ are specified, the matrix $\mathbb{G}(w,t\,|\,w',t')$ can be obtained from the matrix $\tilde{\mathbb{G}}(s,t\,|\,t')$ using the inverse Laplace transform.

In closing this Sec. let us note that if one adopts the specific form of the transition rates

$$\begin{aligned}\lambda_{\mathrm{R}} &= \frac{D}{\epsilon^2}q_0\exp\left(-\frac{1}{2}\epsilon\beta v t\right) \ , \\ \lambda_{\mathrm{L}} &= \frac{D}{\epsilon^2}q_0^{-1}\exp\left(\frac{1}{2}\epsilon\beta v t\right) \ ,\end{aligned} \quad (2.51)$$

where $q_0 = \exp(-\epsilon\beta f_0/2)$, the present model becomes in the limit $\epsilon \to 0$ equivalent to the diffusion of a particle driven by the time-dependent potential $\mathcal{F}(x,t) = \mathcal{E}(x,t) = \epsilon\, i f(t) = x f(t)$, $f(t) = f_0 + vt$. In such case D stands for the diffusion constant, the particle position reads $x = \epsilon\, i$ and $-f(t)$ is a spatially independent force applied on the particle. It can be seen from Eqs. (1.37) and (1.43) that, for this setting, both the particle position $\mathsf{X}(t)$ and the thermodynamic work done on the particle $\mathsf{W}(t,t')$ are linear functions of the Gaussian white noise $\mathsf{N}(t)$. Therefore both the solution of Eq. (1.38) and that of Eq. (1.45) are given by a Gaussian distribution [125]. Calculation of the WPD for a similar model is presented in Sec. 3.2.

2.4 Kittel zipper

The following work was published with minor modifications in [93].

2.4.1 Introduction

The Watson-Crick double-stranded form represents the thermodynamically stable state of DNA in a wide range of temperature and salt conditions. However, even at standard physiologic conditions, there always exists possibility that the double-helix is locally unzipped into two strands both at its ends and in its interior [13, 68, 85, 127, 141]. If the interior unzipping is neglected, the unfolding of the two strands can be described by a simple zipper model [46, 75, 110]. This model, while including several simplifications, emphasizes the essential ingredient of the unzipping process, that means the competition between the entropic forces which tend to open the macromolecule, and the energetic forces that tend to condense it into its double-stranded form.

In the last two decades, new experimental techniques have been developed for detailed analysis of unzipping processes. A powerful technique are single molecule manipulations by optical tweezers [115, 117, 118, 137, 150, 151], where biomolecules are unfolded and refolded by applying mechanical forces. Because

single molecules are subject to strong fluctuations, a stochastic description of the unfolding/refolding kinetics becomes necessary. Investigation of these stochastic processes can be useful to understand how biomolecules unfold and fold under locally applied forces [67, 123, 183, 184], as, for example, when mRNA passes through the ribosome during the translation process [81, 144], or when DNA is unzipped by helicase during the replication process [111, 180].

A particularly interesting part in the analysis of unzipping processes is the application of integral or detailed fluctuation theorems [22, 56, 57, 138, 151, 165] (see also SEC. 1.3) to estimate free energy differences between folded and unfolded states (see, e.g., [19]). Their advantage is that they can be applied also to protocols, which drive the considered system far from equilibrium. It is thus not necessary to perform the unfolding/folding under quasi-static near-equilibrium conditions, where the process becomes reversible. Most popular theorems are the Crooks fluctuation theorem [43] and Jarzynski equality [104]. These relate to the distribution of work performed on the molecule during the process. Unfortunately it is not easy to get theoretical insight into characteristics of the underlying work distributions in far-from-equilibrium processes, since the work is a functional of the whole stochastic trajectory. Investigations have been conducted for simple spin systems driven by a time-dependent external field [30, 31, 35, 52, 90, 179] and for diffusion processes in the presence of a time-dependent potential [11, 125]. Analytical solutions are known for two-level systems [31, 35, 122, 179] and for systems with one continuous state variable [11, 125].

In this SEC. we present analytical results for the work distribution for a multi-state system, which is motivated by a model proposed by Kittel for describing the melting transition of DNA molecules [110]. In order to derive analytical results, we had to consider a stochastic process with directed forward and forbidden backward transitions between states. As a consequence, detailed balance (1.4) is broken and fluctuation theorems, as mentioned above, will not hold true. On the other hand, kinetic Monte Carlo simulations of the stochastic process show that, for at least certain parameter settings in the model, the restriction of forbidden backward transitions is not so severe and events dominating the integrand in the Jarzynski equality are not very rare. It is important to point out that these parameter settings are not related to any experimental conditions. In more realistic settings rare events would play the decisive role and in such cases it becomes difficult to determine tails of the work distribution with sufficient accuracy (see, for example, APP. B). Also the relation of the work considered in our study to the thermodynamic work measured in an unzipping experiments needs to be treated with care. These problems are discussed in detail in SUBS. 2.4.2 and they imply that the theory cannot be applied to experiments at this stage. Nevertheless, our findings should be useful because the connection to experiments seems not completely out of reach and because they widen the range of hopping models, where analytical results for work distributions are available.

2.4.2 Unzipping in an extended Kittel model

Kittel's model [110] is a simplified version of the Poland-Scheraga model [141] for the equilibrium properties of DNA molecules, which got renewed attention in the last ten years [119]. In contrast to the Poland-Scheraga model, it disregards

the possibility of any interior openings (bubbles) of double-stranded parts of the molecule. Despite this simplification, it is already sufficient to understand the origin of a melting transition.

A molecule in Kittel's model [110] has N links in its fully folded state, see FIG. 2.3. Different energy levels $k = 1, \ldots, N$ of the molecule refer to configurations, where $(k-1)$ of the links are opened in a row. The difference $\mathcal{U}_k - \mathcal{U}_1$ of the internal energy of a microstate with $(k-1)$ open links and the ground level $k = 1$ (no open links) is equal to $(k-1)\Delta$, corresponding to a loss of chemical bond energy Δ per broken link. With each broken link, the molecule gains G degrees of freedom, which characterize the win of conformational degrees of freedom when double-stranded DNA is transferred to single stranded DNA. The entropy difference $\mathcal{S}_k - \mathcal{S}_1$ between the level k and the ground level then becomes $k_\mathrm{B} \ln G^{k-1} = k_\mathrm{B}(k-1)\ln G$, i.e., the multiplicity Ω_k of the level k is G^{k-1}. The free energy $\mathcal{G}_k$ of the level k at a temperature T is thus given by $\mathcal{G}_k = G_0 + (k-1)[\Delta - k_\mathrm{B}T \ln G]$ and the equilibrium properties can be readily worked out by considering the partition sum $Z = \sum_{k=1}^{N} \exp(-\beta \mathcal{G}_k)$.

In extending this model to treat unfolding kinetics, the molecule is supposed to unzip successively, one link in each step, as a consequence of a strong external driving. Such external driving can be caused by a local force or a pH gradient, as indicated in FIG. 2.3. With respect to pulling experiments on single DNA molecules out of equilibrium, there is evidence that a neglect of interior openings can become even less relevant than for the equilibrium properties. For example, far away from the melting temperature, e.g. at standard room temperature conditions (298 K), the unfolding kinetics of DNA hairpin molecules could be successfully described by assuming no interior openings and thermally activated unzipping transitions [122, 123]. Moreover, molecular fraying can be identified in individual unzipping trajectories by considering the size of force jumps. Thereby microstates with interior openings can be systematically excluded from the analysis [54].

We assume that the driving lowers the energy differences by an amount proportional to $(k-1)t$, i.e., open microstates with a larger number of broken links are favored with increasing time. If we take the ground level energy as the reference point, $\mathcal{E}_1 = 0$, we obtain for the free energies (1.1) and energies (1.2) of the individual levels

$$\mathcal{F}_k(t) = (k-1)(\Delta - vt - k_\mathrm{B}T \ln G)\,, \qquad k = 1, \ldots, N\,, \tag{2.52}$$

$$\mathcal{E}_k(t) = (k-1)(\Delta - vt)\,, \qquad k = 1, \ldots, N\,, \tag{2.53}$$

where the parameter v has the dimension of an energy rate and characterizes different speeds of the unfolding in response to different strengths of the external driving.

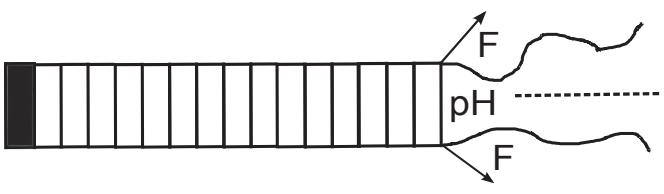

FIG. 2.3: The zipper model.

Following established theoretical descriptions for the rupture kinetics of the bonds [54, 122, 129], the Kramers-Bell form [12] is used for the time-dependent transition rate λ_{kk+1} from level k to level $(k+1)$,

$$\lambda_{kk+1}(t) = \tilde{\nu} \exp[-\beta \mathcal{F}_{kk+1}(t)] \,. \tag{2.54}$$

Here $\tilde{\nu}$ is an attempt frequency and $\mathcal{F}_{k,k+1}(t)$ denotes the free energy barrier for the transition, i.e., the difference of the free energy at the saddle point separating levels k, $(k+1)$ and the free energy $\mathcal{F}_k$ in level k, see FIG. 2.1. The barrier $\mathcal{F}_{kk+1}(t)$ is considered to be composed of a bare, k-independent free energy barrier, $F_{\rm b}$, which is modified by an amount proportional to the free energy difference, $[\mathcal{F}_{k+1}(t) - \mathcal{F}_k(t)]$,

$$\mathcal{F}_{kk+1}(t) = F_{\rm b} + \gamma[\mathcal{F}_{k+1}(t) - \mathcal{F}_k(t)] = F_{\rm b} + \gamma[\Delta - vt - k_{\rm B}T \ln G] \,. \tag{2.55}$$

In the following we set $\gamma = 1$ [2]. Note that $\mathcal{F}_{kk+1}(t)$ and thus $\lambda(t) \equiv \lambda_{kk+1}(t)$ in EQ. (2.54) are independent of k. The attempt frequency $\tilde{\nu}$ in EQ. (2.54) was reported [37] to be approximately proportional to the ratio of the diffusion constant of the molecule in water to the water viscosity. We assume here a linear dependence of this ratio on the temperature T, i.e., we take $\tilde{\nu} = \nu(T/T_0)$, where ν and T_0 are positive constants. Thus we obtain

$$\lambda(t) = \lambda_{kk+1}(t) = g \exp[-\beta(d - vt)] \,, \tag{2.56}$$

where

$$g = \nu G \frac{T}{T_0} \,, \qquad d = \Delta + F_{\rm b} \,. \tag{2.57}$$

If the (time local) detailed balance (1.4) is obeyed, i.e., $\lambda_{kk+1}(t) \exp[-\beta \mathcal{F}_k(t)] = \lambda_{k+1k}(t) \exp[-\beta \mathcal{F}_{k+1}(t)]$, the rates $\lambda_{k+1k}(t) \equiv \lambda_{\rm b}$ for backward (refolding) transitions become both independent of k and t,

$$\lambda_{\rm b} = \lambda_{k+1,k}(t) = \frac{g}{G} \exp(-\beta F_{\rm b}) \,. \tag{2.58}$$

Note that G appears here in the denominator, which means that the ratio $\lambda_{\rm b}/\lambda(t) = \exp(\beta\Delta - \beta vt)/G$ of backward to forward rates becomes small for large degeneracy factors G. This reflects the fact that it is difficult for the flexible unfolded part of the molecule to find proper configurations, which would allow for a reformation of (hydrogen) bonds. The model with the rates given by (2.56) and (2.57) for $N = 2$ (the molecule represented by a two-level system) is exactly solvable (for details see SUBS. 2.1.2).

If the model would refer to the hopping motion of a particle between time-dependent energy levels $\mathcal{E}_k(t)$, the work performed on the system (for one real-

[2] Smaller (larger) γ would correspond to saddle points lying closer to level $k(k+1)$ in configuration space. The derivations in SECS. 2.4.3 and 2.4.4 can be performed analogously for any γ and $F_{\rm b}$.

ization of the stochastic process), (1.10), would be

$$\begin{aligned}
\mathsf{W}(t,0) &= \mathsf{W}(t) = \int_0^t \mathrm{d}t' \sum_{k=1}^{N} \dot{\mathcal{E}}_k(t')\delta_{k\mathsf{D}(t')} \\
&= [\mathcal{E}_{\mathsf{D(t)}}(t) - \mathcal{E}_{\mathsf{D(t)}}(t_{\mathsf{D(t)}})] + \sum_{k=1}^{\mathsf{D}(t)-1} [\mathcal{E}_k(t_{k+1}) - \mathcal{E}_k(t_k)] \\
&= [\mathcal{F}_{\mathsf{D(t)}}(t) - \mathcal{F}_{\mathsf{D(t)}}(t_{\mathsf{D(t)}})] + \sum_{k=1}^{\mathsf{D}(t)-1} [\mathcal{F}_k(t_{k+1}) - \mathcal{F}_k(t_k)] \ , \qquad (2.59)
\end{aligned}$$

where $\mathsf{D}(t)$ denotes the (random) microstate of the molecule at time t and t_k is the (random) time at which the transition from level k to $(k+1)$ (rupture of kth bond) takes place ($t_1 = t' = 0$ being the initial time). The last line in Eq. (2.59) follows from the fact that the entropy in the extended Kittel model is not dependent on time, i.e., for given k, differences between internal energies and between free energies at distinct times equal.

The work in Eq. (2.59) can be related to the thermodynamic work W_f in an unzipping experiment under force control. As pointed out in [3], work in thermodynamics is the internal energy transferred to a system upon changing the control parameters for given system configuration (see also Secs. 1.2.3 and 3.1). This means that, when the force $f = f(t)$ is the control variable and the molecular extension X the conjugate configurational variable, one has $\mathsf{W}_f(t) = -\int_{f(0)}^{f(t)} \mathrm{d}f\, \mathsf{X}$ [3]. Stochastic changes of the molecular extension occur mainly due to bond rupture, while in between transitions the response will be rather smooth and, under neglect of small thermal fluctuations, can be represented by a function $x(k,f)$. This specifies the *mean* end-to-end distance of the unfolded part in microstate k at force f (as often modeled by, e.g., the freely jointed or worm-like chain models from polymer physics). With $f_k \equiv f(t_k)$ we then have

$$\mathsf{W}_f(t) = -\int_{f(0)}^{f(t)} \mathrm{d}f\, \mathsf{X} = -\int_{f_{\mathsf{D}(t)}}^{f(t)} \mathrm{d}f\, \mathsf{X}(\mathsf{D}(t),f) - \sum_{k=1}^{\mathsf{D}(t)-1} \int_{f_k}^{f_{k+1}} \mathrm{d}f\, x(k,f) \ . \quad (2.60)$$

In more detailed energy landscape models, the free energy $\mathcal{F}_{\mathrm{tot}}(k,f)$ of the molecule in level k under loading f can be represented as $\mathcal{F}_{\mathrm{tot}}(k,f) = F\mathcal{F}_0(k) - fx(k,f) + \mathcal{F}_{\mathrm{str}}(k,f)$ (see, e.g., [123]), where $\mathcal{F}_0(k)$ is the free energy in the absence of loading and $\mathcal{F}_{\mathrm{str}}(k,f)$ the elastic energy of the unfolded part upon stretching. For smooth response under stretching the latter is given by [123]

$$\mathcal{F}_{\mathrm{str}}(k,f) = \int_{x(k,0)}^{x(k,f)} \mathrm{d}x\, \tilde{f}(k,x) = fx(k,f) - \int_0^f \mathrm{d}f'\, x(k,f') \,, \qquad (2.61)$$

where $\tilde{f}(k,x)$ denotes the inverse function of $x(k,f)$ with respect to f. Accordingly, at a given k, the work for stretching upon increasing the force from f_a to

[3] Force controlled experiments are achievable with magnetic tweezers or with optical tweezers operating in the force clamp mode. In the latter case, the conjugate variable to the applied force f should better be taken as the trap-pipette distance (rather than the molecular extension) because for this definition the fluctuation theorems are obeyed. Both definitions differ only by a boundary term involving the final and initial forces f_{f} and f_{i}, respectively (for details, see [3]).

f_b becomes

$$-\int_{f_a}^{f_b} \mathrm{d}f\, x(k,f) = \mathcal{F}_{\mathrm{str}}(k,f_b) - f_b x(k,f_b) - \mathcal{F}_{\mathrm{str}}(k,f_a) + f_a x(k,f_a)$$
$$= \mathcal{F}_{\mathrm{tot}}(k,f_b) - \mathcal{F}_{\mathrm{tot}}(k,f_a)\ . \qquad (2.62)$$

This just means that the stretching at fixed k is assumed to take place quasi-statically, i.e., the variation of the force is supposed to occur on a time scale much slower than the correlation time of end-to-end distance fluctuations. Inserting this result into Eq. (2.60) yields

$$\mathsf{W}_f(t) = [\mathcal{F}_{\mathrm{tot}}(k,f(t)) - \mathcal{F}_{\mathrm{tot}}(k,\mathsf{D}(t))] + \\ + \sum_{k=1}^{\mathsf{D}(t)-1} [\mathcal{F}_{\mathrm{tot}}(k,f(t_{k+1})) - F_{\mathrm{tot}}(k,f(t_k))]\,, \qquad (2.63)$$

from which it becomes clear that $\mathsf{W}_f(t)$ equals $\mathsf{W}(t)$, if $\mathcal{F}_{\mathrm{tot}}[k,f(t)]$ is identified with the free energy $\mathcal{F}_k(t)$ in the extended Kittel model.

As said above, we were able to find analytical results for the work distributions if $N = 2$ (Subs. 2.1.2), or if the backward rates in Eq. (2.58) were negligible. We are interested here in the model itself and will not make attempts to assign values to the parameters in the transition rates $\lambda(t)$ [Eq. (2.56)] and λ_b [Eq. (2.58)], and appearing also in the level free energies in Eq. (2.52), which are connected to real experiments. Nevertheless, with respect to the value of the analytical results for $N > 2$ in connection with fluctuation theorems, the question arises whether a neglect of backward rates could be acceptable, at least for certain parameter settings. To check this, we have performed kinetic Monte Carlo simulations of the stochastic process. Because the forward rate from Eq. (2.56) can be written as $\lambda(t) = \lambda_b G \exp(-\beta\Delta + \beta v t)$ and the free energy differences appearing in Eq. (2.59) by $[\mathcal{F}_k(t_{k+1}) - \mathcal{F}_k(t_k)] = -v(k-1)(t_{k+1} - t_k)$, the dynamics and energetics of the model is completely specified by the parameters λ_b, G, v, and T (and N if we consider a complete unfolding). For illustration and discussion of representative results, we use Δ, Δ/k_{B}, and ν^{-1} as units for energy, temperature and time, respectively.

Simulations were performed for fixed $N = 10$, $T = 1$ and $\lambda_b = 1$, and a set of v and G values varying in the intervals $v = 0.01 - 3.3$ and $G = 10 - 1000$, respectively. We always started the unfolding from the fully closed microstate, i.e., $p_k(0) = \delta_{k,1}$ [4]. Probabilities $p_N(t)$ of complete unfolding (occupation of level N) until time t were determined and an unfolding time t_{U} defined by requiring that at $t = t_{\mathrm{U}}$ the zipper has unfolded with a probability of 99.9%, i.e., $p_N(t_{\mathrm{U}}) = 0.999$ (see Subs. 2.4.5). We then considered the work distributions

[4] In this case one can show (cf. Sec. 1.3) that $\langle \exp(-\beta w)\rangle = \phi(t) \exp\{-\beta[F(t) - \mathcal{F}_1(0)]\} = \phi(t)\exp[-\beta F(t)]$, where $\mathcal{F}_1(0) = 0$ from Eq. (2.52) and $F(t) = -\beta^{-1}\ln[(A^N - 1)/(A - 1)]$, $A = \exp[-\beta(\Delta + vt)]/G$, is the free energy for an equilibrated system with level free energies $\mathcal{F}_k(t)$ (protocol variables) at time t; $\phi(t)$ is the probability for the zipper to be in the fully closed microstate $k = 1$ under the reversed protocol, if the system is initially in to the equilibrium state $\exp\{\beta[F(t) - \mathcal{F}_k(t)]\}$. The situation when the system is initially in thermal equilibrium, and hence the standard Jarzynski equality (1.61) is valid, is discussed in App. B). It turns out that in this case, in order to get the tails of the WPD correctly, the refolding can not be neglected.

$\rho(w, t_{\mathrm{U}})$ at $t = t_{\mathrm{U}}$ and the weighted distributions $\exp(-\beta w)\rho(w, t_{\mathrm{U}})$, corresponding to the integrand in the average $\langle \exp(-\beta w) \rangle = \int \mathrm{d}w \, \exp(-\beta w)\rho(w, t_{\mathrm{U}})$ as it appears in the Jarzynski equality. It was found that backward rates turn out to have a minor importance when the forward rates are much larger than the backward rates during the whole unfolding process or when v is large enough. Specifically, the error in calculating $\langle \exp(-\beta w) \rangle$ is smaller than 5% when $v \gtrsim 3$ for $G = 10$, $v \gtrsim 0.1$ for $G = 100$, and $v \gtrsim 0.01$ for $G = 1000$. As representative examples we show in FIG. 2.4 simulated results (blue lines) with nonzero backward rates in comparison with analytical results (green circles) for zero backward rates (see SUBS. 2.4.4) for $p_N(t)$, $\rho(w, t_{\mathrm{U}})$, and $\exp(-\beta w)\rho(w, t_{\mathrm{U}})$, and parameters $v = 0.25$, $G = 10$ [panels labeled with a)] and $G = 1000$ [panels labeled with b)]. As can be seen from the figure, for the case of large G (small backward transitions), the simulated results for $p_N(t)$, $\rho(w, t_{\mathrm{U}})$, and $\exp(-\beta w)\rho(w, t_{\mathrm{U}})$ are almost indistinguishable from the analytical results.

The remaining part of this SEC. is organized as follows. In SUBS. 2.4.3 we specify the equations for the time evolution of the system state [EQ. (1.3)] and for the quantities describing the energy transformations [EQ. (1.13)]. In SUBS. 2.4.4 we derive exact analytical solutions of these equations and in SUBS. 2.4.5 we discuss our findings.

2.4.3 Formalization of the model

Let $p_k(t)$, $k = 1, \ldots, N$, be the occupation probabilities of the k-th level. The dynamics of these functions for the above described model is governed by master EQ. (1.3) with the $(N \times N)$ matrix of the transition rates

$$\mathbb{L}(t) = \frac{1}{\nu} \begin{pmatrix} \lambda(t) & 0 & \ldots & \ldots & 0 \\ -\lambda(t) & \lambda(t) & \ddots & & \vdots \\ 0 & \ddots & \ddots & \ddots & \vdots \\ \vdots & \ddots & \ddots & \lambda(t) & 0 \\ 0 & \ldots & 0 & -\lambda(t) & 0 \end{pmatrix} , \tag{2.64}$$

where $\lambda(t)$ is given by (2.56). Without loose of generality we will consider only the case when the initial condition is set at the time $t' = 0$. In such case we can simplify the notation used in SEC. 1.1. We will write $\mathbb{R}(t \,|\, 0) \equiv \mathbb{R}(t)$ for the solution of EQ. (1.3), $\mathbb{G}(w, t \,|\, 0, 0) \equiv \mathbb{G}(w, t)$ for the solution of EQ. (1.13) and we will omit the variable t' for other quantities such as work and heat. Moreover, in the following, we always start with the completely closed zipper, that means $p_k(0) = \delta_{k1}$. The individual occupation probabilities (1.6) then read

$$p_i(t) = R_{i1}(t) \ . \tag{2.65}$$

The energetics of the zipper is described by EQ. (1.13), where the matrix $\dot{\mathbb{E}}(t)$ is the $(N \times N)$ diagonal matrix

$$\dot{\mathbb{E}}(t) = \mathrm{diag}\{\dot{\mathcal{E}}_1(t), \ldots, \dot{\mathcal{E}}_N(t)\} = -v \, \mathrm{diag}\{0, 1 \ldots, N-1\} \ . \tag{2.66}$$

Exact solutions of EQS. (1.3) and (1.13) with the $(N \times N)$ matrices $\mathbb{L}(t)$ and $\dot{\mathbb{E}}(t)$ given by EQS. (2.64) and (2.66) will be derived the following SUBS. 2.4.4. The

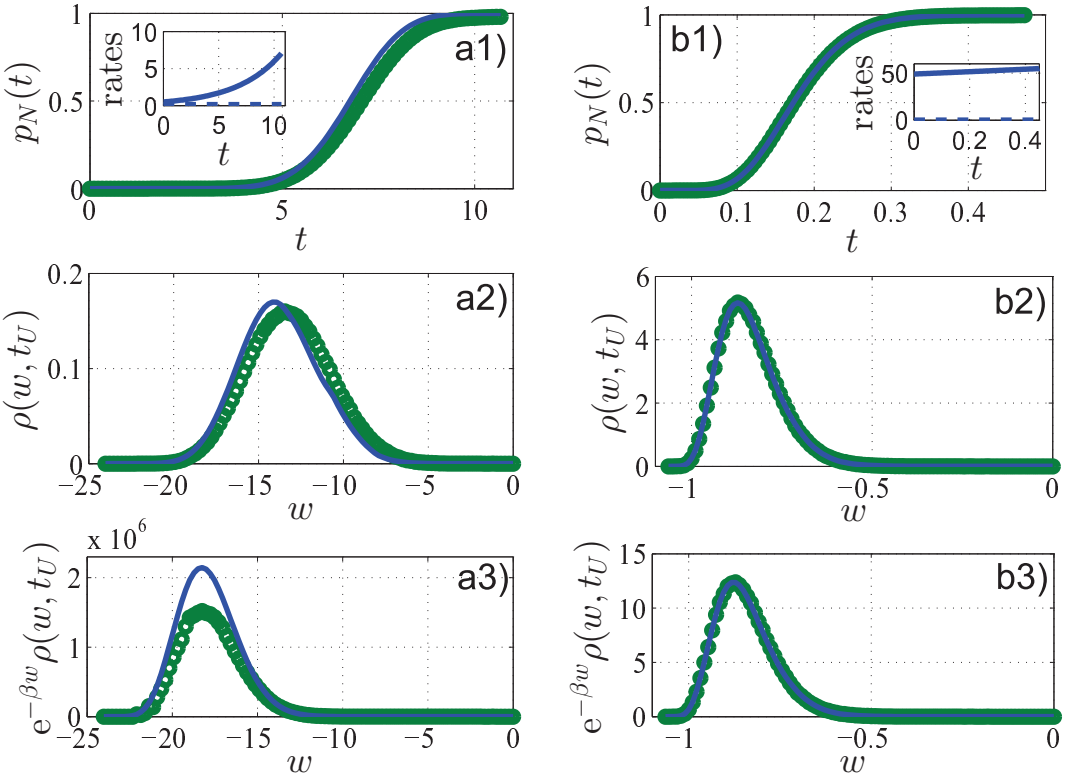

FIG. 2.4: Simulated results of the model presented in SUBS. 2.4.2 with backward transition rate $\lambda_b = 0.133$ (blue lines) in comparison with analytical results (see SUBS. 2.4.4) when neglecting backward transitions (green circles). Panels labeled with a) and b) refer to degeneracy factors $G = 10$ and $G = 1000$, respectively. The remaining parameters are $T = 1$, $v = 0.25$, and $N = 10$. Panels a1) and b1) show the probability $p_N(t)$ that the zipper has unfolded up to time t and the insets depict the time-dependence of the forward transition rates (solid line); the constant backward rate is indicated by the dashed line. Panels a2) and b2) display the probability densities $\rho(w, t_U)$ at the unfolding time t_U ($t_U = 10.67$ for $G = 10$ and $t_U = 0.47$ for $G = 1000$), and panels a3) and b3) the weighted probability densities $\exp(-\beta w)\rho(w, t_U)$.

WPD $\rho(w,t)$ follows from from Eq. (1.16), the mean values and variances of the internal energy, the work and the heat can be calculated from Eqs. (1.22)-(1.24) and (1.28)-(1.30).

2.4.4 Solution of the model

Owing to the simple two-diagonal structure of the matrix $\mathbb{L}(t)$ in Eq. (2.64), the system (1.3) can be solved by simple integrations. By defining

$$\Lambda(t,t') = \int_{t'}^{t} \mathrm{d}t'' \lambda(t'') = \frac{\alpha}{\beta v} \left[\exp(\beta v t) - \exp(\beta v t')\right] \ , \tag{2.67}$$

where $\alpha = g \exp(-\beta d)$, a recursive treatment of Eq. (1.3) yields

$$\begin{aligned}
R_{ij}(t) &= 0 \ , && i < j \ , \\
R_{jj}(t) &= \mathrm{e}^{-\Lambda(t,0)} \ , && j = 1, \ldots, N \ , \\
R_{ij}(t) &= \int_0^t \mathrm{d}t' \mathrm{e}^{-\Lambda(t,t')} \, \lambda(t') \, R_{i-1j}(t') \ , && j < i < N \ , \\
R_{Nj}(t) &= \int_0^t \mathrm{d}t' \lambda(t') \, R_{N-1j}(t') \ , && j = 1, \ldots, N \ .
\end{aligned} \tag{2.68}$$

When solving these recursive relations, we obtain the lower triangular matrix with the nonzero matrix elements

$$R_{j+kj}(t) = \frac{[\Lambda(t,0)]^k}{k!} \, \mathrm{e}^{-\Lambda(t,0)} \ , \quad j = 1, \ldots, N-1 \ ; \ k = 0, \ldots, N-1-j \ , \tag{2.69}$$

$$R_{Nj}(t) = \frac{[\Lambda(t,0)]^{N-j}}{(N-j)!} \, \mathrm{e}^{-\Lambda(t,0)} \, {}_1\mathrm{F}_1[1, N+1-j; \Lambda(t,0)] \ , \quad j = 1, \ldots, N \ , \tag{2.70}$$

where ${}_1\mathrm{F}_1(a,b;x)$ denotes the confluent hypergeometric function [2, 173].

For solving Eq. (1.13) we first perform a Laplace transform with respect to the work variable w. It yields the system of ordinary differential equations

$$\frac{\mathrm{d}}{\mathrm{d}t} \tilde{\mathbb{G}}(s,t) = \left[-s \, \dot{\mathbb{E}}(t) + \mathbb{L}(t) \right] \, \tilde{\mathbb{G}}(s,t) \ , \qquad \tilde{\mathbb{G}}(s,0) = \mathbb{I} \ . \tag{2.71}$$

The matrix which multiplies $\tilde{\mathbb{G}}(s,t)$ on the right hand side is again a lower two-diagonal one. Therefore, as in the case of Eq. (2.68), we find the recursive relation

$$\begin{aligned}
\tilde{G}_{ij}(s,t) &= 0 \ , && i < j \ , \\
\tilde{G}_{jj}(s,t) &= \mathrm{e}^{-\Lambda(t,0)} \mathrm{e}^{-s[\mathcal{E}_j(t) - \mathcal{E}_j(0)]} \ , && j = 1, \ldots, N \ , \\
\tilde{G}_{ij}(s,t) &= \int_0^t \mathrm{d}t' \mathrm{e}^{-\Lambda(t,t')} \mathrm{e}^{-s[\mathcal{E}_i(t) - \mathcal{E}_i(t')]} \, \lambda(t') \, \tilde{G}_{i-1j}(s,t') \ , && j < i < N \ , \\
\tilde{G}_{Nj}(s,t) &= \int_0^t \mathrm{d}t' \mathrm{e}^{-s[\mathcal{E}_N(t) - \mathcal{E}_N(t')]} \, \lambda(t') \, \tilde{G}_{N-1j}(s,t') \ , && j = 1, \ldots, N \ .
\end{aligned} \tag{2.72}$$

Notice that the matrix $\tilde{\mathbb{G}}(s,t)$ is again a lower triangular one. We now want to solve these recursive relations. It turns out that all matrix elements of the matrix $\tilde{\mathbb{G}}(s,t)$, except the matrix elements $\tilde{G}_{Nj}(s,t)$, $j=1,\ldots,N-1$, can be explicitly evaluated by simple integrations:

$$\tilde{G}_{j+kj}(s,t) = \mathrm{e}^{-\Lambda(t,0)}\,\frac{\exp\left[s(j-1)vt\right]}{k!}\left\{\frac{\alpha}{v(\beta-s)}\left[\exp(\beta vt)-\exp(svt)\right]\right\}^k \quad , \quad (2.73)$$

for $j=N$, $k=0$ and also for $j=1,\ldots,N-1$, $k=0,\ldots,N-1-j$. Moreover, we were able to carry out the inverse Laplace transform of these functions. The resulting diagonal elements $G_{jj}(w,t)$, $j=1,\ldots,N$ are proportional to Dirac δ-functions. The remaining ones possess a finite support, i.e., they are proportional to the differences of the unit-step functions $\Theta(a,b;x)=\Theta(x-a)-\Theta(x-b)$,

$$\begin{aligned} G_{jj}(w,t) &= \delta[w+(j-1)vt]\,\mathrm{e}^{-\Lambda(t,0)} \quad , \qquad j=1,\ldots,N \quad , & (2.74)\\ G_{j+kj}(w,t) &= \mathrm{e}^{-\Lambda(t,0)}\left(-\frac{\alpha}{v}\right)^k \frac{\exp\left\{\beta[w+(k+j-1)vt]\right\}}{(k-1)!}\times \\ &\times \sum_{l=0}^{k}\frac{(-1)^l}{l!\,(k-l)!}\,\frac{\Theta[(1-j-l)vt,(1-j)vt;w]}{[w+(j+l-1)vt]^{1-k}} \quad . & (2.75) \end{aligned}$$

Eq. (2.75) is valid for $j=1,\ldots,N-1$ and $k=1,\ldots,N-1-j$.

It remains to calculate the matrix elements $\tilde{G}_{Nj}(s,t)$, $j=1,\ldots,N$. The inverse Laplace transform of the last formula in the recursive scheme (2.72) is

$$G_{Nj}(w,t) = \int_0^t \mathrm{d}t'\lambda(t')\,G_{N-1j}\left\{w-[\mathcal{E}_N(t)-\mathcal{E}_N(t')],t'\right\} \quad , \quad (2.76)$$

where $j=1,\ldots,N-1$. We insert herein the explicit forms of Eqs. (2.74) and (2.75). After some algebra we finally obtain

$$\begin{aligned} G_{NN-1}(w,t) &= \frac{\alpha}{v}\exp\left\{\beta[w+(N-1)vt]\right\}\times \\ &\exp\left\{-\Lambda\left[\frac{w}{v}+(N-1)t,0\right]\right\}\times\Theta[-(N-1)vt,-(N-2)vt;w] \quad , \quad (2.77) \end{aligned}$$

$$\begin{aligned} G_{Nj}(w,t) &= \frac{\alpha\left(-\frac{\alpha}{v}\right)^{N-1-j}}{(N-2-j)!}\,\exp\{\beta[w+(N-1)vt]\}\sum_{l=0}^{N-1-j}\frac{(-1)^l}{l!\,(N-1-j-l)!}\times \\ &\times\left\{F_{jl}\left[\frac{w+(N-1)vt}{v(N-j)},\frac{w+(N-1)vt}{v(N-j-l)};w,t\right]\Theta[-(N-1)vt,-(j+l-1)vt;w]+\right. \\ &\left.+F_{jl}\left[\frac{w+(N-1)vt}{v(N-j)},t;w,t\right]\Theta[-(j+l-1)vt,-(j-1)vt;w]\right\} \quad , \quad (2.78) \end{aligned}$$

In Eq. (2.78) $j \in \{1, \ldots, N-2\}$ and we have introduced the abbreviation

$$F_{jl}(a,b;w,t) = \int_a^b \mathrm{d}t' \, \exp\left[-\Lambda\left(t',0\right)\right] \times \\ \left[w + (N-1)vt - (N-j-l)vt'\right]^{N-j-2} \ . \quad (2.79)$$

The main results of this Subs. are Eqs. (2.69) and (2.70), which give the solution of the master Eq. (1.3), and Eqs. (2.74)-(2.79) which present the solution of Eq. (1.13). We now turn to the discussion of these results.

2.4.5 Discussion

In Kittel's work [110] the *equilibrium* properties of the zipper are studied. The mean number of open links in equilibrium always increases with increasing temperature, but the form of this increase is different for the degeneracy factor $G = 1$ [cf. Fig. 2.5a1)] and for $G > 1$ [cf. Fig. 2.5a2)]. For $G = 1$, the mean number of open links increases smoothly with a concave curvature, while for $G > 1$, the curve exhibits a sharp increase in a narrow temperature interval and resembles a first-order phase transition. In the following discussion of representative results for the non-equilibrium dynamics and energetics, we use d, d/k_B, and ν^{-1} as units for energy, temperature and time, respectively.

In the unidirectional unzipping process, the time evolution towards the completely unzipped microstate is again sensitive to the degeneracy factor G. Let us define an unfolding time t_U by the condition that at $t = t_\mathrm{U}$ the zipper has completely unfolded with a probability of 99,9%, i.e.,

$$p_N(t_\mathrm{U}) = R_{N1}(t_\mathrm{U}) = 1 - \epsilon \ , \quad (2.80)$$

where $\epsilon = 0.001$. With respect to the N dependence of t_U (and other quantities to be discussed below), we found that its behavior is similar for $N = 2$ and $N > 2$, and we therefore restrict the following discussion to the two-level case $N = 2$. Eq. (2.80) can then be inverted after inserting $R_{N1}(t_\mathrm{U})$ from Eq. (2.70) in Eq. (2.80), yielding

$$t_\mathrm{U} = \frac{1}{\beta v} \ln\left[1 - \frac{\beta v}{\alpha} \ln \epsilon\right] \ . \quad (2.81)$$

For small temperatures [large argument of the exponential and/or small prefactor g in Eq. (2.56)] the transitions are driven predominantly by the magnitude of the energy gap between the closed and the opened microstate. For large temperatures [small argument of the exponential and/or large prefactor g in Eq. (2.56)] by contrast, the dynamics is governed by the entropy difference between the closed and the opened microstate, and hence by the degeneracy factor G. The dependence of the unfolding time t_U on G and T is plotted in Fig. 2.5b) for a representative set of parameters. For any fixed nonzero temperature, the unfolding time decreases with increasing G, while for fixed G, the temperature-dependence of the unfolding time exhibits a maximum at a temperature $T = T_\mathrm{max}(G)$, where $T_\mathrm{max}(G)$ decreases with increasing G, see Fig. 2.5b).

Let us now consider a certain temperature T_0 and call, for this temperature, the *fast-unzipping regime* and *slow-unzipping regime* the ranges of G-values,

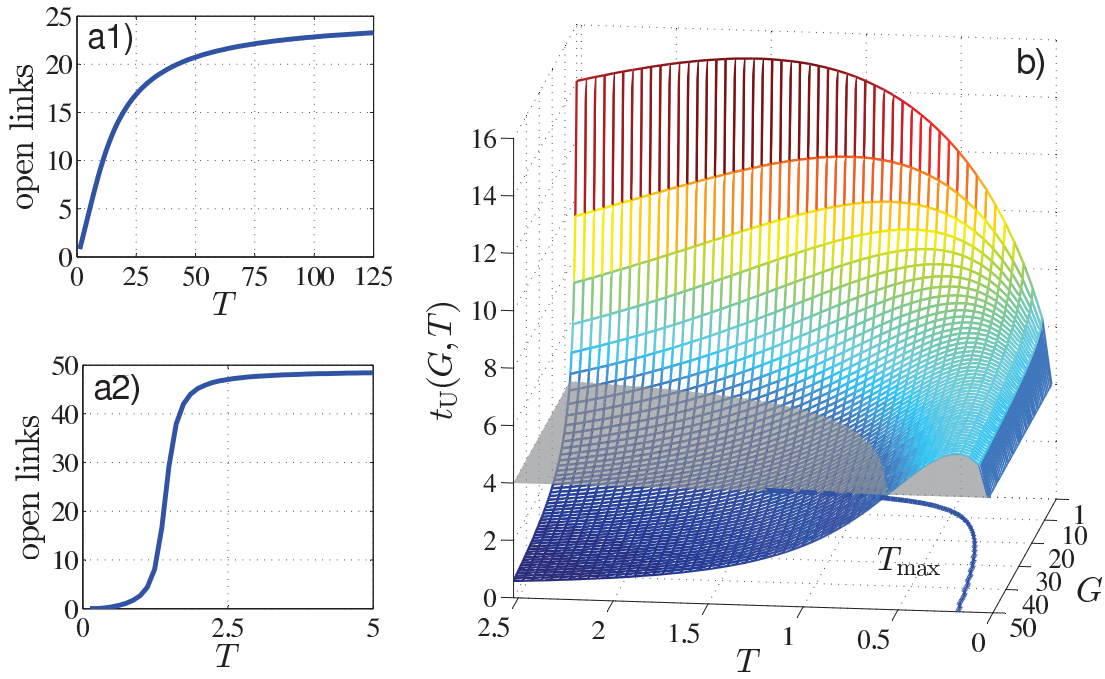

FIG. 2.5: Left two panels: Mean number of open links in equilibrium for Kittel's molecular zipper as a function of the reservoir temperature T for $N = 50$ links, and [a1)] $G = 1$ and [a2)] $G = 2$. Right panel b): Unfolding time t_U, EQ. (2.81), as a function of T and G for $T_0 = 7.5$, $v = 0.25$, and $N = 2$. Above (below) the horizontal plane in the graph, the opened (closed) microstate is energetically favored. In the base plane, the temperature T_{max} of maximal unfolding time in dependence of the degeneracy factor G is shown.

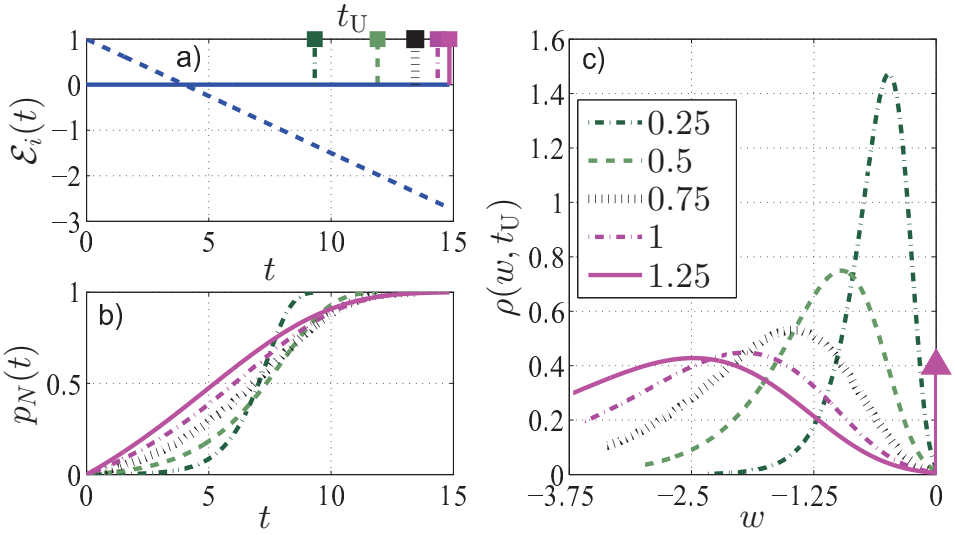

FIG. 2.6: Dynamics of a) the energy levels [EQ. (2.53)], b) the occupation probability $p_N(t)$ of the opened microstate [EQ. (2.65)], and c) the probability density $\rho(w, t_U)$ of the work [EQ. (1.16)] for $G = 1$ and several values of the reservoir temperature T. The other parameters are the same as in FIG. 2.5. The assignment of the line styles to the temperature given in the legend of c) applies also to parts a) and b). In a) we compare the dynamics of the two energy levels with the unfolding time t_U [EQ. (2.81)] at different temperatures marked by the vertical lines. The solid (dashed) line gives the energy $\mathcal{E}_1(t)$ [$\mathcal{E}_2(t)$] of the closed (unzipped) microstate. The arrows in c) represent the weights and the positions of the δ-functions, which form the singular part of the probability density.

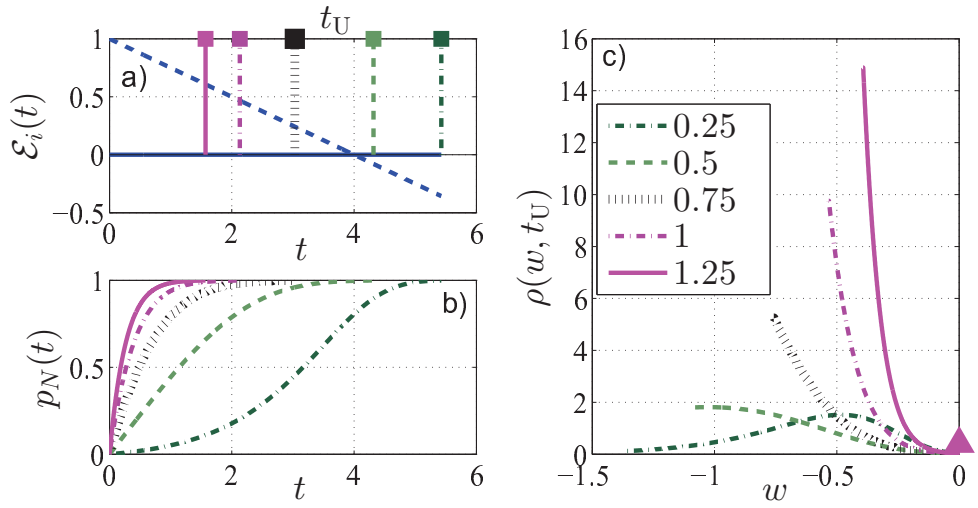

FIG. 2.7: Same quantities as in FIG. 2.6 for $G = 50$ and otherwise the same set of parameters.

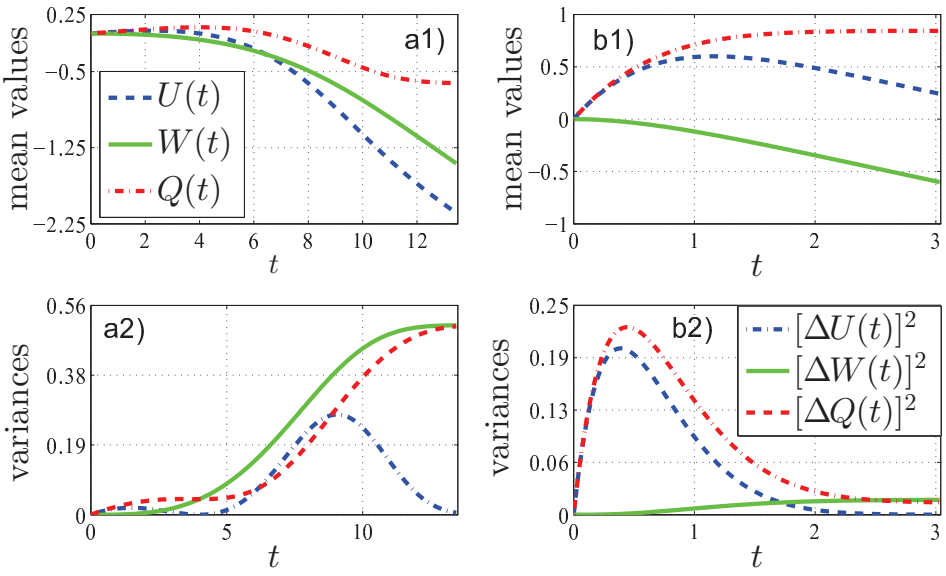

FIG. 2.8: Upper two panels: Mean value of the internal energy [EQ. (1.22)], work [EQ. (1.23)] and heat [EQ. (1.24)] as a function of time for a1) $G = 1$ and b1) $G = 50$. Lower two panels: Variances of internal energy [EQ. (1.28)], work [EQ. (1.29)] and heat [EQ. (1.30)] as a function of time for a2) $G = 1$ and b2) $G = 50$. The temperature is $T = 0.75$ and the other parameters are the same as in FIG. 2.5.

where $T_{\max}(G) < T_0$ and $T_{\max}(G) > T_0$, respectively. In these two regimes the dynamics and energetics of the molecular zipper exhibit a qualitatively different behavior. In particular we find (i) a different time-dependence of the N-th level's occupation probability, cf. FIGS. 2.6b) and 2.7b), (ii) a different form of the curves describing the work needed to open the zipper, cf. FIGS. 2.6c) and 2.7c), (iii) a different mean value of heat accepted by the zipper during the unzipping, cf. FIGS. 2.8a1) and 2.8b1), and iv) different values of the variances of the internal energy and heat during the unzipping, cf. FIGS. 2.8a2) and 2.8b2). These features will be now discussed in more detail.

FIG. 2.6 illustrates the slow-unzipping regime. The probability $p_N(t)$ that the zipper has reached the opened microstate until time t first increases slowly. After the time d/v the energy of the opened microstate becomes lower than that of the closed one. This leads to more frequent transitions and accordingly $p_N(t)$ increases more rapidly. Notice that the curves exhibit a change of their second derivative. The WPD during the unzipping has a maximum located inside its finite support, cf. FIG. 2.6c). The value of the work at the left (right) border of the support equals the work done on the zipper when it dwells during the time interval $[0, t_U]$ in the opened (closed) microstate. From the position of the WPD peak we can conclude that, for a typical trajectory of the stochastic process $\mathsf{D}(t)$, the work consists of two comparable fractions. The first (second) part of the work is performed while the system dwells in the closed (opened) microstate. At time t_{U}, 0.1% of the trajectories will give molecules still residing in the zipped microstate. These trajectories contribute to the singular (δ-function) components of WPDs, which are depicted in FIG. 2.6c) by the vertical arrows [31, 35, 52, 179].

Note that the curves plotted for the temperatures $T = 1$ and $T = 1.25$, which are close to the temperature $T_{\max}(\mathrm{G})$ for $G = 1$, cf. FIG. 2.5b), become similar to the curves for these temperatures obtained in the fast-unzipping regime for $G = 50$, see FIG. 2.7.

FIG. 2.7 illustrates the fast-unzipping regime. The probability $p_N(t)$ rapidly increases from the very beginning of the process, cf. FIG. 2.7b), i.e., the zipper opens before the opened microstate becomes energetically preferred. The maximum of the WPD is located at the left border of its support, cf. FIG. 2.7c). This means that, for the majority of the trajectories, the substantial part of the work is done while the system dwells in the opened microstate. Note that the curves plotted for the temperature $T = 0.25$, which is close to the boundary temperature $T_{\max}(\mathrm{G})$ for $G = 50$, cf. FIG. 2.5b), become similar to the curves for this temperature in the fast-unzipping regime for $G = 1$, see FIG. 2.6.

FIG. 2.8 illustrates the dynamics of the thermodynamic quantities (1.22)–(1.30) in the two unzipping regimes. For an arbitrary trajectory of $\mathsf{D}(t)$ which resides during the time interval $[t', t]$ in the i-th level, the work performed on the system is $\mathcal{E}_i(t) - \mathcal{E}_i(t')$, cf. EQ. (2.59). In our model, the energies of the levels decrease linearly with time and accordingly the mean work is a monotonically decreasing function of time, see FIGS. 2.8a1) and 2.8b1). Heat is exchanged with the reservoir when the molecule changes its microstate. It is absorbed by the molecule if the transition brings the molecular zipper to a level with higher energy. Since in our setting the transitions are unidirectional, the molecule necessarily absorbs heat up to the time $t_E = d/v$, where the energies of the levels become the same, cf. FIGS. 2.6a) and 2.7a). For times $t > t_E$, the molecule delivers heat to the environment. In the slow-unzipping regime we have $t_{\mathrm{U}} > t_E$. This implies that the mean heat first increases and then decreases, cf. FIG. 2.8a1). By contrast, in the fast-unzipping regime where $t_{\mathrm{U}} < t_E$, the mean heat monotonically increases, cf. FIG. 2.8b1). Finally, due to the transitions to the level with higher energy at the very beginning of the process, cf. FIGS. 2.6 and 2.7, the mean internal energy (1.22) develops a single maximum.

The variances of $\mathsf{U}(t)$, $\mathsf{W}(t)$ and $\mathsf{Q}(t)$, cf. EQS. (1.28)–(1.30), are plotted in FIGS. 2.8a2) and FIGS. 2.8b2). If the variance of the internal energy approaches zero, the variance of the work becomes equal to that of the heat. All variances approach constant values at large times. In fact, for $t > t_U$, almost all trajectories have brought the molecule into the opened microstate. As a consequence, the increments to the work, heat and internal energy are nearly constant during the time interval $[t_{\mathrm{U}}, t]$. Therefore the form of their probability densities does not change, the curves just move along the energy axis.

The probability density for the internal energy has no continuous component. In general it consists of N δ-functions located at the energies of the individual levels. The corresponding weights are given by the occupation probabilities of the levels. In the slow-unzipping regime, $[\Delta U(t)]^2$ vanishes at time $t = 0$ and at time $t_E = d/v$, when the level energies are equal, and it becomes very close to zero for $t \gtrsim t_{\mathrm{U}}$. In between these time instants, the variance develops a maximum, cf. FIG. 2.8a2). In the fast-unzipping regime, the function $[\Delta U(t)]^2$ displays just one maximum, cf. FIG. 2.8b2), because $t_{\mathrm{U}} < t_E$.

In both the fast and slow unzipping regime, the variance of the work monotonically increases and approaches a constant for large times, cf. FIG. 2.8a2) and

FIG. 2.8b2). The absolute value of the first derivate of the variance $[\Delta Q(t)]^2$ is given by the product of the two quantities, the energy difference between the closed and the opened microstates at time t and the probability that the zipper opens at the time t, which were shown in FIGS. 2.6 and 2.7. In the slow-unzipping regime, the majority of the transitions occurs during the time interval $[t_E, t_{\mathrm{U}}]$. During this time interval, the energy difference between the levels monotonically increases. In the fast-unzipping regime, by contrast, nearly all transitions take place before time $t_E/2$. The sooner the transition, the larger is the amount of transferred heat. As a result, at small times, the heat probability density has one peak at a large value, coming from the trajectories with a transition to the opened microstate, and another peak at zero heat exchange, originating from trajectories without a transition. With increasing time the amount of the trajectories with a transition to the opened microstate increases rapidly, and the peak close to zero heat moves towards the peak at a large heat value. This explains the behavior of the heat variances in FIGS. 2.8a2) and 2.8b2).

Finally, one may ask how our results are affected if the variation ("static disorder") in base pairing energies is included in the modeling. To this end we have performed Monte Carlo simulations [92] of the stochastic process for a molecular zipper with $N = 10$ energy levels, where the initial energies $\mathcal{E}_k(0) = \mathcal{U}_k$, $k = 1, \ldots, N$, in EQ. (2.53) are given by $\mathcal{U}_k = (k-1)(\Delta + \eta_k)$, corresponding to different losses of energies due to variations in base pair bondings. The η_k were chosen as random numbers from a box distribution in the interval $[-\Delta/3, \Delta/3]$. Results from these simulations for a number of realizations of this disorder were compared to the predictions of the analytical theory for the "ordered case", where $\mathcal{U}_k = (k-1)\Delta$. We found that, for typical realizations of sets of η_k, the shapes of the work distributions are very similar, while the peak positions and peak heights are shifted slightly. Also the probability distributions $p_N(t)$ for the zipper to fully open until time t are, for these sets of η_k, very similar in shape. Analogous to the peak positions of the work distributions, the onset of opening shifts slightly from realization to realization. The shifts of the peaks and of the onset of the opening are controlled by the largest base pair bonding (largest η_k), which governs the unfolding time.

3. Continuous State Space Models

3.1 The two works – a toy model

In this Sec. we illustrate the difference between the two work definitions (1.44) and (1.53) on two specific models. Specifically, we demonstrate validity of the individual formulas presented in Subs. 1.2.3. Moreover, we introduce two examples of externally controlled parameters $\boldsymbol{Y}(t)$ used in single molecule experiments [3, 40, 150, 151].

Consider a microscopic spring in contact with a heat reservoir, which is, by one of its ends, attached to a wall located at $x = 0$. For sake of mathematical simplicity we assume that the force exerted by the spring equals zero when its elongation vanish, i.e., when its free end is at $x = 0$, and that the spring can be stretched either in the positive and in the negative direction. Our goal will be simple: to stretch the spring.

In such situation the microstate of the system is determined by the random spring elongation $\mathsf{X}(t) \in (-\infty, \infty)$ and the energy (free energy) landscape of the system alone (the spring) assumes the form

$$\mathcal{U}(x) = \mathcal{G}(x) = \frac{1}{2} k_{\mathrm{m}} x^2 \ , \tag{3.1}$$

where k_{m} denotes the spring stiffness. Having in mind that we perform our experiment at microscale, it seems difficult, although possible, to apply a controllable force on the free end of the spring *directly* [3]. Instead one would rather stretch the spring *indirectly* by inserting its free end into an externally controlled potential. This setup is sketched in Fig. 3.1, the setup when the spring is stretched by a directly controlled force is depicted in Fig. 3.2. We first analyze the setup where the force is applied indirectly.

3.1.1 Indirectly controlled force

Assume that the interaction potential applied on the spring is parabolic and that the single control parameter is the position of its minimum $\boldsymbol{Y}(t) = Y(t) = Y$, i.e.,

$$\tilde{\mathcal{V}}(x, Y) = \frac{1}{2} k_{\mathrm{o}} (x - Y)^2 \ . \tag{3.2}$$

Eqs. (3.1) and (3.2) yield the total energy (free energy) of the compound system via Eqs. (1.35) and (1.36). Specifically we have

$$\mathcal{E}(x, t) = \mathcal{F}(x, t) = \frac{1}{2} k_{\mathrm{m}} x^2 + \frac{1}{2} k_{\mathrm{o}} [x - Y(t)]^2 \ . \tag{3.3}$$

The whole setting is depicted in Fig. 3.1. Assume that the minimum of the potential is shifted during the time interval $[t', t]$ from the position $Y(t') = 0$ to a new one, $Y(t)$. In such case the thermodynamic work (1.44) and the mechanical

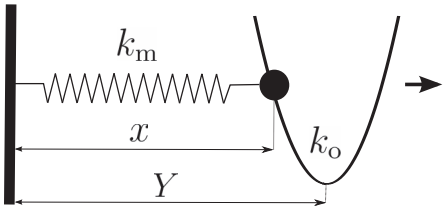

FIG. 3.1: Stretching of a spring via force controlled indirectly by the position of the minimum of an external potential.

work (1.53) are given by

$$\mathsf{W}(t,t') = k_{\rm o}\int_{t'}^{t} {\rm d}t''\,[Y(t'') - \mathsf{X}(t'')]\dot{Y}(t'')\ , \tag{3.4}$$

$$\mathsf{W}_{\rm E}(t,t') = k_{\rm o}\int_{t'}^{t} {\rm d}t''\,[Y(t'') - \mathsf{X}(t'')]\frac{{\rm d}\mathsf{X}(t'')}{{\rm d}t''}\ , \tag{3.5}$$

respectively.

Mean values

Assume that the potential changes quasi-statically, then the mean values of these two integrals can be evaluated using the mean equilibrium length of the spring

$$\langle[\mathsf{X}(t)]_{\rm eq}\rangle = \frac{k_{\rm o}}{k_{\rm o}+k_{\rm m}}Y(t)\ . \tag{3.6}$$

If we substitute this expression for $\mathsf{X}(t)$ in EQS. (3.4) and (3.5), we obtain

$$\langle[\mathsf{W}(t,t')]_{\rm eq}\rangle = \frac{1}{2}\frac{k_{\rm o}k_{\rm m}}{k_{\rm o}+k_{\rm m}}[Y(t)]^2\ , \tag{3.7}$$

$$\langle[\mathsf{W}_{\rm E}(t,t')]_{\rm eq}\rangle = \frac{1}{2}\frac{k_{\rm o}^2k_{\rm m}}{(k_{\rm o}+k_{\rm m})^2}[Y(t)]^2\ . \tag{3.8}$$

On the other hand, the increase of the free energy of the compound system (system-interaction) and that of the system itself are given by

$$\Delta F(t,t') = \mathcal{F}\left(\langle[\mathsf{X}(t)]_{\rm eq}\rangle,t\right) - \mathcal{F}\left(\langle[\mathsf{X}(t')]_{\rm eq}\rangle,t'\right) = \frac{1}{2}\frac{k_{\rm o}k_{\rm m}}{k_{\rm o}+k_{\rm m}}[Y(t)]^2\ , \tag{3.9}$$

$$\Delta F_0(t,t') = \mathcal{G}\left(\langle[\mathsf{X}(t)]_{\rm eq}\rangle\right) - \mathcal{G}\left(\langle[\mathsf{X}(t')]_{\rm eq}\rangle\right) = \frac{1}{2}\frac{k_{\rm o}^2k_{\rm m}}{(k_{\rm o}+k_{\rm m})^2}[Y(t)]^2\ , \tag{3.10}$$

respectively, and hence the relations (1.55) and (1.57) for the given model are verified. Similarly, one can check also the relation (1.60):

$$-\mathcal{V}\left(\langle[\mathsf{X}(t)]_{\rm eq}\rangle,t\right) + \mathcal{V}\left(\langle[\mathsf{X}(t')]_{\rm eq}\rangle,t'\right) + \Delta F(t,t') = \frac{1}{2}\frac{k_{\rm o}^2k_{\rm m}}{(k_{\rm o}+k_{\rm m})^2}[Y(t)]^2\ . \tag{3.11}$$

Fluctuations

The dynamics of the spring is described by the Langevin EQ. (1.37) (we take $\Gamma = 1$)

$$\frac{\rm d}{{\rm d}t}\mathsf{X}(t) = -k_{\rm m}\mathsf{X}(t) + k_{\rm o}[Y(t) - \mathsf{X}(t)] + \mathsf{N}(t)\ . \tag{3.12}$$

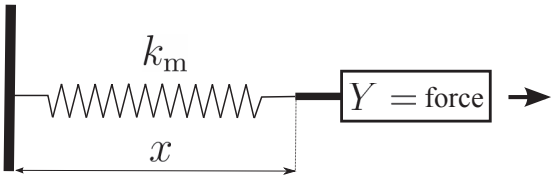

FIG. 3.2: Stretching of a spring via force controlled directly.

The spring elongation $\mathsf{X}(t)$ can be formally integrated. It turns out that $\mathsf{X}(t)$ is a linear function of the Gaussian white noise $\mathsf{N}(t)$ and hence its probability distribution is Gaussian. Similarly, the thermodynamic work (3.4) is a linear function of the system state $\mathsf{X}(t)$. Therefore its probability density must be also Gaussian [125] specified solely by the mean work and work variance, which can be calculated from EQS. (3.4) and (3.12) for an arbitrary function $Y(t)$ [94, 125]. Derivation of the WPD for a similar model is presented in SEC. 3.2. The mechanical work is a quadratic function of $\mathsf{X}(t)$ and its probability density is not Gaussian. WPD for a similar model, the so called "breathing parabola", was investigated in [53, 134, 152, 176] (see also SEC. 4.2). The exact WPD can be also obtained by numerical integration of EQS. (3.5) and (3.12). Nevertheless, no matter the densities are, they must obey the fluctuation theorems (1.61)-(1.65).

3.1.2 Directly controlled force

Assume that the single control parameter $\boldsymbol{Y}(t) = Y(t) = Y$ is the force exerted on the spring itself (see FIG. 3.2). In such case the interaction energy (- work done on the spring by the constant force Y to stretch it by the amount x) reads

$$\tilde{\mathcal{V}}(x, Y) = -xY \ . \tag{3.13}$$

EQS. (3.1) and (3.13) yield the total energy (free energy) of the compound system via EQS. (1.35) and (1.36). Specifically we have

$$\mathcal{E}(x,t) = \mathcal{F}(x,t) = \frac{1}{2}k_{\mathrm{m}}x^2 - xY(t) \ . \tag{3.14}$$

Assume that the force is increased during the time interval $[t', t]$ from the value $Y(t') = 0$ to a new one, $Y(t)$. In such case the thermodynamic work (1.44) and the mechanical work (1.53) are given by

$$\mathsf{W}(t,t') = -\int_{t'}^{t} \mathrm{d}t''\, \mathsf{X}(t'')\dot{Y}(t'') \ , \tag{3.15}$$

$$\mathsf{W}_{\mathrm{E}}(t,t') = \int_{t'}^{t} \mathrm{d}t'' \, \frac{\mathrm{d}\mathsf{X}(t'')}{\mathrm{d}t''} Y(t'') \ , \tag{3.16}$$

respectively.

Mean values

Assume that the force changes quasi-statically, then the mean values of these two integrals can be evaluated using the mean equilibrium length of the spring

$$\langle [\mathsf{X}(t)]_{\mathrm{eq}} \rangle = \frac{1}{k_{\mathrm{m}}} Y(t) \ . \tag{3.17}$$

If we substitute this expression for $\mathsf{X}(t)$ in Eqs. (3.15)-(3.16), we obtain

$$\langle[\mathsf{W}(t,t')]_{\mathrm{eq}}\rangle = -\frac{1}{2k_{\mathrm{m}}}[Y(t)]^2 \ , \tag{3.18}$$

$$\langle[\mathsf{W}_{\mathrm{E}}(t,t')]_{\mathrm{eq}}\rangle = \frac{1}{2k_{\mathrm{m}}}[Y(t)]^2 \ . \tag{3.19}$$

On the other hand, the increase of the free energy of the compound system (system and interaction) and that of the system itself are given by

$$\Delta F(t,t') = \mathcal{F}\left(\langle[\mathsf{X}(t)]_{\mathrm{eq}}\rangle, t\right) - \mathcal{F}\left(\langle[\mathsf{X}(t')]_{\mathrm{eq}}\rangle, t'\right) = -\frac{1}{2k_{\mathrm{m}}}[Y(t)]^2 \ , \tag{3.20}$$

$$\Delta F_0(t,t') = \mathcal{G}\left(\langle[\mathsf{X}(t)]_{\mathrm{eq}}\rangle\right) - \mathcal{G}\left(\langle[\mathsf{X}(t')]_{\mathrm{eq}}\rangle\right) = \frac{1}{2k_{\mathrm{m}}}[Y(t)]^2 \ , \tag{3.21}$$

respectively, and hence the relations (1.55) and (1.57) for the given model are verified. Similarly, one can check also the relation (1.60):

$$-\mathcal{V}\left(\langle[\mathsf{X}(t)]_{\mathrm{eq}}\rangle, t\right) + \mathcal{V}\left(\langle[\mathsf{X}(t')]_{\mathrm{eq}}\rangle, t'\right) + \Delta F(t,t') = \frac{1}{2k_{\mathrm{m}}}[Y(t)]^2 \ . \tag{3.22}$$

Fluctuations

The dynamics of the spring can be described by the Langevin Eq. (1.37) (we take $\Gamma = 1$)

$$\frac{\mathrm{d}\mathsf{X}(t)}{\mathrm{d}t} = -k_{\mathrm{m}}\mathsf{X}(t) + Y(t) + \mathsf{N}(t) \ . \tag{3.23}$$

$\mathsf{X}(t)$ is a linear function of the Gaussian white noise and its probability distribution is Gaussian. Further, both the thermodynamic work (3.15) and the mechanical work (3.16) are linear functions of the system state $\mathsf{X}(t)$. Therefore their probability densities must also be Gaussian [125] specified solely by the individual mean works and work variances, which can be calculated from Eqs. (3.15), (3.16) and (3.23) for an arbitrary function $Y(t)$. Derivation of the WPD for a similar model is presented in Sec. 3.2. However, no matter the densities are, they must obey the fluctuation theorems (1.61)-(1.65).

3.2 Sliding parabola

The following work was published, with small modifications, in [94]. Consider a particle in contact with a thermal bath at the temperature T. Let the particle move in the externally driven time-dependent parabolic potential [125]

$$\tilde{\mathcal{V}}[x, Y(t)] = \frac{k}{2}[x - Y(t)]^2 \ . \tag{3.24}$$

We assume that $\mathcal{G}(x) = 0$ and thus $\mathcal{E}(x,t) = \mathcal{F}(x,t) = \tilde{\mathcal{V}}[x, Y(t)]$, cf. Eqs. (1.35) and (1.36). One can regard the particle as being attached to a spring the other end of which moves with an instantaneous velocity $\dot{Y}(t)$. Such situation is depicted in Fig. 1.1 if one assumes that $\dot{Y}(t)$ denotes the speed of the car. The Langevine Eq. (1.37) for the particle position is given by

$$\Gamma\frac{\mathrm{d}}{\mathrm{d}t}\mathsf{X}(t) = -k\left[\mathsf{X}(t) - Y(t)\right] + \mathsf{N}(t) \tag{3.25}$$

with the initial condition $\mathsf{X}(t') = x'$. The work (1.44) is driven by the formula

$$\frac{\mathrm{d}}{\mathrm{d}t}\mathsf{W}(t,t') = -k\dot{Y}(t)[\mathsf{X}(t) - Y(t)] \tag{3.26}$$

with the initial condition $\mathsf{W}(t',t') = 0$. The Fokker-Planck Eq. (1.45) corresponding to Eqs. (3.25) and (1.43) reads

$$\frac{\partial}{\partial t}G(x,w,t\,|\,x',w',t') = \left\{ D\,\frac{\partial^2}{\partial x^2} + \frac{k}{\Gamma}\frac{\partial}{\partial x}\,[x - Y(t)] + \right. \\ \left. + [x - Y(t)]\,\dot{Y}(t)\frac{\partial}{\partial w} \right\} G(x,w,t\,|\,x',w',t') \tag{3.27}$$

with the initial condition $G(x,w,t'\,|\,x',w',t') = \delta(x-x')\delta(w-w')$. This Eq. can be solved by several methods. For example, one can use the Lie algebra operator methods [191, 192], or one can calculate the joint generating functional for the coupled process in question [10]. In the following we present two methods of the solution.

The first one is based on the following property of Eq. (3.27): if at an arbitrary fixed instant the probability density $G(x,w,t\,|\,x',w',t')$ is of the Gaussian form, then it will preserve this form for all subsequent times. This follows from the fact that all the coefficients on the right hand side of Eq. (3.27) are polynomials of the degree at most one in the independent variables x and w [187]. Accordingly, the function $G(x,w,t\,|\,x',w',t')$ corresponds to the bivariate Gaussian distribution [125]

$$G(x,w,t\,|\,x',w',t') = \frac{1}{2\pi\sqrt{[\Delta X(t,t')]^2\,[\Delta W(t,t')]^2 - [c_{xw}(t,t')]^2}}\times \\ \times \exp\left\{ -\frac{1}{2}\frac{[\Delta W(t,t')]^2[w - W(t,t')]^2 + [\Delta X(t,t')]^2[x - X(t,t')]^2}{[\Delta X(t,t')]^2\,[\Delta W(t,t')]^2 - [c_{yw}(t,t')]^2} \right\}\times \\ \times \exp\left\{ \frac{c_{xw}(t,t')[w - W(t,t')][x - X(t,t')]}{[\Delta X(t,t')]^2\,[\Delta W(t,t')]^2 - [c_{yw}(t,t')]^2} \right\}, \tag{3.28}$$

which is uniquely defined by the averages:

$$\begin{aligned} X(t,t') &= \langle \mathsf{X}(t) \rangle\ , \\ W(t,t') &= \langle \mathsf{W}(t,t') \rangle\ , \\ [\Delta X(t,t')]^2 &= \langle [\mathsf{X}(t)]^2 \rangle - [X(t,t')]^2\ , \\ [\Delta W(t,t')]^2 &= \langle [\mathsf{W}(t,t')]^2 \rangle - [W(t,t')]^2\ , \\ c_{xw}(t,t') &= \langle \mathsf{X}(t)\mathsf{W}(t,t') \rangle - X(t,t')W(t,t')\ . \end{aligned} \tag{3.29}$$

The simplest way to calculate these averages is to use Eqs. (3.25) and (3.26) [78, 187]. The result is given by Eqs. (3.32) and (3.38). An alternative way to solve Eq. (3.27) is to adopt the operator method introduced in [191,192] and used in [152] during the derivation of WPD for the diffusion in a time-dependent log-harmonic potential. The differential operators $\partial_{xx} = \partial^2/\partial x^2$, $\partial_x = \partial/\partial x$, $x\partial/\partial x$, $\partial_w = \partial/\partial w$, $x\partial/\partial w$ acting in Eq. (3.27) generate a closed Lie algebra. Their commutation relations are given in Tab. 3.1. Because the operators form the

	∂_{xx}	∂_x	$\partial_x x$	$x\partial_w$	∂_w	∂_{wx}	∂_{ww}
∂_{xx}	0	0	$2\,\partial_{xx}$	$2\,\partial_{wx}$	0	0	0
∂_x	0	0	∂_x	∂_w	0	0	0
$\partial_x x$	$-2\,\partial_{xx}$	$-\,\partial_x$	0	$x\partial_w$	0	$-\,\partial_{wx}$	0
$x\partial_w$	$-2\,\partial_{wx}$	$-\,\partial_w$	$-\,x\partial_w$	0	0	$-\,\partial_{ww}$	0
∂_w	0	0	0	0	0	0	0
∂_{wx}	0	0	∂_{wx}	∂_{ww}	0	0	0
∂_{ww}	0	0	0	0	0	0	0

TAB. 3.1: Closed Lie algebra generated by the differential operators contained in EQ. (3.27). Here $\partial_{wx} = \partial^2/\partial w \partial x$ etc.

closed Lie algebra, one can assume the solution of EQ. (3.27) in the form [191,192]

$$G(x,w,t' \,|\, x',w',t') = \mathrm{e}^{a_{wx}(t)\,\partial_{wx}} \mathrm{e}^{a_{ww}(t)\,\partial_{ww}} \mathrm{e}^{a_{xx}(t)\,\partial_{xx}} \times \\ \times \mathrm{e}^{a_x(t)\,\partial_x} \mathrm{e}^{a_w(t)\,\partial_w} \mathrm{e}^{{}_x a_x(t)\,\partial_x [x - Y(t)]} \mathrm{e}^{{}_x a_w(t) [x-Y(t)]\,\partial_w} G(x,w,t' \,|\, x',w',t') \ . \quad (3.30)$$

Inserting this ansatz into EQ. (3.27), performing the partial derivatives and collecting the terms containing the individual differential operators brings us to the following system of the first order ordinary differential equations for the time dependent coefficients ${}_x a_y(t)$:

$$\begin{aligned}
{}_x\dot{a}_x(t) &= \frac{k}{\Gamma} \ , \\
\exp\left[{}_x a_x(t)\right] {}_x\dot{a}_w(t) &= k\,\dot{Y}(t) \ , \\
\dot{a}_x(t) + a_x(t)\,{}_x\dot{a}_x(t) &= \dot{Y}(t) \ , \\
\dot{a}_w(t) + a_x(t) \exp\left[{}_x a_x(t)\right] {}_x\dot{a}_w(t) &= 0 \ , \\
\dot{a}_{xx}(t) + 2a_{xx}(t)\,{}_x\dot{a}_x(t) &= D \ , \\
\dot{a}_{wx}(t) + a_{wx}(t)\,{}_x\dot{a}_x(t) + 2a_{xx}(t) \exp\left[{}_x\, a_x(t)\right] {}_x\dot{a}_w(t) &= 0 \ , \\
\dot{a}_{ww}(t) + a_{wx}(t) \exp\left[{}_x a_x(t)\right] {}_x\dot{a}_w(t) &= 0 \ .
\end{aligned} \quad (3.31)$$

Initial condition for all the coefficients is ${}_x a_y(t') = 0$.

Solution of the system (3.31) reads

$$\begin{aligned}
{}_x a_x(t) &= \frac{k}{\Gamma}(t-t') \ , \\
{}_x a_w(t) &= k \int_{t'}^{t} \mathrm{d}t''\, \dot{Y}(t'') \exp\left[-\frac{k}{\Gamma}(t''-t')\right] \ , \\
a_x(t) &= \exp\left[-\frac{k}{\Gamma}(t-t')\right] \int_{t'}^{t} \mathrm{d}t''\, \dot{Y}(t'') \exp\left[\frac{k}{\Gamma}(t''-t')\right] \ , \\
a_w(t) &= -k \int_{t'}^{t} \mathrm{d}t''\, \dot{Y}(t'')\, a_x(t'') \ , \\
a_{xx}(t) &= \frac{\Gamma D}{2k}\left(1 - \exp\left[-2\frac{k}{\Gamma}(t-t')\right]\right) \ , \\
a_{wx}(t) &= -2\Gamma D \exp\left[-\frac{k}{\Gamma}(t-t')\right] \int_{t'}^{t} \mathrm{d}t''\, \dot{Y}(t'') \sinh\left[\frac{k}{\Gamma}(t''-t')\right] \ , \\
a_{ww}(t) &= -k \int_{t'}^{t} \mathrm{d}t''\, \dot{Y}(t'')\, a_{wx}(t'') \ .
\end{aligned} \quad (3.32)$$

The explicit form of the function $G(x,w,t\,|\,x',w',t')$ is found by applying the individual operators in Eq. (3.30) on the initial condition $G(x,w,t'\,|\,x',w',t') = \delta(w-w')\delta(x-x')$. The operators involved act in the following way

$$\begin{aligned}
\exp\left[a\,\partial_x\right] g(x) &= g(x+a)\ , && (3.33)\\
\exp\left[ax\,\partial_x\right] g(x) &= g(\mathrm{e}^a x)\ , && (3.34)\\
\exp\left[a\partial_{xx}\right] g(x) &= \frac{1}{\sqrt{4\pi a}}\int_{-\infty}^{\infty}\mathrm{d}y\, g(y)\exp\left[-\frac{(x-y)^2}{4a}\right]\ , && (3.35)\\
\exp\left[-a\partial x\, x\right] g(x) &= \mathrm{e}^{-a} g(x\mathrm{e}^{-a})\ , && (3.36)
\end{aligned}$$

and

$$\begin{aligned}
\exp\left[c_{xw}\,\partial_{xw}\right]\exp\left[-\frac{(w-W)^2}{2\sigma_w^2}\right]\exp\left[-\frac{(x-X)^2}{2\sigma_x^2}\right] = \sqrt{\frac{\sigma_x^2\sigma_w^2}{\sigma_x^2\sigma_w^2-c_{xw}^2}}\times\\
\times\exp\left[-\frac{1}{2}\frac{\sigma_w^2(w-W)^2-2c_{xw}(w-\overline{w})(x-X)+\sigma_x^2(x-X)^2}{\sigma_x^2\sigma_w^2-c_{xw}^2}\right]\ . \qquad (3.37)
\end{aligned}$$

The resulting function $G(x,w,t\,|\,x',w',t')$ is given by Eq. (3.28), where

$$\begin{aligned}
X(t,t') &= Y(t)+[x'-Y(t')]\exp[-{}_x a_x(t)]-a_x(t)\ ,\\
W(t,t') &= w'-a_w(t)-{}_x a_w(t)[x-Y(t')]\ ,\\
[\Delta X(t,t')]^2 &= 2a_{xx}(t)\ , \qquad (3.38)\\
[\Delta W(t,t')]^2 &= 2a_{ww}(t)\ ,\\
c_{xw}(t,t') &= a_{wx}(t)\ .
\end{aligned}$$

Surprisingly, the variance $[\Delta X(t,t')]^2$ does not depend on the function $Y(t)$. Moreover, in the asymptotic regime $t \gg \Gamma/k$, the variance $[\Delta X(t,t')]^2$ attains the saturated value $\Gamma D/k$. This means that the marginal probability density for the particle position, $R(x,t\,|\,x',t') = \int_{-\infty}^{\infty}\mathrm{d}w\, G(x,w,t\,|\,x',0,t')$, eventually attains a time-independent shape.

Up to now our considerations were valid for an arbitrary form of the function $Y(t)$. We now focus on the piecewise linear periodic driving. We take $Y(t+t_\mathrm{p}) = Y(t)$ and

$$Y(t) = -2vt \quad \text{for} \quad t\in[0,t_1]\ , \qquad Y(t) = -2vt_1+vt \quad \text{for} \quad t\in[t_1,t_\mathrm{p}]\ , \qquad (3.39)$$

where $v>0$ and $0<t_1<t_\mathrm{p}$. The parabola is first moving to the left with the velocity $2v$ during the time interval $[0,t_1)$. Then, at the time t_1, it abruptly changes its velocity and moves to the right with the velocity v during the rest of the period t_p, cf. Fig. 3.3 d).

Due to the periodic driving the system response (3.38) eventually approaches the limit cycle (cf. Subs. 1.4.1). Fig. 3.3 illustrates the response during two such limit cycles, i.e., we take $t \gg t' = 0$. First, note that the mean position of the particle $X(t,0)$ "lags behind" the minimum of the potential well $Y(t)$ [cf. the panel a)], the fact which once again reminds the horse-carrot analogy (Fig. 1). The magnitude of this phase shift is given by the second term in $X(t,t')$, Eq. (3.38), and therefore it is proportional to the velocity v. In the quasi-static limit of the infinitely slow velocity $v\to 0$ the probability distribution for the particle position is centered at the instantaneous minimum of the parabola.

Consider now the mean work done on the system by the external agent during the time interval $[0, t]$ [panel b)]. $W(t, 0)$ increases if either simultaneously $Y(t) > X(t, 0)$ and $\dot{Y}(t) > 0$, or if simultaneously $Y(t) < X(t, 0)$ and $\dot{Y}(t) < 0$. For instance, assume the parabola moves to the right and, at the same time, the probability packet for the particle coordinate is concentrated on the left from the instantaneous position of the parabola minimum $Y(t)$. Then the dragging rises the potential energy of the particle, i.e., the work is done on it and the mean input power is positive. Similar reasoning holds if either simultaneously $Y(t) > X(t, 0)$ and $\dot{Y}(t) < 0$, or if simultaneously $Y(t) < X(t, 0)$ and $\dot{Y}(t) > 0$. Than the mean work $W(t, 0)$ decreases and hence the mean input power is negative. The magnitude of the instantaneous input power is proportional to the instantaneous velocity $\dot{Y}(t)$. Therefore it is bigger during the first part of the period of the limit cycle in comparison with the second part of the period. Finally, let us stress that the mean work per cycle, $W_{\mathrm{p}} = W(t + t_{\mathrm{p}}, t) = W(t + t_{\mathrm{p}}, 0) - W(t, 0)$, is always positive, as required by the second law of thermodynamics. The variance of the work done on the particle by the external agent, $[\Delta W(t, 0)]^2$, shows qualitatively the same behavior as $W(t, 0)$.

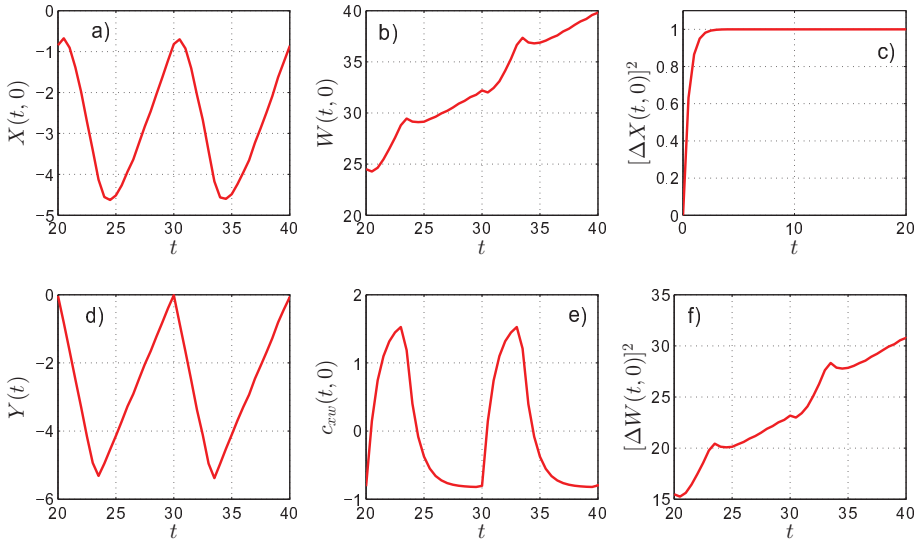

FIG. 3.3: The central moments (3.38) in the time-asymptotic regime. The driving is represented by the position of the potential minimum $Y(t)$ and it is depicted in the panel d). In all panels [except the panel c)] the curves are plotted for two periods t_{p} of the driving. The panel a) shows the mean position of the particle, $X(t, 0)$, which lags behind the minimum of the potential well. The panel b) shows the mean work $W(t, 0)$ done on the particle by the external agent. In the panel c) we observe the saturation of the variance of the particle position $[\Delta X(t, 0)]^2$. In the panel e) we present the correlation function $c_{xw}(t, 0)$. The panel f) illustrates the variance $[\Delta W(t, 0)]^2$ of the work done on the particle by the external agent. The parameters used are: $k = 1\,\mathrm{kg\,s^{-2}}$ $D = 1\,\mathrm{m^2\,s^{-1}}$, $\Gamma = 1\,\mathrm{kg\,s^{-1}}$, $v = 0.825\,\mathrm{m\,s^{-1}}$, $t_{\mathrm{p}} = 10\,\mathrm{s}$, $t_1 = 10/3\,\mathrm{s}$.

4. Heat Engines

4.1 Two state heat engine

The following work was published with minor modifications in [31, 32].

4.1.1 Introduction

In this Sec. we study a simple model of mesoscopic heat engine (Sec. 1.4) operating between two different heat baths under non-equilibrium conditions. The working medium consist of the two-level system described in Subs. 2.1.2. We consider that the cycle of operation includes just two isothermal branches, or strokes. Within each stroke, the system is driven by changing the energies of the two states and we assume a constant driving rate, i.e., a linear time-dependence of the energies. The response of the working medium is governed by the master Eq. (1.3) with time-dependent transition rates given by Eqs. (2.5) and (2.19). The specific form of the rates guarantees that, provided the two energies were fixed, the system would relax towards the Gibbs equilibrium state, cf. Fig. 1. Of course, during the motor operation, the Gibbs equilibrium is never achieved because the energies are cyclically modulated. At a given instant, the system dynamics just reflects the instantaneous position of the energy levels. After a transient regime, with the periodicity of the driving force, the system (engine) state approaches a limit cycle (see Subs. 1.4.1). We will focus on its properties. In particular, we calculate the distribution of the work during the limit cycle.

Our two-isotherm setting imposes one important feature which is worth emphasizing. As stated above, at the end of each branch we remove the present bath and we allow the thermal interaction with another reservoir. This exchange of reservoirs necessarily implies a finite difference between the new reservoir temperature and the actual system (effective) temperature. Even if the driving period tends to infinity, we will observe a positive entropy production originating from the relaxation processes initiated by the abrupt change of the contact temperature. Differently speaking, our engine operates in an inherently irreversible way and there exists no reversible limit. [1]

This Sec. is organized as follows. In Subs. 4.1.2 we solve the dynamical equation for the externally driven working medium. For the sake of clarity we first give the solution just for an unrestricted linear driving protocol using a generic driving rate and a generic reservoir. Thereupon we particularize the generic solution to individual branches and, using the Chapman-Kolmogorov condition (1.7), we derive the solution for the limit cycle. In Subs. 4.1.3 we employ the recently derived (see [179] and Subs. 2.1.2) analytical result for the work probability density under linear driving. Again, we first give the result for the generic linear driving and then we combine two such particular solutions into the final work distribution valid for the limit cycle. The results from Subs. 4.1.2 and Subs. 4.1.3 enable a detailed calculation of the energy and entropy flows during the limit cycle in Subs. 4.1.4 and allow for a discussion of the engine performance in Subs. 4.1.5.

[1] In Sec. 4.2 we show that if one considers also adiabatic branches, the reversible limit can be obtained [170].

4.1.2 Description of the engine and its limit cycle

Consider a two-level system with the time-dependent energies $\mathcal{E}_i(t)$, $i = 1, 2$, in contact with a single thermal reservoir at the temperature T. In general, the heat reservoir temperature T may also be time-dependent. The time evolution of the occupation probabilities $p_i(t)$, $i = 1, 2$, is governed by the master EQ. (1.3) with time-dependent rate matrix (2.1) specified by the reservoir temperature and by the external parameters. We will adopt the Glauber form of the transition rates, which, in contrast to the more common exponential rates ($\propto \exp\{\pm -\beta(t)[\mathcal{E}_2(t)-\mathcal{E}_1(t)/2]$), saturate at large energy differences ("driving forces"; see [51] and SUBS. 2.1.2 for a further discussion),

$$\lambda_{\rm U}(t) = \frac{1}{1+\exp\left\{-\beta(t)\left[\mathcal{E}_1(t)-\mathcal{E}_2(t)\right]\right\}}\,, \tag{4.1}$$

$$\lambda_{\rm D}(t) = \frac{\exp\left\{-\beta(t)\left[\mathcal{E}_1(t)-\mathcal{E}_2(t)\right]\right\}}{1+\exp\left\{-\beta(t)\left[\mathcal{E}_1(t)-\mathcal{E}_2(t)\right]\right\}}\,. \tag{4.2}$$

The general solution of the master equation (1.3) for these transition rates is given by EQ. (2.2). It can be rewritten as

$$\mathbb{R}(t\,|\,t') = \mathbb{1} - \frac{1}{2}\begin{pmatrix} 1 & -1 \\ -1 & 1 \end{pmatrix}\left\{1-\mathrm{e}^{-\nu(t-t')}\right\} + \frac{1}{2}\begin{pmatrix} -1 & -1 \\ 1 & 1 \end{pmatrix}\xi(t,t')\,, \tag{4.3}$$

where

$$\xi(t,t') = \nu\int_{t'}^{t}\mathrm{d}\tau\,\exp\left[-\nu(t-\tau)\right]\,\tanh\left\{\frac{\beta(\tau)}{2}\,\left[\mathcal{E}_1(\tau)-\mathcal{E}_2(\tau)\right]\right\}\,. \tag{4.4}$$

The resulting propagator satisfies the Chapman-Kolmogorov condition (1.7) for any intermediate time t''. Its validity can be easily checked by direct matrix multiplication. The condition simply states that the initial state for the evolution in the time interval $[t'', t]$ can be taken as the final state reached in the interval $[t', t'']$. This is true even if the parameters of the process in the second interval differ from those in the first one, cf. SUBS. 1.4.1. Of course, if this is the case, we should use an appropriate notation which distinguishes the two corresponding propagators. This procedure will be actually implemented below. Keeping in mind this possibility, we will first analyze the propagator for a *generic* linear driving protocol.

Generic case – linear driving protocol

Let us consider the linear driving protocol (2.3). Concretely, we take $\mathcal{E}_1(t) = h + v(t-t')$, and $\mathcal{E}_2(t) = -\mathcal{E}_1(t)$, where $h = \mathcal{E}_1(0)$ denotes the energy of the first level at the initial time t', and v is the driving velocity (energy change per time). The rates (4.1) can then be written in the form

$$\lambda_{\rm U}(t) = \nu\frac{1}{1+c\exp[-\Omega(t-t')]}\,,\quad \lambda_{\rm D}(t) = \nu\frac{c\exp[-\Omega(t-t')]}{1+c\exp[-\Omega(t-t')]}\,, \tag{4.5}$$

where $\Omega = 2\beta v$ is the temperature-reduced driving velocity, and $c = \exp(-2\beta h)$ incorporates the initial values of the energies.

Under this linear driving protocol one can evaluate the definite integral in (4.4) explicitly. Specifically, writing $\xi(t,t') = 1 - \exp[-\nu(t-t')] - 2\gamma(t,t')$, we are to calculate the definite integral

$$\begin{aligned}\gamma(t,t') &= \nu\, c \int_{t'}^{t} \mathrm{d}\tau\, \exp\left[-\nu(t-\tau)\right] \frac{\exp\left[-\Omega(\tau-t')\right]}{1+c\exp\left[-\Omega(\tau-t')\right]} \\ &= a\, c \exp\left(\Omega t'\right) \exp\left(-\nu t\right) \int_{\Omega t'}^{\Omega t} \mathrm{d}\tau\, \frac{\exp\left[(a-1)\tau\right]}{1+c\exp\left(\Omega t'\right)\exp\left(-\tau\right)} \,.\end{aligned}$$

Here we have introduced the dimensionless ratio $a = \nu/\Omega$ of the attempt frequency characterizing the time scale of the system dynamics and the time scale of the external driving, respectively. Naturally, this ratio will describe the degree of irreversibility of the process. Depending on the value $a \in (0,\infty)$, the explicit form of the function $\gamma(t,t')$ reads

$$\begin{cases} \frac{ac}{1-a} \exp\left(\Omega t'\right) \exp\left(-\nu t\right) \left\{ \exp\left[(a-1)\Omega t'\right] {}_2\mathrm{F}_1(1,1-a;2-a;-c) \right. \\ \quad \left. - \exp\left[(a-1)\Omega t\right] {}_2\mathrm{F}_1(1,1-a;2-a;-c\exp\left[-\Omega(t-t')\right]) \right\} \,, & a \in (0,1)\,, \\ c\exp\left[-\Omega(t-t')\right] \left[\Omega(t-t') + \ln \dfrac{1+c\exp\left[-\Omega(t-t')\right]}{1+c} \right] \,, & a = 1\,, \\ {}_2\mathrm{F}_1\left(1,a;1+a;-\dfrac{1}{c}\exp\left[\Omega(t-t')\right]\right) \\ -\exp\left[-a\,\Omega(t-t')\right] {}_2\mathrm{F}_1\left(1,a;1+a;-\dfrac{1}{c}\right) \,, & a > 1\,, \end{cases} \tag{4.6}$$

where ${}_2\mathrm{F}_1(\alpha,\beta;\gamma;z)$ denotes the Gauss hypergeometric function [2, 173].

Piecewise linear periodic driving

We now specify the setup for the operational cycle of the engine under periodic driving introduced in Subs. 1.4.1. Within a given period, two branches with linear time-dependence of the state energies are considered with different velocities. Starting from the value h_1, the energy $\mathcal{E}_1(t)$ linearly increases in the first branch until it attains the value $h_2 > h$, at time t_+ and in the second branch, the energy $\mathcal{E}_1(t)$ linearly decreases towards its original value h_1 in a time t_- (see Fig. 4.1). We always assume $\mathcal{E}_2(t) = -\mathcal{E}_1(t)$, i.e.,

$$\mathcal{E}_1(t) = -\mathcal{E}_2(t) = \begin{cases} h_1 + \dfrac{h_2-h_1}{t_+}\, t \,, & t \in [0,t_+] \,, \\ h_2 - \dfrac{h_2-h_1}{t_-}\,(t-t_+) \,, & t \in [t_+, t_+ + t_-] \,. \end{cases} \tag{4.7}$$

This pattern will be periodically repeated, the period being $t_\mathrm{p} = t_+ + t_-$.

As the second ingredient, we need to specify the temperature schedule. The two-level system will be alternately exposed to a hot and a cold reservoir, which means that the function $\beta(t)$ in equation (4.1) will be a piecewise constant periodic function. During the first branch, it assumes the value β_+, during the second branch it attains the value β_-.

This completes the description of the model. Any quantity describing the engine performance can only depend on the parameters h_1, h_2, $\beta_\pm$, $t_\pm$, and ν. In

the following we will focus on the characterization of the limit cycle, which the engine will approach at long times after a transient period.

We start from the general solution (4.3) of the master EQ. (1.3). Owing to the Chapman-Kolmogorov condition (1.75), the propagator within the cycle is

$$\mathbb{R}_{\rm p}(t) \equiv \mathbb{R}_{\rm p}(t\,|\,0) = \begin{cases} \mathbb{R}_+(t)\,, & t \in [0, t_+]\,, \\ \mathbb{R}_-(t)\mathbb{R}_+(t_+)\,, & t \in [t_+, t_{\rm p}]\,. \end{cases} \tag{4.8}$$

Here the matrixes $\mathbb{R}_\pm(t)$ evolve the state vector within the respective branches and have the form

$$\mathbb{R}_+(t) = \mathbb{1} - \frac{1}{2}\begin{pmatrix} 1 & -1 \\ -1 & 1 \end{pmatrix}\left[1 - {\rm e}^{-\nu t}\right] + \frac{1}{2}\begin{pmatrix} -1 & -1 \\ 1 & 1 \end{pmatrix}\xi_+(t)\,, \tag{4.9}$$

$$\mathbb{R}_-(t) = \mathbb{1} - \frac{1}{2}\begin{pmatrix} 1 & -1 \\ -1 & 1 \end{pmatrix}\left\{1 - {\rm e}^{-\nu(t-t_+)}\right\} + \frac{1}{2}\begin{pmatrix} -1 & -1 \\ 1 & 1 \end{pmatrix}\xi_-(t)\,, \tag{4.10}$$

where

$$\xi_+(t) = \nu\int_0^t {\rm d}\tau\, \exp\left[-\nu(t-\tau)\right] \tanh\left\{\beta_+\left[h_1 + \frac{h_2 - h_1}{t_+}\tau\right]\right\}, \tag{4.11}$$

$$\xi_-(t) = \nu\int_{t_+}^t {\rm d}\tau\, \exp\left[-\nu(t-\tau)\right] \tanh\left\{\beta_-\left[h_2 - \frac{h_2 - h_1}{t_-}(\tau - t_+)\right]\right\}. \tag{4.12}$$

Notice that the both propagators $\mathbb{R}_+(t)$ and $\mathbb{R}_-(t)$ are given by the generic propagator (4.3). In order to get $\mathbb{R}_+(t)$, we replace in equation (4.4) the initial position of the first energy h by h_1, the driving velocity v by $v_+ = (h_2 - h_1)/t_+$, and we set $t' = 0$. Analogously, the propagator $\mathbb{R}_-(t)$ follows from the generic propagator, if we replace h by h_2, v by $v_- = (h_1 - h_2)/t_-$, and t' by t_+.

The periodic state of the system during the cycle, $\boldsymbol{p}(t) = \mathbb{R}_+(t)\,\boldsymbol{p}^{\rm stat}$, is determined by the solution of the eigenvalue problem (1.76). The solution reads

$$p_1^{\rm stat} = 1 - p_2^{\rm stat} = \frac{1}{2}\left[1 - \frac{\xi_+(t_+)\exp\left(-\nu t_-\right) + \xi_-(t_-)}{1 - \exp\left(-\nu t_{\rm p}\right)}\right]. \tag{4.13}$$

These probabilities, and hence also the specific form of the limit cycle, depend solely on the model parameters. The driving only contain a single component and hence the limit cycle can be depicted using a single diagram (SUBS. 1.4.2). The parametric plot of the occupation difference $p(t) \equiv p_1(t) - p_2(t)$ (the response) versus the energy of the first level $\mathcal{E}_1(t) = \mathcal{E}(t)$ (the driving). It exhibits two possible forms which are exemplified in FIG. 4.1. First, we have a one-loop form which is oriented either clockwise or anticlockwise. For clockwise orientation, the work done by the engine on the environment during the limit cycle is negative, while for counter-clockwise orientation it is positive. Secondly, we can obtain a two-loops shape exhibiting again either positive or negative work on the environment. Slowing down the driving, the branches gradually approach the corresponding equilibrium isotherms $p_\pm(\mathcal{E}) = -\tanh(\beta_\pm\mathcal{E}/2)$. We postpone the further discussion of the limit cycle to SUBS. 4.1.4. In next two SUBS. we investigate fluctuations of work and heat during the cycle.

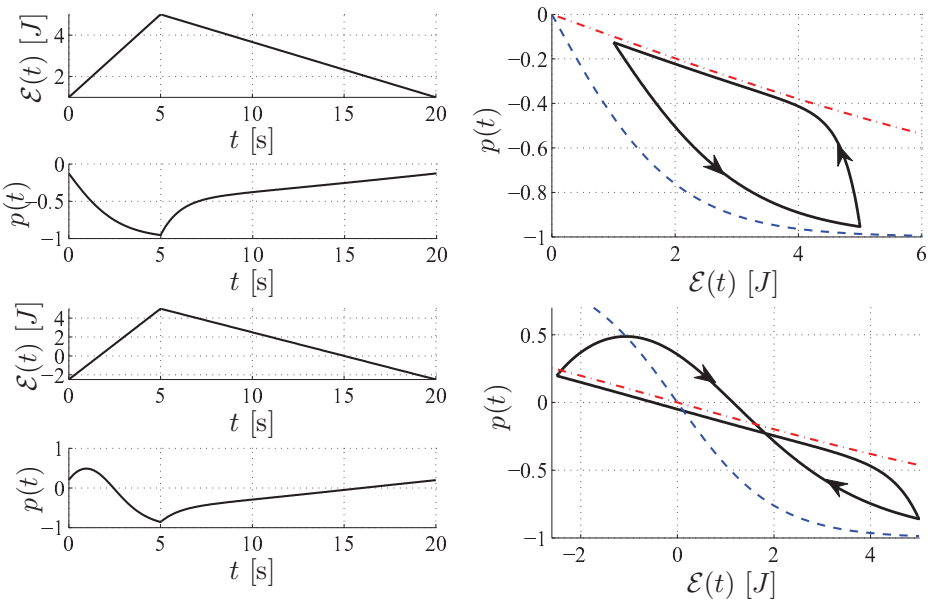

FIG. 4.1: The limit cycle for the two-stroke engine. The three graphs in the upper panel illustrate the case where $h_2 > h_1 > 0$ and the energy levels do not cross during their driving. On the left side we show $\mathcal{E}(t) = \mathcal{E}_1(t) = -\mathcal{E}_2(t)$ and the response $p(t) = p_1(t) - p_2(t)$. On the right hand side the parametric plot of the limit cycle in the p–$\mathcal{E}$ plane is displayed. The cycle starts in the upper vertex and proceeds counterclockwise, cf. the arrows. The dashed and the dot-dashed curves show the equilibrium isotherms corresponding to the baths during the first and the second stroke, respectively. The parameters are: $h_1 = 1$ J, $h_2 = 5$ J, $t_+ = 5$ s, $t_- = 15$ s, $\beta_+ = 0.5$ J^{-1}, $\beta_- = 0.1$ J^{-1}, $\nu = 1$ s^{-1}. The three graphs in the lower panel depict the case where $h_1 < 0 < h_2$ and the energies cross twice during the cycle. Except $h_1 = -2.5$ J, all parameters are as above.

4.1.3 Probability density for work and heat

For the linear driving protocol $\mathcal{E}_1(t) = h + v(t - t') = -\mathcal{E}_2(t)$ the solution of EQ. (1.13) is given by EQS. (2.21)-(2.24) where the reduced work variable η is given by $\eta = \eta(w, w') = 2\beta(w - w')$, the reduced time variable τ equals $\tau = \tau(t, t') = 2\beta|v|(t - t')$ and the parameters a and c are $a = \nu/2\beta|v|$ and $c = \exp(-2\beta h|v|/v)$, respectively. The generic result (2.21)-(2.24) immediately yields the work propagator for the individual branches in the protocol according to EQ. (4.7). We simply carry out the replacements described in the text following EQ. (4.11). We denote the corresponding matrices as $\mathbb{G}_\pm(w, t \,|\, w')$. Then the Chapman-Kolmogorov condition (1.77) yields the propagator

$$\mathbb{G}_{\rm p}(w,t) = \begin{cases} \mathbb{G}_+(w,t\,|\,0)\,, & t \in [0,t_+]\,, \\ \displaystyle\int_{-(h_2-h_1)}^{h_2-h_1} \mathrm{d}w'\, \mathbb{G}_-(w,t\,|\,w')\,\mathbb{G}_+(w',t_+\,|\,0)\,, & t \in [t_+,t_{\rm p}]\,. \end{cases} \tag{4.14}$$

As demonstrated in Subs. 1.1 and 1.4.1, the energetics during the limit cycle is described by the function

$$\xi(u,w,t;u') = \sum_{i,\,j=1}^{2} \delta\left[u - \mathcal{E}_i(t)\right] \delta\left[u' - \mathcal{E}_j(0)\right] \left[\mathbb{G}_{\rm p}(w,t)\right]_{ij} p_j^{\rm stat} \ . \tag{4.15}$$

Specifically the probability density for the work reads

$$\rho_{\rm p}(w,t) = \int_{-\infty}^{\infty} {\rm d}u \int_{-\infty}^{\infty} {\rm d}u' \ \xi(u,w,t;u') \ . \tag{4.16}$$

Similarly, the probability density for the heat accepted within the limit cycle is

$$\chi_{\rm p}(q,t) = \int_{-\infty}^{\infty} {\rm d}u \int_{-\infty}^{\infty} {\rm d}u' \int_{-\infty}^{\infty} {\rm d}w \ \delta\left[q - (u - u' - w)\right] \ \xi(u,w,t;u') \ . \tag{4.17}$$

These two functions represent the main results of the present Subs. They are illustrated in Figs. 4.2-4.4. We discuss their main features in Subs. 4.1.5.

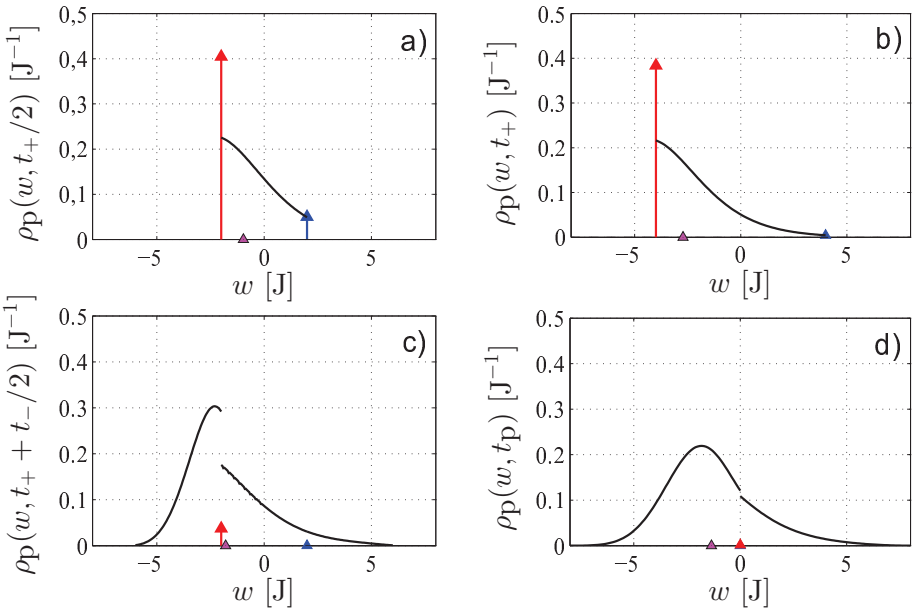

Fig. 4.2: The probability density $\rho_{\rm p}(w,t)$ as a function of the work w for the same parameters as in Fig. 4.1 (with positive h_1): a) $t = t_+/2$ (middle of the first stroke), b) $t = t_+$ (end of the first stroke), c) $t = t_+ + t_-/2$ (middle of the second stroke), and d) $t = t_+ + t_-$ (end of the limit cycle). The triangle on the work axis marks the mean work $W(t) \equiv W(t + t_{\rm p}, t_{\rm p})$ at the corresponding times. The singular parts of $\rho_{\rm p}(w,t)$ are marked by arrows, where the arrow heights equal the weights of the corresponding delta functions [for example, in panel a), the left arrow height gives the probability that the system is initially in the second state and remains in it between the beginning of the cycle and the time $t = t_+/2$; then the work done on the system equals $-(h_2 - h_1)/2$].

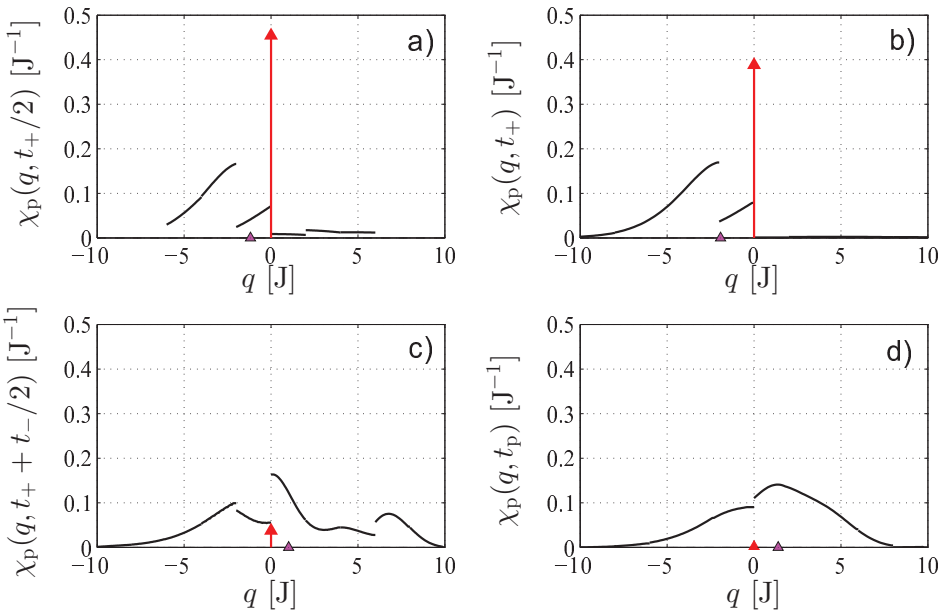

FIG. 4.3: The probability density $\chi_{\rm p}(q,t)$ as a function of the heat q and for the same parameters as in FIG. 4.1 (with positive h_1): a) $t = t_+/2$ (middle of the first stroke), b) $t = t_+$ (end of the first stroke), c) $t = t_+ + t_-/2$ (middle of the second stroke), and d) $t = t_+ + t_-$ (end of the limit cycle). The triangles on the heat axis mark the mean heat $Q(t) \equiv Q(t + t_{\rm p}, t_{\rm p})$ at the corresponding times. The singular parts of $\chi_{\rm p}(q,t)$ are marked by the arrow, where the arrow height equals the weight of the corresponding δ-function. For example, in a), the height of the arrow gives the probability that there was no transition between the states from the beginning of the cycle till the observation time $t = t_+/2$. The heat exchanged in this case is zero.

4.1.4 Engine performance

As shown in SUBS. 4.1.2, the occupation probabilities during the limit cycle are $\boldsymbol{p}(t) = \mathbb{R}_+(t)\,\boldsymbol{p}^{\rm stat}$ with $\mathbb{R}_{\rm p}(t)$ given by equation (4.8). Via EQS. (1.22)-(1.24) these probabilities render the energetics in terms of mean values as we discuss now. We denote as $Q(t) = Q(t + t_{\rm p}, t_{\rm p})$ the mean heat received from the reservoirs during the period between the beginning of the limit cycle and the time t. Analogously, $W(t) = W(t + t_{\rm p}, t_{\rm p})$ stands for the mean work done on the system from the beginning of the limit cycle till the time t. If $W(t) < 0$, the positive work $-W(t)$ is done by the system on the environment. Therefore the oriented areas enclosed by the limit cycle in FIG. 4.1 and in FIG. 4.4 represent the work $W_{\rm out} = -W(t_{\rm p})$ done by the engine on the environment per cycle, cf. SUBS. 1.4.2. These areas approach maximal absolute values in the quasi-static limit. The internal energy, being a state function, fulfills $U(t_{\rm p}) = U(0)$. Therefore, if the work $W_{\rm out}$ is positive, the same total amount of heat has been transferred from the two reservoirs during the cycle. The case $W_{\rm out} > 0$ cannot occur if both reservoirs would have the same temperature. That the *perpetuum mobile* is actually forbidden can be traced back to the detailed balance condition in (2.5).

We denote the system entropy at time t as $S_{\rm s}(t)$, and the reservoir entropy at

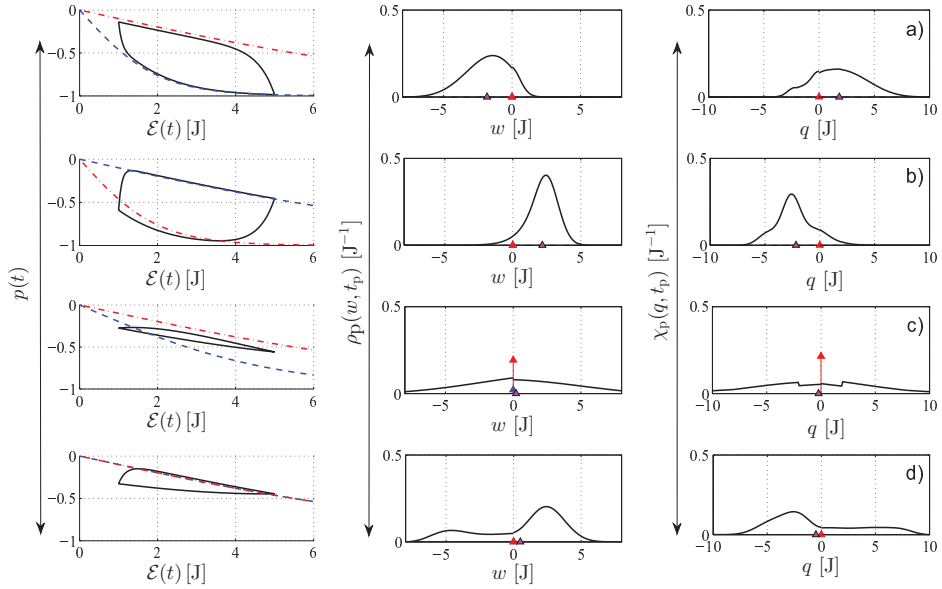

FIG. 4.4: Probability densities $\rho_{\rm p}(w,t_{\rm p})$ and $\chi_{\rm p}(q,t_{\rm p})$ for the work and heat for four representative sets of the engine parameters. For every set we show also the limit cycle in the p–$\mathcal{E}$ plane, where the corresponding equilibrium isotherms are marked by dashed (first stroke) and dot-dashed (second stroke) lines. In all cases we choose $h_1 = 1$ J, $h_2 = 5$ J, and $\nu = 1$ s^{-1}. The remaining parameters are a) $t_+ = 50$ s, $t_- = 10$ s, $\beta_+ = 0.5$ J^{-1}, $\beta_- = 0.1$ J^{-1} (bath of the first stroke is colder than of the second stroke), b) $t_+ = 50$ s, $t_- = 10$ s, $\beta_+ = 0.1$ J^{-1}, $\beta_- = 0.5$ J^{-1} [exchange of β_+ and β_- as compared to case a), leading to a change of the traversing of the cycle from counter-clockwise to clockwise and a sign reversal of the mean values $W(t_{\rm p})$ and $Q(t_{\rm p})$ denoted by the triangles on the work and heat axis], c) $t_+ = 2$ s, $t_- = 2$ s, $\beta_+ = 0.2$ J^{-1}, $\beta_- = 0.1$ J^{-1} (a strongly irreversible cycle traversed clockwise with positive work), d) $t_+ = 20$ s, $t_- = 1$ s, $\beta_\pm = 0.1$ J^{-1} (no change in temperatures, but large difference in duration of the two strokes; $W(t_{\rm p})$ is necessarily positive).

time t as $S_{\rm r}(t) = S_{\rm r}(t,0)$. They are given by [cf. EQS. (1.31) and (4.42)]

$$\frac{S_{\rm s}(t)}{k_{\rm B}} = -\left[p_1(t)\ln p_1(t) + p_2(t)\ln p_2(t)\right] \ , \tag{4.18}$$

$$\frac{S_{\rm r}(t)}{k_{\rm B}} = \begin{cases} -\beta_+ \int_0^t {\rm d}t' \mathcal{E}_1(t')\dot{p}(t') \ , & t \in [0,t_+] \\ -\beta_+ \int_0^{t_+} {\rm d}t' \mathcal{E}_1(t')\dot{p}(t') - \beta_- \int_{t_+}^t {\rm d}t' \mathcal{E}_1(t')\dot{p}(t') \ , & t \in [t_+,t_{\rm p}] \end{cases} , \tag{4.19}$$

where $p(t) = p_1(t) - p_2(t)$. Upon completing the cycle, the system entropy reassumes its value at the beginning of the cycle. On the other hand, the reservoir entropy is controlled by the heat exchange. Owing to the inherent irreversibility of the cycle we observe always a positive entropy production per cycle, $S_{\rm r}(t_{\rm p}) - S_{\rm r}(0) = S_{\rm r}(t_{\rm p}) > 0$. The total entropy produced by the engine up to the time t, $S_{\rm tot}(t) = S_{\rm tot}(t,0) = S_{\rm s}(t) - S_{\rm s}(0) + S_{\rm r}(t)$ increases for any $t \in [0,t_{\rm p}]$. The rate of

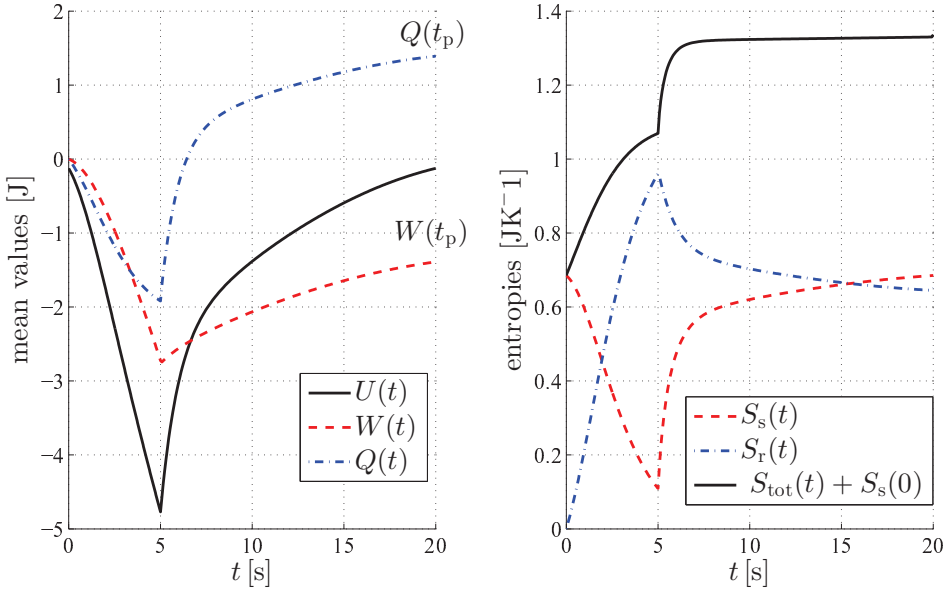

FIG. 4.5: Thermodynamic quantities as functions of time during the limit cycle for the same set of parameters as in the upper panel of FIG. 4.1 (positive h_1). Left panel: internal energy, mean work done on the system, and mean heat received from both reservoirs; the final position of the mean work curve marks the work done on the system per cycle $W(t_\mathrm{p})$. Since $W(t_\mathrm{p}) < 0$, the work W_out has been done on the environment. The internal energy returns to its original value and, after completion of the cycle, the absorbed heat $Q(t_\mathrm{p})$ equals the negative work $-W(t_\mathrm{p})$. Right panel: entropy $S_\mathrm{s}(t)$ of the system and $S_\mathrm{r}(t)$ of the bath, and their sum $S_\mathrm{tot}(t) + S(0)$; after completing the cycle, the system entropy re-assumes its initial value. $S_\mathrm{tot}(t_\mathrm{p}) > 0$ equals the entropy production per cycle. It is always positive and quantifies the degree of irreversibility of the cycle.

the increase is the larger the stronger the representative point in the p–$\mathcal{E}$ diagram deviates from the corresponding equilibrium isotherm (a strong deviation, e.g., can be seen in the p–$\mathcal{E}$ diagram in FIG. 4.4c). Due to the instantaneous exchange of the baths at times t_+ and $t_+ + t_-$ and absence of adiabatic branches [170], a strong increase of $S_\mathrm{tot}(t)$ always occurs after these time instants. A representative example of the overall behavior of the thermodynamic quantities (mean work and heat, and entropies) during the limit cycle is shown in FIG. 4.5. See also FIGS. 4.12 and 4.10 for a different model where the adiabatic branches are considered.

Important characteristics of the engine are its power output P_out and its efficiency η. They are defined by EQS. (1.70) and (1.69), i.e.,

$$P_\mathrm{out} = \frac{W_\mathrm{out}}{t_\mathrm{p}} \quad , \quad \eta = \frac{W_\mathrm{out}}{Q_\mathrm{in}} \, , \tag{4.20}$$

where Q_in is the total heat absorbed by the system per cycle. The performance of the engine characterized by the output work, efficiency, output power, and entropies from equations (4.18) and (4.19) are shown in FIG. 4.6 and FIG. 4.7.

In FIG. 4.6 the performance is displayed as a function of the cycle duration t_p for $t_+ = t_- = t_\mathrm{p}/2$. With increasing t_p, the output work and the efficiency

increase whereas the output power and the entropy production first increase up to a maximum and thereafter they decrease when approaching the quasi-static limit ($t_\mathrm{p} \to \infty$). Notice that the maximum efficiency and output power occur at different values of t_p. In FIG. 4.6a) we show also the standard deviation of the output work, which was calculated from the work probability density $\rho_\mathrm{p}(w, t_\mathrm{p})$. Finally, let us note that the values $\beta_+ = 0.5\ \mathrm{J}^{-1}$ and $\beta_- = 0.1\ \mathrm{J}^{-1}$ used in FIG. 4.6 give the Carnot efficiency $\eta_\mathrm{C} = 0.8$. This should be compared with the efficiency of the engine for a long period t_p, that is, with the value $\eta \approx 0.6$. As discussed above, the Carnot efficiency cannot be reached here even for $t_\mathrm{p} \to \infty$, due to the immediate temperature changes at the times t_+ and $t_\mathrm{p} = t_+ + t_-$.

In FIG. 4.7 we have fixed t_p and plotted the performance of the engine as a function of the time asymmetry (or time splitting) parameter $\Delta = (t_+ - t_-)/t_\mathrm{p}$. As can be seen from the upper three panels in FIG. 4.7, there exist also a maximal efficiency and a maximal output power with respect to a variation of the time asymmetry parameter (as long as the engine performs work, i.e., $W_\mathrm{out} > 0$). Again, the optimal parameter Δ, where these maxima occur, is different for the efficiency and for the output power. In a reversed situation, considered in the lower three panels in FIG. 4.7, where the work is performed on the engine ($W_\mathrm{out} < 0$), minima of the efficiency and output power occur.

4.1.5 Discussion

The overall properties of the engine critically depend on the two dimensionless parameters $a_\pm = \nu/(2\beta_\pm|v_\pm|)$. We call them *reversibility parameters* [2]. For a given branch, say the first one, the parameter a_+ represents the ratio of two characteristic time scales. The first one, $1/\nu$, is given by the attempt rate of the internal transitions [3]. The second scale is proportional to the reciprocal driving velocity. Contrary to the first scale, the second one is fully under the external control. Moreover, the reversibility parameter is proportional to the absolute temperature of the heat bath.

Let us first consider the work probability density (4.16) within the first stroke in the case $h_2 > h_1$, cf. FIG. 4.2a). In essence, $\rho_\mathrm{p}(w, t)$ is given by a linear combination of the functions (2.21)-(2.21). It vanishes outside the common support $[\,-v_+t, v_+t\,]$ which broadens linearly in time. Besides the continuous part located within the support, the diagonal elements $[\mathbb{G}_\mathrm{p}(w, t\,|\,, 0)]_{ii}$ display a singular part represented by δ-functions at the borders of the support. The δ-functions correspond to the paths with no transitions between the states, cf. APP. B. Specifically, the weight of the δ-function located at $w = v_+t$ represents the probability that the system starts in the first state and remains there up to time t. The weight corresponding to the first level decreases with increasing time and vanishes for $t \to \infty$. On the contrary, the weight of the delta function at $-v_+t$ approaches the nonzero limit $(1 + c_+)^{-a_+}$ for $t \to \infty$, which is the probability that a trajectory starts in the second state *and* never leaves it.

[2] The reversibility here refers to the individual branches. As pointed out in SUBS. 4.1.1, the abrupt change in temperature, when switching between the branches, implies that there exists no reversible limit for the complete cycle.

[3] Note that due to the choice of the Glauber rates in EQ. 4.1, the relaxation rate $[\lambda_\mathrm{U}(t)+\lambda_\mathrm{D}(t)]$ (for frozen energy levels at any time instant t) is bounded by 2ν.

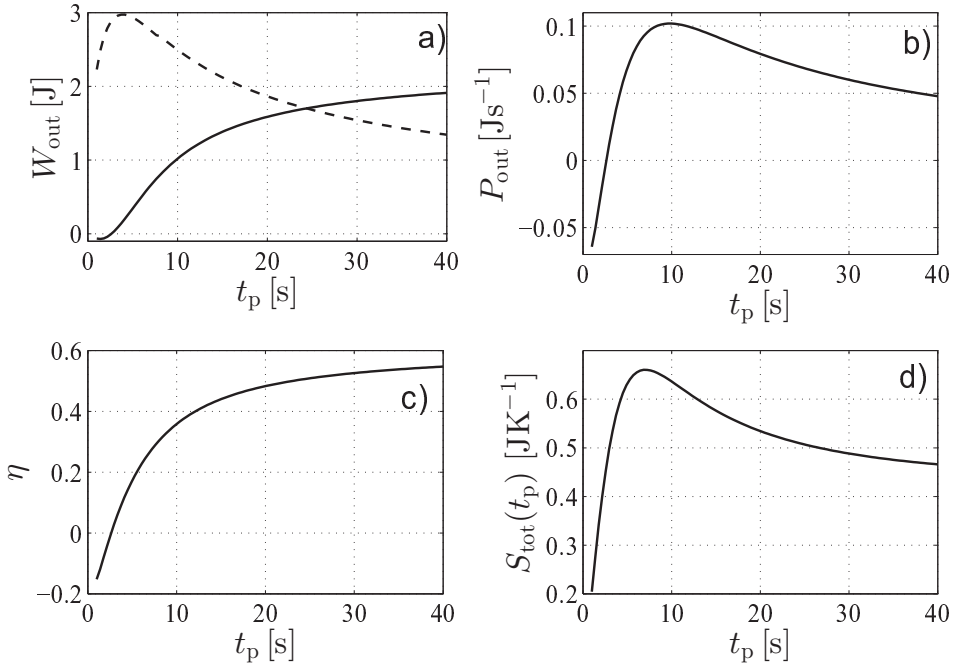

FIG. 4.6: The engine performance versus the duration of the limit cycle $t_{\pm}$ for $t_{+} = t_{-} = \frac{1}{2}t_{\mathrm{p}}$ and otherwise the same parameters as in the upper part of FIG. 4.6 (positive h_1). Both the output work W_{out} in a) and the efficiency η in b) increase with t_{p}. The output power P_{out} in c) assumes a maximum at a special cycle duration. The dashed line in a) marks the standard deviation of the output work, calculated from the work density $\rho_{\mathrm{p}}(w, t_{\mathrm{p}})$. Notice that the work fluctuation is comparatively high close to the cycle duration, where the maximal output power is found. In the long-period limit $t_{\mathrm{p}} \to \infty$, the cycle still represents a non-equilibrium process (due to the construction of the model, see text), and hence the entropy production $S_{\mathrm{tot}}(t_{\mathrm{p}})$ in d) remains positive, approaching a specific asymptotic value.

Within the second stroke, the density $\rho_{\mathrm{p}}(w, t)$ results from the integral of the propagators for the individual strokes, cf. EQ. (4.14). Due to the integration, the singular parts of the cycle propagator $\mathbb{G}_{+}(w, t \,|\, 0)$ are now situated inside the support, at the values $w = \pm[-v_{+}t_{+} + v_{-}(t - t_{+})]$. The two δ-functions approach each other and, upon completing the cycle, they coincide at the point $w = 0$. The nonsingular component of the density is no more continuous [4]. The jumps are located at the positions of the δ-functions and their magnitudes correspond to the weights of the δ-functions (for a discussion of the origin of these jumps, see [52]).

If both reversibility parameters $a_{\pm}$ are small, the isothermal processes during both branches strongly differ from the equilibrium ones. The signature of this case is a flat continuous component of the density $\rho_{\mathrm{p}}(w, t)$ and a well pronounced singular part. The strongly irreversible dynamics occurs if one or more of the following conditions hold. First, if ν is small, the transitions are rare and the

[4] Only δ-functions are referred to as singularities here.

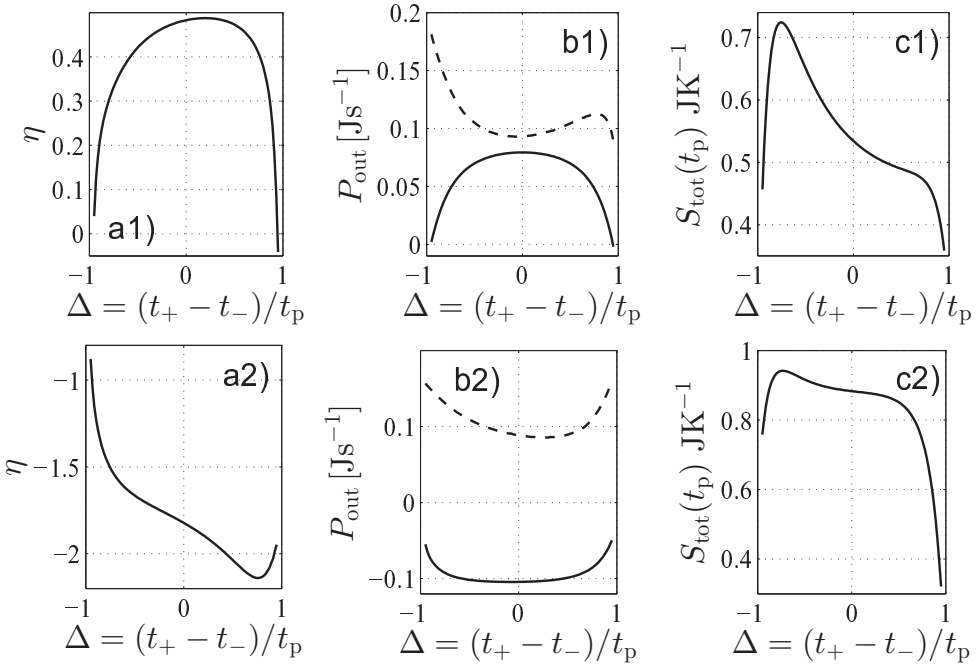

FIG. 4.7: The engine performance characterized by the efficiency η, output power $P_{\rm out}$, and entropy production $S_{\rm tot}(t_{\rm p})$, as a function of the asymmetry parameter $\Delta = (t_+ - t_-)/t_{\rm p}$ for a fixed period $t_{\rm p} = 20$ s and the same parameters $h_1 = 1$ J, $h_2 = 5$ J, $\nu = 1$ s^{-1} as in the upper panel of FIG. 4.1. In a1)–c1) the bath during the first stroke is colder than during the second stroke: $\beta_+ = 0.5$ J^{-1} and $\beta_- = 0.1$ J^{-1}. Notice that the value Δ of maximum efficiency does not correspond to that of maximum output power. In a2)-c2) the reciprocal bath temperatures are interchanged compared to cases a1)-c1), $\beta_+ = 0.1$ J^{-1} and $\beta_- = 0.5$ J^{-1}. The dashed curves in b1) and b2) show the standard deviation of the output power calculated from $\rho_{\rm p}(w, t_{\rm p})$.

occupation probabilities of the individual energy levels are effectively frozen during long periods of time. Therefore they lag behind the Boltzmann distribution which would correspond to the instantaneous positions of the energy levels, cf. FIG. 1. More precisely, the population of the ascending (descending) energy level is larger (smaller) than it would be during the corresponding reversible process. As a result, the mean work done on the system is necessarily larger than the equilibrium work. Secondly, a similar situation occurs for large driving velocities $v_\pm$. Due to the rapid motion of the energy levels, the occupation probabilities again lag behind the equilibrium ones. Thirdly, the strong irreversibility occurs also in the low temperature limit. In the limit $a_\pm \to 0$, the continuous part vanishes and $\rho_{\rm p}(w, t_{\rm p}) = \delta(w)$.

In the opposite case of large reversibility parameters $a_\pm$, both branches in the p–$\mathcal{E}$ plane are located close to the reversible isotherms. The singular part of the density $\rho_{\rm p}(w, t)$ is suppressed and the continuous part exhibits a well pronounced peak. From general considerations [53,177], the density must approach, around its maximum, a Gaussian shape. Our results allow a detailed study of this approach.

Let us denote as $F(\beta,\mathcal{E})$ the free energy of a two level system with energies $\pm\mathcal{E}$ at temperature $T=1/(k_{\mathrm{B}}\beta)$, i.e., $F(\beta,\mathcal{E})=-\ln[2\cosh(\beta\mathcal{E})]/\beta$. Let us further define the function $W_{\mathrm{rev}}(t)$ as

$$\begin{cases} F[\beta_+,\mathcal{E}_1(t)]-F[\beta_+,\mathcal{E}_1(0)]\ , & t\in[0,t_+],\\ F[\beta_-,\mathcal{E}_1(t)]-F[\beta_-,\mathcal{E}_1(t_+)]+F[\beta_+,\mathcal{E}_1(t_+)]-F[\beta_+,\mathcal{E}_1(0)], & t\in[t_+,t_{\mathrm{p}}]. \end{cases} \tag{4.21}$$

This is simply the reversible work (1.55) done on the system if we transform its state from the initial equilibrium state [with the energies fixed at $\pm\mathcal{E}_1(0)$] to another equilibrium state [with the energies fixed at the values $\pm\mathcal{E}_1(t)$]. For large reversibility parameters $a_\pm$, the peak of the work density $\rho_{\mathrm{p}}(w,t_{\mathrm{p}})$ occurs in the vicinity of the value $W_{\mathrm{rev}}(t)$ and with increasing $a_\pm$, the peak collapses to a δ-function (for a general prove see App. A)

$$\lim_{a_\pm\to\infty}\rho_{\mathrm{p}}(w,t)=\delta[w-W_{\mathrm{rev}}(t)]\ . \tag{4.22}$$

The main features of the heat probability density $\chi_{\mathrm{p}}(q,t)$ from Eq. (4.17) are, as we have seen in Subs. 4.1.3, closely related to the work through simple shifts of the independent variable q. However, there are some interesting differences. While the work is conditioned by the external driving, the heat exchange occurs as a consequence of the transitions between the system energy levels. The instantaneous positions of the energies at the instant of the transition give the magnitude of the heat exchange related with the given transition. From this perspective, if there are no transitions, the exchanged heat is zero. As a consequence, the singular part of the probability density $\chi_{\mathrm{p}}(q,t)$ is always situated at $q=0$ and the weight of the δ-function at origin equals the sum of the weights of the δ-functions in the work density $\rho_{\mathrm{p}}(w,t)$. The support of the heat density is given by the largest possible value of the level splitting during the limit cycle. Within the first stroke the support broadens linearly with time as $[-2h_1-2v_+t,2h_1+2v_+t]$, up to its maximum width $[-2h_2,2h_2]$ at the end of the stroke. Within the second stroke the energy difference decreases and the support remains unchanged. The non-singular part of the heat density always displays discontinuities inside the support, even during the first stroke.

In the strongly reversible regime each element $\langle\, i\,|\,\mathbb{G}_{\mathrm{p}}(w,t)|\,j\,\rangle$ exhibits a Gaussian shape situated at $W_{\mathrm{rev}}(t)$. The transformation (4.15) maps the Gaussian function onto four different positions in the heat probability density $\chi_{\mathrm{p}}(q,t)$. In the reversible limit we have

$$\lim_{a_\pm\to\infty}\chi_{\mathrm{p}}(q,t)\rangle=\sum_{i,j=1}^{2}\delta\left\{q-[\mathcal{E}_i(t)-\mathcal{E}_j(0)-W_{\mathrm{rev}}(t))]\right\}[\mathbb{R}_{\mathrm{p}}(t)]_{ij}\,p_j^{\mathrm{stat}}\ . \tag{4.23}$$

If we calculate the mean accepted heat using this form, we get $Q(t)=U(t)-U(0)-W_{\mathrm{rev}}(t)$. In the opposite limit, if $a_\pm\to 0$, we have $\chi_{\mathrm{p}}(q,t)\to\delta(q)$ for any t.

According to the second law of thermodynamics, the mean work $W(t)$ must fulfill $|W(t)|\geq|W_{\mathrm{rev}}(t)|$. On the other hand, there always exists a fraction of trajectories which, individually, display the inequality $|\widetilde{w}(\mathrm{tr},t)|<|W_{\mathrm{rev}}(t)|$, where $\widetilde{w}(\mathrm{tr},t)$ denotes the work done on the system if it evolves along the indicated

trajectory. Using the exact work probability density, we can calculate the total weight of these trajectories. Specifically, in the case $W_{\rm rev}(t) > 0$,

$$\text{Prob}\,\{\,\mathsf{W}(t,0) < W_{\rm rev}(t)\,\} = \int_{-\infty}^{W_{\rm rev}(t)} \mathrm{d}w\,\rho_{\rm p}(w,t)\ . \tag{4.24}$$

If $W_{\rm rev}(t) < 0$, we would have to integrate over the interval $(W_{\rm rev}(t), \infty)$.

Let us finally note that in view of the rather complex structure of the work and heat probability densities, we performed several independent tests. First of all, the densities $\rho_{\rm p}(w,t)$ and $\chi_{\rm p}(q,t)$ must be nonnegative functions fulfilling the normalization conditions, i.e., $\int_{-\infty}^{\infty} \mathrm{d}w\,\rho_{\rm p}(w,t) = 1$ for any $t \in [0, t_{\rm p}]$. Secondly, we have two different procedures to calculate the first moment $W(t)$. One can either start with the density $\rho_{\rm p}(w,t)$ and evaluate the required w-integral, or one directly employs the solution of the rate equation as in SUBS. 4.1.4. Another inspection is based on the Jarzynski identity [43,104]. In our setting, consider the case $\beta_{\pm} = \beta$. After completing the cycle, the system returns to the original state. Therefore we have $W_{\rm rev}(t_{\rm p}) = F[\beta, \mathcal{E}_1(t_{\rm p})] - F[\beta, \mathcal{E}_1(0)] = 0$ and the Jarzynski identity (1.61) reduces to $\langle \exp\,[-\beta\,\mathsf{W}(t_{\rm p}, 0)]\,\rangle = 1$. Using the explicit form of the work probability density we have verified that the integral $\int_{-\infty}^{\infty} \mathrm{d}w\,\exp(-\beta w)\rho_{\rm p}(w, t_{\rm p})$ actually equals one. Finally, we have studied the probability densities $\rho_{\rm p}(w,t)$, $\chi_{\rm p}(q,t)$ by computer simulation. In fact, we have developed two exact simulation methods which are discussed in APP. C. Each of them uses a specific algorithm to generate paths of the time-non-homogeneous Markov process $\mathsf{D}(t)$. Parts of these simulation results have been published in [52,92] and confirm the analytical results.

4.1.6 Conclusions

We have investigated a simple example of a microscopic heat engine, which is exactly solvable. Based on mean thermodynamic quantities, the engine performance is characterized by the occupation probabilities of the energy levels following from the master equation. The more challenging exact calculation of the work and heat probability densities allowed us to study the fluctuation properties in detail. A notable result is that the engine can be tuned to maximize its output power, but the fluctuations of this quantity in the corresponding optimal regime of control parameters are comparatively high.

The present setting can be expanded in various directions. One can address various problems concerning the thermodynamic optimization. Another option would be the embodiment of additional (e.g., adiabatic) branches. The role of the working medium can be assigned to other systems that exhibit more complicated dynamics (e.g., diffusing particles in the presence of time-dependent forces, or, variants of the generalized master equation). It would be also interesting to investigate settings with a nonlinear driving of the energy levels. A nontrivial generalization would be the inclusion of a third energy level. Having the three levels one can couple the system (different pairs of forth-back transitions between the levels) *simultaneously* to reservoirs at different temperatures, so that the system approaches a non-equilibrium steady state without driving [196]. Including a driving and forming an operational cycle, there is no serious obstacle in repeating

the present analysis for this system, which has some additional intriguing properties compared to the two-level system considered here (as, e.g., negative specific heats).

Another possibility is an incorporation of specific forms of transition rates [122] that describe the stretching of biomolecules in some realistic manner. In such problem, the histogram of the work is experimentally accessible [122]. Particularly, in the experiments one can also determine the probability of having certain number of transitions between the folded and the unfolded conformation of the biomolecule during its mechanical stretching [122]. In our formulation, this information is encoded in the counting statistics of the underlying random point process [175] and can be extracted from the perturbation expansion of the propagators which solve our dynamical equations.

4.2 Diffusive heat engine

4.2.1 Introduction

In this Sec. we focus on stochastic heat engines based on Brownian particles diffusing in a periodically driven potential. In [159] strong general results concerning the efficiency at maximum power for a wide class of such engines were obtained. Nevertheless it turned out that exactly solvable is only an engine driven by a *symmetric* harmonic potential [159], which was also realized experimentally [14]. We give an exactly solvable example of a stochastic heat engine based on a particle diffusing in the *asymmetric* log-harmonic potential (4.25). Such potential was considered in theoretical studies [73, 152, 178] and can be also realized experimentally using the optical tweezers [38]. Within our specific setting we verify the universal results regarding the efficiency at maximum power obtained in [59, 61, 159] (see also Subs. 1.4) and discuss properties of the optimal driving. In particular we propose a physical explanation for occurrence of the jumps in the optimal driving as a consequence of the equivalence between the power maximization and minimization of the total entropy production [190]. Moreover, we investigate the performance of the engine for two other protocols and discuss the possibility to minimize fluctuations of the output power.

This Sec. is organized as follows: in Subs. 4.2.2 we describe the working medium of the motor and present the Green's function for its dynamics, which we further use for constructing the working cycle of the engine. In Subs. 4.2.3 we specify the thermodynamic quantities used in our analysis. Subs. 4.2.4 contains the discussion concerning the possibility to depict the operational cycle of the engine by a stochastic thermodynamics analogue of the well known p-V diagrams (see also Subs. 1.4.2). In Subs. 4.2.5 we introduce three examples of the driving. First, we derive the driving which maximizes the output power. Second, we define the driving, which yields the smallest power fluctuations from the three protocols. These two protocols inevitably incorporate two isothermal and two adiabatic branches. The third protocol is different and may consists of two isotherms only. Finally, in Subs. 4.2.6, we discuss the obtained results.

4.2.2 Description of the engine and its limit cycle

Consider an externally driven Brownian particle diffusing on the interval $[0, \infty]$ with a reflecting boundary at $x = 0$. Assume that the external driving is represented by a time-periodic log-harmonic potential [73,152,178]. Let the microstate degeneracies $\Omega(x) = 1$. Moreover, assume the FEL (1.1) is given solely by the external potential, $\mathcal{V}(x,t)$, i.e., we have

$$\mathcal{F}(x,t) = \mathcal{E}(x,t) = \mathcal{V}(x,t) = -g(t)\log x + \frac{k(t)}{2}x^2 \ , \tag{4.25}$$

where $-g(t) < k_{\mathrm{B}}T$ and $k(t) > 0$. The requirement $-g(t) < k_{\mathrm{B}}T$ secures the existence of a nontrivial steady state. For $-g(t) \geq k_{\mathrm{B}}T$ are, in the long time limit, all particles trapped at $x = 0$. Dynamics of the particle is described by Eq. (1.38). In further we take $\Gamma = k_{\mathrm{B}} = 1$. Then Eq. (1.38) reads

$$\frac{\partial}{\partial t}R(x,t\,|\,x',t') = \left\{T(t)\frac{\partial^2}{\partial^2 x} - \frac{\partial}{\partial x}\left[\frac{g(t)}{x} - k(t)\,x\right]\right\}R(x,t\,|\,x',t') \tag{4.26}$$

with the initial condition $R(x,t\,|\,x',t') = \delta(x - x')$. Note that the temperature in Eq. (4.26) is also time dependent. The control parameters are the functions $g(t)$ and $k(t)$, i.e., the vector of control parameters, $\boldsymbol{Y}(t)$, has two components (cf. Subs. 1.4.1).

Generic case – isothermal process

In order to solve Eq. (4.26) we first consider an isothermal process $[T(t) = T]$ with the driving

$$\mathcal{V}(x,t) = -g\log x + \frac{k(t)}{2}x^2 \ . \tag{4.27}$$

In this generic case $[T(t) = T,\ g(t) = g]$ it is possible to solve Eq. (4.26) analytically (see, for example, [152]). The solution is

$$R(x,t\,|\,x',t') = \frac{x'\mathrm{e}^{\frac{\nu+2}{2}a(t,t')}}{2\,b(T;t,t')}\left(\frac{x}{x'}\right)^{\nu+1}\times \\ \times\exp\left[-\frac{x^2\mathrm{e}^{a(t,t')} + (x')^2}{4\,b(T;t,t')}\right]\ \mathrm{I}_\nu\left[\frac{xx'\mathrm{e}^{\frac{1}{2}a(t,t')}}{2\,b(T;t,t')}\right] \ , \tag{4.28}$$

where $\mathrm{I}_\nu(x)$ stands for the modified Bessel function of the first kind [2],

$$\nu = \frac{1}{2}\left(\frac{g}{T} - 1\right) \ , \qquad \nu > -1 \tag{4.29}$$

and

$$\begin{aligned} a(t,t') &= 2\int_{t'}^{t}\mathrm{d}t''\,k(t'') \ , \\ b(T;t,t') &= T\int_{t'}^{t}\mathrm{d}t''\,\exp\left[2\int_{t'}^{t''}\mathrm{d}t'''\,k(t''')\right] \ . \end{aligned} \tag{4.30}$$

Note that the parameter g enters the generic solution (4.28) only through the dimensionless combination ν.

Operational cycle of the engine

Let the periodic driving of the engine (4.25) consist of two isotherms and two adiabatic branches as it is described in SUBS. 1.4.1. To completely specify the protocol it is enough to describe the concrete form of the driving during the isothermal branches. To this end we assume that, during the isotherms, the potential energy $\mathcal{V}(x,t)$ has the generic form (4.27), i.e., we have

$$\mathcal{V}(x,t) = \begin{cases} -g_+ \log x + \dfrac{k(t)}{2}x^2 \ , & t \in [0, t_+^-] \\ \\ -g_- \log x + \dfrac{k(t)}{2}x^2 \ , & t \in [t_+^+, t_{\rm p}^-] \end{cases} \ . \tag{4.31}$$

During the first adiabatic branch the potential changes from $\mathcal{V}(x,t_+^-)$ to $\mathcal{V}(x,t_+^+)$. During the second adiabatic branch the potential regains its initial value, i.e., it changes from $\mathcal{V}(x,t_{\rm p}^-)$ to $\mathcal{V}(x,t_{\rm p}) = \mathcal{V}(x,0)$. This pattern is periodically repeated, the period being $t_{\rm p}$. The durations of the adiabatic branches $t_+^+ - t_+^-$ and $t_{\rm p} - t_{\rm p}^-$ are considered as infinitesimally short as compared to the durations of the isotherms $t_+ = t_+^-$ and $t_- = t_{\rm p}^- - t_+^+$. During the first (the second) isotherm the temperature T assumes the value T_+ (T_-). For the sake of mathematical simplicity we choose the parameters $g_\pm$ proportional to the corresponding reservoir temperatures. Specifically we take $g_\pm = (2\nu+1)T_\pm$ [5]. This setting allows us to investigate the cases when the logarithmic part of the potential $\mathcal{V}(x,t)$ is during the whole cycle repulsive (attractive). The model with general $g_\pm$ would describe also the situation when the two constants have different sign and thus the logarithmic part of the potential (4.31) is during the first isotherm repulsive (attractive) and vice versa during the second one.

The hereby considered driving is depicted in FIG. 4.8. The resulting limit cycle for $\nu = -1/2$ coincides with that discussed in [159]. The fact that the protocol contains adiabatic branches II and IV, where the potential and the temperature change infinitely fast while the particle distribution remains unchanged, may look artificial. However, it is not as was shown in experiments [14]. Onwards we will focus on the characterization of the limit cycle, which the engine will approach at long times after a transient period.

We start from the generic solution (4.28) of the Fokker-Planck EQ. (4.26). Owing to the Chapman-kolmogorov condition (1.80), the propagator within the cycle still assumes the form (4.28). Specifically it reads

$$R_{\rm p}(x,t\,|\,x',t') = \frac{x' \mathrm{e}^{\frac{\nu+2}{2}a(t,t')}}{2b(t,t')} \left(\frac{x}{x'}\right)^{\nu+1} \times \\ \times \exp\left[-\frac{x^2 \mathrm{e}^{a(t,t')} + (x')^2}{4b(t,t')}\right] \ \mathrm{I}_\nu\left[\frac{x x' \mathrm{e}^{\frac{1}{2}a(t,t')}}{2b(t,t')}\right] \ , \tag{4.32}$$

[5] It turns out that for general parameters $g_\pm$ the Green's function (4.32) is given by a sum of Gauss hypergeometric functions [142] and the integral EQ. (1.81) becomes quite complicated.

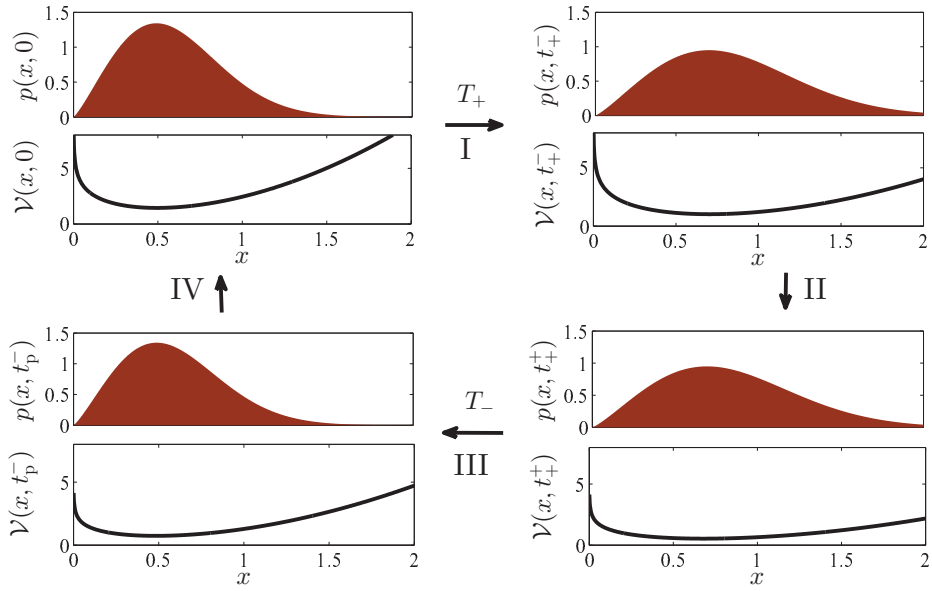

FIG. 4.8: Scheme of the operating cycle of the engine driven by the optimal protocol (4.57). The particle distribution (4.34) is depicted by the filled curve. The solid line represents the potential energy (4.25). Parameters used: $t_+ = 4$, $t_- = 6$, $T_+ = 1$, $T_- = 0.5$, $f_0 = 0.1$, $f_1 = 0.2$, $\nu = 0.1$.

where the function $b(t,t')$ is given by

$$b(t,t') = \begin{cases} b(T_+;t,t') \;, & t',t \in [0,t_+^+] \;, \\ b(T_+;t_+,t') + \mathrm{e}^{a(t_+,t')}\, b(T_-;t,t_+) \;, & t' \in [0,t_+^+] \;\wedge\; t \in [t_+^+,t_\mathrm{p}] \;, \\ b(T_-;t,t') \;, & t',t \in [t_+^+,t_\mathrm{p}] \;, \end{cases} \tag{4.33}$$

and the functions $a(t,t')$ and $b(T;t,t')$ are defined in EQ. (4.30).

The periodic state of the system during the limit cycle is determined by the solution of the integral EQ. (1.81), which reads $p(x,t) = \int_0^\infty \mathrm{d}x'\, R_\mathrm{p}(x,t\,|\,x',0)p(x,0)$. For our present setting, EQ. (1.81) can be solved analytically. The result

$$p(x,t) = \frac{1}{\Gamma(\nu+1)} \left[\frac{1}{f(t)}\right]^{\nu+1} \left(\frac{x}{2}\right)^{2\nu+1} \exp\left[-\frac{x^2}{4f(t)}\right] \tag{4.34}$$

was already mentioned in [152] as a time-asymptotic distribution for a periodically driven system. The function $f(t) = \langle [x(t)]^2 \rangle / (4\nu+4)$ determines the width of the distribution (4.34). It obeys the formula

$$f(t) = \begin{cases} [f_0 + b(t,0)] \exp[-a(t,0)] \;, & t \in [0,t_+] \\ [f_1 + b(t,t_+)] \exp[-a(t,t_+)] \;, & t \in [t_+,t_\mathrm{p}] \end{cases} \;, \tag{4.35}$$

where $f_0 = f(0) = f(t_\mathrm{p}) = \{b(t_+,0) + b(t_\mathrm{p},t_+) \exp[a(t_+,0)]\}/f$, $f_1 = f(t_+^-) = f(t_+^+) = \{b(t_\mathrm{p},t_+) + b(t_+,0) \exp[a(t_\mathrm{p},t_+)]\}/f$, and $f = \exp[a(t_\mathrm{p},0)] - 1$. Note that the system response is continuous regardless the discontinuities in the driving. The probability distribution (4.34), and hence also the specific form of the limit cycle, is determined solely by the parameters ν, $T_\pm$, $t_\pm$, and by the function $k(t)$.

4.2.3 Thermodynamic quantities

Mean values

As in the model discussed in SUBS. (4.1), the probability distribution $p(x,t)$ renders the energetics of the engine in terms of mean values as we discuss now. The periodic potential energy $\mathcal{V}(x,t)$ can be rewritten as $\mathcal{V}(x,t) = \tilde{\mathcal{V}}[x, g(t), k(t)]$. According to EQ. (1.83) the thermodynamic work done by the engine during the time interval $[t,t']$, $W_{\rm out}(t,t') = -W(t,t')$, reads

$$W_{\rm out}(t,t') = \int_{t'}^{t} {\rm d}t''\ \langle \log x(t'')\rangle\ \frac{{\rm d}g(t'')}{{\rm d}t''} - \int_{t'}^{t} {\rm d}t''\ \frac{1}{2}\left\langle [x(t)]^2\right\rangle \frac{{\rm d}k(t'')}{{\rm d}t''}\ , \qquad (4.36)$$

where the two averages are given by

$$\langle \log x(t)\rangle = \int_0^\infty {\rm d}x\ \log x\, \rho(x,t) = \frac{1}{2}\left\{ \log[4f(t)] + \frac{\rm d}{{\rm d}\nu} \log \Gamma\left(\nu+1\right)\right\}\ , \qquad (4.37)$$

$$\frac{1}{2}\left\langle [x(t)]^2\right\rangle = \int_0^\infty {\rm d}x\, x^2 \rho(x,t) = 2(\nu+1) f(t)\ . \qquad (4.38)$$

These two averages also determine the mean internal energy of the system at the time t, $U(t) = -g(t)\,\langle \log x(t)\rangle + \frac{1}{2} k(t)\,\langle [x(t)]^2\rangle$, cf. EQ. (1.47). Its increase from the beginning of the cycle

$$\Delta U(t) = U(t) - U(0) \qquad (4.39)$$

and the mean work done from the beginning of the cycle up to the time t, $W_{\rm out}(t) \equiv W_{\rm out}(t,0)$, yield via the second law of thermodynamics the mean heat uptake during the time interval $[0,t]$

$$Q(t) \equiv Q(t,0) = \Delta U(t) + W_{\rm out}(t)\ . \qquad (4.40)$$

The total work done by the engine per cycle, $W_{\rm out} = W_{\rm out}(t_{\rm p})$, determines its average output power: $P_{\rm out} = W_{\rm out}/t_{\rm p}$. The engine efficiency is given by EQ. (1.69), i.e., $\eta = W_{\rm out}/Q_{\rm in}$, where $Q_{\rm in}$ stands for the total heat transfered to the system from the reservoirs, cf. EQ. (1.68). The entropy of the system at the time t, (1.52), is $S_{\rm s}(t) = -\int_0^\infty {\rm d}x\, p(x,t) \log\left[p(x,t)\right]$. Its increase from the beginning of the cycle [EQ. (1.32)] reads

$$S_{\rm s}(t,0) = S_{\rm s}(t) - S_{\rm s}(0) = (\nu+1) \log \frac{f(t)}{f(0)}\ . \qquad (4.41)$$

Due to the time dependence of the temperature during the cycle the entropy transfered to the reservoirs during the time interval $[0,t]$ [EQ. (1.33)] needs to be redefined as

$$S_r(t) = S_r(t,0) = -\int_0^t {\rm d}t'\ \frac{1}{T(t')} \frac{\rm d}{{\rm d}t'} Q(t')\ . \qquad (4.42)$$

Finally, the total entropy produced by the engine during the time interval $[0,t]$ is given by EQ. (1.34), i.e.,

$$S_{\rm tot}(t) = S_{\rm tot}(t,0) = S_{\rm s}(t,0) + S_r(t) \geq 0\ . \qquad (4.43)$$

Work and power fluctuations

In the previous model [Sec. (4.1)] we examined the work and power fluctuations using the work probability density (4.16). Here we employ Eq. (1.50), i.e., we study the work and power fluctuations using the propagator $R_{\rm p}(x,t\,|\,x',t')$, which yields the time-correlation function (1.51). Specifically we calculate the relative fluctuation of the work done by the engine during the time interval (t',t)

$$\tilde{\sigma}_w(t,t') = \frac{\sqrt{\langle[\mathsf{W}(t,t')]^2\rangle - [W_{\rm out}(t,t')]^2}}{|W_{\rm out}(t,t')|} \tag{4.44}$$

which determines the relative power fluctuation

$$\delta P_{\rm out} = \tilde{\sigma}_w(t_{\rm p},0) \tag{4.45}$$

and, hence, in a sense, also the stability of engine performance. In Eq. (4.45) the second moment $\langle[\mathsf{W}(t,t')]^2\rangle$ is given by Eq. (1.50), i.e., it reads

$$\left\langle[\mathsf{W}(t,t']^2\right\rangle = \int_{t'}^{t}{\rm d}t\int_{t'}^{t}{\rm d}t'\left\langle\frac{\partial\mathcal{V}[\mathsf{X}(t),t]}{\partial t}\frac{\partial\mathcal{V}[\mathsf{X}(t'),t']}{\partial t'}\right\rangle_{\rm C}\,, \tag{4.46}$$

where $\partial\mathcal{V}[x(t),t]/\partial t = -\log[x(t)]\,{\rm d}g(t)/{\rm d}t + [x(t)]^2/2\,{\rm d}k(t)/{\rm d}t$ and the time-correlation function $\langle h([\mathsf{X}(t)]\,f[(\mathsf{X}(t')]\rangle_{\rm C}$ obeys Eq. (1.51). Note that, due to the jumps in the driving, the functions ${\rm d}g(t)/{\rm d}t$ and ${\rm d}k(t)/{\rm d}t$ may also contain singular terms proportional to δ-functions. For example ${\rm d}k(t)/{\rm d}t = [k(t_+^+)-k(t_+^-)]\delta(t-t_+) + [k(t_F^+)-k(t_F^-)]\delta(t-t_F) + {\rm d}k(t)/{\rm d}t\,[\Theta(t_+-t)+\Theta(t_F-t)\Theta(t-t_+)]$, where $\Theta(t)$ equals 1 for $t>0$ and 0 otherwise. For an isothermal process the function $\tilde{\sigma}_w(t,t')$ can be obtained from the work characteristic function derived in [152].

4.2.4 Diagrams of the limit cycle

The driving $\boldsymbol{Y}(t)$ has two components, $g(t)$ and $k(t)$. The mean work done by the engine per cycle can thus be written as $W_{\rm out} = W_{\rm g} + W_{\rm k}$ (cf. Subs. 1.4.2). From Eq. (4.36) the two terms are identified:

$$W_{\rm g} = \int_0^{t_{\rm p}}{\rm d}t\;\langle\log x(t)\rangle\;\left[\frac{{\rm d}g(t)}{{\rm d}t}\right]\,, \tag{4.47}$$

$$W_{\rm k} = -\int_0^{t_{\rm p}}{\rm d}t\,\frac{1}{2}\left\langle[x(t)]^2\right\rangle\frac{{\rm d}k(t)}{{\rm d}t}\,. \tag{4.48}$$

The first contribution equals the area enclosed by the parametric plot of the average $\langle\log x(t)\rangle$ (system response) versus the driving component $g(t)$, where the parameter t runs from 0 to $t_{\rm p}$. Similarly the second contribution corresponds to the area enclosed by the parametric plot of the response $\langle[x(t)]^2\rangle/2$ versus the driving component $-k(t)$, cf. Figs. 4.9 and 4.11. In context of stochastic thermodynamics such parametric plots, which represent an analogy of the well known p-V diagrams, were introduced in [31]. From now on we call the parametric plot corresponding to $W_{\rm g}$ ($W_{\rm k}$) as *g-cycle* (*k-cycle*). $W_{\rm g}$ and $W_{\rm k}$ are proportional to $(2\nu+1)$ and to $(\nu+1)$, respectively. Consequently, it is possible to tune the sign of the total output power $P_{\rm out} = (W_{\rm g}+W_{\rm k})/t_{\rm p}$ by changing the parameter $\nu > -1$, cf. Fig. 4.14.

An important eye-guide in FIGS. 4.9 and 4.11 are the two equilibrium isotherms $\langle \log x(t) \rangle_{\rm eq}$ and $\langle [x(t)]^2 \rangle_{\rm eq}/2$, where $\langle \bullet \rangle_{\rm eq} = -\int_0^\infty {\rm d}x \, \bullet \exp\left[-\mathcal{V}(x,t)/T(t)\right]/Z(t)$, $Z(t) = \Gamma(\nu+1) 2^\nu [T(t)/k(t)]^{\nu+1}$. They correspond to the values of the averages (4.37)-(4.38) if a given cycle would be carried out quasi-statically. The specific form of $\langle \log x(t) \rangle_{\rm eq}$ and $\langle [x(t)]^2 \rangle_{\rm eq}/2$ is obtained if one substitutes

$$f_{\rm eq}(t) = \frac{T(t)}{2k(t)} \tag{4.49}$$

for the function $f(t)$ in EQS. (4.37) and (4.38), respectively. The farther a non-equilibrium isotherm is from the corresponding equilibrium one the more irreversible this branch is, cf. FIG. 4.11. Close to equilibrium the work probability density is reasonably approximated by a Gaussian distribution [134, 176, 177]. From Jarzynski equality (1.61), valid during the isothermal branches, then follows $T(t)\, \log[Z(t')/Z(t)] \approx -W_{\rm out}(t,t') - [W_{\rm out}(t,t')\, \tilde{\sigma}_w(t,t')]^2/[2T(t)]$. We have used this formula for verification of the calculated functions (4.36) and (4.44). The further discussion of the cycle diagrams is postponed to SUBS. 4.2.6. In the next SUBS. we specify several forms of the driving component $k(t)$ with respect to the engine performance.

4.2.5 External driving

The quantities $P_{\rm out}$, $\delta P_{\rm out}$ and η naturally determine the "quality" of a Brownian engine. The ideal engine should work, at the same time, at the largest possible output power (1.70) with the smallest possible fluctuation (4.45) and with the largest possible efficiency (1.69). However, such engine can not be constructed. For example, the *maximum possible efficiency* (1.71) is obtained in the reversible limit, when the output power vanishes. Therefore one has to either maximize a single characteristic of the engine alone or settle with a compromise.

Maximum power:

Let the parameters $k_0 = k(0)$, $k_1 = k(t_+^+)$, $t_\pm$, $T_\pm$ and ν are given. In this SUBS. we will find the specific form of the function $k(t)$ which yields the maximum power (1.70) for these parameters. Later on we will identify also ideal durations of the two isothermal branches, $t_\pm$. The mean work (4.36) represents a complicated, non-local, functional of $k(t)$ (see for example [182] where the procedure is performed for an isothermal process). Therefore, instead of finding the optimal protocol $k(t)$ directly, we will adopt a little bit tricky approach introduced in [159] (see also [195]). The limit cycle (4.34) corresponding the (unknown) optimal protocol $k(t)$ is inevitably described by a certain function $f(t)$. This function can be obtained from $k(t)$ via EQ. (4.35) and, similarly, the function $k(t)$ can be obtained from the function $f(t)$ using the formula

$$k(t) = -\frac{\dot{f}(t) - T(t)}{2f(t)} \ . \tag{4.50}$$

EQS. (4.35) and (4.50) represent a one-to-one correspondence between the functions $k(t)$ and $f(t)$ and hence it does not matter if one first finds the optimal

driving $k(t)$ or the optimal response $f(t)$. During the isothermal branches the work (4.36) assumes the generic form

$$W_{\rm out}(t_{\rm f},t_{\rm i}) = -\int_{t_{\rm i}}^{t_{\rm f}} {\rm d}t\, \frac{1}{f(t)} \left[\dot f(t)\right]^2 - \\ - 2(\nu+1)[k(t_{\rm f})f_{\rm f} - k(t_{\rm i})f_{\rm i}] + (\nu+1)T\log\frac{f_{\rm f}}{f_{\rm i}} \ . \quad (4.51)$$

The work done during the first isothermal branch (branch I) is obtained after the substitution $t_{\rm i}=0$, $t_{\rm f}=t_+^-$, $f_{\rm i}=f(0)=f_0$, $f_{\rm f}=f(t_+)=f_1$ and $T=T_+$. The substitution $t_{\rm i}=t_+^+$, $t_{\rm f}=t_{\rm p}^-$, $f_{\rm i}=f(t_+)=f_1$, $f_{\rm f}=f(t_{\rm p})=f_0$ and $T=T_-$ yields the work done during the second isothermal branch (branch III). The integral in Eq. (4.51) equals the *irreversible work*

$$W_{\rm ir}(t_{\rm f},t_{\rm i}) = -\int_{t_{\rm i}}^{t_{\rm f}} {\rm d}t\, \frac{1}{f(t)} \left[\dot f(t)\right]^2 = -T[S_{\rm tot}(t_{\rm f}) - S_{\rm tot}(t_{\rm i})] \le 0 \ , \quad (4.52)$$

the second term Eq. (4.51) corresponds to the increase of the internal energy, $-[U(t_{\rm f})-U(t_{\rm i})]$, and the third term is given by $TS_{\rm s}(t_{\rm f},t_{\rm i})$. Using the definition (4.52), the total entropy produced per cycle, the work done per cycle and the engine efficiency can be rewritten as

$$S_{\rm tot} = S_{\rm tot}(t_{\rm p}) = -\left[\frac{W_{\rm ir}(t_+,0)}{T_+} + \frac{W_{\rm ir}(t_{\rm p},t_+)}{T_-}\right] \ , \quad (4.53)$$

$$W_{\rm out} = (T_+ - T_-)S_{\rm s}(t_+,0) + [W_{\rm ir}(t_+,0) + W_{\rm ir}(t_{\rm p},t_+)] \ , \quad (4.54)$$

$$\eta = \left(1-\frac{T_-}{T_+}\right)\frac{W_{\rm out}}{W_{\rm out}+T_-S_{\rm tot}} \ , \quad (4.55)$$

respectively. The increase of the system entropy during the first isothermal branch, $S_{\rm s}(t_+,0)$, equals $(\nu+1)\log(f_1/f_0)$. Assume that the parameters $T_\pm$, $t_\pm$, f_0 and f_1 are given. Moreover, let the function $f(t)$ maximize the irreversible work (4.52) during the both isothermal branches. Then, for these given parameters, this function also minimizes the total entropy production (4.53) and maximizes the output work (4.54) and the efficiency (4.55), cf. [190] and Figs. 4.13, 4.14.

Heaving in mind the above discussion, we find the function $k(t)$, which maximizes the work per cycle for a given k_0, k_1, $t_\pm$, $T_\pm$ and ν, in the following three steps. First, we find the function $f(t)$ which maximizes the work for a given f_0 and f_1, etc. Second, we use Eq. (4.50) and calculate the corresponding function $k(t)$. Finally, we determine the constants f_0 and f_1 as the functions of k_0 and k_1.

The function $f(t)$ maximizing the integral (4.52) solves the Euler-Lagrange equation $[\dot f(t)]^2 - 2f(t)\,[\ddot f(t)] = 0$ with the boundary conditions $f(t_{\rm i})=f_{\rm i}$, $f(t_{\rm f})=f_{\rm f}$. Its solution for the isothermal branches I and III reads [158, 159, 182]

$$f(t) = \begin{cases} f_0\,(1+A_1 t)^2 \ , \quad A_1 = \dfrac{1}{t_+}\left(\sqrt{\dfrac{f_1}{f_0}}-1\right) \ , & t\in[0,t_+] \\ f_1\,[1+A_2(t-t_+)]^2 \ , \quad A_2 = \dfrac{1}{t_-}\left(\sqrt{\dfrac{f_0}{f_1}}-1\right) \ , & t\in[t_+,t_{\rm p}] \end{cases} . \quad (4.56)$$

For this optimal response, Eq. (4.50) yields the following *optimal protocol*:

$$k(t) = \begin{cases} \dfrac{T_+}{2f_0}\dfrac{1}{(1+A_1 t)^2} - \dfrac{A_1}{1+A_1 t} \ , & t \in [0, t_+^-] \\ \dfrac{T_-}{2f_1}\dfrac{1}{[1+A_2(t-t_+)]^2} - \dfrac{A_2}{1+A_2(t-t_+)} \ , & t \in [t_+^+, t_{\mathrm{p}}^-] \end{cases} \ . \tag{4.57}$$

This protocol already determines the jumps in $k(t)$ and thus the adiabatic branches II and IV. The assumptions we have imposed on the function $k(t)$ during the derivation of the optimal protocol (4.57) are the following: 1) $k(t)$ is continuous within the isothermal branches (otherwise the time derivative $\dot{f}(t)$ in Eq. (4.52) would not exist); 2) the optimal system response $f(t)$ corresponding to $k(t)$ is periodic and assumes the values f_0 and f_1 at the times 0 and t_+, respectively. Finally, from Eq. (4.57), we have for f_0 and f_1

$$f_0 = \frac{2(D-B) + ABC + 2\sqrt{(D-B)^2 + ABCD}}{A(AC-4)} \ , \tag{4.58}$$

$$f_1 = \frac{2(B-D) + ACD + 2\sqrt{(D-B)^2 + ABCD}}{C(AC-4)} \ , \tag{4.59}$$

where the individual constants are given by

$$\begin{aligned} A &= 2(k_0 t_+ + 1) \ , & B &= t_+ T_+ \ , \\ C &= 2(k_1 t_- + 1) \ , & D &= t_- T_- \ . \end{aligned} \tag{4.60}$$

Eqs. (4.57)-(4.60) represent the solution of the problem proposed in the beginning of this Subs., i.e., they describe the driving $k(t)$ which, for the given parameters $k_0 = k(0)$, $k_1 = k(t_+^+)$, $t_\pm$, $T_\pm$ and ν, yields the maximal output work and thus also the maximum power. Note that for any positive $k_0 = k(0)$, $k_1 = k(t_+^+)$, $t_\pm$, $T_\pm$ the corresponding f_0 and f_1 are also positive and hence the optimal cycle exists for any reasonable parameters. The power corresponding to the optimal protocol (4.57) reads

$$P_{\mathrm{out}} = \frac{T_+ - T_-}{2(\nu+1)}\frac{1}{t_+ + t_-}\Delta S - A_{\mathrm{ir}}\frac{1}{t_+ t_-} \ , \tag{4.61}$$

where $\Delta S = S(t_+, 0)$ is given by (4.41) and $A_{\mathrm{ir}} = 4(\nu+1)\left(\sqrt{f_1} - \sqrt{f_0}\right)^2$ stands for the irreversible action [159], which determines the heat uptake during the isothermal branches, $Q_\pm = \pm T_\pm \Delta S/[2(\nu+1)] - A_{\mathrm{ir}}/t_\pm$, and thus also the total entropy produced per cycle, $S_{\mathrm{tot}} = -Q_+/T_+ - Q_-/T_- = (t_+ + t_-)/(t_+ t_-)A_{\mathrm{ir}}$. The authors of [159] already noted that, in the long time limit $t_\pm \to \infty$, the produced entropy converges to zero and the cycle becomes reversible regardless the instantaneous interchanges of the reservoirs. This feature of the driving, which in fact means that the system is in the long time limit during the *whole cycle* in thermal equilibrium, cf. Figs. 4.11 and 4.12, stems from the fact that, during the derivation, one actually minimizes the irreversible entropy production S_{tot}, cf. [190]. Indeed, from Eqs. (4.56) and (4.57) follow that $\lim_{t_\pm \to \infty} f(t) = f_{\mathrm{eq}}(t)$. As was already noted by Sekimoto [170], this would not be possible if the driving would not include the jumps, which ensure that the system response $f(t)$

converges to its equilibrium value (4.49) also at the instants when the temperature suddenly changes. For the protocols where $\lim_{t_\pm \to \infty} f(t) \neq f_{\rm eq}(t)$ there is, due to the sudden changes of the temperature and subsequent inevitable relaxation processes, always produced a positive amount of entropy $S_{\rm tot}$, cf. [31], Sec. 4.1 and Figs. 4.11, 4.12.

Maximization of (4.61) with respect to the times $t_\pm$ leads to the optimal duration of the branches

$$\tilde{t}_1 = \tilde{t}_2 = \frac{8(\nu+1)A_{\rm ir}}{(T_+ - T_-)\,\Delta S} \ . \tag{4.62}$$

Without loose of generality we assume that the first reservoir is hot ($T_+ > T_-$). In such case the efficiency (1.69) corresponding to the optimal protocol (4.57) with the optimal period durations (4.62) can be written as

$$\eta_{\rm P} = \frac{2\eta_{\rm C}}{4 - \eta_{\rm C}} \ , \tag{4.63}$$

where $\eta_{\rm C} = 1 - T_-/T_+$ denotes the Carnot efficiency (1.71). Note that $\eta_{\rm p}$ depends, contrary to the corresponding optimal power $P_{\rm out} = (T_+ - T_-)^2 \Delta S/[64(\nu+1)^2 A_{\rm ir}]$, only on the reservoir temperatures T_+ and T_-, not on the parameters f_0, f_1 or k_0, k_1 etc. Under the assumption of small temperature difference ($\eta_{\rm C}$ small) one can perform Taylor expansion of the efficiency at maximum power (4.63), the result is

$$\eta_{\rm P} \approx \eta_{\rm CA} \approx \frac{\eta_{\rm C}}{2} + \frac{\eta_C^2}{8} + O\left(\eta_C^3\right) \ , \tag{4.64}$$

where $\eta_{\rm CA} = 1 - \sqrt{T_-/T_+}$ stands for the Curzon-Ahlbron efficiency (1.72). The formulas (4.63) and (4.64) represent another example which verifies validity of general considerations of the works [59, 61, 101, 159] where the authors prove that the efficiency at maximum power (4.63) is bounded as $\eta_{\rm C}/2 < \eta_{\rm P} < \eta_{\rm C}/(2 - \eta_{\rm C})$ and that the expansion (4.64) is universal for strong coupling models that possess a left-right symmetry, cf. Sec. 1.4. In Fig. 4.8 we show one example of the potential (4.25) and of the corresponding particle distribution (4.34) during the limit cycle driven by the optimal protocol (4.57).

Minimum relative power fluctuation

Minimization of the relative power fluctuation (4.45) is a task which is beyond the scope of the present Sec. (the functional, which yields the protocol minimizing the power fluctuation, is to complicated). Using the physical intuition, one can guess that the driving, which minimizes the work fluctuation $|W_{\rm tot}|\,\tilde{\sigma}_w(t_{\rm p}, 0)$, should perform all the work at the instants when the width of the particle distribution (4.38) is minimal. However, such driving would also perform zero amount of work $W_{\rm out}$. Nevertheless, we decided to investigate a class of protocols where the work is performed only during the adiabatic branches. To this end we introduce the *adiabatic driving*:

$$k(t) = \begin{cases} r_1 \ , & t \in [0, t_+^-] \\ r_2 \ , & t \in [t_+^+, t_{\rm p}^-] \end{cases} \ . \tag{4.65}$$

The two isotherms where no work is produced can also be referred to as *isochoric* branches. It is worth noting that, due to the jumps in $k(t)$, the resulting cycle can be performed quasi-statically. However, the only equilibrium cycle consistent with the driving (4.65) dwells during the whole period in the same state.

Fractional driving

Except the protocols (4.57) and (4.65) we have examined also the *fractional driving*:

$$k(t) = \begin{cases} \dfrac{k_1}{1+\gamma_1 t}\,, & t \in [0, t_+^-] \\ \dfrac{k_2}{1+\gamma_2 (t - t_+^+)}\,, & t \in [t_+^+, t_{\rm p}^-] \end{cases} . \tag{4.66}$$

Our results for this protocol coincide with those obtained in [152]. Contrary to the protocols (4.57) and (4.65), this driving may consists of two isotherms only (cf. with the driving used in SEC. 4.1). In the figures we always take continuous $k(t)$, then the adiabatic branches vanish for $\nu = -1/2$. If the jumps in the driving are allowed, the engine corresponding to the fractional driving can be tuned so it differs from the one driven by the optimal protocol (4.57) nearly negligibly. In the next SUBS. we discuss the results obtained for these three protocols.

4.2.6 Discussion

Assume that we want to realize the described engine experimentally using the optical tweezers. Then the control parameters $g(t)$ and $k(t)$ can be driven by the laser intensity. The response function $f(t)$ is proportional to the particle variance. Therefore its maximum value in a sense determines the engine size. In this SUBS. we compare performance of the three protocols described above. In the most illustrations we assume that the protocols are specified by the parameters f_0, f_1, $t_\pm$, $T_\pm$ and ν. In all the figures the constant f_0 (f_1) represents the smallest (largest) value of the function $f(t)$ during the cycle. This means that we compare the engines characterized by the same minimum and maximum particle variance (system size). To perform a similar analysis for a given $k_0 = k(0)$, $k_1 = k(t_+^+)$ etc is straightforward. For a given f_0, f_1, $t_\pm$, $T_\pm$ and ν the parameters of the individual drivings are calculated using the closure conditions on the driving and system response which read $k(t_{\rm p}) = k(0)$, $f(t_+^-) = f(t_+^+)$, $f(t_{\rm p}) = f(0)$ and, for the fractional driving, $k(t_+^-) = k(t_+^+)$, $k(t_{\rm p}^-) = k(t_{\rm p})$. For arbitrary reasonable parameters (positive f_0, f_1, $t_\pm$, $T_\pm$) these formulas yield solution only for the optimal protocol. Therefore, in FIGS. 4.13 and 4.14, we were pushed to take different f_1 for the fractional driving than that used for the other two protocols.

Two representative working cycles for the optimal protocol (4.57) are depicted in FIGS. 4.9 and 4.11. The time resolved thermodynamic quantities (4.36), (4.39-4.40), (4.41-4.43) and (4.44), for these two engines, are depicted in FIGS. 4.10 and 4.12. In FIGS. 4.9, 4.10 and 4.11, 4.12 we show an example of the working cycle together with the corresponding time resolved thermodynamic quantities for the fractional driving (4.66) and for the adiabatic driving (4.65), respectively. Contrary to the equilibrium situation, where two isotherms corresponding to different temperatures can never cross, the simplest non-equilibrium cycle can be formed just by two isothermal branches. For the drivings used the g-cycle forms always a rectangle, while the k-cycle can be formed by two loops of a general shape. An example of such two-loop cycle is depicted in FIG. 4.9.

FIGS. 4.11 and 4.12 demonstrate the case of very slow driving. The cycle driven by the optimal protocol is close to the quasi-static realization and its efficiency nearly attains the Carnot's upper bound (1.71). In the limit of infinitely slow

driving ($t_\pm \to \infty$), the adiabatic changes of the optimal driving at the instants when the reservoirs are interchanged guarantees that the equilibrium states before and after the adiabatic branches coincide, cf. [170]. On the other hand, during the cycle driven by the fractional driving, where the adiabatic branches are not considered, the system is brought far from equilibrium whenever the temperature changes and the quasi-static limit does not exist. In SUBS. 4.2.5 we have shown that, for a given parameters f_0, f_1, $t_\pm$, $T_\pm$ and ν, the optimal protocol (4.57) yields the maximal efficiency and output power and that it minimizes the entropy produced per cycle. This result is verified in FIGS. 4.10 and 4.12. More detailed discussion of FIGS. 4.9-4.12 is contained in the captions below the individual figures.

The efficiency (1.69), the output power (1.70), the power fluctuation (4.45) and the total entropy production (4.43) of engines driven by the protocols (4.57), (4.65) and (4.66) are depicted in FIGS. 4.13 and 4.14. In FIG. 4.13 we study the dependence of these variables on the allocation of a given period t_p between the two isotherms. In FIG. 4.14 the engine performance as a function of the parameter ν is studied. It turns out that all the depicted quantities except the relative power fluctuation, which exhibits a well pronounced minimum, are monotonic functions of ν. The curves corresponding to the optimal protocol and to the adiabatic driving in FIGS. 4.13 and 4.14 verify that, for a given parameters f_0, f_1, $t_\pm$, $T_\pm$ and ν, the optimal protocol (4.57) yields the maximal efficiency, output power and that it minimizes the entropy produced per cycle. On the other hand, for the fractional driving we use different f_1 and hence the corresponding efficiency and even the power output exceeds, for some parameters, the results obtained for the optimal protocol. For the parameters taken in FIGS. 4.13 and FIG. 4.14 the maximum power (4.61) is obtained for $\Delta = 0.5$ and for $\nu = -0.499$, respectively. In the both FIGS. the efficiency at maximum power (4.63) lies between the general bounds (1.74), which are depicted by the solid red and green horizontal lines. For more detailed discussion see the captions below the individual figures.

The smallest relative power fluctuation observed for the three protocols is achieved by the adiabatic driving. From macroscopic world we know that the power fluctuations towards large values can be handled by enlarging the capacity of the system where the power is delivered. On the other hand the fluctuations towards small power values can be balanced only by adapting a standby power supply. An example is the discussion about wind power plants, which cause current fluctuations in transmission-grids [55]. The natural Brownian motors [9, 82, 83, 106] are exposed to large fluctuations of the environment and hence they are quite adapted, indeed. Nevertheless it is an interesting question whether the principle of minimal power fluctuations, the principle of maximum output power, or some other principle eventually applies in this field. In any case, these principles should be considered during the design of artificial Brownian motors [82].

To conclude we have studied a simple, exactly solvable, model of a stochastic heat engine with the continuous state space. The working medium of the engine is a particle diffusing in a time-periodic log-harmonic potential described by two control parameters. We have examined the efficiency at maximum power for this engine. Specifically, we have verified the general results obtained by Schmiedl and Seifert [159] and by Esposito et al. [59, 61]. Further we have focused on output

power fluctuations and discussed the possibility to minimize them. Concretely, we have presented a protocol which yields smaller power fluctuations than the one which gives the maximum power. Finally, we have introduced the driving which, contrary to the two mentioned protocols, does not incorporate the adiabatic branches and thus the corresponding limit cycle can never approach the quasi-static limit. For the three drivings we have discussed the possibility to depict the corresponding limit cycles in a PV-like diagram.

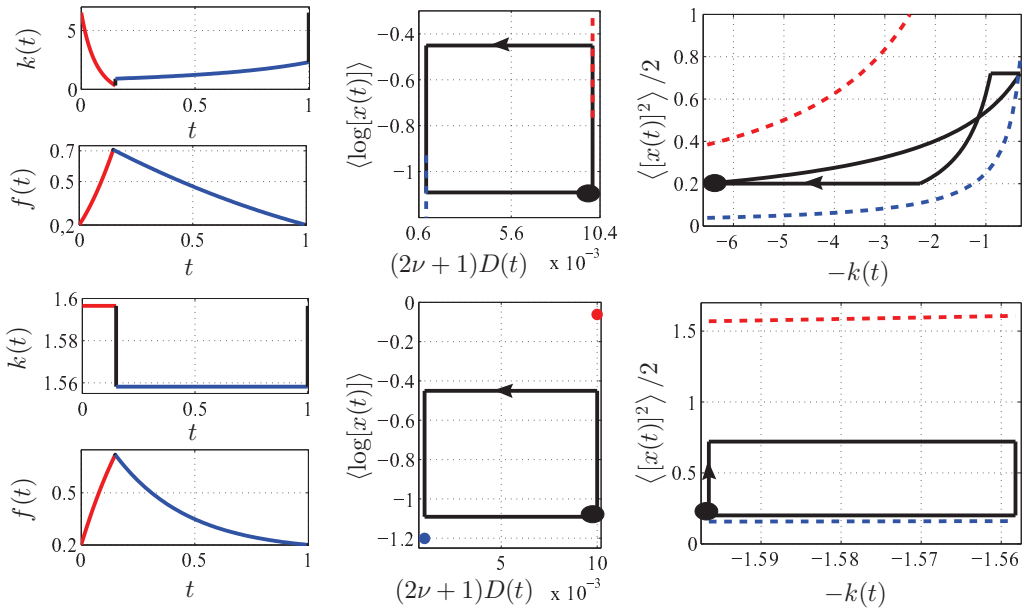

FIG. 4.9: Upper figures depict the driving $k(t)$, the systems response $f(t)$ [EQ. (4.35)], the g-cycle (4.47) formed by one counter-clockwise loop ($W_g < 0$) and the k-cycle (4.48) formed by one clockwise loop ($W_k > 0$) for the optimal protocol (4.57), respectively. Lower three figures show the same for the adiabatic driving (4.65). The total work output for the both cycles is positive ($W_{\rm out} > 0$). In the left figures the red (blue) curve corresponds to the first (second) isotherm. The curves corresponding to the (infinitely fast) adiabatic branches are depicted in black. Red/blue dashed lines in the middle and in the right figures stand for the hot/cold equilibrium isotherms. In the both figures the black circles denote the initial points of the cycles, the directions of the circulations are marked by the arrows. During the isothermal branches of the both g-cycles (and also during the isotherms of the k-cycle for the adiabatic driving) the driving is constant and hence no work is produced. These branches thus represent an analogue of isochores from the classical thermodynamics. Another consequence of the constant $k(t)$ during the isotherms of the adiabatic driving is the fact that the equilibrium isotherms corresponding to the g-cycle degenerate to points. The system response $f(t)$ for the two different protocols [in particular compare the ranges of used $k(t)$ values] is quite similar. Parameters used: $t_+ = 0.15$, $t_- = 0.85$, $T_+ = 5$, $T_- = 0.5$, $f_0 = 0.2$, $f_1 = 0.7198$, $\nu = -0.499$. Here and in all other figures the remaining parameters are calculated from the closure conditions on the driving and system response which read $k(t_{\rm p}) = k(0)$, $f(t_+^-) = f(t_+^+)$ and $f(t_{\rm p}) = f(0)$.

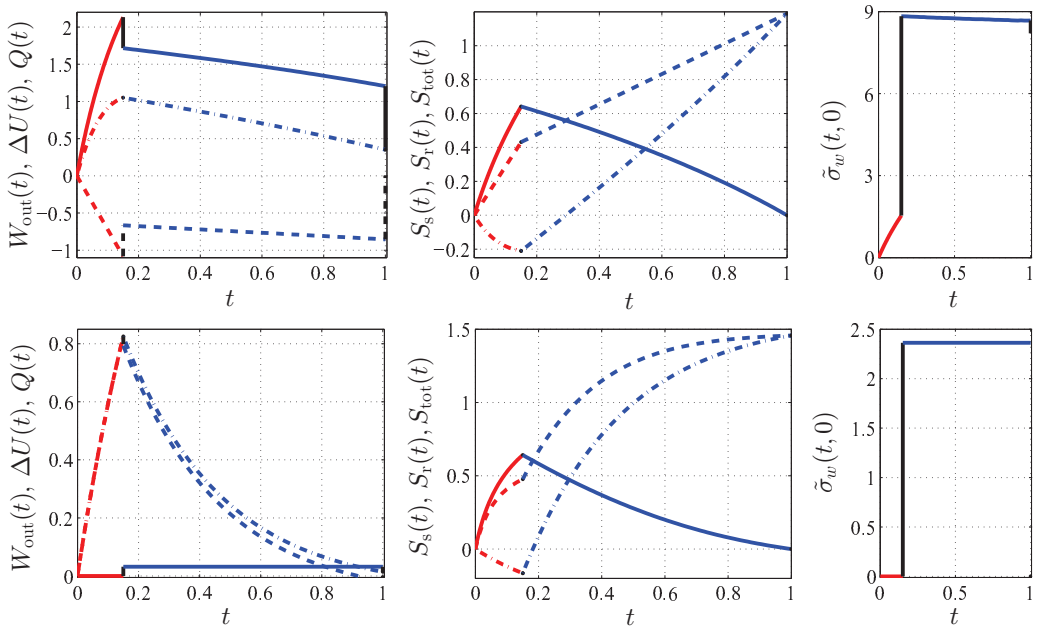

FIG. 4.10: Time-resolved thermodynamics of the engines depicted in FIG. 4.9. In all the panels the red (blue) curve stands for the first (second) isotherm. The curves corresponding to the (infinitely fast) adiabatic branches are depicted in black. The upper (lower) figures in FIG. 4.9 stand for the upper (lower) figures herein. Left: The mean work done on the environment (solid line), the mean heat accepted by the system (dot-dashed line) and the internal energy of the system (broken line). Note that these curves verify the first law of thermodynamics. Middle: The entropy of the system (solid line), the entropy transfered to the reservoirs (dot-dashed line) and the total entropy production of the engine (solid line). The total entropy produced per cycle, $S_{\rm tot}(t_{\rm p})$, is always positive and equals the amount of entropy transfered to the reservoirs, $S_{\rm r}(t_{\rm p})$. Right: The relative work fluctuation. The cycle driven by the optimal protocol (upper figures) produces larger work with larger relative fluctuation than the cycle driven by the adiabatic driving (lower figures), which performs work only during the adiabatic branches. More entropy is produced during the cycle with the adiabatic driving. Note that the relative work fluctuation changes, during the adiabatic branches of the cycle, discontinuously. Although this function can also decrease, the total fluctuation at the end of the cycle is always positive.

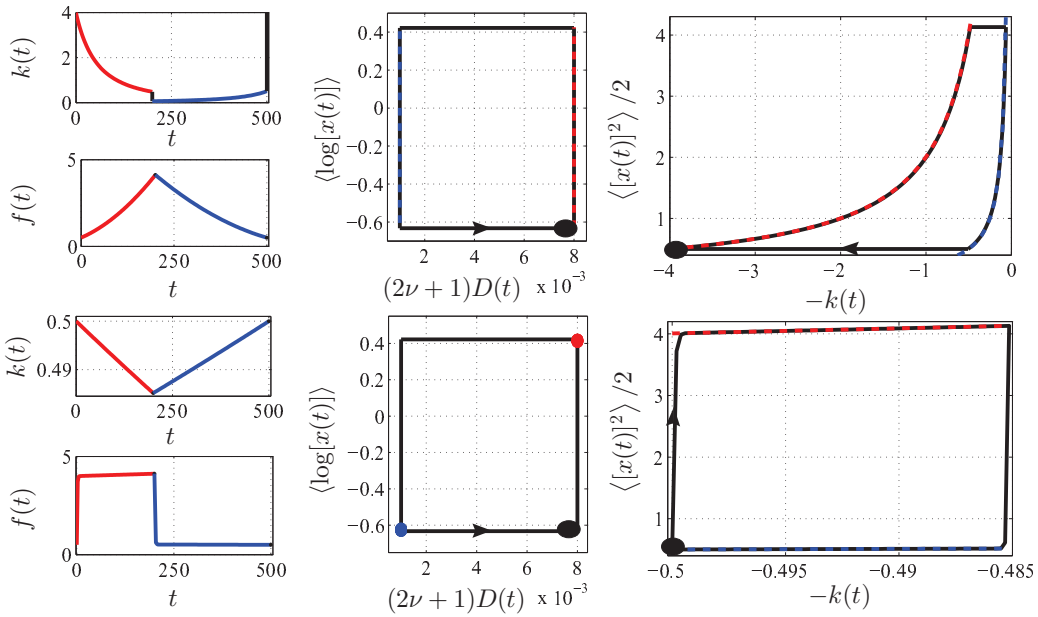

FIG. 4.11: The same quantities as in FIG. 4.9. Upper (lower) three figures correspond to the optimal protocol (4.57) [fractional driving (4.66)]. For the both cycles we have taken very slow driving ($t_+ = 200$, $t_- = 300$). During the cycle driven by the optimal protocol the system is at all times very close to the equilibrium state. The cycle is nearly quasi-static and its efficiency $\eta \approx 0.868$ almost reaches the Carnot's upper bound $\eta_C = 0.875$. On the other hand, during the cycle driven by the fractional driving the system is brought far from equilibrium at the instants when the heat reservoirs are interchanged. During the emerging relaxation processes a large amount of entropy is produced (cf. FIG. 4.12) and the engine efficiency $\eta \approx 0.352$ is far from η_C. Note also that the system response $f(t)$ after these time instants changes quite rapidly as compared to the system response for the optimal protocol. It may seem that the equilibrium isotherms in the g-cycle corresponding to the fractional driving again degenerate to points. This illusion is caused by the fact that the driving $k(t)$ changes during these isotherms only slightly. The range of $k(t)$ used for the optimal protocol is much larger. Other parameters used: $T_+ = 4$, $T_- = 0.5$, $f_0 = 0.5$, $f_1 = 4.1219$, $\nu = -0.499$.

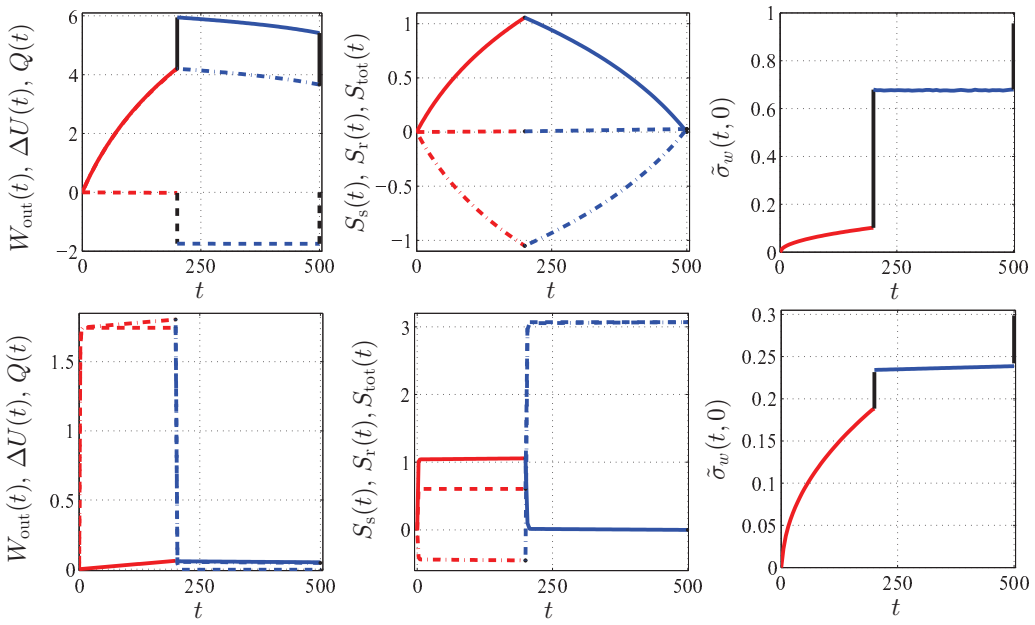

FIG. 4.12: Same quantities as in FIG. 4.10 for the engines depicted in FIG. 4.11. The engine driven by the optimal protocol works during the whole cycle close to the quasi-static regime (cf. FIG. 4.11). On the contrary the cycle driven by the fractional driving is brought far from equilibrium at the instants when the heat reservoirs are interchanged. This is reflected in large (small) output work and small (large) entropy production corresponding to the optimal (fractional) protocol. Note that a considerable amount of the total entropy produced during the cycle with the fraction driving is created just after the two heat reservoirs are interchanged. The fractional driving is favored by the relative work fluctuation, which is much smaller than that corresponding to the optimal protocol.

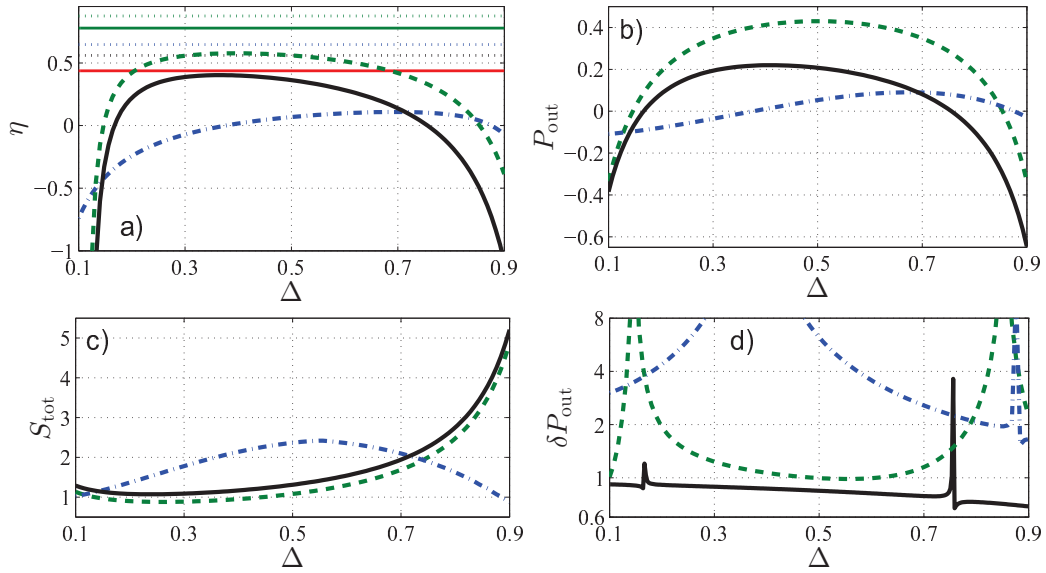

FIG. 4.13: Performance of the engine as a function of the asymmetry parameter $\Delta = t_+/t_\mathrm{p}$ for the optimal driving (4.57) (dashed lines), for the adiabatic driving (4.65) (solid lines) and for the fractional driving (4.66) (dashed-dotted lines). The fixed $t_\mathrm{p} = 2.2344$ is chosen in order to obtain the optimal time distribution (4.62) for $\Delta = 0.5$. a) The efficiency (1.69) of the engine. The upper, middle and lower dotted horizontal lines correspond to the Carnot efficiency η_C, Curzon-Ahlborn effciency η_CA and efficiency at maximum power η_P given by (4.63), respectively. The upper green and lower red solid horizontal lines correspond to the upper and lower bounds for the efficiency at maximum power (1.74). For $\Delta = 0.5$ the efficiency for the optimal driving fulfills this limitation. Note that the upper bound for the efficiency at maximum power is larger than the Curzon-Ahlborn efficiency. b) The output power (1.70). The maximal power for the optimal driving is achieved for $\Delta = 0.5$. c) The total entropy produced per cycle (4.43). d) The relative power fluctuation (4.45) tends to $+\infty$ if the corresponding output power vanishes. We restricted the vertical limits in order to show the most interesting region of the figure in sufficient detail. The smallest power fluctuations are achieved by the adiabatic driving. For all the protocols we took $T_+ = 4$, $T_- = 0.5$, $f_0 = 0.5$, $\nu = -0.499$. Moreover, for the optimal and for the adiabatic driving we used $f_1 = 1.5$, and for the fractional driving we took $k_1 = 1.8$, which results in a different f_1. According to the discussion in SUBS. 4.2.5, the optimal protocol yields, for a given f_0, f_1, $t_\pm$, $T_\pm$ and ν, maximum efficiency, maximum output power and minimum amount of entropy. This is verified on the adiabatic driving which corresponds to the same parameters as the used optimal protocol. On the other hand, for the fractional driving we have used different f_1, which means that, for some values of the parameter Δ, the resulting efficiency and even the output power may exceed the values obtained for the optimal protocol. Similar situation arises if one specifies the parameters $k(0)$, $k(t_+^+)$, $t_\pm$, $T_\pm$ and ν.

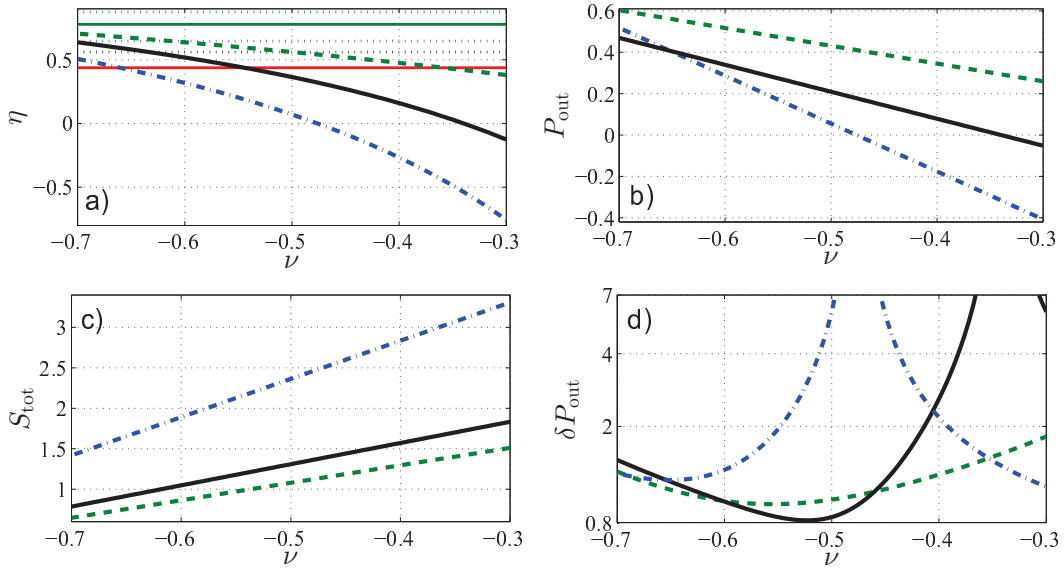

FIG. 4.14: Performance of the engine as a function of the parameter ν (4.29). For $\nu > -0.5$ ($\nu < -0.5$) the logarithmic part of the potential (4.25) is repulsive (attractive). The meaning of the individual curves is the same as in FIG. 4.13. The duration of the isothermal branches $t_+ = t_- = 1.1172$ is chosen in order to obtain the optimal time distribution (4.62) for $\nu = -0.499$. The efficiency, the output power and the entropy produced per cycle are monotonic functions of ν. Note that the efficiency at maximum power ($\nu = -0.499$) fulfills the restriction (1.74). For the parameters taken, the optimal protocol yields the maximum efficiency, maximum output power and minimum entropy production from the three drivings. The power fluctuation both for the optimal protocol and for the adiabatic driving exhibits well pronounced minimum, which is deeper for the adiabatic driving. Other parameters used for all protocols: $T_+ = 4$, $T_- = 0.5$, $f_0 = 0.5$. For the optimal and adiabatic drivings we, moreover, used $f_1 = 1.5$. For the fractional driving we took $k_1 = 1.8$.

Conclusion

In this thesis we have presented several exactly solvable models from the field of stochastic thermodynamics, which we have reviewed in Chap. 1. First, in Chaps. 2 and 3, we have focused on driven mesoscopic systems with both discrete (Chap. 2) and continuous (Chap. 3) state space which, moreover, interact with a thermal reservoir at a constant temperature. We have analytically investigated the dynamics and energetics during the emerging isothermal processes. In particular, we have calculated the probability density for work, heat and internal energy. Although, from the theoretical point of view, these results are themselves interesting, they can also help to better utilize the experimental data. For instance in many experiments the Jarzynski equality (1.61) is used in order to extract the equilibrium free energy differences from non-equilibrium stretching experiments [151]. The extracted free energy difference strongly depends on the tail of the work distribution for large negative work values, which correspond to highly improbable realizations of the experiment and hence can not be measured accurately enough. Therefore it is important to use the correct fit (the Jarzynski estimator) of the measured work distributions in order to obtain the tail accurately enough [138]. Although complicated from the mathematical point of view, the models where the work fluctuations can be treated analytically are often too simple from the physical point of view. More realistic models can be studied using computer simulations, which can also help to find suitable Jarzynski estimators. In App. C we present a new algorithm which can be used for these simulations.

In the second part of the thesis (Chap. 4) we have focused on periodically driven mesoscopic systems which communicate with two heat reservoirs at different temperatures. During the cyclic process the system can perform a positive mean work on the environment. Such stochastic heat engines have been studied during the last decade. We have presented two exactly solvable models. In the first one we have derived the probability density for the work performed per operational cycle, and we have discussed its properties. In the second example we have found the exact form of the periodic driving which yields the maximum output power of the engine and we have verified the recent general results concerning the corresponding efficiency [195]. In the both models we have also discussed the possibility to minimize the power fluctuations. Majority of the available studies concerning stochastic heat engines focus on calculating the mean values of the thermodynamic quantities. Our analysis of the corresponding fluctuations provides new insights into the performance of the engines.

The results presented in the thesis can be extended in several directions. For instance one can focus on stochastic thermodynamics of interacting systems, which did not received much attention in the literature, yet. Further, it would be interesting to investigate the possibility to optimize the performance of the stochastic heat engines under different requirements than that of maximum power or minimal power fluctuations. One can draw inspiration from many studies concerning macroscopic heat engines, where several ecological, economical and size criteria are considered [49]. "Natural" engines working in living cells usually do not use temperature gradients. Therefore, it would be interesting to extend the presented analysis on the processes driven by chemical gradients, which, moreover,

involve chemical reactions. Several studies in this direction were performed in the field of Brownian motors [9, 82, 83, 106]. However, in these papers, the work fluctuations are studied only seldom, which opens possibilities for further research.

Appendixes

A. Work Distributions for Slow and for Fast Processes

In this App. we investigate the probability density for the work done during an infinitely fast (slow) isothermal process. Without loose of generality we consider only the situation when the initial condition is set at the time $t' = 0$. In such case we can simplify the notation. We write $\mathbb{R}(t\,|\,0) \equiv \mathbb{R}(t)$ and $\mathbb{G}(w, t\,|\,0, 0) \equiv \mathbb{G}(w, t)$ for the solution of the master Eq. (1.3) and that of Eq. (1.13), respectively. Further we assume that the detail balance condition (1.4) is fulfilled.

Laplace transform of the probability distribution for the work given initial and final state of the system [elements of the matrix $\mathbb{G}(w, t)$], if exists, obeys the set of ordinary differential equations

$$\frac{\mathrm{d}}{\mathrm{d}t}\tilde{\mathbb{G}}(s, t) = -\Big[s\,\dot{\mathbb{E}}(t) + \nu\mathbb{L}(t)\Big]\,\tilde{\mathbb{G}}(s, t), \qquad \tilde{\mathbb{G}}(s, 0) = \mathbb{1}\ , \tag{A.1}$$

where s is the Laplace variable corresponding to the work variable w. Note that $\tilde{\mathbb{G}}(0, t) = \mathbb{R}(t)$. Its solution for an infinitely slow (fast) process can be obtained by taking the limit $\nu \to \infty$ ($\nu \to 0$) in Eq. (A.1), i.e., by assuming infinitely fast (slow) intrinsic relaxation processes.

A.1 Infinitely fast process

If $\nu = 0$, the solution of the master Eq. (1.3) is the constant matrix $\mathbb{R}(t) = 1/N\,\mathbb{1}$ and Eq. (A.1) reduces to

$$\frac{\mathrm{d}}{\mathrm{d}t}\tilde{\mathbb{G}}(s, t) = -s\,\dot{\mathbb{E}}(t)\,\tilde{\mathbb{G}}(s, t), \qquad \mathbb{G}(s, 0) = \mathbb{1}\ . \tag{A.2}$$

Its solution reads

$$\tilde{\mathbb{G}}(s, t) = \frac{1}{N}\exp\left\{-s\left[\mathbb{E}(t) - \mathbb{E}(0)\right]\right\}\,\mathbb{1}\ , \tag{A.3}$$

which gives after the inverse Laplace transform [the matrix $\mathbb{E}(t)$ is diagonal]

$$[\mathbb{G}(w, t)]_{ij} = \frac{1}{N}\delta\left\{w - \left[\mathcal{E}_i(t) - \mathcal{E}_i(0)\right]\right\}\delta_{ij}\ . \tag{A.4}$$

As expected, during an infinitely fast process, the system dwells in its initial state and the work equals the change of its internal energy (there is no time to accept any heat from the reservoir). In this thesis we call these processes as adiabatic.

A.2 Infinitely slow process

If $\nu = \infty$, the master Eq. (1.3) translates into the eigenvalue problem

$$\mathbb{L}(t)\,\mathbb{R}(t) = 0\ . \tag{A.5}$$

Assuming the detailed balance condition (1.4), the solution of Eq. (A.5) is the matrix containing the equilibrium occupation probability vector corresponding to the instantaneous value of the potential in all its columns: $[\mathbb{R}(t)]ij = \pi_j(t) = \exp\left[-\beta\mathcal{F}_j(t)\right]/Z(t)$, where $Z(t) = \sum_{i=1}^{N} \exp[-\beta\mathcal{F}_i(t)]$ denotes the partition function. Differently speaking, any initial state $\boldsymbol{p}(0)$ immediately relaxes into the equilibrium state $\boldsymbol{\pi}(0) = \mathbb{R}(0)\,\boldsymbol{p}(0)$. Note that the individual matrix elements are discontinuous. Initially $\mathbb{R}(t)$ equals the unity matrix and at any larger time ($t > 0$) it consists of the equilibrium vectors $\boldsymbol{\pi}(t)$.

Let us integrate the work variable out of the work propagator $\mathbb{G}(w,t)$, what remains is the transition matrix $\mathbb{R}(t)$:

$$\int_{-\infty}^{\infty} \mathrm{d}w\, \mathbb{G}(w,t) = \mathbb{R}(t)\ . \tag{A.6}$$

Now we multiply this Eq. from the left by the rate matrix $\mathbb{L}(t)$ and we employ Eq. (A.5). The result is

$$\int_{-\infty}^{\infty} \mathrm{d}w\, \mathbb{L}(t)\mathbb{G}(w,t) = 0\ . \tag{A.7}$$

This formula is valid for any external driving $\mathcal{E}_i(t)$, even for those for which the matrix $\mathbb{L}(t)\,\mathbb{G}(w,t)$ does not vanish after the integration. This means that the matrix $\mathbb{G}(w,t)$ factorizes as $\mathbb{G}(w,t) = \mathbb{R}(t)\,\mathbb{F}(w,t)$, where the unknown matrix $\mathbb{F}(w,t)$ obeys the formula $\int_{-\infty}^{\infty} \mathrm{d}w\, \mathbb{F}(w,t) = \mathbb{1}$. Using the same argumentation as above, in order to fulfill the last formula, the matrix $\mathbb{F}(w,t)$ must be diagonal. Moreover, if we consider that any initial state $\boldsymbol{p}(0)$ immediately relaxes into the equilibrium state $\boldsymbol{\pi}(0)$, it is reasonable to assume that for any initial state of the system one obtains the same work distribution. Altogether we conclude that the work propagator should have the form $\mathbb{G}(w,t) = f(w,t)\mathbb{R}(t)$, where $f(w,t)$ is an unknown function. After inserting this ansatz into Eq. (A.1) we obtain

$$\tilde{f}(s,t)\,\frac{\mathrm{d}}{\mathrm{d}t}\mathbb{R}(t) + \left[\frac{\mathrm{d}}{\mathrm{d}t}\tilde{f}(s,t)\right]\,\mathbb{R}(t) = -s\tilde{f}(s,t)\,\left[\frac{\mathrm{d}}{\mathrm{d}t}\mathbb{E}(t)\right]\,\mathbb{R}(t)\ , \tag{A.8}$$

where $\tilde{f}(s,t)$ stands for the Laplace transformed function $f(w,t)$. The work probability density is obtained from the work propagator as $\rho(w,t) = \mathbf{1}^{\mathrm{T}}\,\mathbb{G}(w,t)\,\boldsymbol{p}(0)$, where $\mathbf{1}^{\mathrm{T}}$ stands for the line vector of ones, cf. equations (1.15) and (1.16). Therefore, in order to obtain the function $f(s,t)$ we multiply Eq. (A.8) by $\mathbf{1}^{\mathrm{T}}$ from the left and by $\boldsymbol{p}(0)$ from the right. We get the formula

$$\frac{\mathrm{d}}{\mathrm{d}t}\tilde{f}(s,t) = -s\sum_{i=1}^{N} \dot{\mathcal{E}}_i(t)\,\pi_i(t)\tilde{f}(s,t)\ , \tag{A.9}$$

where we have used the following relations

$$\mathbf{1}^{\mathrm{T}}\,\mathbb{R}(t)\,\boldsymbol{p}(0) = \mathbb{1}\ , \tag{A.10}$$

$$\mathbf{1}^{\mathrm{T}}\,\dot{\mathbb{R}}(t)\,\boldsymbol{p}(0) = \frac{\mathrm{d}}{\mathrm{d}t}\left[\mathbf{1}^{\mathrm{T}}\,\mathbb{R}(t)\,\boldsymbol{p}(0)\right] = 0\ , \tag{A.11}$$

$$\mathbf{1}^{\mathrm{T}}\,\dot{\mathbb{E}}(t)\,\mathbb{R}(t)\,\boldsymbol{p}(0) = \mathbf{1}^{\mathrm{T}}\,\dot{\mathbb{E}}(t)\,\boldsymbol{\pi} = \sum_{i=1}^{N} \dot{\mathcal{E}}_i(t)\,\pi_i(t)\ . \tag{A.12}$$

Solution of Eq. (A.9) is similar to that of Eq. (A.1). We will continue with its inverse Laplace transform

$$f(w,t) = \rho(w,t) = \delta\left\{ w - \int_0^t \mathrm{dt}' \sum_{i=1}^{N} \dot{\mathcal{E}}_i(t')\, \pi_i(t') \right\} \ . \tag{A.13}$$

The integral inside the δ-function yields the mean work done on the system (1.23). Since the process is quasi-static, the mean work equals the increase of the Helmholtz free energy $F(t) = -\log[Z(t)]/\beta$ of the system. We get the expected result

$$\rho(w,t) = \delta\left\{ w - [F(t) - F(0)] \right\} \ . \tag{A.14}$$

This results was already obtained by Speck and Seifert [177] using Langevin and Fokker-Planck formalism. In their setting these authors have also shown that for slow (but finite) driving WPD has always Gaussian form. We were not able to repeat such calculation within the master equation dynamics. For example if one attempts to expand the matrices $\mathbb{R}(t)$ and $\mathbb{G}(w,t)$ in the small parameter $1/\nu$, he is pushed to calculate the matrix $[\mathbb{L}(t)]^{-1}$. However, the rate matrix $\mathbb{L}(t)$ is singular and thus it can not be inversed. Nevertheless, such result could be expected, because the WPD in discrete models poses (for finite times) a finite support and hence it can be approximated by a Gaussian near its maximum at best [134].

B. Validity of Jarzynksi Equality for an Unidirectional Process

In this App. we investigate whether the analytical results obtained for the work probability density in the Kittel zipper model (Sec. 2.4) can be used as an approximation of work distributions measured during single molecule experiments [3, 40, 150, 151]. Specifically, we examine the validity of the experimentally important Jarzynski equality (1.61) for this approximate model. To this end we consider a more realistic model of a DNA hairpin unfolded by a linearly increasing force $f(t) = f_0 + rt$, where r is the loading rate (cf. Fig. 2.3). With the help of Mfold folding predictions [155, 198], it is possible to design a periodic DNA sequence [135] which unfolds like a N-level system with the (forward) free energy barriers between the individual levels (cf. Fig. 2.1) and the level free energies given by

$$\Delta(t) = E - Ff(t) = E - Ff_0 - Frt \;, \tag{B.1}$$
$$\mathcal{F}_i(t) = (i-1)[A - Bf(t)] = (i-1)(A - Bf_0 - Brt) \;, \tag{B.2}$$

respectively. The unfolding of such periodic DNA molecule can be described by Eq. (1.3) with the rate matrix

$$\mathbb{L}(t) = \frac{1}{\nu} \begin{pmatrix} \lambda_{\mathrm{U}}(t) & -\lambda_{\mathrm{R}}(t) & & & & \\ -\lambda_{\mathrm{U}}(t) & \lambda_{\mathrm{U}}(t) + \lambda_{\mathrm{R}}(t) & \ddots & & & \\ & \ddots & \ddots & \ddots & & \\ & & \ddots & \lambda_{\mathrm{U}}(t) + \lambda_{\mathrm{R}}(t) & -\lambda_{\mathrm{R}}(t) & \\ & & & -\lambda_{\mathrm{U}}(t) & \lambda_{\mathrm{R}}(t) \end{pmatrix} \;, \tag{B.3}$$

where the empty elements are 0. The unfolding and refolding rates in (B.3) are

$$\lambda_{\mathrm{U}}(t) = \nu \exp[-\beta(E - Ff_0)] \exp(\beta Frt) \;, \tag{B.4}$$
$$\lambda_{\mathrm{R}}(t) = \exp[\beta(A - Bf_0)] \exp(-\beta Frt) \lambda_{\mathrm{U}}(t) \;. \tag{B.5}$$

The work fluctuations during the unfolding can be studied using the solution of Eq. (1.13) with the matrix $\mathbb{L}(t)$ given by Eq. (B.3) and with

$$\dot{\mathbb{E}}(t) = \mathrm{diag}\{\dot{\mathcal{F}}_1(t), \ldots, \dot{\mathcal{F}}_N(t)\} = -Br\,\mathrm{diag}\{0, \ldots, N-1\} \;. \tag{B.6}$$

From Subs. 2.1.2 we know that, even for $N = 2$, this model is exactly solvable only for the case $F = B$. The approximate solution for the case $\lambda_{\mathrm{U}}(t) \gg \lambda_{\mathrm{R}}(t) \approx 0$ is discussed in Sec. 2.4.

WPD for any N-level system assumes the generic form

$$\rho(w,t) = \rho_{\mathrm{C}}(w,t) + \sum_{i=1}^{N} R_{ii}(t)\, p_i(0)\, \delta\{w - [\mathcal{F}_i(t) - \mathcal{F}_i(0)]\} \;, \tag{B.7}$$

where $\rho_{\mathrm{C}}(w,t)$ stands for the non-singular part of the probability density and the singular part, proportional to the δ-functions, is determined by the diagonal of the

matrix $\mathbb{R}(t) \equiv \mathbb{R}(t\,|\,0)$ and by the initial state of the system, $p_i(0)$. Contrary to the function $\rho_{\rm C}(w,t)$, the singular part of $\rho(w,t)$ can be always obtained analytically. Specifically, let us define the two auxiliary functions

$$\Lambda_{\rm U}(t) = \int_0^t {\rm d}t'\,\lambda_{\rm U}(t') = \frac{\alpha_{\rm U}}{\beta F r}\left[\exp(\beta F r t) - 1\right] , \tag{B.8}$$

$$\Lambda_{\rm R}(t) = \int_0^t {\rm d}t'\,\lambda_{\rm R}(t') = \frac{\alpha_{\rm R}}{\beta (F-B) r}\left\{\exp[\beta (F-B) r t] - 1\right\} , \tag{B.9}$$

where $\alpha_{\rm U} = \nu \exp[-\beta(E - F f_0)]$ and $\alpha_{\rm R} = \nu \exp[-\beta(E - F f_0)] \exp[\beta(A - B f_0)]$. Then the weights $R_{ii}(t)$ for the present model read

$$R_{11}(t) = \exp[-\Lambda_{\rm U}(t)] , \tag{B.10}$$

$$R_{ii}(t) = \exp[-\Lambda_{\rm U}(t) - \Lambda_{\rm R}(t))] , \quad i = 2, \ldots, N-1 , \tag{B.11}$$

$$R_{NN}(t) = \exp[-\Lambda_{\rm R}(t)] . \tag{B.12}$$

Realistic values of the model parameters obtained in [135] are $\nu = 5 \times 10^6$ Hz, $A = 66.75\, k_{\rm B}T$, $B = 4.64\, k_{\rm B}T/{\rm pN}$, $E = 34.61\, k_{\rm B}T$ and $F = 1.55\, k_{\rm B}T/{\rm pN}$. Moreover, assume that the constant pulling rate is $r = 5$ pN/s, the force applied on the molecule is initially $f(0) = f_0 = 10$ pN and that we stop the pulling at the time $t_{\rm U} = 1.0876$ s when the molecule is already unfolded with the probability larger than 99%. In order to fulfill the Jarzynksi equality

$$\int_{-\infty}^{\infty} {\rm d}w \exp\left(-\beta w\right) \rho(w, t_{\rm U}) = \exp[-\beta \Delta F(t_{\rm U}, 0)] , \tag{B.13}$$

the molecule must be initially in thermal equilibrium. For the parameters above, we have for the partition function $Z(0) = \sum_{i=1}^{N} \exp[-\beta \mathcal{F}_i(0)] \approx \exp[-\beta \mathcal{F}_1(0)]$ and thus $p_i(0) \approx \exp[-\beta \mathcal{F}_i(0)] / \exp[-\beta \mathcal{F}_1(0)]$. Similarly, $Z(t_{\rm U}) \approx \exp[-\beta \mathcal{F}_N(t_{\rm U})]$ and thus we can write for the equilibrium free energy difference $\Delta F(t_{\rm U}, 0) = \log[Z(t_F)/Z(0)] \approx \mathcal{F}_N(t_F) - \mathcal{F}_1(0)$. For the present model Eq. (B.13) is precisely fulfilled. Let us now examine Eq. (B.13) for the unidirectional model, i.e., we take $\lambda_{\rm R}(t) = 0$. In that case $\Lambda_{\rm R}(t) = 0$ and thus $R_{ii}(t) = \exp[-\Lambda_{\rm U}(t)]$, $\forall\, i \neq N$ and $R_{NN}(t) = 1$. For the parameters above we have $\Lambda_{\rm U}(t_{\rm U}) \approx 15$, $\Lambda_{\rm R}(t_{\rm U}) \approx 10^6$ and hence these weights of the δ-functions differ significantly from the values valid for the exact model. Using Eq. (B.7) the integral in Eq. (B.13) assumes the form

$$J_{\rm int} = \int_{-\infty}^{\infty} {\rm d}w \exp\left(-\beta w\right) \rho(w, t_{\rm U}) = I_{\rm C} + I_{\rm S} , \tag{B.14}$$

where the two non-negative terms are $I_{\rm C} = \int_{-\infty}^{\infty} {\rm d}w \exp\left(-\beta w\right) \rho_{\rm C}(w, t_{\rm U})$ and $I_{\rm S} = \sum_{i=1}^{N} R_{ii}(t_{\rm U}) p_i(0) \exp\{-\beta[\mathcal{F}_i(t_{\rm U}) - \mathcal{F}_i(0)]\}$. Using the parameters above and considering the unidirectional model, the second term can be rewritten as

$$\begin{aligned} I_{\rm S} &\approx R_{NN}(t_{\rm U}) p_N(0) \exp\{-\beta[\mathcal{F}_N(t_{\rm U}) - \mathcal{F}_N(0)]\} = \\ &= \exp\left\{-\beta\left[\mathcal{F}_N(t_F) - \mathcal{F}_1(0)\right]\right\} \approx \exp\left[-\beta \Delta F(t_{\rm U}, 0)\right] . \end{aligned} \tag{B.15}$$

The right-hand side of the Jarzynski identity (B.13) is thus, for the unidirectional model, given solely by the singular part of the work distribution. This means

that, although for high enough pulling rates r the work distribution for the unidirectional process and that for the exact model are very similar on a first glance, their tails corresponding to the large negative work values differ significantly. These results are depicted in FIG. B.1.

For small pulling rates ($r = 5\text{pN/s}$) both the probability that the molecule is at the time t fully unfolded, $p_N(t)$, and the WPD for the two models significantly differ, cf. FIGS. B.1a1) and a2). On the other hand for large pulling rates ($r = 500\text{pN/s}$) these two functions are, on a first glance, identical, cf. FIGS. B.1b1) and b2). Note that neither in the case $r = 5\text{pN/s}$ nor in the case $r = 500\text{pN/s}$ the refolding rates can be neglected during the whole pulling, see FIGS. B.1a1) and b1). Indeed, if the backward rates could be neglected also in the very beginning of the pulling experiment, the molecule would be with large probability already unfolded, cf. FIG. 2.4 and the discussion of the backward rates in SUBS. 2.4.2. FIG. B.1a) demonstrates that the correct value of the Jarzynski integral (B.13) is for the unidirectional model given solely by the singular part of the WPD, cf. EQS. (B.14) and (B.15). Note that the Jarzynski integral is in the unidirectional model always overestimated, i.e., the corresponding free energy is underestimated [cf. EQ. (B.14)].

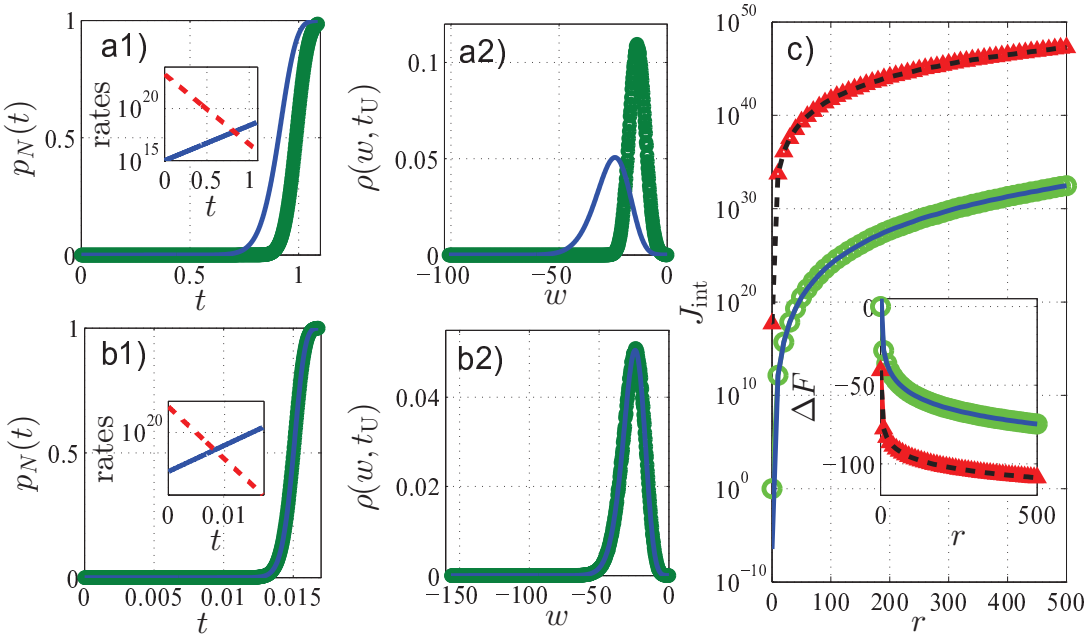

FIG. B.1: Comparison of the unidirectional model (analytical results) and exact model (Monte Carlo results) for the molecule described in APP. B. Panels a1) and a2) [b1) and b2)] correspond to the pulling rate $r = 5\text{pN/s}$ [$r = 500\text{pN/s}$]. The panels a1) and b1) show the probability $p_N(t)$ as a function of time. In the panels a2) and b2) the probability density $\rho(w, t_U)$ for the work done on the molecule during the pulling experiment is presented. In all four panels the results for the exact (unidirectional) model are depicted by the green circles (solid blue lines). The insets in the panels a1) and b1) show the transition rates $\lambda_U(t)$ (solid blue line) and $\lambda_R(t)$ (dashed red line) as the functions of time. The unfolding time t_U in all the panels is given by the implicit equation $p_N(t_U) = 0.99$. Panel c) depicts the Jarzynski integral (B.14) calculated for the unidirectional process as the function of the pulling rate r. Specifically, the red triangles stand for the whole integral, J_{int}, the dashed black line stands for the continuous part of the integral, I_C, and the solid blue line depicts the singular part of the integral, I_S. The green circles stand for the value of the Jarzynski integral for the exact model. The inset shows the free energies calculated from the individual parts of the Jarzynski integral using EQ. (B.13). For each point in the panel c) a different unfolding time t_U is used. Note that the Jarzynski integral is, in the unidirectional model, always overestimated, i.e., the corresponding free energy is underestimated (cf. EQ. (B.14)).

C. Simulations

The following work was, in a slightly modified version, published in [92].

C.1 Introduction

Stochastic jump processes with time-dependent transition rates are of general importance for many applications in physics and chemistry, in particular for describing the kinetics of chemical reactions [5, 8, 76] and the non-equilibrium dynamics of driven systems in statistical mechanics [43, 56, 164]. With respect to applications in interdisciplinary fields they play an important role in connection with queuing theories.

In general a system with N-levels is considered that, at random time instants, performs transitions from one microstate to another. In case of a Markovian jump dynamics the probability for the system to change its microstate in the time interval $[t, t + \Delta t)$ is independent of the history and given by $\lambda_{ij}(t)\Delta t + o(\Delta t)$, where j and $i \neq j$ are the initial and target levels, respectively, and $\lambda_{ij}(t)$ the corresponding transition rate at the time t ($\lambda_{jj}(t) = 0$). That is, if the system is in the level j at the time t', it will stay in this level until a time $t > t'$ with the probability $\phi_j(t, t') = \exp[-\int_{t'}^{t} \mathrm{d}\tau\, \lambda_j^{\mathrm{tot}}(\tau)]$, where $\lambda_j^{\mathrm{tot}}(\tau) = \sum_{i=1}^{N} \lambda_{ij}(\tau)$ is the total escape rate from the level j at the time τ. The probability to perform a transition to the target level i in the time interval $[t, t+\mathrm{d}t)$ then is $\lambda_{ij}(t)\phi_j(t, t')\,\mathrm{d}t$, i.e.,

$$\psi_{ij}(t, t') = \lambda_{ij}(t) \exp\left[-\int_{t'}^{t} \mathrm{d}\tau\, \lambda_j^{\mathrm{tot}}(\tau)\right] \tag{C.1}$$

stands for the probability density for the first transition to the level i to occur at the time t after the system was in the level j at the time t'. Any algorithm that evolves the system according to Eq. (C.1) generates stochastic trajectories with the correct path probabilities.

The first algorithm of this kind was developed by Gillespie [77] in generalization of the continuous-time Monte-Carlo algorithm introduced by Bortz *et al.* [18] for time-independent rates. We call it the reaction time algorithm (RTA) in the following. The RTA consists of drawing a random time t from the first transition time probability density $\psi_j^{\mathrm{tot}}(t, t') = \sum_{i=1}^{N} \psi_{ij}(t, t') = \lambda_j^{\mathrm{tot}}(t)\phi_j(t, t') = -\partial_t \phi_j(t, t')$ to any other microstate $i \neq j$, and a subsequent random selection of the target level i with probability $\lambda_{ij}(t)/\lambda_j^{\mathrm{tot}}(t)$. In practice these two steps can be performed by generating two uncorrelated and uniformly distributed random numbers r_1, r_2 in the unit interval $[0, 1)$ with some random number generator, where the first one is used to specify the transition time t via

$$\Lambda_j(t, t') = \int_{t'}^{t} \mathrm{d}\tau \lambda_j^{\mathrm{tot}}(\tau) = -\log(1 - r_1) \tag{C.2}$$

and the second one is used to select the target level i by requiring

$$\sum_{k=1}^{i-1} \frac{\lambda_{kj}(t)}{\lambda_j^{\mathrm{tot}}(t)} \leq r_2 < \sum_{k=1}^{i} \frac{\lambda_{kj}(t)}{\lambda_j^{\mathrm{tot}}(t)} \tag{C.3}$$

Both steps, however, lead to some unpleasant problems in the practical realization.

The first step according to Eq. (C.2) requires the calculation of $\Lambda_j(t,t')$ and the determination of its inverse $\tilde{\Lambda}_j(.,t')$ with respect to t in order to obtain the transition time $t = \tilde{\Lambda}_j[-\log(1-r_1),t']$. While this is always possible, since $\lambda_j^{\rm tot} > 0$ and accordingly $\Lambda_j(t,t')$ is a monotonously increasing function of t, it can be CPU time consuming in the case when $\tilde{\Lambda}_j(t,t')$ cannot be explicitly given in an analytical form and one needs to implement a root finding procedure.

The second step according to Eq. (C.3) can be cumbersome if there are many levels (N large) and a systematic grouping of the $\lambda_{ij}(t)$ to only a few classes is not possible. This situation in particular applies to many-particle systems, where N typically grows exponentially with the number of particles, and the interactions (or a coupling to spatially inhomogeneous time-dependent external fields) can lead to a large number of different transitions rates. Moreover, even for systems with simple interactions (as, for example, Ising spin systems), where a grouping is in principle possible, the subdivision of the unit interval underlying Eq. (C.3) cannot be strongly simplified for time-dependent rates.

A way to circumvent Eq. (C.3) is the use of the First Reaction Time Algorithm (FRTA) for time dependent rates [102], or modifications of it [5]. In the FRTA one first draws random transition times t_k from the probability densities $\psi_{kj}(t_k,t') = \lambda_{kj}(t_k)\exp[-\int_{t'}^{t_k} {\rm d}\tau\, \lambda_{kj}(\tau)]$ for the individual transitions to each of the target microstates k and then performs the transition i with the smallest $t_i = \min_k\{t_k\}$ at the time t_i. This is statistically equivalent to the RTA, since for the given initial microstate j, the possible transitions to all target microstates are independent of each other. In short-range interacting systems, in particular, many of the random times t_k can be kept for determining the next transition following i. In fact, all transitions from the new level i to target levels k can be kept for which $\lambda_{ki}(\tau) = \lambda_{kj}(\tau)$ for $\tau > t$ (see Ref. [52] for details). However, the random times t_k need to be drawn from $\psi_{kj}(t_k,t')$ and this unfortunately involves the same problems as discussed above in connection with Eq. (C.2).

C.2 Algorithms

We now present a new "attempt time algorithm" (ATA) that allows one to avoid the problems associated with the generation of the transition time in Eq. (C.2). Starting with the system in the level j at the time t_0, one first considers a large time interval T and determines a number $\mu_j^{\rm tot}$ satisfying

$$\mu_j^{\rm tot} \geq \max_{t_0 \leq \tau \leq t_0+T} \{\lambda_j^{\rm tot}(\tau)\} \tag{C.4}$$

In general this can by done easily, since $\lambda_j^{\rm tot}(\tau)$ is a known function. In particular for bounded transition rates it poses no difficulty, as, for example, in the case of Glauber rates or a periodic external driving, where T could be chosen as the time period. If an unlimited growth of $\lambda_j^{\rm tot}$ with time were present (an unphysical situation for long times), T can be chosen self-consistently by requiring that the time t for the next transition to another level $i \neq j$ (see below) must be smaller than $t_0 + T$.

Next an attempt time interval Δt_1 is drawn from the exponential density $F_j(\Delta t_1) = \mu_j^{\rm tot} \exp(-\mu_j^{\rm tot} \Delta t_1)$ and the resulting attempt transition time $t_1 = t_0 + \Delta t_1$ is rejected with probability $p_j^{\rm rej}(t_1) = 1 - \lambda_j^{\rm tot}(t_1)/\mu_j^{\rm tot}$. If it is rejected, a further attempt time interval Δt_2 is drawn from $F_j(\Delta t_2)$, corresponding to an attempt transition time $t_2 = t_1 + \Delta t_2$, and so on until an attempt time $t < t_0 + T$ is eventually accepted. Then a transition to a target level i is performed at the time t with probability $\lambda_{ij}(t)/\lambda_j^{\rm tot}(t)$, using the target level selection of Eq. (C.3).

In order to show that this method yields the correct first transition probability density $\psi_{ij}(t, t_0)$ from Eq. (C.1), let us first consider a sequence, where exactly $n \geq 0$ attempts at some times $t_1 < \ldots < t_n$ are rejected and then the $(n+1)$th attempt leads to a transition to the target level i in the time interval $[t, t + {\rm d}t)$. The corresponding probability density $\psi_{ij}^{(n)}(t, t_0)$ is given by

$$\begin{aligned}
\psi_{ij}^{(n)}(t, t_0) &= \int_{t_0}^{t} {\rm d}t_n \int_{t_0}^{t_{n-1}} {\rm d}t_{n-1} \ldots \int_{t_0}^{t_2} {\rm d}t_1 \frac{\lambda_{ij}(t)}{\lambda_j^{\rm tot}(t)} \\
&\times \left[1 - p_j^{\rm rej}(t)\right] F_j(t - t_n) \prod_{m=1}^{n} p_j^{\rm rej}(t_m) F_j(t_m - t_{m-1}) \qquad \text{(C.5)} \\
&= \frac{\lambda_{ij}(t) e^{-\mu_j^{\rm tot}(t-t_0)}}{n!} \left[\int_{t_0}^{t} {\rm d}\tau \, \mu_j^{\rm tot} p_j^{\rm rej}(\tau)\right]^n \\
&= \frac{\lambda_{ij}(t) e^{-\mu_j^{\rm tot}(t-t_0)}}{n!} \left[\mu_j^{\rm tot}(t - t_0) - \int_{t_0}^{t} {\rm d}\tau \, \lambda_j^{\rm tot}(\tau)\right]^n .
\end{aligned}$$

Summing over all possible n hence yields

$$\psi_j(t, t_0) = \sum_{n=0}^{\infty} \psi_{ij}^{(n)}(t, t_0) = \lambda_{ij}(t) \exp\left[-\int_{t_0}^{t} {\rm d}\tau \, \lambda_j^{\rm tot}(\tau)\right] \qquad \text{(C.6)}$$

from Eq. (C.1).

It is clear that for avoiding the root finding of Eq. (C.2) by use of the ATA, one has to pay the price for introducing rejections. If the typical number of rejections can be kept small and an explicit analytical expression for t cannot be derived from Eq. (C.2), the ATA should become favorable in comparison to the RTA. Moreover, the ATA can be implemented in a software routine independent of the special form of the $\lambda_{ij}(\tau)$ for applicants who are not interested to invest special thoughts on how to solve Eq. (C.2).

One may object that the ATA still entails the problem connected with the cumbersome target microstate selection by Eq. (C.3). However, as the RTA has the first reaction variant FRTA, the ATA has a first attempt variant. In this first attempt time algorithm (FATA) one first determines, instead of $\mu_j^{\rm tot}$ from Eq. (C.4), upper bounds for the individual transitions to all target microstates $k \neq j$ ($\mu_{jj} = 0$),

$$\mu_{kj} \geq \max_{t_0 \leq \tau \leq t_0 + T} \{\lambda_{kj}(\tau)\} \qquad \text{(C.7)}$$

Thereupon random time intervals Δt_k are drawn from the probability density $F_{kj}(\Delta t_k) = \mu_{kj} \exp(-\mu_{kj} \Delta t_k)$, yielding corresponding attempt times $t_k^{(1)} = t_0 + \Delta t_k$. The transition to the target level k' with the minimal $t_{k'}^{(1)} = \min_k\{t_k^{(1)}\} = t_1$ is attempted and rejected with probability $p_{k'k}^{\rm rej}(t_{k'}^{(1)}) = 1 - \lambda_{k'k}(t_{k'}^{(1)})/\mu_{k'k}$. If

it is rejected, a further time interval $\Delta t_{k'}^{(2)}$ is drawn from $F_{k'j}(\Delta t_{k'}^{(2)})$, yielding $t_{k'}^{(2)} = t_{k'}^{(1)} + \Delta t_{k'}^{(2)}$, while the other attempt transition times are kept, $t_k^{(2)} = t_k^{(1)}$ for $k \neq k'$ (it is not necessary to draw new time intervals for these target levels due to the absence of memory in the Poisson process). The target level k'' with the new minimal $t_{k''}^{(2)} = \min_k\{t_k^{(2)}\} = t_2$ is then attempted and so on until eventually a transition to a target level i is accepted at a time $t < t_0 + T$. The determination of the minimal times can be done effectively by keeping an ordered stack of the attempt times. Furthermore, as in the FRTA, one can, after a successful transition to a target level i at the time t, keep the (last updated) attempt times t_k for all target levels that are not affected by this transition (i.e., for which $\lambda_{ki}(\tau) = \lambda_{kj}(\tau)$ for $\tau \geq t$). Overall one can view the procedure implied by the FATA as that each level k has a next attempt time t_k (with $t_j = \infty$ if the system is in the level j) and that the next attempt is made to the target level with the minimal t_k. After each attempt, updates of some of the t_k are made as described above in dependence of whether the attempt was rejected or accepted.

In order to prove that the FATA gives the $\psi_j(t, t_0)$ from Eq. (C.1), we show that the probability densities $\chi_{ij}(t, t_n) = [\lambda_{ij}(t)/\lambda_j^{\mathrm{tot}}(t)](1 - p_j^{\mathrm{rej}}(t))F_j(t - t_n) = \lambda_{ij}(t)\exp[-\mu_j^{\mathrm{tot}}(t - t_n)]$ and $\eta_j(t_m, t_{m-1}) = p_j^{\mathrm{rej}}(t_m)F_j(t_m - t_{m-1}) = [\mu_j^{\mathrm{tot}} - \lambda_j^{\mathrm{tot}}]$ $\exp[-\mu_j^{\mathrm{tot}}(t_m - t_{m-1})]$ appearing in Eq. (C.5) are generated, if we set $\mu_j^{\mathrm{tot}} = \sum_k^N \mu_{kj}$ (note that Eq. (C.4) is automatically satisfied by this choice). These probability densities have the following meaning: $\chi_{ij}(t, t_n)\mathrm{d}t$ is the probability that, if the system is in the level j at the time t_n, the next attempt to a target microstate occurs in the time interval $[t, t + \mathrm{d}t)$, the attempt is accepted, and it changes the level from j to i; $\eta_j(t_m, t_{m-1})\,\mathrm{d}t_m$ is the probability that, after the attempt time t_m, the next attempt occurs in $[t_m, t_m + \mathrm{d}t_m)$ with $t_m > t_{m-1}$ and is rejected.

In the FATA the probability $\kappa_{lj}(t_m, t_{m-1})\,\mathrm{d}t_m$ that, when starting at the time t_{m-1}, the next attempt is occurring in $[t_m, t_m + \mathrm{d}t_m)$ to a target level l is given by

$$\begin{aligned}\kappa_{lj}(t_m, t_{m-1}) &= \mu_{lj}\exp[-\mu_{lj}(t_m - t_{m-1})] \\ &\quad \times \prod_{k\neq l}\int_{t_m - t_{m-1}}^{\infty} \mathrm{d}\tau\, \mu_{kj}\exp(-\mu_{kj}\tau) \\ &= \mu_{lj}\exp[-\mu_j^{\mathrm{tot}}(t_m - t_{m-1})]\ . \end{aligned} \tag{C.8}$$

The product ensures that t_m is the minimal time (the lower bound in the integral can be set equal $(t_m - t_{m-1})$ for all $k \neq l$ due to the absence of memory in the Poisson process). The probability that this attempted transition is rejected is $p_{lj}^{\mathrm{rej}}(t_m) = 1 - \lambda_{lj}(t_m)/\mu_{lj}$ and accordingly, by summing over all target levels l, we obtain

$$\begin{aligned}\eta_j(t_m, t_{m-1}) &= \sum_{l=1}^{N} p_{lj}^{\mathrm{rej}}(t_m)\mu_{lj}\exp[-\mu_j^{\mathrm{tot}})(t_m - t_{m-1})] \\ &= [\mu_j^{\mathrm{tot}} - \lambda_j^{\mathrm{tot}}(t_m)]\exp[-\mu_j^{\mathrm{tot}}(t_m - t_{m-1})] \end{aligned} \tag{C.9}$$

in agreement with the expression appearing in Eq. (C.5). Furthermore, when starting from time t_n, the probability density $\chi_{ij}(t, t_n)$ referring to the joint probability that the next attempted transition occurs in $[t, t + \mathrm{d}t)$ to level i and is

accepted is given by

$$\chi_{ij}(t,t_n) = \frac{\lambda_{ij}(t)}{\mu_{ij}}\kappa_{ij}(t,t_n) = \lambda_{ij}(t)\exp[-\mu_j^{\rm tot}(t-t_n)] \ . \tag{C.10}$$

Hence one recovers the decomposition in Eq. (C.5) with $\mu_j^{\rm tot} = \sum_{k=1}^N \mu_{kj}$.

Before discussing an example, it is instructive to see how the ATA (and RTA) can be associated with a solution of the underlying master Eq. (1.3)

$$\frac{\rm d}{{\rm d}t}\,\mathbb{R}(t\,|\,t') = -\mathbb{M}(t)\,\mathbb{R}(t\,|\,t') \ , \qquad \mathbb{R}(t'\,|\,t') = \mathbb{1} \tag{C.11}$$

where $\mathbb{R}(t\,|\,t')$ is the matrix of transition probabilities $R_{ij}(t\,|\,t')$ for the system to be in the level i at the time t if it was in the level j at the time $t' \le t$, and $\mathbb{M}(t) = \nu\mathbb{L}(t)$ is the transition rate matrix with elements $M_{ij}(t) = -\lambda_{ij}(t)$ for $i \neq j$ and $M_{jj}(t) = -\sum_{\forall\, i\neq j} M_{ij}(t) = \lambda_j^{\rm tot}(t)$. Let us decompose $\mathbb{M}(t)$ as $\mathbb{M}(t) = \mathbb{D} + \mathbb{A}(t)$, where $\mathbb{D} = {\rm diag}\,\{\mu_1^{\rm tot},\ldots,\mu_N^{\rm tot}\}$. If $\mathbb{A}(t)$ were missing, the solution of the master equation (C.11) would be $\mathbb{R}_0(t\,|\,t') = {\rm diag}\,\{\exp(-\mu_1^{\rm tot}(t-t'),\ldots,\exp(-\mu_N^{\rm tot}(t-t')\}$. Hence, when introducing $\tilde{\mathbb{A}}(t\,|\,t') = \mathbb{R}_0^{-1}(t\,|\,t')\mathbb{A}(t)\mathbb{R}_0(t\,|\,t') = \mathbb{R}_0(t'\,|\,t)\mathbb{A}(t)\mathbb{R}_0(t\,|\,t')$ in the "interaction picture", the solution of the master Eq. can be written as

$$\begin{aligned}\mathbb{R}(t\,|\,t') = \mathbb{R}_0(t\,|\,t')\Bigg[\mathbb{1} &+ \int_{t'}^t {\rm d}t_1 \tilde{\mathbb{A}}(t_1\,|\,t') \\ &+ \int_{t'}^t {\rm d}t_2 \int_{t'}^{t_2} {\rm d}t_1 \tilde{\mathbb{A}}(t_2\,|\,t')\tilde{\mathbb{A}}(t_1\,|\,t') + \ldots\Bigg]\end{aligned} \tag{C.12}$$

Inserting $\mathbb{1} = \mathbb{D}^{-1}\mathbb{D}$ after each matrix $\tilde{\mathbb{A}}$, one arrives at

$$\begin{aligned}\mathbb{R}(t\,|\,t') &= \mathbb{R}_0(t\,|\,t') + \int_{t'}^t {\rm d}t_1 \mathbb{R}_0(t\,|\,t_1)\mathbb{B}(t_1)F_0(t_1\,|\,t') \\ &+ \int_{t'}^t {\rm d}t_2 \int_{t'}^{t_2} {\rm d}t_1 \mathbb{R}_0(t\,|\,t_2)\mathbb{B}(t_2)\mathbb{F}_0(t_2\,|\,t_1)\mathbb{B}(t_1)\mathbb{F}_0(t_1\,|\,t') \\ &+ \ldots\end{aligned} \tag{C.13}$$

where $\mathbb{F}_0(t\,|\,t') = \mathbb{D}\,\mathbb{R}_0(t\,|\,t') = {\rm diag}\{\mu_1^{\rm tot}\exp[-\mu_1^{\rm tot}(t-t')],\ldots,\ \mu_N^{\rm tot}\exp[-\mu_N^{\rm tot}(t-t')]\}$, and $\mathbb{B}(t) = \mathbb{A}(t)\mathbb{D}^{-1}$ has the matrix elements $B_{ij}(t) = -\lambda_{ij}(t)/\mu_j^{\rm tot}$ for $i \neq j$ and $B_{jj}(t) = 1 - \lambda_j^{\rm tot}(t)/\mu_j^{\rm tot}$.

Eq. (C.13) resembles the ATA: The transition probabilities $R_{ij}(t\,|\,t')$ are decomposed into paths with an arbitrary number $n = 0, 1, 2, \ldots$ of "Poisson points", where transitions are attempted. The times between successive attempted transitions are exponentially distributed according to the matrix elements of $\mathbb{F}_0$ and the attempted transitions are accepted or rejected according to the probabilities encoded in the diagonal and non-diagonal elements of the $\mathbb{B}$ matrix, respectively. The $\mathbb{R}_0$ entering Eq. (C.13) takes care that after the last attempt in a path with exactly n attempted transitions no further attempt occurs and the system remains in the target level i. The RTA can be associated with an analogous formal solution of the master equation if one replaces $\mathbb{R}_0(t\,|\,t')$ by $\mathbb{R}_0^{\rm RTA}(t\,|\,t') = {\rm diag}\left\{\lambda_1^{\rm tot}(t)\exp[-\int_{t'}^t {\rm d}\tau\,\lambda_1^{\rm tot}(\tau)],\ldots,\ \ \lambda_N^{\rm tot}(t)\exp[-\int_{t'}^t {\rm d}\tau\,\lambda_N^{\rm tot}(\tau)]\right\}$ and $\mathbb{B}(t)$ by $\mathbb{B}^{\rm RTA}(t)$ with elements $B_{ij}^{\rm RTA}(t) = (1-\delta_{ij})\,\lambda_{ij}(t)/\lambda_j^{\rm tot}(t)$ (the diagonal elements are zero since the RTA is rejection-free).

C.3 Example

An implementation of FATA was used for simulated results depicted in FIGS. 2.4 and B.1. Another example is presented in [92]. Here we will introduce an example where EQ. (C.2) must be inevitably solved numerically and, hence, ATA is advantaged before RTA. Specifically, we consider a two-level system with stochastic time-dependent level energies (free energies) $\mathsf{E}_1(t)$ and $\mathsf{E}_2(t)$. We choose a simple linear protocol

$$\mathsf{E}_1(t) = 0 \ , \qquad \mathsf{E}_2(t) = at + \Theta(t)\Theta(\tau - t)\,\mathsf{I}(t) \ . \tag{C.14}$$

The constant a governs the deterministic component of $\mathsf{E}_2(t)$ and $\mathsf{I}(t)$ denotes its stochastic (zero-mean) component. We considered the evolution within the time-interval $t \in [0, \tau]$. The unit-step functions $\Theta(z)$ secure that the stochastic component of the driving is switched on (of) after (before) the beginning (end) of the process. The time-evolution of the system for a given noise realization is driven by EQ. (1.3). The work done on the system fulfills EQ. (1.10). We consider the detailed balanced Glauber transition rates (2.19). Due to the stochastic level energies, the rates themselves are stochastic:

$$\begin{aligned} \nu\,\mathsf{L}_{21}(t) &= \frac{\nu}{1 + \exp\{\beta[(\mathsf{E}_2(t) - \mathsf{E}_1(t))]\}} \ , \\ \nu\,\mathsf{L}_{12}(t) &= \frac{\nu}{1 + \exp\{\beta[(\mathsf{E}_1(t) - \mathsf{E}_2(t))]\}} \ . \end{aligned} \tag{C.15}$$

Our goal in this example is to verify the Crooks relation (1.62) as it can be, using the results derived in [86], generalized for models with stochastic driving. Let us define the entropy for a given realization of the external noise, $I \equiv I(t)$, $t \in (0, \tau)$, by the formula

$$\sigma(I) = \ln \left[\frac{\text{Prob } \{\mathsf{I}(t) = I(t) \ , \ \ \forall\, t \in (0, \tau)\}}{\text{Prob } \{\mathsf{I}(t) = \widetilde{I}(t) \ , \ \ \forall\, t \in (0, \tau)\}} \right] \ , \tag{C.16}$$

where $\widetilde{I} \equiv \widetilde{I}(t) = I(\tau - t)$, $t \in (0, \tau)$. The external noise is *time-reversible* if its arbitrary realization I is as probable to occur as the corresponding time-reversed realization $\widetilde{I}$, i.e., if the entropy (C.16) vanishes for any realization of the noise (see [48, 109]). The generalized Crooks relation reads [95]

$$\frac{\rho_{\mathrm{F}}(w)}{\rho_{\mathrm{R}}(-w)} \left\langle \exp[-\sigma(I)] \right\rangle_{\sigma(I)|w} = \exp\{-\beta[\Delta F(\tau, 0) - w]\} \ . \tag{C.17}$$

Here, $\rho_{\mathrm{F}}(w)$ stands for the probability density for the work (1.10) done during the forward stochastic process $\mathsf{D}(t)$ when the system starts form thermal equilibrium distribution $\pi_1 = \pi_2 = 1/2$ corresponding to the instantaneous value of the energies (C.14) at the time $t = 0$ (cf. SEC. 1.3). Similarly $\rho_{\mathrm{R}}(w)$ denotes the probability density for the work done during the time-reversed process when the system starts form the thermal equilibrium distribution $\tilde{\pi}_1 = 1/(1 + \mathrm{e}^{-\beta a \tau})$ $\tilde{\pi}_2 = \mathrm{e}^{-\beta a \tau}/(1 + \mathrm{e}^{-\beta a \tau})$ corresponding to the instantaneous value of the energies (C.14) at the time $t = \tau$. It is assumed that during the reversed process only the deterministic part of the energies (C.14) is reversed. The average

$\langle \exp[-\sigma(I)] \rangle_{\sigma(I)|w}$ is taken over all trajectories of the forward process $\mathsf{D}(t)$ (for each of these trajectories a new realization I of the noise $\mathsf{I}(t)$ is taken) that yield the work w.

The generalized Crooks theorem (C.17) implies that the Crooks theorem $\rho_{\rm F}(w)/\rho_{\rm R}(-w) = \exp\{-\beta[\Delta F(\tau,0) - w]\}$ is exact if and only if the external noise is time-reversible (the entropy production for each individual realization I vanishes). This is verified in FIG. C.1 where the external noise $\mathsf{I}(t)$ is the Ornstein-Uhlenbeck process [78, 187]. The process driven by the Langevin EQ. (1.37) with the parabolic potential $\mathcal{F}(x,t) = kx^2/2$. Using ATA we calculate the probability densities of work for both the forward process, $\rho_{\rm F}(w)$, and the corresponding time-reversed process, $\rho_{\rm R}(-w)$. During the time-reversed process we reverse only the deterministic component of $\mathsf{E}_2(t)$. The stochastic component for the both processes starts at the initial time $t = 0$ from the value drawn from a Gaussian distribution with zero mean and a given variance V_0. Whenever the initial variance differs from $D/(2k)$ the corresponding Ornstein-Uhlenbeck process is non-stationary, the relaxation occurs, and the entropy $\sigma(I)$ is positive for most realizations of the process.

In the illustrations we take $a = 1$, so in the forward process the deterministic part of $\mathsf{E}_2(t)$ increases. Notice that under the deterministic driving alone, the support of the work distributions $\rho_{\rm F}(w)$ and $\rho_{\rm R}(-w)$ would be $w \in [0,\tau]$. The tail $w < 0$ arises purely due to the action of the noise. In FIG. C.1 there are two δ-functions situated at the origin. Their weights correspond to the relative frequencies of the trajectories that reside in the level 1 during $[0,\tau]$. If the external noise is time-irreversible [as illustrated in FIG. C.1b)] then, for a given w, one of the three cases

$$\begin{aligned}
\left\langle \mathrm{e}^{-\sigma(I)} \right\rangle_{\sigma(I)|w} &< 1 \ldots \rho_{\rm F}(w)\, \mathrm{e}^{-\beta(w-\Delta F(\tau,0))} > \rho_{\rm R}(-w) \ , \\
\left\langle \mathrm{e}^{-\sigma(I)} \right\rangle_{\sigma(I)|w} &= 1 \ldots \rho_{\rm F}(w)\, \mathrm{e}^{-\beta(w-\Delta F(\tau,0))} = \rho_{\rm R}(-w) \ , \\
\left\langle \mathrm{e}^{-\sigma(I)} \right\rangle_{\sigma(I)|w} &> 1 \ldots \rho_{\rm F}(w)\, \mathrm{e}^{-\beta(w-\Delta F(\tau,0))} < \rho_{\rm R}(-w) \ ,
\end{aligned}$$

may be observed.

The case $\left\langle \mathrm{e}^{-\sigma(I)} \right\rangle_{\sigma(I)|w} < 1$ is *normal*, that is, a typical situation which is highly probable to be observed in experiments or simulations. In this case, majority of the noise realizations possess a positive entropy. The values of w, for which $\left\langle \mathrm{e}^{-\sigma(I)} \right\rangle_{\sigma(I)|w} < 1$ holds, are highly probable values situated mostly in a vicinity of $W(\tau,0)$ and/or $\Delta F(\tau,0)$ [$W(\tau,0)$ denotes the mean work performed during the forward process]. The case $\left\langle \mathrm{e}^{-\sigma(I)} \right\rangle_{\sigma(I)|w} = 1$ is *marginal*. For such w the Crooks relation is valid pointwise. This case serves as a borderline between the first and the third cases. The case $\left\langle \mathrm{e}^{-\sigma(I)} \right\rangle_{\sigma(I)|w} > 1$ is *anomalous*. For these values of w the entropy corresponding to the majority of the noise realizations is negative, i.e., these realizations occur with a lower probability then their time-reversals. The values of w for which this case arises are rather unexpected. They are situated in the tails of the work distributions. For more irreversible noise the effect of such noise realizations on the tail $w < 0$ (works that are inaccessible without the noise) becomes more pronounced.

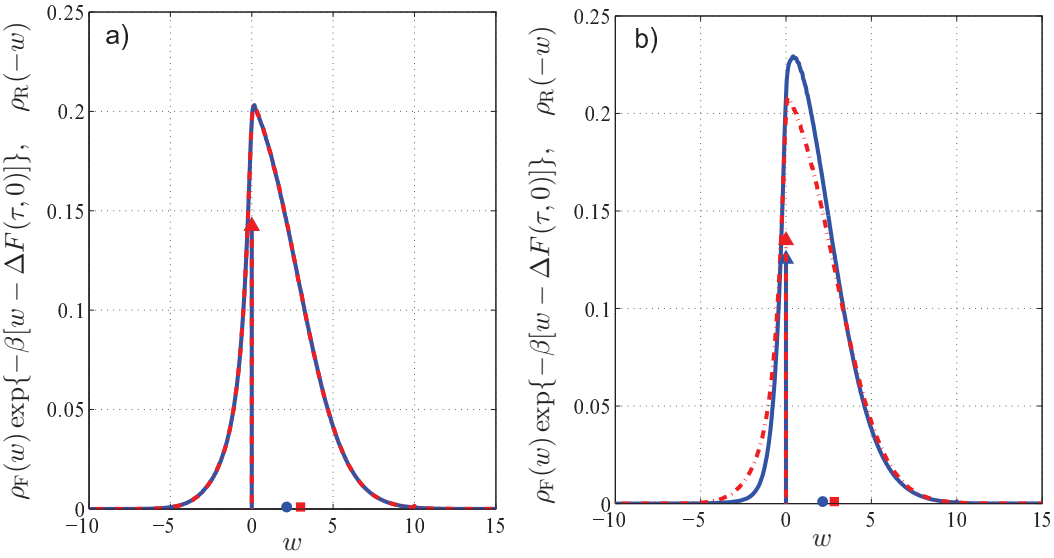

FIG. C.1: The illustration of the fluctuation theorem (C.17). The blue solid line stands for the function $\rho_{\rm R}(-w)$. The red dot-dashed line corresponds to $\rho_{\rm R}(-w)\exp\{-\beta[w-\Delta F(\tau,0)]\}$. The blue circle (red square) on the horizontal axis depicts the mean work $W(\tau,0)$ [free energy difference $\Delta F(\tau,0)$]. a) The noise I(t) is the stationary reversible Ornstein-Uhlenbeck process ($\langle\sigma(I)\rangle_I=0$). We take $V_0=5$. b) The noise I(t) is the non-stationary irreversible Ornstein-Uhlenbeck process with $\langle\sigma(I)\rangle_I\doteq 20.76$ and $V_0=0.1$. Other parameters used: $D=0.5$, $k=0.05$, $a=1$, $\beta=0.3$, $\tau=10$, $\nu=1$.

C.4 Summary

In summary, we have presented new simulation algorithms for Markovian jump processes with time-dependent transition rates, which avoid the often cumbersome or unhandy calculation of inverse functions. The ATA and FATA rely on the construction of a series of Poisson points, where transitions are attempted and rejected with certain probabilities. As a consequence, both algorithms are easy to implement, and their efficiency will be good as long as the number of rejections can be kept small. For complex interacting systems, the FATA has the same merits as the FRTA with respect to the FRA. Both the ATA and FATA generate exact realizations of the stochastic process. Their connection to perturbative solutions of the underlying master equation may allow one to include in future work also non-Markovian features of a stochastic dynamics by letting the rejection probabilities to depend on the history [33]. Compared to the RTA and FRTA, the new algorithms should in particular be favorable, when considering periodically driven systems with interactions. Such systems are of much current interest in the study of non-equilibrium stationary states and we thus hope that our findings will help to investigate them more conveniently and efficiently.

Bibliography

[1] Abah, O.; Roßnagel, J.; Jacob, G.; et. al.: Single-Ion Heat Engine at Maximum Power. *Phys. Rev. Lett.*, volume 109, Nov 2012: page 203006, doi: 10.1103/PhysRevLett.109.203006.
URL http://link.aps.org/doi/10.1103/PhysRevLett.109.203006

[2] Abramowitz, M.; Stegun, I.: *Handbook of Mathematical Functions: With Formulars, Graphs, and Mathematical Tables*. Applied mathematics series, New York: Dover Publications, Incorporated, 1964, ISBN 9780486612720.
URL http://books.google.se/books?id=MtU8uP7XMvoC

[3] Alemany, A.; Ribezzi, M.; Ritort, F.: Recent progress in fluctuation theorems and free energy recovery. *AIP Conference Proceedings*, volume 1332, nr. 1, 2011: pages 96–110, doi:10.1063/1.3569489.
URL http://link.aip.org/link/?APC/1332/96/1

[4] Allahverdyan, A. E.; Johal, R. S.; Mahler, G.: Work extremum principle: Structure and function of quantum heat engines. *Phys. Rev. E*, volume 77, Apr 2008: page 041118, doi:10.1103/PhysRevE.77.041118.
URL http://link.aps.org/doi/10.1103/PhysRevE.77.041118

[5] Anderson, D. F.: A modified next reaction method for simulating chemical systems with time dependent propensities and delays. *The Journal of Chemical Physics*, volume 127, nr. 21, 2007: 214107, doi:10.1063/1.2799998.
URL http://link.aip.org/link/?JCP/127/214107/1

[6] Arnaud, J.; Chusseau, L.; Philippe, F.: A simple model for Carnot heat engines. *American Journal of Physics*, volume 78, nr. 1, 2010: pages 106–110, doi:10.1119/1.3247983.
URL http://link.aip.org/link/?AJP/78/106/1

[7] Astumian, R. D.: Thermodynamics and Kinetics of a Brownian Motor. *Science*, volume 276, nr. 5314, 1997: pages 917–922, doi:10.1126/science.276.5314.917, http://www.sciencemag.org/content/276/5314/917.full.pdf.
URL http://www.sciencemag.org/content/276/5314/917.abstract

[8] Astumian, R. D.: Adiabatic operation of a molecular machine. *Procl. Natl. Acad. Sci. U.S.A.*, volume 104, 2007: page 19715.
URL http://www.pnas.org/content/104/50/19715.full.pdf+html

[9] Astumian, R. D.; Hanggi, P.: Brownian Motors. *Physics Today*, volume 55, nr. 11, 2002: pages 33–39, doi:10.1063/1.1535005.
URL http://link.aip.org/link/?PTO/55/33/1

[10] Baule, A.; Cohen, E. G. D.: Fluctuation properties of an effective nonlinear system subject to Poisson noise. *Phys. Rev. E*, volume 79, Mar 2009: page 030103, doi:10.1103/PhysRevE.79.030103.
URL http://link.aps.org/doi/10.1103/PhysRevE.79.030103

[11] Baule, A.; Cohen, E. G. D.: Steady-state work fluctuations of a dragged particle under external and thermal noise. *Phys. Rev. E*, volume 80, Jul 2009: page 011110, doi:10.1103/PhysRevE.80.011110.
URL http://link.aps.org/doi/10.1103/PhysRevE.80.011110

[12] Bell, G.: Models for the specific adhesion of cells to cells. *Science*, volume 200, nr. 4342, 1978: pages 618–627, doi:10.1126/science.347575, http://www.sciencemag.org/content/200/4342/618.full.pdf.
URL http://www.sciencemag.org/content/200/4342/618.abstract

[13] Bicout, D. J.; Kats, E.: Bubble relaxation dynamics in double-stranded DNA. *Phys. Rev. E*, volume 70, Jul 2004: page 010902, doi:10.1103/PhysRevE.70.010902.
URL http://link.aps.org/doi/10.1103/PhysRevE.70.010902

[14] Blickle, V.; Bechinger, C.: Realization of a micrometre-sized stochastic heat engine. *Nature Physics*, volume 8, nr. 2, 2011: pages 143–146, doi:10.1038/nphys2163.
URL http://dx.doi.org/10.1038/nphys2163

[15] Blickle, V.; Speck, T.; Helden, L.; et. al.: Thermodynamics of a Colloidal Particle in a Time-Dependent Nonharmonic Potential. *Phys. Rev. Lett.*, volume 96, Feb 2006: page 070603, doi:10.1103/PhysRevLett.96.070603.
URL http://link.aps.org/doi/10.1103/PhysRevLett.96.070603

[16] Bochkov, G.; Kuzovlev, Y.: Nonlinear fluctuation-dissipation relations and stochastic models in nonequilibrium thermodynamics: I. Generalized fluctuation-dissipation theorem. *Physica A: Statistical Mechanics and its Applications*, volume 106, nr. 3, 1981: pages 443 – 479, ISSN 0378-4371, doi:10.1016/0378-4371(81)90122-9.
URL http://www.sciencedirect.com/science/article/pii/0378437181901229

[17] Bochkov, G.; Kuzovlev, Y.: Nonlinear fluctuation-dissipation relations and stochastic models in nonequilibrium thermodynamics: II. Kinetic potential and variational principles for nonlinear irreversible processes. *Physica A: Statistical Mechanics and its Applications*, volume 106, nr. 3, 1981: pages 480 – 520, ISSN 0378-4371, doi:10.1016/0378-4371(81)90123-0.
URL http://www.sciencedirect.com/science/article/pii/0378437181901230

[18] Bortz, A.; Kalos, M.; Lebowitz, J.: A new algorithm for Monte Carlo simulation of Ising spin systems. *Journal of Computational Physics*, volume 17, nr. 1, 1975: pages 10 – 18, ISSN 0021-9991, doi:10.1016/0021-9991(75)90060-1.
URL http://www.sciencedirect.com/science/article/pii/0021999175900601

[19] Braun, O.; Hanke, A.; Seifert, U.: Probing Molecular Free Energy Landscapes by Periodic Loading. *Phys. Rev. Lett.*, volume 93, Oct 2004: page 158105, doi:10.1103/PhysRevLett.93.158105.
URL http://link.aps.org/doi/10.1103/PhysRevLett.93.158105

[20] Bressloff, P. C.; Newby, J. M.: Stochastic models of intracellular transport. *Rev. Mod. Phys.*, volume 85, Jan 2013: pages 135–196, doi:10.1103/RevModPhys.85.135.
URL http://link.aps.org/doi/10.1103/RevModPhys.85.135

[21] Brey, J. J.; Prados, A.: Residual properties of a two-level system. *Phys. Rev. B*, volume 43, Apr 1991: pages 8350–8361, doi:10.1103/PhysRevB.43.8350.
URL http://link.aps.org/doi/10.1103/PhysRevB.43.8350

[22] Van den Broeck, C.; Esposito, M.: Three faces of the second law. II. Fokker-Planck formulation. *Phys. Rev. E*, volume 82, Jul 2010: page 011144, doi:10.1103/PhysRevE.82.011144.
URL http://link.aps.org/doi/10.1103/PhysRevE.82.011144

[23] Van den Broeck, C.; Kawai, R.; Meurs, P.: Microscopic Analysis of a Thermal Brownian Motor. *Phys. Rev. Lett.*, volume 93, Aug 2004: page 090601, doi:10.1103/PhysRevLett.93.090601.
URL http://link.aps.org/doi/10.1103/PhysRevLett.93.090601

[24] Bustamante, C.; Liphardt, J.; Felix, R.: The Nonequilibrium Thermodynamics of Small Systems. *Physics Today*, volume 58, 2005: page 43, doi:http://dx.doi.org/10.1063/1.2012462.

[25] Calderon, C. P.; Harris, N. C.; Kiang, C.-H.; et. al.: Quantifying Multiscale Noise Sources in Single-Molecule Time Series. *The Journal of Physical Chemistry B*, volume 113, nr. 1, 2009: pages 138–148, doi:10.1021/jp807908c, http://pubs.acs.org/doi/pdf/10.1021/jp807908c.
URL http://pubs.acs.org/doi/abs/10.1021/jp807908c

[26] Callen, H.: *THERMODYNAMICS & AN INTRO. TO THERMOSTATISTICS*. Student Edition, Wiley India Pvt. Limited, 2006, ISBN 9788126508129.
URL http://books.google.cz/books?id=uOiZB_2y5pIC

[27] Campisi, M.; Hänggi, P.; Talkner, P.: *Colloquium* : Quantum fluctuation relations: Foundations and applications. *Rev. Mod. Phys.*, volume 83, Jul 2011: pages 771–791, doi:10.1103/RevModPhys.83.771.
URL http://link.aps.org/doi/10.1103/RevModPhys.83.771

[28] Carberry, D. M.; Reid, J. C.; Wang, G. M.; et. al.: Fluctuations and Irreversibility: An Experimental Demonstration of a Second-Law-Like Theorem Using a Colloidal Particle Held in an Optical Trap. *Phys. Rev. Lett.*, volume 92, Apr 2004: page 140601, doi:10.1103/PhysRevLett.92.140601.
URL http://link.aps.org/doi/10.1103/PhysRevLett.92.140601

[29] Chambadal, P.: *Les Centrales nucléaires*. Collection Armand Colin, Colin, 1957.
URL http://books.google.cz/books?id=TX8KAAAAMAAJ

[30] Chatelain, C.; Karevski, D.: Probability distributions of the work in the two-dimensional Ising model. *Journal of Statistical Mechanics: Theory and*

Experiment, volume 2006, nr. 06, 2006: page P06005.
URL http://stacks.iop.org/1742-5468/2006/i=06/a=P06005

[31] Chvosta, P.; Einax, M.; Holubec, V.; et. al.: Energetics and performance of a microscopic heat engine based on exact calculations of work and heat distributions. *Journal of Statistical Mechanics: Theory and Experiment*, volume 2010, nr. 03, 2010: page P03002.
URL http://stacks.iop.org/1742-5468/2010/i=03/a=P03002

[32] Chvosta, P.; Holubec, V.; Ryabov, A.; et. al.: Thermodynamics of two-stroke engine based on periodically driven two-level system. *Physica E: Low-dimensional Systems and Nanostructures*, volume 42, nr. 3, 2010: pages 472 – 476, ISSN 1386-9477, doi:http://dx.doi.org/10.1016/j.physe.2009.06.031, proceedings of the international conference Frontiers of Quantum and Mesoscopic Thermodynamics {FQMT} '08.
URL http://www.sciencedirect.com/science/article/pii/S1386947709002380

[33] Chvosta, P.; Reineker, P.: Dynamics under the influence of semi-Markov noise. *Physica A: Statistical Mechanics and its Applications*, volume 268, 1999: pages 103 – 120, ISSN 0378-4371, doi:10.1016/S0378-4371(99)00021-7.
URL http://www.sciencedirect.com/science/article/pii/S0378437199000217

[34] Chvosta, P.; Reineker, P.: Analysis of stochastic resonances. *Phys. Rev. E*, volume 68, Dec 2003: page 066109, doi:10.1103/PhysRevE.68.066109.
URL http://link.aps.org/doi/10.1103/PhysRevE.68.066109

[35] Chvosta, P.; Reineker, P.; Schulz, M.: Probability distribution of work done on a two-level system during a nonequilibrium isothermal process. *Phys. Rev. E*, volume 75, Apr 2007: page 041124, doi:10.1103/PhysRevE.75.041124.
URL http://link.aps.org/doi/10.1103/PhysRevE.75.041124

[36] Ciliberto, S.; Joubaud, S.; Petrosyan, A.: Fluctuations in out-of-equilibrium systems: from theory to experiment. *Journal of Statistical Mechanics: Theory and Experiment*, volume 2010, nr. 12, 2010: page P12003.
URL http://stacks.iop.org/1742-5468/2010/i=12/a=P12003

[37] Cocco, S.; Monasson, R.; Marko, J. F.: Force and kinetic barriers to unzipping of the DNA double helix. *Proceedings of the National Academy of Sciences*, volume 98, nr. 15, 2001: pages 8608–8613, doi:10.1073/pnas.151257598, http://www.pnas.org/content/98/15/8608.full.pdf+html.
URL http://www.pnas.org/content/98/15/8608.abstract

[38] Cohen, A. E.: Control of Nanoparticles with Arbitrary Two-Dimensional Force Fields. *Phys. Rev. Lett.*, volume 94, Mar 2005: page 118102, doi:10.1103/PhysRevLett.94.118102.
URL http://link.aps.org/doi/10.1103/PhysRevLett.94.118102

[39] Cohen-Tannoudji, C.; Diu, B.; Laloe, F.: *Quantum Mechanics*. John Wiley & Sons, 1996, ISBN 9780471569527.
URL http://books.google.cz/books?id=CjeNnQEACAAJ

[40] Collin, D.; Ritort, F.; Jarzynski, C.; et. al.: Verification of the Crooks fluctuation theorem and recovery of RNA folding free energies. *Nature*, volume 473, 2005: page 231, doi:http://dx.doi.org/10.1038/nature04061M3.

[41] Creutz, M.; Jacobs, L.; Rebbi, C.: Experiments with a Gauge-Invariant Ising System. *Phys. Rev. Lett.*, volume 42, May 1979: pages 1390–1393, doi:10.1103/PhysRevLett.42.1390.
URL http://link.aps.org/doi/10.1103/PhysRevLett.42.1390

[42] Crooks, G.: Nonequilibrium Measurements of Free Energy Differences for Microscopically Reversible Markovian Systems. *Journal of Statistical Physics*, volume 90, nr. 5-6, 1998: pages 1481–1487, ISSN 0022-4715, doi:10.1023/A:1023208217925.
URL http://dx.doi.org/10.1023/A%3A1023208217925

[43] Crooks, G. E.: Entropy production fluctuation theorem and the nonequilibrium work relation for free energy differences. *Phys. Rev. E*, volume 60, Sep 1999: pages 2721–2726, doi:10.1103/PhysRevE.60.2721.
URL http://link.aps.org/doi/10.1103/PhysRevE.60.2721

[44] Crooks, G. E.: Path-ensemble averages in systems driven far from equilibrium. *Phys. Rev. E*, volume 61, Mar 2000: pages 2361–2366, doi:10.1103/PhysRevE.61.2361.
URL http://link.aps.org/doi/10.1103/PhysRevE.61.2361

[45] Crooks, G. E.; Jarzynski, C.: Work distribution for the adiabatic compression of a dilute and interacting classical gas. *Phys. Rev. E*, volume 75, Feb 2007: page 021116, doi:10.1103/PhysRevE.75.021116.
URL http://link.aps.org/doi/10.1103/PhysRevE.75.021116

[46] Crothers, D.; Kallenbach, N. R.; Zimm, B.: The melting transition of low-molecular-weight DNA: Theory and experiment. *Journal of Molecular Biology*, volume 11, nr. 4, 1965: pages 802 – 820, ISSN 0022-2836, doi:10.1016/S0022-2836(65)80037-7.
URL http://www.sciencedirect.com/science/article/pii/S0022283665800377

[47] Curzon, F. L.; Ahlborn, B.: Efficiency of a Carnot engine at maximum power output. *American Journal of Physics*, volume 43, nr. 1, 1975: pages 22–24, doi:10.1119/1.10023.
URL http://link.aip.org/link/?AJP/43/22/1

[48] Dubkov, A. A.: Statistical time-reversal symmetry and its physical applications. *Chemical Physics*, volume 375, nr. 2-3, 2010: pages 364 – 369, ISSN 0301-0104, doi:http://dx.doi.org/10.1016/j.chemphys.2010.05.033, stochastic processes in Physics and Chemistry (in honor of Peter Hänggi).
URL http://www.sciencedirect.com/science/article/pii/S0301010410002661

[49] Durmayaz, A.; Sogut, O. S.; Sahin, B.; et. al.: Optimization of thermal systems based on finite-time thermodynamics and thermoeconomics. *Progress in Energy and Combustion Science*, volume 30, nr. 2, 2004: pages 175 – 217, ISSN 0360-1285, doi:10.1016/j.pecs.2003.10.003.
URL http://www.sciencedirect.com/science/article/pii/S0360128503000777

[50] Ehrenfest, P.; Ehrenfest, T.: Über zwei bekannte Einwände gegen das Boltzmannsche H-Theorem. *Phys. Z.*, volume 8, 1907: page 311.

[51] Einax, M.; Korner, M.; Maass, P.; et. al.: Nonlinear hopping transport in ring systems and open channels. *Phys. Chem. Chem. Phys.*, volume 12, 2010: pages 645–654, doi:10.1039/B916827C.
URL http://dx.doi.org/10.1039/B916827C

[52] Einax, M.; Maass, P.: Work distributions for Ising chains in a time-dependent magnetic field. *Phys. Rev. E*, volume 80, Aug 2009: page 020101, doi:10.1103/PhysRevE.80.020101.
URL http://link.aps.org/doi/10.1103/PhysRevE.80.020101

[53] Engel, A.: Asymptotics of work distributions in nonequilibrium systems. *Phys. Rev. E*, volume 80, Aug 2009: page 021120, doi:10.1103/PhysRevE.80.021120.
URL http://link.aps.org/doi/10.1103/PhysRevE.80.021120

[54] Engel, S.; Alemany, A.; Forns, N.; et. al.: Folding and unfolding of a triple-branch DNA molecule with four conformational states. *Philosophical Magazine*, volume 91, nr. 13-15, 2011: pages 2049–2065, doi:10.1080/14786435.2011.557671, http://www.tandfonline.com/doi/pdf/10.1080/14786435.2011.557671.
URL http://www.tandfonline.com/doi/abs/10.1080/14786435.2011.557671

[55] Eriksen, P.; Ackermann, T.; Abildgaard, H.; et. al.: System operation with high wind penetration. *Power and Energy Magazine, IEEE*, volume 3, nr. 6, nov.-dec. 2005: pages 65 – 74, ISSN 1540-7977, doi:10.1109/MPAE.2005.1524622.

[56] Esposito, M.; Van den Broeck, C.: Three Detailed Fluctuation Theorems. *Phys. Rev. Lett.*, volume 104, Mar 2010: page 090601, doi:10.1103/PhysRevLett.104.090601.
URL http://link.aps.org/doi/10.1103/PhysRevLett.104.090601

[57] Esposito, M.; Van den Broeck, C.: Three faces of the second law. I. Master equation formulation. *Phys. Rev. E*, volume 82, Jul 2010: page 011143, doi:10.1103/PhysRevE.82.011143.
URL http://link.aps.org/doi/10.1103/PhysRevE.82.011143

[58] Esposito, M.; Harbola, U.; Mukamel, S.: Nonequilibrium fluctuations, fluctuation theorems, and counting statistics in quantum systems. *Rev. Mod. Phys.*, volume 81, Dec 2009: pages 1665–1702, doi:10.1103/RevModPhys.

81.1665.
URL http://link.aps.org/doi/10.1103/RevModPhys.81.1665

[59] Esposito, M.; Kawai, R.; Lindenberg, K.; et. al.: Efficiency at Maximum Power of Low-Dissipation Carnot Engines. *Phys. Rev. Lett.*, volume 105, Oct 2010: page 150603, doi:10.1103/PhysRevLett.105.150603.
URL http://link.aps.org/doi/10.1103/PhysRevLett.105.150603

[60] Esposito, M.; Kawai, R.; Lindenberg, K.; et. al.: Quantum-dot Carnot engine at maximum power. *Phys. Rev. E*, volume 81, Apr 2010: page 041106, doi:10.1103/PhysRevE.81.041106.
URL http://link.aps.org/doi/10.1103/PhysRevE.81.041106

[61] Esposito, M.; Lindenberg, K.; Van den Broeck, C.: Universality of Efficiency at Maximum Power. *Phys. Rev. Lett.*, volume 102, Apr 2009: page 130602, doi:10.1103/PhysRevLett.102.130602.
URL http://link.aps.org/doi/10.1103/PhysRevLett.102.130602

[62] Esposito, M.; Mukamel, S.: Fluctuation theorems for quantum master equations. *Phys. Rev. E*, volume 73, Apr 2006: page 046129, doi:10.1103/PhysRevE.73.046129.
URL http://link.aps.org/doi/10.1103/PhysRevE.73.046129

[63] Evans, D.; Morriss, G.: *Statistical Mechanics of Nonequilibrium Liquids*. Theoretical chemistry, Cambridge University Press, 2008, ISBN 9780521857918.
URL http://books.google.cz/books?id=65URS_vPwuQC

[64] Evans, D. J.; Cohen, E. G. D.; Morriss, G. P.: Probability of second law violations in shearing steady states. *Phys. Rev. Lett.*, volume 71, Oct 1993: pages 2401–2404, doi:10.1103/PhysRevLett.71.2401.
URL http://link.aps.org/doi/10.1103/PhysRevLett.71.2401

[65] Evans, D. J.; Searles, D. J.: Equilibrium microstates which generate second law violating steady states. *Phys. Rev. E*, volume 50, Aug 1994: pages 1645–1648, doi:10.1103/PhysRevE.50.1645.
URL http://link.aps.org/doi/10.1103/PhysRevE.50.1645

[66] Evans, D. J.; Searles, D. J.: The Fluctuation Theorem. *Advances in Physics*, volume 51, nr. 7, 2002: pages 1529–1585, doi:10.1080/00018730210155133, http://www.tandfonline.com/doi/pdf/10.1080/00018730210155133.
URL http://www.tandfonline.com/doi/abs/10.1080/00018730210155133

[67] Finkelstein, A.: Course 12: Proteins: Structural, Thermodynamic and Kinetic Aspects. In *Slow Relaxations and nonequilibrium dynamics in condensed matter*, *Les Houches-École d'Été de Physique Theorique*, volume 77, edby J.-L. Barrat; M. Feigelman; J. Kurchan; J. Dalibard, Springer Berlin Heidelberg, 2003, ISBN 978-3-540-40141-4, pages 649–703, doi:10.1007/978-3-540-44835-8_12.
URL http://adsabs.harvard.edu/abs/2004srnd.conf..649F

[68] Fogedby, H. C.; Metzler, R.: DNA Bubble Dynamics as a Quantum Coulomb Problem. *Phys. Rev. Lett.*, volume 98, Feb 2007: page 070601, doi:10.1103/PhysRevLett.98.070601.
URL http://link.aps.org/doi/10.1103/PhysRevLett.98.070601

[69] Gallavotti, G.; Cohen, E. G. D.: Dynamical Ensembles in Nonequilibrium Statistical Mechanics. *Phys. Rev. Lett.*, volume 74, Apr 1995: pages 2694–2697, doi:10.1103/PhysRevLett.74.2694.
URL http://link.aps.org/doi/10.1103/PhysRevLett.74.2694

[70] Gammaitoni, L.; Hänggi, P.; Jung, P.; et. al.: Stochastic resonance. *Rev. Mod. Phys.*, volume 70, Jan 1998: pages 223–287, doi:10.1103/RevModPhys.70.223.
URL http://link.aps.org/doi/10.1103/RevModPhys.70.223

[71] García-García, R.; Domínguez, D.; Lecomte, V.; et. al.: Unifying approach for fluctuation theorems from joint probability distributions. *Phys. Rev. E*, volume 82, Sep 2010: page 030104, doi:10.1103/PhysRevE.82.030104.
URL http://link.aps.org/doi/10.1103/PhysRevE.82.030104

[72] Gaspard, P.: Hamiltonian dynamics, nanosystems, and nonequilibrium statistical mechanics. *Physica A: Statistical Mechanics and its Applications*, volume 369, nr. 1, 2006: pages 201 – 246, ISSN 0378-4371, doi:http://dx.doi.org/10.1016/j.physa.2006.04.010, ¡ce:title¿Fundamental Problems in Statistical Physics¡/ce:title¿ ¡ce:subtitle¿Proceedings of the 11th International Summerschool on 'Fundamental problems in statistical physics', September 4–17, 2005, Leuven, Belgium¡/ce:subtitle¿ ¡xocs:full-name¿11th International Summerschool on 'Fundamental problems in statistical physics'¡/xocs:full-name¿.
URL http://www.sciencedirect.com/science/article/pii/S0378437106004055

[73] Giampaoli, J. A.; Strier, D. E.; Batista, C.; et. al.: Exact expression for the diffusion propagator in a family of time-dependent anharmonic potentials. *Phys. Rev. E*, volume 60, Sep 1999: pages 2540–2546, doi:10.1103/PhysRevE.60.2540.
URL http://link.aps.org/doi/10.1103/PhysRevE.60.2540

[74] Gibbs, J.: *Elementary Principles in Statistical Mechanics: Developed with Especial Reference to the Rational Foundation of Thermodynamics*. Cambridge Library Collection - Mathematics, Cambridge University Press, 2010, ISBN 9781108017022.
URL http://www.google.cz/books?id=7VbC-15f0SkC

[75] Gibbs, J. H.; DiMarzio, E. A.: Statistical Mechanics of Helix-Coil Transitions in Biological Macromolecules. *The Journal of Chemical Physics*, volume 30, nr. 1, 1959: pages 271–282, doi:10.1063/1.1729886.
URL http://link.aip.org/link/?JCP/30/271/1

[76] Gibson, M. A.; Bruck, J.: Efficient Exact Stochastic Simulation of Chemical Systems with Many Species and Many Channels. *The Journal of Physical Chemistry A*, volume 104, nr. 9, 2000: pages 1876–1889, doi:10.1021/

jp993732q, http://pubs.acs.org/doi/pdf/10.1021/jp993732q.
URL http://pubs.acs.org/doi/abs/10.1021/jp993732q

[77] Gillespie, D. T.: Monte Carlo simulation of random walks with residence time dependent transition probability rates. *Journal of Computational Physics*, volume 28, nr. 3, 1978: pages 395 – 407, ISSN 0021-9991, doi:10.1016/0021-9991(78)90060-8.
URL http://www.sciencedirect.com/science/article/pii/0021999178900608

[78] Gillespie, D. T.: *Markov Processes: An Introduction for Physical Scientist*. Gulf Professional Publishing, 1992.

[79] Glauber, R. J.: Time-Dependent Statistics of the Ising Model. *Journal of Mathematical Physics*, volume 4, nr. 2, 1963: pages 294–307, doi:10.1063/1.1703954.
URL http://link.aip.org/link/?JMP/4/294/1

[80] Gomez-Solano, J. R.; Bellon, L.; Petrosyan, A.; et. al.: Steady-state fluctuation relations for systems driven by an external random force. *EPL (Europhysics Letters)*, volume 89, nr. 6, 2010: page 60003.
URL http://stacks.iop.org/0295-5075/89/i=6/a=60003

[81] Green and, R.; Noller, H. F.: RIBOSOMES AND TRANSLATION. *Annual Review of Biochemistry*, volume 66, nr. 1, 1997: pages 679–716, doi:10.1146/annurev.biochem.66.1.679, pMID: 9242921, http://www.annualreviews.org/doi/pdf/10.1146/annurev.biochem.66.1.679.
URL http://www.annualreviews.org/doi/abs/10.1146/annurev.biochem.66.1.679

[82] Hänggi, P.; Marchesoni, F.: Artificial Brownian motors: Controlling transport on the nanoscale. *Rev. Mod. Phys.*, volume 81, Mar 2009: pages 387–442, doi:10.1103/RevModPhys.81.387.
URL http://link.aps.org/doi/10.1103/RevModPhys.81.387

[83] Hänggi, P.; Marchesoni, F.; Nori, F.: Brownian motors. *Annalen der Physik*, volume 14, nr. 1-3, 2005: pages 51–70, ISSN 1521-3889, doi:10.1002/andp.200410121.
URL http://dx.doi.org/10.1002/andp.200410121

[84] Hänggi, P.; Talkner, P.; Borkovec, M.: Reaction-rate theory: fifty years after Kramers. *Rev. Mod. Phys.*, volume 62, Apr 1990: pages 251–341, doi:10.1103/RevModPhys.62.251.
URL http://link.aps.org/doi/10.1103/RevModPhys.62.251

[85] Hanke, A.; Metzler, R.: Bubble dynamics in DNA. *Journal of Physics A: Mathematical and General*, volume 36, nr. 36, 2003: page L473.
URL http://stacks.iop.org/0305-4470/36/i=36/a=101

[86] Harris, R. J.; Schütz, G. M.: Fluctuation theorems for stochastic dynamics. *Journal of Statistical Mechanics: Theory and Experiment*, volume 2007,

nr. 07, 2007: page P07020.
URL http://stacks.iop.org/1742-5468/2007/i=07/a=P07020

[87] Hatano, T.; Sasa, S.-i.: Steady-State Thermodynamics of Langevin Systems. *Phys. Rev. Lett.*, volume 86, Apr 2001: pages 3463–3466, doi: 10.1103/PhysRevLett.86.3463.
URL http://link.aps.org/doi/10.1103/PhysRevLett.86.3463

[88] Hauert, C.; Nagler, J.; Schuster, H.: Of Dogs and Fleas: The Dynamics of N Uncoupled Two-State Systems. *Journal of Statistical Physics*, volume 116, nr. 5-6, 2004: pages 1453–1469, ISSN 0022-4715, doi:10.1023/B:JOSS.0000041725.70622.c4.
URL http://dx.doi.org/10.1023/B%3AJOSS.0000041725.70622.c4

[89] Henrich, M. J.; Rempp, F.; Mahler, G.: Quantum thermodynamic Otto machines: A spin-system approach. *The European Physical Journal Special Topics*, volume 151, nr. 1, 2007: pages 157–165, ISSN 1951-6355, doi:10.1140/epjst/e2007-00371-8.
URL http://dx.doi.org/10.1140/epjst/e2007-00371-8

[90] Híjar, H.; Quintana-H, J.; Sutmann, G.: Non-equilibrium work theorems for the two-dimensional Ising model. *Journal of Statistical Mechanics: Theory and Experiment*, volume 2007, nr. 04, 2007: page P04010.
URL http://stacks.iop.org/1742-5468/2007/i=04/a=P04010

[91] Holubec, V.: *Nonequilibrium Thermodynamics of Small Systems*. Diploma thesis, Charles University in Prague, Faculty of Mathematics and Physics, 2009.

[92] Holubec, V.; Chvosta, P.; Einax, M.; et. al.: Attempt time Monte Carlo: An alternative for simulation of stochastic jump processes with time-dependent transition rates. *EPL (Europhysics Letters)*, volume 93, nr. 4, 2011: page 40003.
URL http://stacks.iop.org/0295-5075/93/i=4/a=40003

[93] Holubec, V.; Chvosta, P.; Maass, P.: Dynamics and energetics for a molecular zipper model under external driving. *Journal of Statistical Mechanics: Theory and Experiment*, volume 2012, nr. 11, 2012: page P11009.
URL http://stacks.iop.org/1742-5468/2012/i=11/a=P11009

[94] Holubec, V.; Chvosta, P.; Ryabov, A.: *Thermodynamics*, chapter Four Exactly Solvable Examples in Non-Equilibrium Thermodynamics of Small Systems. InTech, 2010, pages 153–176, doi:10.5772/13374.
URL http://www.intechopen.com/books/thermodynamics

[95] Holubec, V.; Ryabov, A.: Work fluctuations in systems under external stochastic driving, 2012, unpublished.

[96] Huang, K.: *Statistical mechanics*. Wiley, 1963.
URL http://books.google.cz/books?id=MolRAAAAMAAJ

[97] Hummer, G.; Szabo, A.: Free energy reconstruction from nonequilibrium single-molecule pulling experiments. *Proceedings of the National Academy of Sciences*, volume 98, nr. 7, 2001: pages 3658–3661, doi:10.1073/pnas.071034098, http://www.pnas.org/content/98/7/3658.full.pdf+html.
URL http://www.pnas.org/content/98/7/3658.abstract

[98] Imparato, A.; Peliti, L.: Work distribution and path integrals in general mean-field systems. *EPL (Europhysics Letters)*, volume 70, nr. 6, 2005: page 740.
URL http://stacks.iop.org/0295-5075/70/i=6/a=740

[99] Imparato, A.; Peliti, L.: Work probability distribution in single-molecule experiments. *EPL (Europhysics Letters)*, volume 69, nr. 4, 2005: page 643.
URL http://stacks.iop.org/0295-5075/69/i=4/a=643

[100] Imparato, A.; Peliti, L.: Work-probability distribution in systems driven out of equilibrium. *Phys. Rev. E*, volume 72, Oct 2005: page 046114, doi:10.1103/PhysRevE.72.046114.
URL http://link.aps.org/doi/10.1103/PhysRevE.72.046114

[101] Izumida, Y.; Okuda, K.: Efficiency at maximum power of minimally nonlinear irreversible heat engines. *EPL (Europhysics Letters)*, volume 97, nr. 1, 2012: page 10004.
URL http://stacks.iop.org/0295-5075/97/i=1/a=10004

[102] Jansen, A.: Monte Carlo simulations of chemical reactions on a surface with time-dependent reaction-rate constants. *Computer Physics Communications*, volume 86, 1995: pages 1 – 12, ISSN 0010-4655, doi:10.1016/0010-4655(94)00155-U.
URL http://www.sciencedirect.com/science/article/pii/001046559400155U

[103] Jarzynski, C.: Equilibrium free-energy differences from nonequilibrium measurements: A master-equation approach. *Phys. Rev. E*, volume 56, Nov 1997: pages 5018–5035, doi:10.1103/PhysRevE.56.5018.
URL http://link.aps.org/doi/10.1103/PhysRevE.56.5018

[104] Jarzynski, C.: Nonequilibrium Equality for Free Energy Differences. *Phys. Rev. Lett.*, volume 78, Apr 1997: pages 2690–2693, doi:10.1103/PhysRevLett.78.2690.
URL http://link.aps.org/doi/10.1103/PhysRevLett.78.2690

[105] Jarzynski, C.: Comparison of far-from-equilibrium work relations. *Comptes Rendus Physique*, volume 8, June 2007: pages 495–506, doi:10.1016/j.crhy.2007.04.010, arXiv:cond-mat/0612305.

[106] Jung, P.; Hänggi, P.: Resonantly driven Brownian motion: Basic concepts and exact results. *Phys. Rev. A*, volume 41, Mar 1990: pages 2977–2988, doi:10.1103/PhysRevA.41.2977.
URL http://link.aps.org/doi/10.1103/PhysRevA.41.2977

[107] Jung, P.; Hänggi, P.: Amplification of small signals via stochastic resonance. *Phys. Rev. A*, volume 44, Dec 1991: pages 8032–8042, doi: 10.1103/PhysRevA.44.8032.
URL http://link.aps.org/doi/10.1103/PhysRevA.44.8032

[108] Kac, M.: *Probability and Related Topics in Physical Sciences*. Lectures in Applied Mathematics Series, Vol 1A, London: Interscience Publishers, 1959, ISBN 9780821800478.
URL http://books.google.cz/books?id=xm-Y9-GKr_EC

[109] Kelly, F. P.: *Reversibility and Stochastic Networks*. New York: John Wiley & Sons Ltd, 1979, doi:10.1002/net.3230130110.

[110] Kittel, C.: Phase Transition of a Molecular Zipper. *American Journal of Physics*, volume 37, nr. 9, 1969: pages 917–920, doi:10.1119/1.1975930.
URL http://link.aip.org/link/?AJP/37/917/1

[111] Kornberg, A.; Baker, T.: *Dna Replication*. University Science Books, 2005, ISBN 9781891389443.
URL http://books.google.cz/books?id=KDsubusF0YsC

[112] Kurchan, J.: Fluctuation theorem for stochastic dynamics. *Journal of Physics A: Mathematical and General*, volume 31, nr. 16, 1998: page 3719.
URL http://stacks.iop.org/0305-4470/31/i=16/a=003

[113] Kurchan, J.: Non-equilibrium work relations. *Journal of Statistical Mechanics: Theory and Experiment*, volume 2007, nr. 07, 2007: page P07005.
URL http://stacks.iop.org/1742-5468/2007/i=07/a=P07005

[114] Lahiri, S.; Rana, S.; Jayannavar, A. M.: Fluctuation relations for heat engines in time-periodic steady states. *Journal of Physics A: Mathematical and Theoretical*, volume 45, nr. 46, 2012: page 465001.
URL http://stacks.iop.org/1751-8121/45/i=46/a=465001

[115] Lang, M. J.; Block, S. M.: Resource Letter: LBOT-1: Laser-based optical tweezers. *American Journal of Physics*, volume 71, nr. 3, 2003: pages 201–215, doi:10.1119/1.1532323.
URL http://link.aip.org/link/?AJP/71/201/1

[116] Lebowitz, J.; Spohn, H.: A Gallavotti–Cohen-Type Symmetry in the Large Deviation Functional for Stochastic Dynamics. *Journal of Statistical Physics*, volume 95, nr. 1-2, 1999: pages 333–365, ISSN 0022-4715, doi:10.1023/A:1004589714161.
URL http://dx.doi.org/10.1023/A%3A1004589714161

[117] Liphardt, J.; Dumont, S.; Smith, S. B.; et. al.: Equilibrium Information from Nonequilibrium Measurements in an Experimental Test of Jarzynski's Equality. *Science*, volume 296, nr. 5574, 2002: pages 1832–1835, doi:10.1126/science.1071152, http://www.sciencemag.org/content/296/5574/1832.full.pdf.
URL http://www.sciencemag.org/content/296/5574/1832.abstract

[118] Liphardt, J.; Onoa, B.; Smith, S. B.; et. al.: Reversible Unfolding of Single RNA Molecules by Mechanical Force. *Science*, volume 292, nr. 5517, 2001: pages 733–737, doi:10.1126/science.1058498, http://www.sciencemag.org/content/292/5517/733.full.pdf.
URL http://www.sciencemag.org/content/292/5517/733.abstract

[119] Lubensky, D. K.; Nelson, D. R.: Pulling Pinned Polymers and Unzipping DNA. *Phys. Rev. Lett.*, volume 85, Aug 2000: pages 1572–1575, doi:10.1103/PhysRevLett.85.1572.
URL http://link.aps.org/doi/10.1103/PhysRevLett.85.1572

[120] Maes, C.: On the origin and the use of fluctuation relations for the entropy. *Séminaire Poincaré*, volume 2, 2003: pages 29–62.

[121] Maes, C.; Netočný, K.: Time-Reversal and Entropy. *Journal of Statistical Physics*, volume 110, nr. 1-2, 2003: pages 269–310, ISSN 0022-4715, doi:10.1023/A:1021026930129.
URL http://dx.doi.org/10.1023/A%3A1021026930129

[122] Manosas, M.; Mossa, A.; Forns, N.; et. al.: Dynamic force spectroscopy of DNA hairpins: II. Irreversibility and dissipation. *Journal of Statistical Mechanics: Theory and Experiment*, volume 2009, nr. 02, 2009: page P02061.
URL http://stacks.iop.org/1742-5468/2009/i=02/a=P02061

[123] Manosas, M.; Ritort, F.: Thermodynamic and Kinetic Aspects of RNA Pulling Experiments. *Biophysical Journal*, volume 88, nr. 5, 2005: pages 3224 – 3242, ISSN 0006-3495, doi:10.1529/biophysj.104.045344.
URL http://www.sciencedirect.com/science/article/pii/S0006349505733749

[124] Maragakis, P.; Ritort, F.; Bustamante, C.; et. al.: Bayesian estimates of free energies from nonequilibrium work data in the presence of instrument noise. *The Journal of Chemical Physics*, volume 129, nr. 2, 2008: 024102, doi:10.1063/1.2937892.
URL http://link.aip.org/link/?JCP/129/024102/1

[125] Mazonka, O.; Jarzynski, C.: Exactly solvable model illustrating far-from-equilibrium predictions. *eprint arXiv:cond-mat/9912121*, December 1999, arXiv:cond-mat/9912121.
URL http://arxiv.org/abs/cond-mat/9912121

[126] Metropolis, N.; Rosenbluth, A. W.; Rosenbluth, M. N.; et. al.: Equation of State Calculations by Fast Computing Machines. *The Journal of Chemical Physics*, volume 21, nr. 6, 1953: pages 1087–1092, doi:10.1063/1.1699114.
URL http://link.aip.org/link/?JCP/21/1087/1

[127] Metzler, R.; Ambjörnsson, T.; Hanke, A.; et. al.: Single DNA denaturation and bubble dynamics. *Journal of Physics: Condensed Matter*, volume 21, nr. 3, 2009: page 034111.
URL http://stacks.iop.org/0953-8984/21/i=3/a=034111

[128] Michael, C.: Fast heat-bath algorithm for the Ising model. *Phys. Rev. B*, volume 33, Jun 1986: pages 7861–7862, doi:10.1103/PhysRevB.33.7861.
URL http://link.aps.org/doi/10.1103/PhysRevB.33.7861

[129] Mossa, A.; Manosas, M.; Forns, N.; et. al.: Dynamic force spectroscopy of DNA hairpins: I. Force kinetics and free energy landscapes. *Journal of Statistical Mechanics: Theory and Experiment*, volume 2009, nr. 02, 2009: page P02060.
URL http://stacks.iop.org/1742-5468/2009/i=02/a=P02060

[130] Motl, L.; Zahradník, M.: *Pěstujeme lineární algebru*. Karolinum, 1995, ISBN 9788071841869.
URL http://books.google.cz/books?id=0shyAAAACAAJ

[131] Mou, C. Y.; li Luo, J.; Nicolis, G.: Stochastic thermodynamics of nonequilibrium steady states in chemical reaction systems. *The Journal of Chemical Physics*, volume 84, nr. 12, 1986: pages 7011–7017.

[132] Müller, I.: *A History of Thermodynamics: The Doctrine of Energy and Entropy*. Springer London, Limited, 2007, ISBN 9783540462279.
URL http://books.google.cz/books?id=u13KiGlz2zcC

[133] Neuman, K. C.; Nagy, A.: Single-molecule force spectroscopy: optical tweezers, magnetic tweezers and atomic force microscopy. *Nature Met*, volume 5, 2008: pages 491–505.
URL http://dx.doi.org/10.1038/nmeth.1218

[134] Nickelsen, D.; Engel, A.: Asymptotics of work distributions: the pre-exponential factor. *The European Physical Journal B*, volume 82, 2011: pages 207–218, ISSN 1434-6028, doi:10.1140/epjb/e2011-20133-y.
URL http://dx.doi.org/10.1140/epjb/e2011-20133-y

[135] Nostheide, S.; Holubec, V.; Chvosta, P.; et. al.: 2013, unpublished.

[136] Novikov, I. I.: The efficiency of atomic power stations. *J. Nucl. Energy II*, volume 7, 1958: page 125.

[137] Onoa, B.; Dumont, S.; Liphardt, J.; et. al.: Identifying Kinetic Barriers to Mechanical Unfolding of the T. thermophila Ribozyme. *Science*, volume 299, nr. 5614, 2003: pages 1892–1895, doi:10.1126/science.1081338, http://www.sciencemag.org/content/299/5614/1892.full.pdf.
URL http://www.sciencemag.org/content/299/5614/1892.abstract

[138] Palassini, M.; Ritort, F.: Improving Free-Energy Estimates from Unidirectional Work Measurements: Theory and Experiment. *Phys. Rev. Lett.*, volume 107, Aug 2011: page 060601, doi:10.1103/PhysRevLett.107.060601.
URL http://link.aps.org/doi/10.1103/PhysRevLett.107.060601

[139] Parrondo, J.; de Cisneros, B.: Energetics of Brownian motors: a review. *Applied Physics A*, volume 75, nr. 2, 2002: pages 179–191, ISSN 0947-8396, doi:10.1007/s003390201332.
URL http://dx.doi.org/10.1007/s003390201332

[140] Peliti, L.: On the work-Hamiltonian connection in manipulated systems. *Journal of Statistical Mechanics: Theory and Experiment*, volume 2008, nr. 05, 2008: page P05002.
URL http://stacks.iop.org/1742-5468/2008/i=05/a=P05002

[141] Poland, D.; Scheraga, H. A.: Occurrence of a Phase Transition in Nucleic Acid Models. *The Journal of Chemical Physics*, volume 45, nr. 5, 1966: pages 1464–1469, doi:10.1063/1.1727786.
URL http://link.aip.org/link/?JCP/45/1464/1

[142] Prudnikov, A.; Brychkov, I.; Maričev, O.: *Integrals and Series: Special functions. Vol.2*. Integrals and Series, C R C Press LLC, 1986, ISBN 9782881240904.
URL http://books.google.cz/books?id=2t2cNs00aTgC

[143] Qian, H.: Mesoscopic nonequilibrium thermodynamics of single macromolecules and dynamic entropy-energy compensation. *Phys. Rev. E*, volume 65, Dec 2001: page 016102, doi:10.1103/PhysRevE.65.016102.
URL http://link.aps.org/doi/10.1103/PhysRevE.65.016102

[144] Ramakrishnan, V.: Ribosome Structure and the Mechanism of Translation. *Cell*, volume 108, 2002: pages 557–572.
URL http://linkinghub.elsevier.com/retrieve/pii/S0092867402006190

[145] Reimann, P.: Brownian motors: noisy transport far from equilibrium. *Physics Reports*, volume 361, nr. 2-4, 2002: pages 57 – 265, ISSN 0370-1573, doi:http://dx.doi.org/10.1016/S0370-1573(01)00081-3.
URL http://www.sciencedirect.com/science/article/pii/S0370157301000813

[146] Rezek, Y.; Kosloff, R.: Irreversible performance of a quantum harmonic heat engine. *New Journal of Physics*, volume 8, nr. 5, 2006: page 83.
URL http://stacks.iop.org/1367-2630/8/i=5/a=083

[147] Risken, H.: *The Fokker-Planck equation: methods of solution and applications*. Springer Verlag, 1985.

[148] Ritort, F.: *Poincaré Seminar 2003: Bose-Einstein Condensation – Entropy*, chapter Work Fluctuations, Transient Violations of the Second Law and Free-Energy Recovery Methods: Perspectives in Theory and Experiments. Basel: Birkhäuser, 2004, pages 63–87, doi:10.1007/978-3-0348-7932-3_9.

[149] Ritort, F.: Work and heat fluctuations in two-state systems: a trajectory thermodynamics formalism. *Journal of Statistical Mechanics: Theory and Experiment*, volume 2004, nr. 10, 2004: page P10016.
URL http://stacks.iop.org/1742-5468/2004/i=10/a=P10016

[150] Ritort, F.: Single-molecule experiments in biological physics: methods and applications. *Journal of Physics: Condensed Matter*, volume 18, nr. 32,

2006: page R531.
URL http://stacks.iop.org/0953-8984/18/i=32/a=R01

[151] Ritort, F.: *Advances in Chemical Physics, Volume 137*, chapter Nonequilibrium Fluctuations in Small Systems: From Physics to Biology. John Wiley & Sons, Inc., 2008, ISBN 9780470238080, pages 31–123, doi:10.1002/9780470238080.ch2.
URL http://dx.doi.org/10.1002/9780470238080.ch2

[152] Ryabov, A.; Dierl, M.; Chvosta, P.; et. al.: Work distribution in a time-dependent logarithmic-harmonic potential: exact results and asymptotic analysis. *Journal of Physics A: Mathematical and Theoretical*, volume 46, nr. 7, 2013: page 075002.
URL http://stacks.iop.org/1751-8121/46/i=7/a=075002

[153] Sagawa, T.; Ueda, M.: Generalized Jarzynski Equality under Nonequilibrium Feedback Control. *Phys. Rev. Lett.*, volume 104, Mar 2010: page 090602, doi:10.1103/PhysRevLett.104.090602.
URL http://link.aps.org/doi/10.1103/PhysRevLett.104.090602

[154] Sagawa, T.; Ueda, M.: Nonequilibrium thermodynamics of feedback control. *Phys. Rev. E*, volume 85, Feb 2012: page 021104, doi:10.1103/PhysRevE.85.021104.
URL http://link.aps.org/doi/10.1103/PhysRevE.85.021104

[155] SantaLucia, J.: A unified view of polymer, dumbbell, and oligonucleotide DNA nearest-neighbor thermodynamics. *Proceedings of the National Academy of Sciences*, volume 95, nr. 4, 1998: pages 1460–1465, http://www.pnas.org/content/95/4/1460.full.pdf+html.
URL http://www.pnas.org/content/95/4/1460.abstract

[156] Schliwa, M.: *Molecular Motors*. Wiley, 2006, ISBN 9783527605651.
URL http://books.google.cz/books?id=6PJMfQlIS1kC

[157] Schliwa, M.; Woehlke, G.: Molecular motors. *Nature*, volume 422, April 2003: pages 759–765, doi:10.1038/nature01601.

[158] Schmiedl, T.; Seifert, U.: Optimal Finite-Time Processes In Stochastic Thermodynamics. *Phys. Rev. Lett.*, volume 98, Mar 2007: page 108301, doi:10.1103/PhysRevLett.98.108301.
URL http://link.aps.org/doi/10.1103/PhysRevLett.98.108301

[159] Schmiedl, T.; Seifert, U.: Efficiency at maximum power: An analytically solvable model for stochastic heat engines. *EPL (Europhysics Letters)*, volume 81, nr. 2, 2008: page 20003.
URL http://stacks.iop.org/0295-5075/81/i=2/a=20003

[160] Schuler, S.; Speck, T.; Tietz, C.; et. al.: Experimental Test of the Fluctuation Theorem for a Driven Two-Level System with Time-Dependent Rates. *Phys. Rev. Lett.*, volume 94, May 2005: page 180602, doi:10.1103/PhysRevLett.94.180602.
URL http://link.aps.org/doi/10.1103/PhysRevLett.94.180602

[161] Schurr, J. M.; Fujimoto, B. S.: Equalities for the Nonequilibrium Work Transferred from an External Potential to a Molecular System. Analysis of Single-Molecule Extension Experiments. *The Journal of Physical Chemistry B*, volume 107, nr. 50, 2003: pages 14007–14019, doi:10.1021/jp0306803, http://pubs.acs.org/doi/pdf/10.1021/jp0306803.
URL http://pubs.acs.org/doi/abs/10.1021/jp0306803

[162] Schuster, H.: *Complex Adaptive Systems: An Introduction*. Scator Verlag, 2001, ISBN 9783980793605.
URL http://books.google.cz/books?id=9GuePQAACAAJ

[163] Searles, D. J.; Evans, D. J.: Fluctuation theorem for stochastic systems. *Phys. Rev. E*, volume 60, Jul 1999: pages 159–164, doi:10.1103/PhysRevE.60.159.
URL http://link.aps.org/doi/10.1103/PhysRevE.60.159

[164] Seifert, U.: Entropy Production along a Stochastic Trajectory and an Integral Fluctuation Theorem. *Phys. Rev. Lett.*, volume 95, Jul 2005: page 040602, doi:10.1103/PhysRevLett.95.040602.
URL http://link.aps.org/doi/10.1103/PhysRevLett.95.040602

[165] Seifert, U.: Stochastic thermodynamics: principles and perspectives. *The European Physical Journal B - Condensed Matter and Complex Systems*, volume 64, 2008: pages 423–431, ISSN 1434-6028, 10.1140/epjb/e2008-00001-9.
URL http://dx.doi.org/10.1140/epjb/e2008-00001-9

[166] Seifert, U.: Stochastic thermodynamics, fluctuation theorems and molecular machines. *Reports on Progress in Physics*, volume 75, nr. 12, 2012: page 126001.
URL http://stacks.iop.org/0034-4885/75/i=12/a=126001

[167] Sekimoto, K.: Kinetic Characterization of Heat Bath and the Energetics of Thermal Ratchet Models. *Journal of the Physical Society of Japan*, volume 66, nr. 5, 1997: pages 1234–1237, doi:10.1143/JPSJ.66.1234.
URL http://jpsj.ipap.jp/link?JPSJ/66/1234/

[168] Sekimoto, K.: Langevin Equation and Thermodynamics. *Progress of Theoretical Physics Supplement*, volume 130, 1998: pages 17–27, doi:10.1143/PTPS.130.17, http://ptps.oxfordjournals.org/content/130/17.full.pdf+html.
URL http://ptps.oxfordjournals.org/content/130/17.abstract

[169] Sekimoto, K.: *Stochastic Energetics*. Lecture notes in physics, Springer, 2010, ISBN 9783642054488.
URL http://books.google.cz/books?id=4cyxd7bvZHgC

[170] Sekimoto, K.; Takagi, F.; Hondou, T.: Carnot's cycle for small systems: Irreversibility and cost of operations. *Phys. Rev. E*, volume 62, Dec 2000: pages 7759–7768, doi:10.1103/PhysRevE.62.7759.
URL http://link.aps.org/doi/10.1103/PhysRevE.62.7759

[171] Sevick, E.; Prabhakar, R.; Williams, S. R.; et. al.: Fluctuation Theorems. *Annual Review of Physical Chemistry*, volume 59, nr. 1, 2008: pages 603–633, doi:10.1146/annurev.physchem.58.032806.104555, http://www.annualreviews.org/doi/pdf/10.1146/annurev.physchem.58.032806.104555.
URL http://www.annualreviews.org/doi/abs/10.1146/annurev.physchem.58.032806.104555

[172] Sinitsyn, N. A.: Fluctuation relation for heat engines. *Journal of Physics A: Mathematical and Theoretical*, volume 44, nr. 40, 2011: page 405001.
URL http://stacks.iop.org/1751-8121/44/i=40/a=405001

[173] Slater, L.: *Confluent hypergeometric functions*. University Press, 1960.
URL http://books.google.cz/books?id=BKUNAQAAIAAJ

[174] Slater, L.: *Generalized Hypergeometric Functions*. London: Cambridge University Press, 1966.
URL http://books.google.cz/books?id=HqONAQAAIAAJ

[175] Snyder, D.: *Random point processes*. A Wiley-Interscience Publication, Wiley, 1975, ISBN 9780471810216.
URL http://books.google.cz/books?id=veRQAAAAMAAJ

[176] Speck, T.: Work distribution for the driven harmonic oscillator with time-dependent strength: exact solution and slow driving. *Journal of Physics A: Mathematical and Theoretical*, volume 44, nr. 30, 2011: page 305001.
URL http://stacks.iop.org/1751-8121/44/i=30/a=305001

[177] Speck, T.; Seifert, U.: Distribution of work in isothermal nonequilibrium processes. *Phys. Rev. E*, volume 70, Dec 2004: page 066112, doi:10.1103/PhysRevE.70.066112.
URL http://link.aps.org/doi/10.1103/PhysRevE.70.066112

[178] Strier, D. E.; Drazer, G.; Wio, H. S.: An analytical study of stochastic resonance in a monostable non-harmonic system. *Physica A: Statistical Mechanics and its Applications*, volume 283, 2000: pages 255 – 260, ISSN 0378-4371, doi:10.1016/S0378-4371(00)00163-1.
URL http://www.sciencedirect.com/science/article/pii/S0378437100001631

[179] Šubrt, E.; Chvosta, P.: Exact analysis of work fluctuations in two-level systems. *Journal of Statistical Mechanics: Theory and Experiment*, volume 2007, nr. 09, 2007: page P09019.
URL http://stacks.iop.org/1742-5468/2007/i=09/a=P09019

[180] Tackett, A. J.; Morris, P. D.; Dennis, R.; et. al.: Unwinding of Unnatural Substrates by a DNA Helicase. *Biochemistry*, volume 40, nr. 2, 2001: pages 543–548, doi:10.1021/bi002122+, pMID: 11148049, http://pubs.acs.org/doi/pdf/10.1021/bi002122%2B.
URL http://pubs.acs.org/doi/abs/10.1021/bi002122%2B

[181] Takagi, F.; Hondou, T.: Thermal noise can facilitate energy conversion by a ratchet system. *Phys. Rev. E*, volume 60, Oct 1999: pages 4954–4957, doi:10.1103/PhysRevE.60.4954.
URL http://link.aps.org/doi/10.1103/PhysRevE.60.4954

[182] Then, H.; Engel, A.: Computing the optimal protocol for finite-time processes in stochastic thermodynamics. *Phys. Rev. E*, volume 77, Apr 2008: page 041105, doi:10.1103/PhysRevE.77.041105.
URL http://link.aps.org/doi/10.1103/PhysRevE.77.041105

[183] Thirumalai, D.; Hyeon, C.: RNA and Protein Folding: Common Themes and Variations. *Biochemistry*, volume 44, nr. 13, 2005: pages 4957–4970, doi:10.1021/bi047314+, pMID: 15794634, http://pubs.acs.org/doi/pdf/10.1021/bi047314%2B.
URL http://pubs.acs.org/doi/abs/10.1021/bi047314%2B

[184] Tinoco Jr, I.; Bustamante, C.: How RNA folds. *Journal of Molecular Biology*, volume 293, nr. 2, 1999: pages 271–281, ISSN 0022-2836, doi:10.1006/jmbi.1999.3001.
URL http://www.sciencedirect.com/science/article/pii/S0022283699930012

[185] Tu, Z. C.: Efficiency at maximum power of Feynman's ratchet as a heat engine. *Journal of Physics A: Mathematical and Theoretical*, volume 41, nr. 31, 2008: page 312003.
URL http://stacks.iop.org/1751-8121/41/i=31/a=312003

[186] Van Den Broeck, C.: Stochastic Thermodynamics. In *Selforganization by Nonlinear Irreversible Processes*, *Springer Series in Synergetics*, volume 33, edby W. Ebeling; H. Ulbricht, Springer Berlin Heidelberg, 1986, ISBN 978-3-642-71006-3, pages 57–61, doi:10.1007/978-3-642-71004-9_6.
URL http://dx.doi.org/10.1007/978-3-642-71004-9_6

[187] Van Kampen, N.: *Stochastic Processes in Physics and Chemistry*. North-Holland Personal Library, Elsevier Science, 2011, ISBN 9780080475363.
URL http://books.google.cz/books?id=N6II-6HlPxEC

[188] Vilar, J. M. G.; Rubi, J. M.: Failure of the Work-Hamiltonian Connection for Free-Energy Calculations. *Phys. Rev. Lett.*, volume 100, Jan 2008: page 020601, doi:10.1103/PhysRevLett.100.020601.
URL http://link.aps.org/doi/10.1103/PhysRevLett.100.020601

[189] Vilar, J. M. G.; Rubi, J. M.: Work-Hamiltonian connection for anisoparametric processes in manipulated microsystems. *Journal of Non-Equilibrium Thermodynamics*, volume 36, 2011: page 123–130, doi:10.1515/jnetdy.2011.008.
URL http://www.degruyter.com/view/j/jnet.2011.36.issue-2/jnetdy.2011.008/jnetdy.2011.008.xml

[190] Wang, Y.; Tu, Z. C.: Efficiency at maximum power output of linear irreversible Carnot-like heat engines. *Phys. Rev. E*, volume 85, Jan 2012: page

011127, doi:10.1103/PhysRevE.85.011127.
URL http://link.aps.org/doi/10.1103/PhysRevE.85.011127

[191] Wilcox, R. M.: Exponential Operators and Parameter Differentiation in Quantum Physics. *Journal of Mathematical Physics*, volume 8, nr. 4, 1967: pages 962–982, doi:10.1063/1.1705306.
URL http://link.aip.org/link/?JMP/8/962/1

[192] Wolf, F.: Lie algebraic solutions of linear Fokker–Planck equations. *Journal of Mathematical Physics*, volume 29, nr. 2, 1988: pages 305–307, doi:10.1063/1.528067.
URL http://link.aip.org/link/?JMP/29/305/1

[193] Xiao, T. J.; Hou, Z.; Xin, H.: Entropy production and fluctuation theorem along a stochastic limit cycle. *The Journal of Chemical Physics*, volume 129, nr. 11, 2008: 114506, doi:10.1063/1.2978179.
URL http://link.aip.org/link/?JCP/129/114506/1

[194] Yellin, J.: Two exact lattice propagators. *Phys. Rev. E*, volume 52, Sep 1995: pages 2208–2215, doi:10.1103/PhysRevE.52.2208.
URL http://link.aps.org/doi/10.1103/PhysRevE.52.2208

[195] Zhan-Chun, T.: Recent advance on the efficiency at maximum power of heat engines. *Chinese Physics B*, volume 21, nr. 2, 2012: page 020513.
URL http://stacks.iop.org/1674-1056/21/i=2/a=020513

[196] Zia, R. K. P.; Praestgaard, E. L.; Mouritsen, O. G.: Getting more from pushing less: Negative specific heat and conductivity in nonequilibrium steady states. *American Journal of Physics*, volume 70, nr. 4, 2002: pages 384–392, doi:10.1119/1.1427088.
URL http://link.aip.org/link/?AJP/70/384/1

[197] Zimanyi, E. N.; Silbey, R. J.: The work-Hamiltonian connection and the usefulness of the Jarzynski equality for free energy calculations. *Journal of Chemical Physics*, volume 130, nr. 17, May 2009: page 171102, doi:10.1063/1.3132747, 0902.3681.

[198] Zuker, M.: Mfold web server for nucleic acid folding and hybridization prediction. *Nucleic Acids Research*, volume 31, nr. 13, 2003: pages 3406–3415, doi:10.1093/nar/gkg595, see also http://mfold.rna.albany.edu/ and http://www.bioinfo.rpi.edu/applications/mfold/, http://nar.oxfordjournals.org/content/31/13/3406.full.pdf+html.
URL http://nar.oxfordjournals.org/content/31/13/3406.abstract

List of Tables

List of Abbreviations

App.	Appendix.
Apps.	Appendixes.
Eq.	Equation.
Eqs.	Equations.
Chap.	Chapter.
Chaps.	Chapters.
Fig.	Figure.
Figs.	Figures.
Sec.	Section.
Secs.	Sections.
Subs.	Subsection.
Subss.	Subsections.
Tab.	Table.
$\boldsymbol{x}$, $\boldsymbol{x}(t)$, $\boldsymbol{X}$, $\boldsymbol{X}(t)$	Column vector.
$\boldsymbol{x}^{\mathrm{T}}$, $[\boldsymbol{x}(t)]^{\mathrm{T}}$	Line vector.
x_i, $[\boldsymbol{x}]_i$	ith component of the vector $\boldsymbol{x}$.
$\mathbb{X}$, $\mathbb{X}(t)$	Matrix.
X_{ij}, $[\mathbb{X}]_{ij}$	Element of the matrix $\mathbb{X}$ at the ith line and jth column.
$\mathrm{diag}\{a, b, \ldots, z\}$	Diagonal matrix with $a, b, \ldots, z$ on the diagonal.
$\mathcal{A}_i(t)$	Variable corresponding to the microstates i of the system with discrete state space.
$\mathcal{A}(x,t)$	Variables corresponding to the microstates x of the system with continuous state space.
X	Random variable.
$\mathsf{X}(t)$	Stochastic process.
$\mathrm{Prob}\{\mathsf{X}(t) = a\}$	Probability that $\mathsf{X}(t) = a$.
$\dot{x}(t)$	Time derivative, $\dot{x}(t) \equiv \mathrm{d}x/\mathrm{d}t$.
$[a, b]$	Closed interval from a to b.
(a, b)	Open interval from a to b.
$\lvert x \rvert$	Absolute value of x.
$\delta(z)$	Dirac δ-function of the variable z.
δ_{ij}	Kronecker δ.
$\exp(z)$, e^z	Exponential function of the variable z.
$\log(z)$	Natural logarithm of the variable z.
$\tanh(z)$	Hyperbolic tangent of the variable z.
$\mathrm{I}_\nu(z)$	Modified Bessel function of the first kind of the variable z with the parameter ν.
${}_1\mathrm{F}_1(a, b; z)$	Kummer function of the variable z with the parameters a, and b.
${}_2\mathrm{F}_1(a, b, c; z)$	Gauss hypergeometric function of the variable z with the parameters a, b and c.
$\Theta(z)$	Unit-step function. $\Theta(z)$ equals to 1 for $z > 0$ and to 0 otherwise.
$\Theta(a, b; z)$	$\Theta(a, b; z) = \Theta(z - a) - \Theta(z - b)$.
FEL	Free energy landscape.
PV diagram	Pressure volume diagram.
WPD	Work probability density.

WPDs	Work probability densities.
RTA	Reaction time algorithm.
FRTA	First reaction time algorithm.
ATA	Attempt time algorithm.
FATA	First attempt time algorithm.

List of Original Publications

Some of the main results of the thesis were already published. Specifically, the zipper model (Sec. 2.4) was published in [93], the sliding parabola model in [94], and the two-level motor (Sec. 4.1) is described in [31, 32]. Finally, the new algorithm for Monte Carlo simulation of stochastic jump processes (App. C) has been published in [92]. Below we present the list of the corresponding citations.

1. [31] Chvosta, P.; Einax, M.; Holubec, V.; et. al.: Energetics and performance of a microscopic heat engine based on exact calculations of work and heat distributions, *Journal of Statistical Mechanics: Theory and Experiment*, 2010, P03002.

2. [32] Chvosta, P.; Holubec, V.; Ryabov, A.; et. al.: Thermodynamics of two-stroke engine based on periodically driven two-level system, *Physica E: Low-dimensional Systems and Nanostructures* **42**, 2010, 472.

3. [94] Holubec, V.; Chvosta, P.; Ryabov, A.: *Thermodynamics*, chapter Four Exactly Solvable Examples in Non-Equilibrium Thermodynamics of Small Systems, InTech, 2010, 153.

4. [92] Holubec, V.; Chvosta, P.; Einax, M.; et. al.: Attempt time Monte Carlo: An alternative for simulation of stochastic jump processes with time-dependent transition rates, *Europhysics Letters* **93**, 2011, 40003.

5. [93] Holubec, V.; Chvosta, P.; Maass, P.: Dynamics and energetics for a molecular zipper model under external driving, *Journal of Statistical Mechanics: Theory and Experiment*, 2012, P11009.